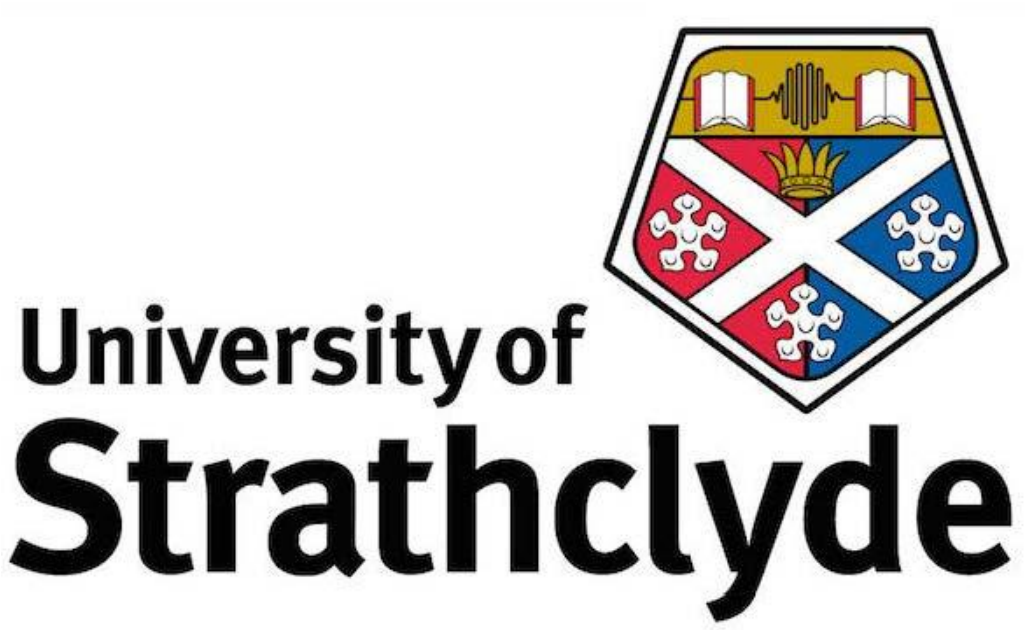

The Department of Biomedical Engineering

Development of an automated plasmapheresis system for the treatment of sepsis

By

Khaled Mohammed Alshareef

Supervisor: Professor. Terence Gourlay

This thesis is submitted in accordance with the regulation governing the award of the Degree of Doctor of Philosophy in Biomedical Engineering

2019

Declaration of Authenticity and Author's Rights:

This thesis is the result of the author's original research. It has been composed by the author and has not been previously submitted for examination which has led to the award of a degree.

Signed:

Date:

Acknowledgement:

First, I would like to thank Allah for his guidance and strength during the PhD course.

Second, I would like to thank my supervisor Professor Terence Gourlay for his support, guidance and patience through this project. His experience and knowledge in the field of extracorporeal devices was able to produce this work.

Also, I would like to thank Dr. Paul Davis for his efforts to help me in this project.

In addition, I would like to thank Dr. Moutaz Hamdan and Dr. Monica Kerr for their help.

Moreover, I would like to thank the staff of the Biomedical Engineering Department for their help in the lab.

I would like to thank my Father and my Mother for their support in my life. Also, I would like to thank my lovely wife, Hanin, and my son, Mohammed, for their patience and their encouragement, without them, this project will be very difficult.

I would like to thank my sponsor, Majmmah University for their financial support for the PhD.

Abstract:

Background:

Sepsis is one of the leading cause of death in ICU. The causes of sepsis could be viral, bacterial, fungal infection, also, and in some instances trauma. When a local response to the infection becomes a systemic response, the immune system becomes chaotic. Cytokines are produced in an uncontrolled way, resulting in a cytokines storm. The immune system enters a hyperactivation status that leads to multiple organ failures. Despite advances in the medical treatment and clinical experience, there is currently no single medication approved for treating sepsis. Thus, removal of the plasma that contains the inflammatory mediators is a potential solution to reduce their effect in the body.

Objectives:

The aim of this project is to develop a device that is able to separate plasma from whole blood. The device should be able to generate secondary flow to enhance the performance by reducing the formation of cake layer. In addition, the device should be fully automated in order to simplify the technology for the end user.

Approach:

Design using computer aided design employing different methods for producing secondary flow, investigate the impact of these techniques on formed blood element, by assessment of shear stress. The design was 3D printed to investigate the performance in term of plasma filtration using different membranes with different effective pore area. The next step was to increase the dimension of the rig and test the increase in surface

area on flux rate. In addition, an automation system was designed and assembled in order to control the transmembrane pressure, blood pump and plasma replacement pump through feedback from sensors read by a microcontroller.

Results:

The device was able to separate the plasma from the blood. The polyethersulfone membrane that has higher effective pore size had higher filtration rate. By increasing the size of the rig, the filtration volume increased. Also, the methods used to increase the flux were able to improve the flux rate. The automation system was tested and functioned well. Different flow rates were tested to investigate the performance of the system, and the results demonstrated the relationship between the flow rate and flux rate. In the TMP range 40-50 mmHg, at 260 ml/min flow rate, was the optimum flux rate. The device had the ability to run for 12 hours with a constant flux rate. The device achieved this with little haemolysis (pfHb <4 mg/L).

List of Abbreviations:

Activated Carbon (AC)

Activated Drotrecogin Alfa (ADF)

Activated Protein C (APC)

Active Clotting Time (ACT)

Acute Kidney Failure (AKF)

American College of Chest Physicians (ACCP)

American Society for Apheresis (ASFA)

American Thoracic Society (ATS)

Analog to Digital Conversion (ADC)

Circulatory Assist Device (CAD)

Compensatory Anti-Inflammatory Response Syndrome (CARS)

Computational Fluid Dynamics (CFD)

Continuous Hemodiafiltration (CHDF)

Continuous Hemofiltration (CHF)

Continuous Renal Replacement Therapies (CRRT)

Continuous Veno-Venous Hemofiltration (CVVHF)

Coupled Plasma Filtration with Adsorption (CPFA)

Disseminated Intravascular Coagulation (DIC)

Effective Pores Area (EPA)

European Society of Intensive Care Medicine (ESICM)

High-Volume Hemofiltration (HVHF)

Human Leukocytes Antigen-DR (HLA-DR)

IL-1 Receptor Antagonist (IL-1ra)

Intercellular Adhesion Molecules (ICAM)

Interleukin (IL)

Lymphocytes Function-Associated Antigen 1 (LFA-1)

Mannose-Binding Lectin (MBL)

Mean Arterial Pressure (MAP)

Membrane Attack Complex (MAC)

Microcontroller (MC)

Microfiltration (MF)

Mixed Antagonists Response Syndrome (MARS)

Molecular Weight (MW)

Multi-Organ Dysfunction Syndrome (MODS)

MW Cut-Off (MWCO)

Myeloperoxidase (MPO)

P-Selectin Glycosylated Ligands 1 (PSGL 1)

Pathogen-Associated Molecular Pattern (PAMP)

Pattern Recognition Receptors (PRRs)

Phase 3 Recombinant Human Activated Protein C Worldwide Evaluation in Sever Sepsis (PROWESS)

Plasma Exchange (PE)

plasma Free Hemoglobin (pfHb)

Plasmapheresis (PP)

PMX Fiber (PMX-F)

Polycarbonate (PC)

Polyethersulfone (PES)

Polyethylene (PE)

Polymyxin-B-Immobilized (PMX)

Printed Circuit Board (PCB)

Pulse Width Modulation (PWM)

Quick SOFA (qSOFA)

Reactive Oxygen Species (ROS)

Red Blood Cells (RBCs)

Scanning Electron Microscope (SEM)

Sequential Organ Failure Assessment (SOFA)

Society of Critical Care Medicine (SCCM)

Surgical Infection Society (SIS)

Surviving Sepsis Campaign (SSC)

Systemic Inflammatory Response Syndrome (SIRS)

Toll-Like Receptors (TLRs)

Transmembrane Pressure (TMP)

Tumor Necrosis Factor α (TNF-α)

Turbulent Kinetic Energy (TKE)

Ultrafiltration (UF)

Uncoated Charcoal (UC)

User Defined Function (UDF)

White blood cells (WBCs)

Thesis Outline:

Chapter one is an introduction to the word sepsis, diagnosis and treatment of sepsis through the history of civilizations. Also, the definition of sepsis and criteria of diagnosing sepsis evolving with time has been discussed. The pathophysiology of sepsis and immune system mechanisms after an insult was mentioned in this chapter.

Chapter two discussed the current treatment of sepsis and the pharmacological clinical trials that deal with finding the treatment of sepsis. Moreover, the clinical trials involving the medical technologies, excluding plasmapheresis.

Chapter three mentioned the plasmapheresis technology in the treatment of sepsis. In this chapter, different clinical trials for treating sepsis were discussed.

Chapter four, the aims of the project and the objective were defined.

Chapter five, literature review of the anatomy of blood, effect of shear stress on blood and membrane characteristics for the plasmapheresis were given. Also, the methods of enhancement of the flux was discussed. In this chapter also, the development of various stages of the device are included that covers the automation system.

Chapter six illustrate the results of the device experiments during different stages of the rig development.

Chapter seven discussed the result and the limitations that have an impact of the project.

Chapter eight concluded the project and proposed the work that improve the device in the future.

Table of Contents:

List of Figures:

List of Tables:

Chapter 1:

Sepsis: An Historical and Aetiological Perspective

1 Sepsis: An Historical and Aetiological Perspective:

1.1 Introduction:

Sepsis is a major disease with a high mortality rate despite great advances in healthcare management. The mortality rate among sepsis patients is 40-80% and the annual cost related to sepsis treatment is approximately 17 Billion USD. Yearly, 31.5 million patients are diagnosed with sepsis globally, and on average 5.3 million sepsis patients die every year (Delano and Ward, 2016, Daniels, 2011, Singer et al., 2016, Fleischmann et al., 2016). Sepsis typically follows a sequence of events starting with the introduction of an insult which leads to the local initiation of inflammatory process involving cellular and plasma borne processes. The un-regulated amplification of these processes provokes the amplification of local events to become a systemic challenge. When an initiator is detected by the immune cells, the immune system targets the invader locally. As part of the local response, the immune system secretes inflammatory mediators, such as cytokines. The aim of these mediators is the destruction of the pathogen by migrating cells that specialize in this process. The cytokines are regulated and in themselves regulate the immune system, but once cytokine production becomes unregulated, the result can be catastrophic. The unregulated cytokines damage epithelial cells, leading to systemic inflammation which can result in widespread organ dysfunction (Schulte et al., 2013b). Up to the date of this thesis, there are no FDA approved medications that target sepsis, even though there are many clinical trials that focus on agents that block pro-inflammatory or anti-inflammatory cytokines. The trials failed due to the complexity of the nature of the immune response that is activated during inflammatory event through

different pathways. So, blocking one pathway will not result in successful sepsis treatment (Chun et al., 2017, Gotts and Matthay, 2016). In order to understand the definition of sepsis and its pathophysiology, the history of the word “sepsis” and the history of associated inflammation will be discussed.

1.2 History:

The mortality from infection can be traced back to ancient civilization. In Europe and Asia, black death caused more than one third of the populations to die at the beginning of the 15th century. In 2,375 BC, the first recorded herbal medicine, ch'ang shan, to treat fever was prescribed by Emperor Shen Nung's doctors (Funk et al., 2009). So, the relationship between inflammation, seen as severe fever and death was recognized and the journey to develop treatment began.

1.2.1 Egyptians:

The Egyptians studied sepsis related to battlefield wounds. The written records, on early papyrus, can be traced back to 1600 BC and were found in Luxor, Egypt. The information found in these papyrus is actually taken from older papyrus recorded around 3000 BC. In the papyrus, 47 cases were recorded details lesions such as bone fracture, open wound, and dislocation, in addition to describing the treatment of these lesions. It was noted that some of these cases had fever as secondary phenomenon, beginning with pus, described as "ryt" as a complication of an infection. The development of pus was described as bad condition. One accurate description of a complication of secondary infection came from a wound case with two stages: The first stage is that the wound was treated, and the second stage is fever associated with skin redness, sweating, stiffness of the neck, convulsion and the strong smell emitted from the wound site. At the second stage, the Egyptians determined that the wound cannot be treated. The Egyptians, introduced a clear description of wounds and their treatment, describes the agents associated with infection in a way akin to microorganisms. They described them as "WHDW" and proposed that they were found in the gut and could enter the bloodstream

and resulted in the intoxication of the body. The Egyptians also tried to find treatments that could stop the formation of pus. The treatments include applying mixture of honey and grease on the wound, and physically removing the pus, and noted that this often led to wound healing (Botero and Pérez, 2012).

1.2.2 Greeks:

The word sepsis comes the Greek word "σηψιζ" that translates to "decomposition of animal or vegetable organic matter in the presence of bacteria". The first use of the word sepsis as medical term was more than 2700 years in the poems of Homer. The word sepsis originally derived from "sepo" "σηπω" that translates to "I rot". The latter word is found in the Hippocratic Corpus written by the philosopher and physician Hippocrates (approximately 400 BC). Hippocrates establish the concept of body humor dysregulation, blood, yellow bile, black bile and phlegm that represent the four elements air, water, fire and earth; imbalance in these body humors was thought to cause disease (Funk et al., 2009, Hernandez Botero and Florian Perez, 2012). Sepsis disease was described by Hippocrates as dangerous, emitting odors and decay that occur in the body. Also, he mentioned that as result of colon decay," dangerous principle" is generated and leads to "auto-intoxication". Hippocrates tested medicines that could cure sepsis such as wine and vinegar (Funk et al., 2009).

The Greek physicians understood the complications associated with continuous skin loss, which were reported by Hippocrates in his book as "When a cut becomes inflamed, the neighboring tissues become intumescent, and the lesion flush and heat spreads through the vessels. If the lesion is located in the leg, the tumours will develop in the

groin; if it is in the arm they will prefer the armpit". In Greek medicine, the treatment of diseases was based on the fundamental aspect of humors. Thus, the treatment of purulent lesions was related to the interaction between skin, humors and their involvement in the development of systemic inflammation. The Greeks took blood samples from septic patients, and they found that the status of the blood was changed as the black bile is increased. Greek physicians believed that the formation of pus could be either harmful or harmless based on the idea of SEPSIS and PEPSIS. Sepsis is similar to the concept of putrefaction that take place inside the colon. While pepsis is similar to the idea of fermentation, for example, food digestion in the stomach was considered by the Greeks as pepsis. The presence of pus formation was described by Hippocrates to be either sepsis or pepsis depending on the lesion suppuration. Hippocrates mentioned if the discharge is darker, abundant, heterogeneous, fetid and bloody it considered as part of sepsis. If the suppuration is part of the wound healing process, this can be described as pepsis. As a result, the lack of pus was considered as good sign. Moreover, part of the treatment of the lesion was to drain the content of the pus, and a Greek barber invented a device similar to syringe to drain pus. The treatment of pus included the use of ointments, bandages and bathing with wine, vinegar and water (Hernandez Botero and Florian Perez, 2012).

1.2.3 Romans:

Galen was a Roman physician who studied sepsis based on observing the symptoms. His findings remained in use for over 1500 years. Galen's idea of treating sepsis is by letting blood and draining abscesses. Also, he invented medicine for treating different diseases such as inflammation and venom, using "theriac", which is made from mixing more than 70 substances. Also, Galen was the first physician to mentioned that wound is healed by secondary intention. His idea that the pus formation "Pus bonum et laudabile" is important since it part of the healing process of wounds. The Romans believed that sepsis came from invisible organisms that released putrid fumes known as "miasma". Thus, hygiene to the romans was important. However, the idea of transferring infection from a person to others by contact was not theorized at that time so measures to reduce contamination were not taken. In addition, Celsus, a Roman physician, was the first person to described the four inflammation symptoms "Notae vera inflammationis sunt quattuor; rubor et tumor cum calore et dolore", which translate to redness and swelling with heat and pain (Hernandez Botero and Florian Perez, 2012, Scott et al., 2004). Celsus treatment techniques consist of two methods, first control the bleeding by applying cloth soaked in mixture of water, vinegar and wine. Second, after the bleeding is controlled, the skin around the wound was moisturized with a combination of butter and rose oil, in addition to dressing the wound with water soaked bandages, proper diet and resting was prescribed. But, if these methods fail, the skin will be burned (cauterization) (Hernandez Botero and Florian Perez, 2012).

1.2.4 Middle Ages:

The Arabs studied medicine through translation from pervious eras. The Arab medicine techniques were influenced by Galen, suppuration being considered as part of the wound healing process. Arabs, also took from the Greeks the painful cauterization method to treat lesions. Performing surgery in Europe was based largely on the same approach as in the middle ages, using the cauterization technique, and the "pus bonum et laudabile" that was proposed by Galen (Hernandez Botero and Florian Perez, 2012).

In the 14th century, the concept that all wounds are subjected to suppuration was recognized for all types of wounds including the ones that cauterization was applied to. Also, middle ages physicians performed pus drainage. However, William of Saliceto theorized that the pus formation was bad for the wound. His method of treatment was applying a dressing contain a mixture of egg white and rose water, to prevent pus formation (Thurston, 2000).

1.2.5 Firearms:

Cuts and pierce from swords and arrows are largely "clean" wounds with little ballistic contamination. The development of firearms introduced different types of lesions and the prospect of contamination with bullet materials, external debris and gunpowder. Hieronymus Brunschwig came with the concept that the gunpowder is poisonous for the wound. For treating the wounds, he proposed to remove the gunpowder from the wound using seton and encourage the formation of suppuration. Giovanni da Vigo proposed using boiling oil to remove the powder and he published his method in the book "Practica copiosa in arte chirurgica". Cauterization and boiling oil were used in combination to treat wounds. However, Ambroise Paré disagreed with the concept of

using boiling oil for removing powder from the wounds. He proposed a lotion consisting of egg yolks, rose oil and turpentine. He applied the lotion to the wound and it was found to be effective (Thurston, 2000, Hernandez Botero and Florian Perez, 2012).

Alfonso Ferri published an article stating that fragments of armour and cloth worn by soldiers could penetrate deeply in the wound and result in suppuration, thus, the penetrated pieces must be removed from the wound. His theory was accepted for more than 200 years.

The first theory of disease transmission was published by Girolamo Fracastoro in 1546. He said there are three paths for diseases to be transmitted: direct contact, indirect contact such contact with infected items and transmission from a distance. Also, he regarded an infection "as being due to the passage of minute bodies from one person to another". Also, that these minute bodies are capable of multiplying (Thurston, 2000). This first genuine suggestion of microorganisms and their role in disease transmission and propagation was revolutionary and will be discussed further in section 1.2.6.

1.2.6 Microorganisms Theory and Discovery:

Aristotle theorized that "sepsis creates small creatures specially in the mud and marshy places" (Majno, 1991). In the 1650s, Francesco Redi experimented with Aristotle's theory by creating putrefaction in meat. He placed meat in two pots, one pot is sealed while the other was exposed. He found that the exposed meat had flies on it and after some time maggots started to appear and cover the meat. The results of Redi suggests a process rather than Galen's idea of spontaneous generation.

The first compound microscope designed to demonstrate the micro-environment and creatures was developed by Galileo by modifying a telescope. However, the images captured from the microscope were blurred and unclear. 300 years after the first microscope, Anthony van Leeuwenhoek, developed his compound microscope that was able to produce clear images. He discovered, what he called, "animacules" and he drew them as seen in figure 1. His drawing of the "animalcules" led scientists to developed germ theories suggesting that these creatures were involved in the development of diseases. In the 19th century, there was a big jump toward the understanding of the transmission of infectious diseases. Ignaz Semmelweiss, a physician in a maternity ward, noticed the mortality rate was high among childbed fever patients, known as puerperal sepsis. Also, he found that the infection among women delivered by a midwife is lower compared to women delivered by a medical student. The reason suggested is that the medical students, who carry out operations, did not wash their hand before delivering babies. As a result, he suggested that "The fingers and hands of students and doctors, soiled by recent dissections, carry those death-dealing cadaver's poisons into the genital organs of women in childbirth". Semmelweiss initiated handwashing a policy

prior to delivery, and the puerperal sepsis rate dropped from 16% to less than 3%. Unfortunately, his concept of handwashing was not accepted by the medical staff at that time, and it was considered somewhat counter-intuitive. Surgical knowledge and practice increase exponentially in the 19th century, leading to an increase in mortality rate associated with postoperative sepsis (Funk et al., 2009).

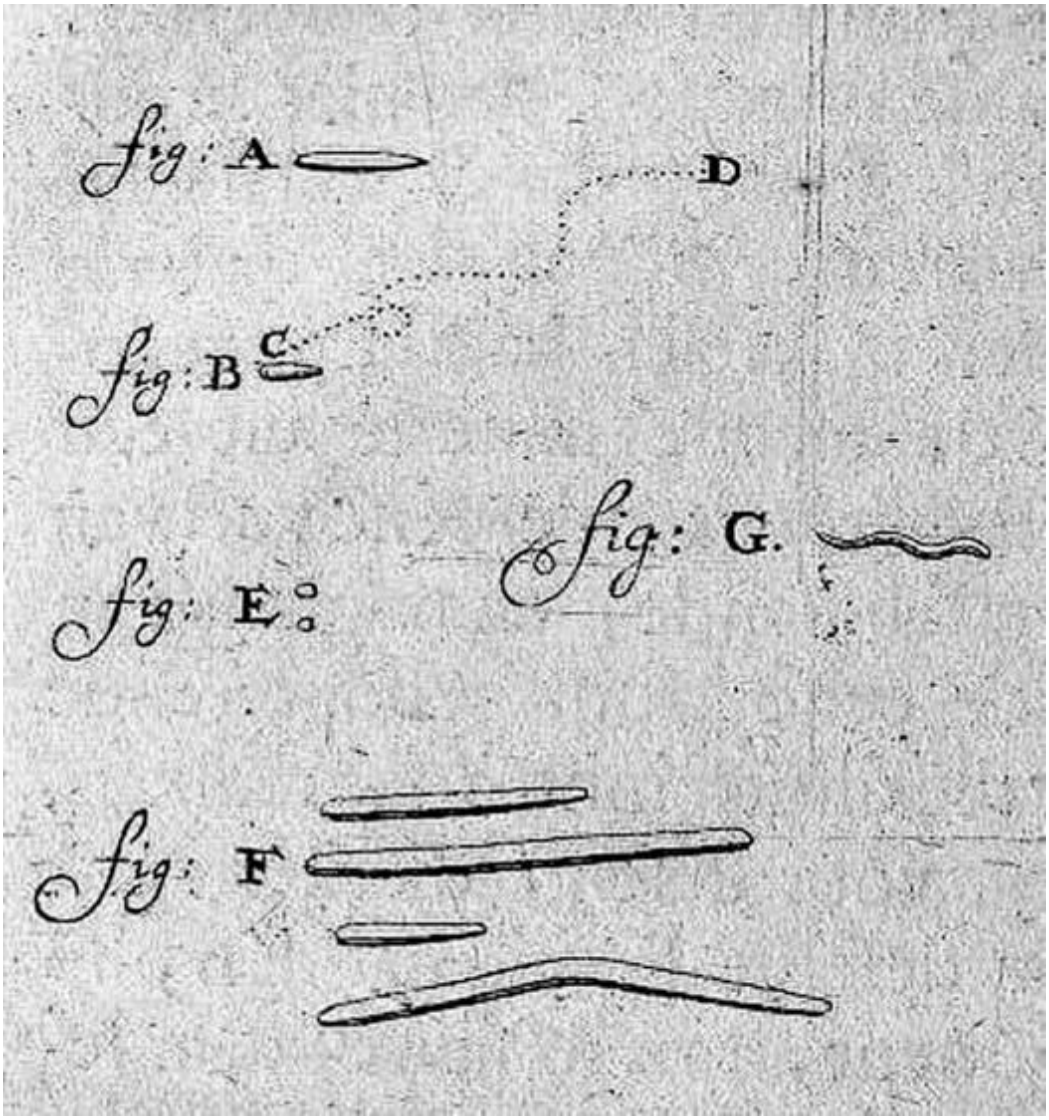

Figure 1 Animacules Drawings (Funk et al., 2009)

Louis Pasteur had performed experiments regarding germ theory. He concluded that the putrefaction process needed a living organisms, so the concept of spontaneous generation was eliminated confirming Leeuwenhoek's work earlier theories (Funk et al., 2009).

Joseph Lister had noticed that a closed skin fracture healed without an infection when compare to open skin fractures where sepsis and pus drainage occur. He came with the idea of "dust of disease" responsible for complication of amputation and infectious wounds. In addition, he made a connection between the wounds and microscopic bacteria responsible for fermentation after reading Pasteur's work. Lister published a paper about antiseptic methods used to manage open skin fracture by carbolic acid. During surgery, Lister sprayed diluted carbolic acid on the wound in order to eliminate bacteria (Thurston, 2000, Hernandez Botero and Florian Perez, 2012). Robert Koch worked on the germ theory by experimenting on sheep. Koch mentioned that infected sheep with anthrax have tiny rod shaped organism growing in their blood. He was culturing and growing these organisms using nutrient gelatin, and infecting healthy sheep with the bacteria, as a result, the healthy sheep were infected with anthrax. Thus, Koch had invented a methodology used for further definition of germ theory (Funk et al., 2009). William MacEwen was studying under Lister, and in 1879 he stopped using carbolic acid and replace it with a boiling method, where he used to boil the gauze that was used for the dressing, sterilizing the materials. Ernst von Bergman invented a steam sterilizing device, and it was used by MacEwen to sterilize tools. In recognition of the developing understanding of the need for sterility in the operating environment and in

the dressing procedures, John Charnley invented a procedure for hip replacement. Feared the infection of hip replacement implant. Thus, he implemented methods for reducing bacteria in the operating rooms. His methods included:

1- The operating team is separated from the others and patient lower part by enclosing them in glass.
2- The surgeon and his assistants were wearing clothes similar to spacesuits, as shown in figure 2, filtered air were supplied to the suit, and communication radio was fitted inside the suit in order to isolate the surgeon and assistance from the wound.
3- The enclosure is ventilated with filtered air, and the air flow is laminar, since the secondary flow will contact the surfaces and will carry bacteria to flow in the operating room.

His method of laminar air flow continues to be used in operating rooms to reduce postoperative infection (Thurston, 2000).

Figure 2 Operating Suit (Thurston, 2000)

1.2.7 The development of anti-biotics:

Paul Erlich (1845-1915) identified a compound that was able to destroy newly discovered bacteria responsible of infection and sepsis. His first focus was staining and identifying the bacteria, and theorized that if bacteria absorbed the dye, there may be a "magic bullet" able to destroy the bacteria. After 600 failed compounds, he was able to create "salvarsan", which contains arsenic, a compound used to treat syphilis.

Gerhard Domagk in 1935 demonstrated that by injecting prontosil red (dye) into mice, they developed an immunity to sepsis caused by streptococci. The dye inside the body is converted into a sulphanilamide compound. As a result, many compounds were created with bactericidal properties (Funk et al., 2009).

The next major step in this field was the work of Alexander Fleming, who discovered penicillin by accident. He noticed some culture plates contaminated with mould, and the area where the mould grew had no bacteria. The mould was Penicillum notatum and he named the compound penicillin that cause the bacteria to die. Unfortunately, Fleming was unable to extract and concentrate the penicillin. Ernest Chain and Howard Florey were able to produce penicillin by identifying its chemical structure. Their work encouraged scientists to develop antibacterial medications leading to a family of "anti-biotics" (Funk et al., 2009). Selman Abraham Waksman, a soil microbiologist, discovered antibiotics from streptomyces griseus fungi, where he extracted streptomycin, used effectively to kill the tubercle bacillus, one of the greatest healthcare challenge of the early 20th century (Thurston, 2000).

1.2.8 White Blood Cells (WBCs) and Cytokines:

In the late of 19th century, Ilya Metchnikoff had discovered phagocytes and he noted that inflammation occurred to bring phagocytes to the infected area to destroy bacteria. F. J. Lang in 1926, had proposed that transformed tissues and migrating monocytes are responsible for upregulation of macrophages. Also, he theorized that injured endothelial cells will cause elongation and differentiation into wound "fibroblasts". Through this work, the role of cellular species was fairly well defined and understood, but it was in the 1950s, the endogenous pyrogen, interleukin(IL)-1, nerve growth factor, and interferon were identified. Rita Levi-Montalcini named the molecule responsible for simulating the growth and differentiation of new developing nerve cells as nerve growth factor. Researchers had discovered lymphokines in 1960s, which are mediators generated by lymphocytes. In 1970s, tumor necrosis factor and its mechanism has been identified. In the 1980s and 1990s, more inflammatory mediators were discovered (Broughton et al., 2006). Latter work, made possible through emergence of new molecular diagnostic techniques uncovered more molecular species involve in the mechanisms of inflammation, and would ultimately lead to the identification of many and varied activation pathways' that brings together the cellular and humoral elements of sepsis and inflammation.

1.3 The definition of Sepsis:

In 1991, the American College of Chest Physicians (ACCP) and the Society of Critical Care Medicine (SCCM) proposed the fundamental definition of sepsis, severe sepsis, septic shock and multi-organ dysfunction syndrome (MODS). They introduced the systemic inflammatory response syndrome (SIRS) as the immune response to infection and non-infection origins. Bone et al. (1992) stated that standardizing the definitions of sepsis would lead to diagnosis and treatment of the disease as soon as it discovered. Also, by standardizing the definitions, it made possible to gather data from clinical trials, which will help to understand the cellular and the immune mechanism of sepsis and its complications (Bone et al., 1992).

Systemic Inflammatory Response Syndrome (SIRS):

SIRS is the whole body inflammatory condition that represent the systemic outcome of the amplification of the local event (figure 3). Critically, SIRS often leads to MODS and death, often is the mechanism of death in sepsis patients. The consensus diagnosis of SIRS is considered to consist of any two of the following conditions:

1- $36C^o$ <Body temperature> $38C^o$.
2- Heart rate > 90 bpm.
3- Respiratory rate > 20 bpm, tachypnea, or if the PaCO2 < 32 mmHg, hyperventilation.
4- White blood count is more than 12000/mm^3 or less than 4000/mm^3or the existing percentage of the immature neutrophils > 10%.

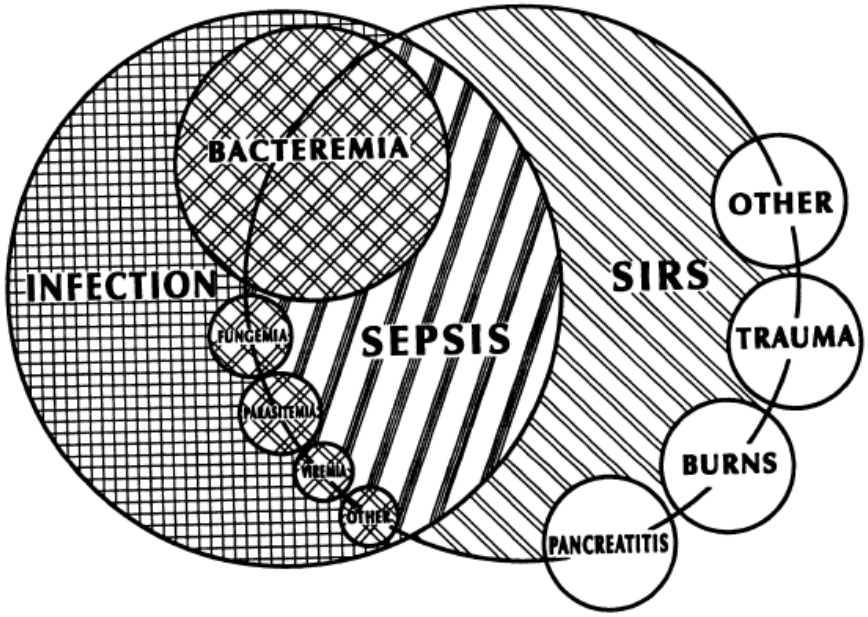

Figure 3 SIRS (Bone et al., 1992)

SIRS complications lead to organ failure, acute lung injury, renal dysfunction, and MODS (Bone et al., 1992). In order to better understand the SIRS, three stages have been suggested, as shown in figure 4.

Stage I: When an injury or insult occurs, the regional cells produce cytokines that will initiate the immune response. The immune response will result in repairing the wound and recruiting reticuloendothelial cells.

Stage II: The locally released cytokines will enter the circulation system causing macrophages and platelets to move into the injured area. The cytokines will also simulate the production of growth factors. The immune response is controlled by the immune system by secreting endogenous antagonist. These antagonists will suppress the production of pro-inflammatory cytokines, this cycle will be terminated once the wound is healed and hemostasis normalized.

Stage III: System response will occur once hemostasis fails to return to normal. The cytokines will begin to initiate humoral cascade, reticular endothelial system, causing damage to the organs (Davies and Hagen, 1997). More detail will be discussed in section 1.4.

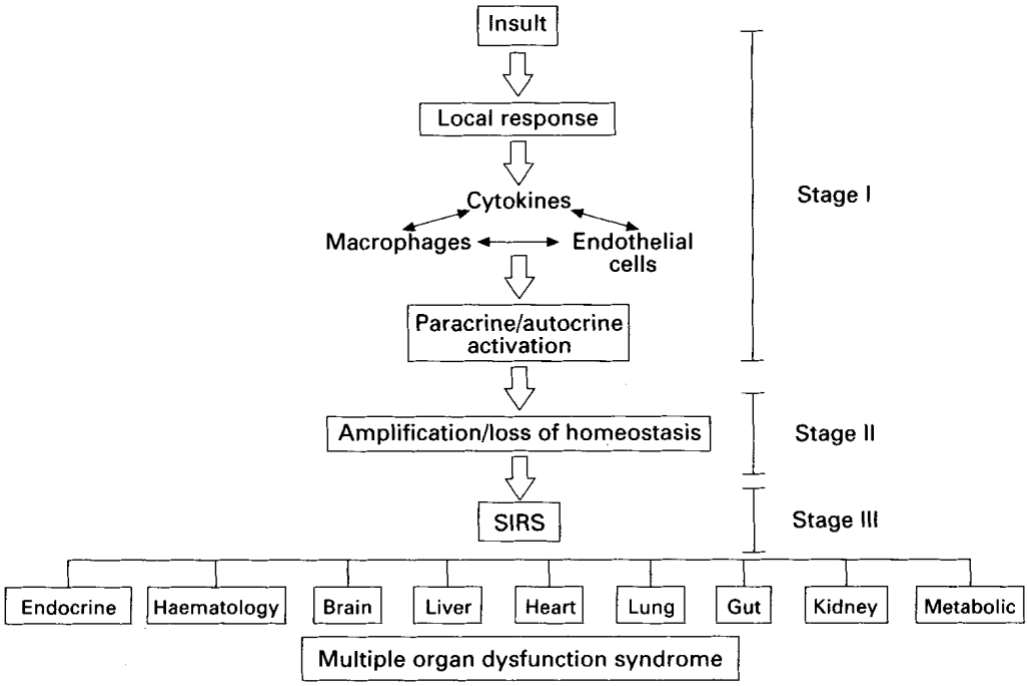

Figure 4 SIRS stages (Davies and Hagen, 1997)

Sepsis:

SIRS leads to sepsis, in the presence of identified infection. The infection could be cause by bacteria, fungi, virus and parasites. If the blood is infected with bacteria, causing sepsis, this medical condition known as bacteremia. Other variants are called viremia, fungemia, parasitemia (Bone et al., 1992). 1.8 million sepsis incidents occur globally (Daniels, 2011). In US, the sepsis incidence is estimated between 240-300 cases per 100000 of populations, and the cost around 17 billion dollars. The rate of sepsis is increasing at 9% yearly (Lewis et al., 2012). In UK, 38600 deaths occur annually due to sepsis. In Europe, 90.4 sepsis cases are diagnosed per 100000 people (Daniels, 2011). Critically, the accurate diagnosis of sepsis events still requires technological development and the incidence could actually be much higher as many cases maybe misdiagnosed if only the clinical indicators are employed, as diagnostic markers.

The basic indicators of various septic states are fairly well defined:

Infection- the normal underlying cause of sepsis:

Bone et al. (1992) define infection as "Microbial phenomenon characterized by an inflammatory response to the presence of microorganisms or the invasion of normally sterile host tissue by those organisms".

Severe Sepsis:

Severe sepsis, known as sepsis with organ dysfunction, hypotension or abnormal hypoperfusion that leads to lactic acidosis, oliguria and acute alteration of mental status (Bone et al., 1992).

In USA, 300 patients per 100000 cases are diagnosed with severe sepsis, and the death rate among these patients is 20-50% (McCormack et al., 2016). 150000 death occur in Europe due to severe sepsis each year (Levy et al., 2003).

Sepsis-induced hypotension:

Sepsis-induced hypotension is present when the systolic pressure is less than 90 mmHg or is less than baseline by 40 mmHg or more when there is no other presenting cause (Bone et al., 1992).

Septic Shock:

Septic shock is diagnosed as sepsis induced hypotension in spite of sufficient fluid in addition to abnormal hypoperfusion and organ dysfunction (Bone et al., 1992).

Multiple Organ Dysfunction Syndrome (MODS):

Mortality associated with MODS is significant. Clinical research shows that the reason for this mortality is "a process of progressive physiological failure of several interdependent organ systems" (Bone et al., 1992). Progressive organ failure, sequential organ failure, multiple organ failure, and multiple system organ failure are names that are used to describe the various mechanisms of organ failure that occur in patients. Previous clinical studies found that the primary cause of multiple organ failure is infection. However, several clinical studies show that multiple organ failure can also result from non-infectious causes (Bone et al., 1992). Studies have shown that the complexity of the interrelationship between the organs, means that failure of one organ can progress into failure of others (Bone et al., 1992). Understanding of organ dysfunction, its diagnosis and treatment, continues to evolve. However, further research is required to accurately diagnose this condition. A series of recommendations have evolved in this regard in recent years, proposed by Bone et al. (1992).

Recommendation I: The "multiple organ dysfunction syndrome" should be used when an organ is functioning abnormally. The term organ dysfunction should be selected when the hemostasis of the organ is abnormal. Also, even in patient with normal cardiac output and oxygen delivery, tissue oxygen levels may be insufficient, known as lactic acidosis. Four points have been proposed to summarize recommendation one, these are:

1- "MODS describe a continuum of organ dysfunction, although the specific descriptions of this continuous process are not currently available."
2- By increasing the knowledge of diagnosing the disease at first stage, an early intervention can be started.

3- The performance of the organ can change with time, which can be used to predict the organ functionality. However, the techniques to diagnose the severity of the disease are time specific, but the organ function can change with time.

4- There are different factors that affect MODS at different time intervals, both interventional and host-related.

Recommendation II: There are two different types of MODS, primary and secondary. The primary pathway is caused by the insult itself. To illustrate, if a patient is diagnosed with rhabdomyolysis, this will lead to renal dysfunction. The secondary MODS is defined as complications of the host response not the insult, figure 5.

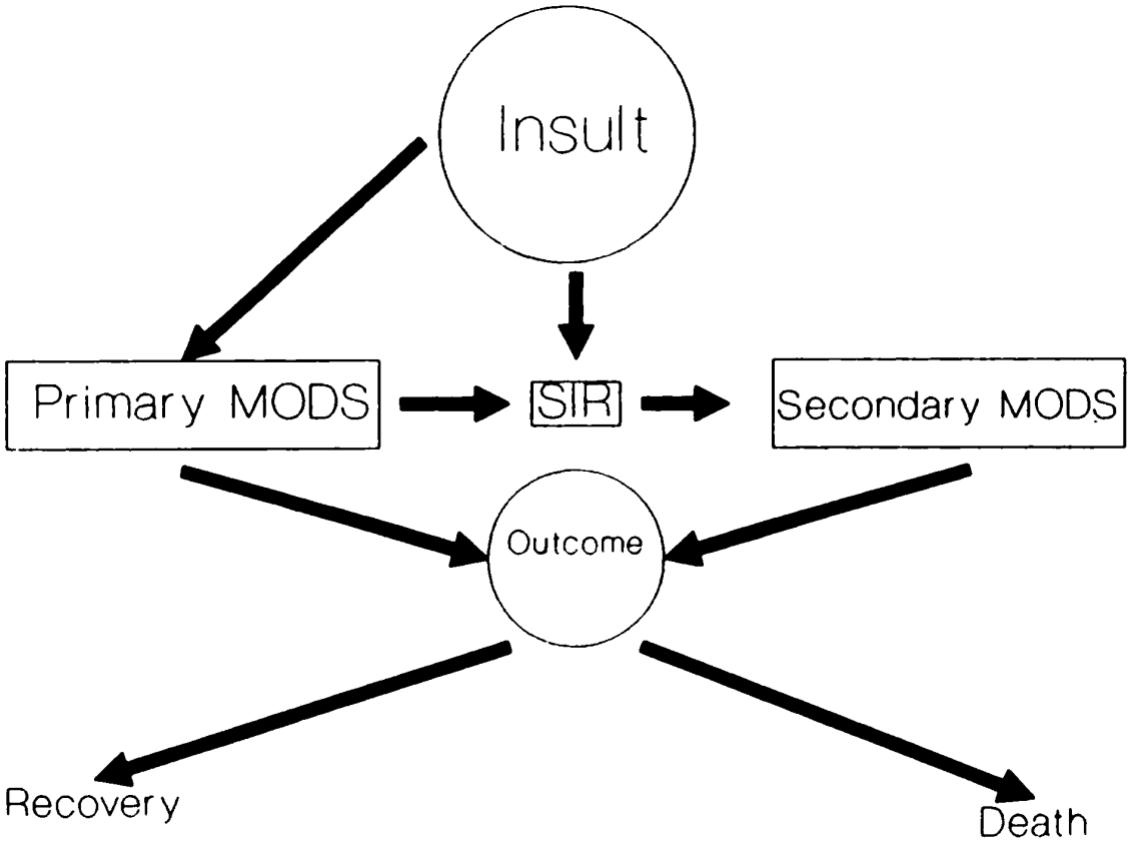

Figure 5 Primary and Secondary MODS (Bone et al., 1992)

Recommendation III: the data collected before the conference cannot be used to set optimum criteria to define MODS. Thus, setting up a database for clinical researchers to update their finding in order to find the optimal definitions to describe the syndrome. The data collected to diagnose organ failure should come from empirical studies (Bone et al., 1992).

The data from clinical research showed that the first sepsis conference definition for sepsis needed to be revised in order to include knowledge about the pathophysiology of sepsis and its complications. Also, some physicians are critical of the conference for not giving a distinctive definition of sepsis. Moreover, a survey established by the European Society of Intensive Care Medicine (ESICM) and Society of Critical Care Medicine found that 71% of the participants have a non-common definition for sepsis even though sepsis has been defined by the 1991 conference. So, in 2001, another international conference was held in Washington, DC sponsored by American College of Chest Physicians (ACCP), Society of Critical Care Medicine (SCCM), European Society of Intensive Care Medicine (ESICM), American Thoracic Society (ATS) and Surgical Infection Society (SIS); where the definition for sepsis was revised. There were three objectives for the conference:

1- Reviewing the strength and weakness of the definition of sepsis.
2- Better understanding about the current sepsis definition to improve it.
3- Find new methods to improve the accuracy, reliability and utility for diagnosing sepsis.

A major issue that arises with diagnosing sepsis is that there is no "gold standard" criteria. "Diagnostic criteria will be judged successful if clinicians regard them as an aid for decision-making at the bedside. The diagnostic scheme requires sufficient sensitivity and specificity to be a clinical aid". The SIRS definition in 1991 was considered to be non-specific and cannot be used to accurately diagnose the disease. Clinicians have found that in SIRS patients the level of various mediators such as IL-6 and active protein-C is detectable. These biomarkers may be used to diagnose SIRS and reduce dependence on the clinical signs. Further research is needed to support this conclusion (Levy et al., 2003).

Levy et al. (2003) have defined sepsis as the 1991 definition, which is SIRS in addition to infection. For physician and researchers, the criteria for diagnosing infection should be widely useful in order to enhance the treatment of sepsis. Also, the sensitivity of the criteria needs to be high for diagnosing patients with sepsis. Infection is defined as that of Bone et al. (1992) at the conference held in 1991, but their definition of infection has a flaw. To illustrate, colitis triggered by Clostridium difficile that leads to the abnormal growth of the bacteria in the colon, which is already filled with bacteria. The clinical symptoms are shown only when the Clostridium difficile infect the tissues and release its endotoxin. So, the infection can be assumed even without confirming the presence of a microbe. Table 1 shows all the possible clinical signs that can be used to identify systemic inflammation in response to infection. However, it must be taken into consideration not all the signs that are found in table 1 can be specifically used to diagnose sepsis. For example, the high cardiac output can be seen in patients who have

had surgical procedures or trauma. Severe sepsis definition is defined by that offered in the first sepsis conference. Septic shock can be defined if the systolic blood pressure is less than 90 mmHg, mean arterial pressure (MAP) is less than 60 mmHg or the systolic blood pressure is reduced more than 40 mmHg from baseline (Levy et al., 2003).

Infection,[a] documented or suspected, and some of the following:[b]
General variables
Fever (core temperature >38.3°C)
Hypothermia (core temperature <36°C)
Heart rate >90 min^{-1} or >2 SD above the normal value for age
Tachypnea
Altered mental status
Significant edema or positive fluid balance (>20 mL/kg over 24 hrs)
Hyperglycemia (plasma glucose >120 mg/dL or 7.7 mmol/L) in the absence of diabetes
Inflammatory variables
Leukocytosis (WBC count >12,000 μL^{-1})
Leukopenia (WBC count <4000 μL^{-1})
Normal WBC count with >10% immature forms
Plasma C-reactive protein >2 SD above the normal value
Plasma procalcitonin >2 SD above the normal value
Hemodynamic variables
Arterial hypotension[b] (SBP <90 mm Hg, MAP <70, or an SBP decrease >40 mm Hg in adults or <2 SD below normal for age)
$S\bar{v}O_2$ >70%[b]
Cardiac index >3.5 $L \cdot min^{-1} \cdot M^{-23}$
Organ dysfunction variables
Arterial hypoxemia (PaO_2/FIO_2 <300)
Acute oliguria (urine output <0.5 $mL \cdot kg^{-1} \cdot hr^{-1}$ or 45 mmol/L for at least 2 hrs)
Creatinine increase >0.5 mg/dL
Coagulation abnormalities (INR >1.5 or aPTT >60 secs)
Ileus (absent bowel sounds)
Thrombocytopenia (platelet count <100,000 μL^{-1})
Hyperbilirubinemia (plasma total bilirubin >4 mg/dL or 70 mmol/L)
Tissue perfusion variables
Hyperlactatemia (>1 mmol/L)
Decreased capillary refill or mottling

Table 1 Clinical Signs of Sepsis (Levy et al., 2003)

Singer et al. (2016) in the third international consensus definitions for sepsis and septic shock (sepsis-3), redefine sepsis and septic shock. They criticized the early efforts at defining these life threating conditions in 1991 and 2001. This task force considered that many of the SIRS clinical signs are not helpful in diagnosing sepsis. WBC count, heart rate and temperature change as the body is infected and they indicate the normal response of the immune system to an insult. The conventional SIRS clinical signs do not reflect if the body is critically ill and if the immune system is unregulated. 1 in 8 patients transferred to ICU with infection and organ dysfunction, do not meet with the minimum SIRS criteria. The current method that is used for describing the severity of the organ failure is sequential organ failure assessment (SOFA). The SOFA scoring system, which grades the abnormalities in organ function, is based on clinical observations, laboratory results, such as PaO2, platelet counts, creatinine level and bilirubin level. The SOFA scoring is illustrated in table 2 (Singer et al., 2016).

	Score				
System	0	1	2	3	4
Respiration					
Pao_2/Fio_2, mm Hg (kPa)	≥400 (53.3)	<400 (53.3)	<300 (40)	<200 (26.7) with respiratory support	<100 (13.3) with respiratory support
Coagulation					
Platelets, $\times 10^3/\mu L$	≥150	<150	<100	<50	<20
Liver					
Bilirubin, mg/dL (μmol/L)	<1.2 (20)	1.2-1.9 (20-32)	2.0-5.9 (33-101)	6.0-11.9 (102-204)	>12.0 (204)
Cardiovascular	MAP ≥70 mm Hg	MAP <70 mm Hg	Dopamine <5 or dobutamine (any dose)[b]	Dopamine 5.1-15 or epinephrine ≤0.1 or norepinephrine ≤0.1[b]	Dopamine >15 or epinephrine >0.1 or norepinephrine >0.1[b]
Central nervous system					
Glasgow Coma Scale score[c]	15	13-14	10-12	6-9	<6
Renal					
Creatinine, mg/dL (μmol/L)	<1.2 (110)	1.2-1.9 (110-170)	2.0-3.4 (171-299)	3.5-4.9 (300-440)	>5.0 (440)
Urine output, mL/d				<500	<200

Table 2 SOFA scoring system (Singer et al., 2016)

The recommendation of the 2016 consensus for sepsis definition is "life-threatening organ dysfunction caused by a dysregulated host response to infection". Also, in a published article, the task force did not find accurate clinical criteria for measuring the immune response. In the 2001 sepsis conference, a list of clinical criteria and blood tests is published to detect inflammation and organ failure, as seen in table 1. Table 3 shows the new definition for sepsis and associated clinical measurement. As mentioned before, the issue with SOFA scoring system requires laboratory tests in addition to clinical signs. As a result, in the 2016 conference, a new fast scoring system has been proposed called quick SOFA (qSOFA). qSOFA can be defined by the following conditions:

1- The respiratory rate is 22 breath per minutes or more.
2- Systolic blood pressure is equal or less than 100 mmHg
3- Altered mental status.

The 2016 task force defines septic shock as "a subset of sepsis in which underlying circulatory and cellular metabolism abnormalities are profound enough to substantially increase mortality." Also, in the consensus, two variables are agreed as diagnostic of septic shock, hypotension with MAP is less than 65 mmHg that require vasopressor and a lactate level more than 2mmol/L. Lactate level is used as an indicator for mortality rate. There is a close association between lactate levels and mortality. Figure 4 shows the diagram for diagnosing sepsis and septic shock (Singer et al., 2016) and defining observations and factors.

- Sepsis is defined as life-threatening organ dysfunction caused by a dysregulated host response to infection.
- Organ dysfunction can be identified as an acute change in total SOFA score ≥2 points consequent to the infection.
  - The baseline SOFA score can be assumed to be zero in patients not known to have preexisting organ dysfunction.
  - A SOFA score ≥2 reflects an overall mortality risk of approximately 10% in a general hospital population with suspected infection. Even patients presenting with modest dysfunction can deteriorate further, emphasizing the seriousness of this condition and the need for prompt and appropriate intervention, if not already being instituted.
- In lay terms, sepsis is a life-threatening condition that arises when the body's response to an infection injures its own tissues and organs.
- Patients with suspected infection who are likely to have a prolonged ICU stay or to die in the hospital can be promptly identified at the bedside with qSOFA, ie, alteration in mental status, systolic blood pressure ≤100 mm Hg, or respiratory rate ≥22/min.
- Septic shock is a subset of sepsis in which underlying circulatory and cellular/metabolic abnormalities are profound enough to substantially increase mortality.
- Patients with septic shock can be identified with a clinical construct of sepsis with persisting hypotension requiring vasopressors to maintain MAP ≥65 mm Hg and having a serum lactate level >2 mmol/L (18 mg/dL) despite adequate volume resuscitation. With these criteria, hospital mortality is in excess of 40%.

Table 3 New Sepsis definition and measurement (Singer et al., 2016)

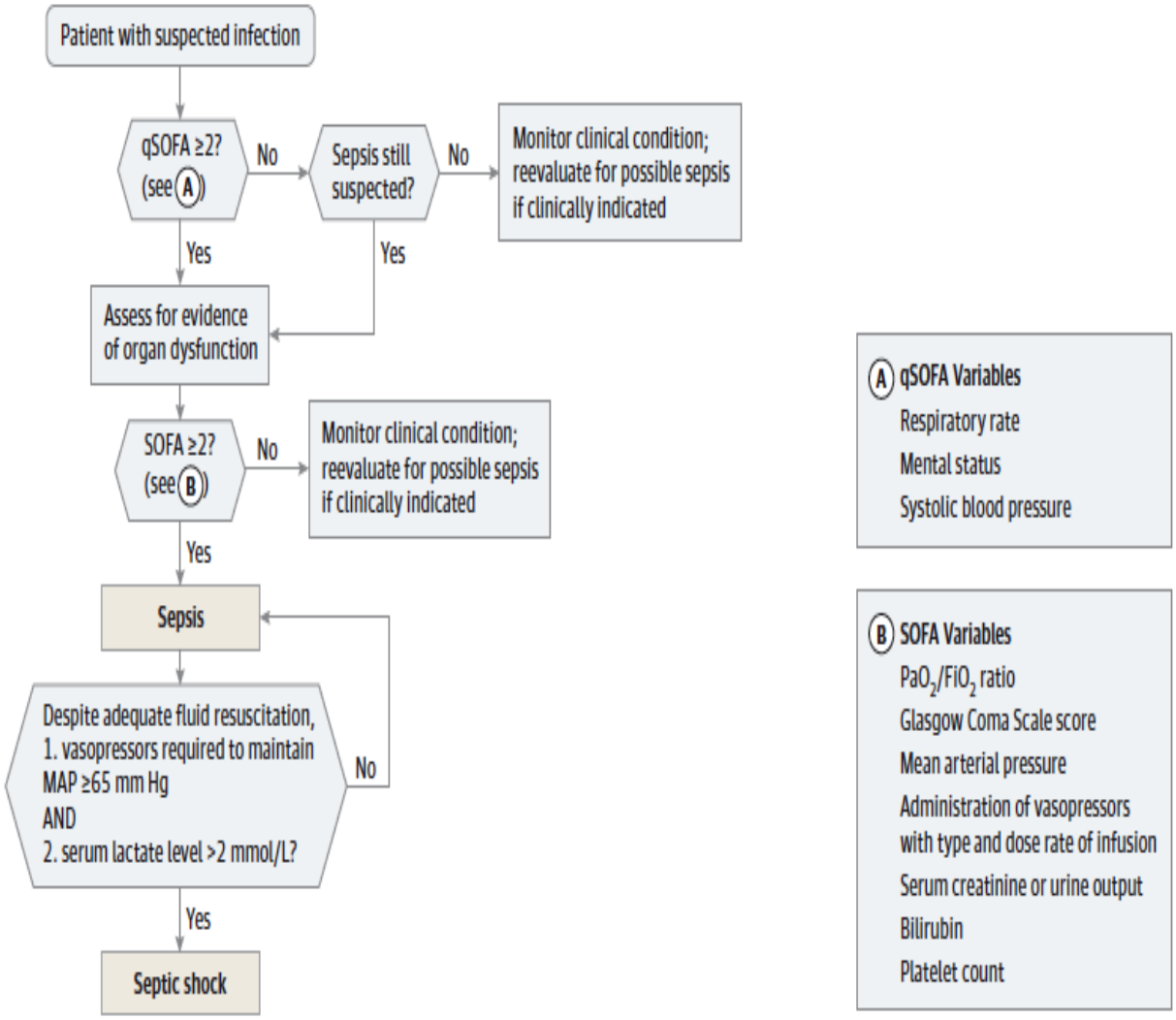

Figure 6 Diagram for diagnosing Sepsis and Septic Shock (Singer et al., 2016)

Compensatory Anti-inflammatory Response Syndrome:

In 1997, (Bone et al.) derived two new terms, compensatory anti-inflammatory response syndrome (CARS) and mixed antagonists response syndrome (MARS) reflecting new mechanisms involved in the immune response. When an insult occurs in the body, the immune system releases pro-inflammatory cytokines. The pro-inflammatory cytokines initiate the cellular defense. Moreover, the immune system will produce anti-inflammatory cytokines that suppress the action and production of pro-inflammatory cytokines to control the immune response and avoid over expression. Normally, the production of cytokines is regulated by inflammatory mediators. If the balance between pro-inflammatory cytokines and anti-inflammatory cytokines is not maintained, this will result in massive inflammatory reaction (SIRS) or compensatory anti-inflammatory reaction (CARS). CARS is defined when human leukocytes antigen-DR (HLA-DR) receptors on monocytes is less than 30% and the monocytes cannot secrete inflammatory cytokines, MARS is defined as SIRS characteristics in patients diagnosed with CARS. Figure 7 demonstrate CARS, SIRS and the clinical sequences (CHAOS) (Bone et al., 1997, Han et al., 2018). If the CARS is predominating SIRS, there will be immune system suppression phase that may lead to secondary infection. For example, the patients could acquire a secondary infection in the form of a nosocomial infection, caused by catheter-associated urinary tract infections, ventilator-associated pneumonia or central line-associated blood stream infections (Chun et al., 2017, P.49).

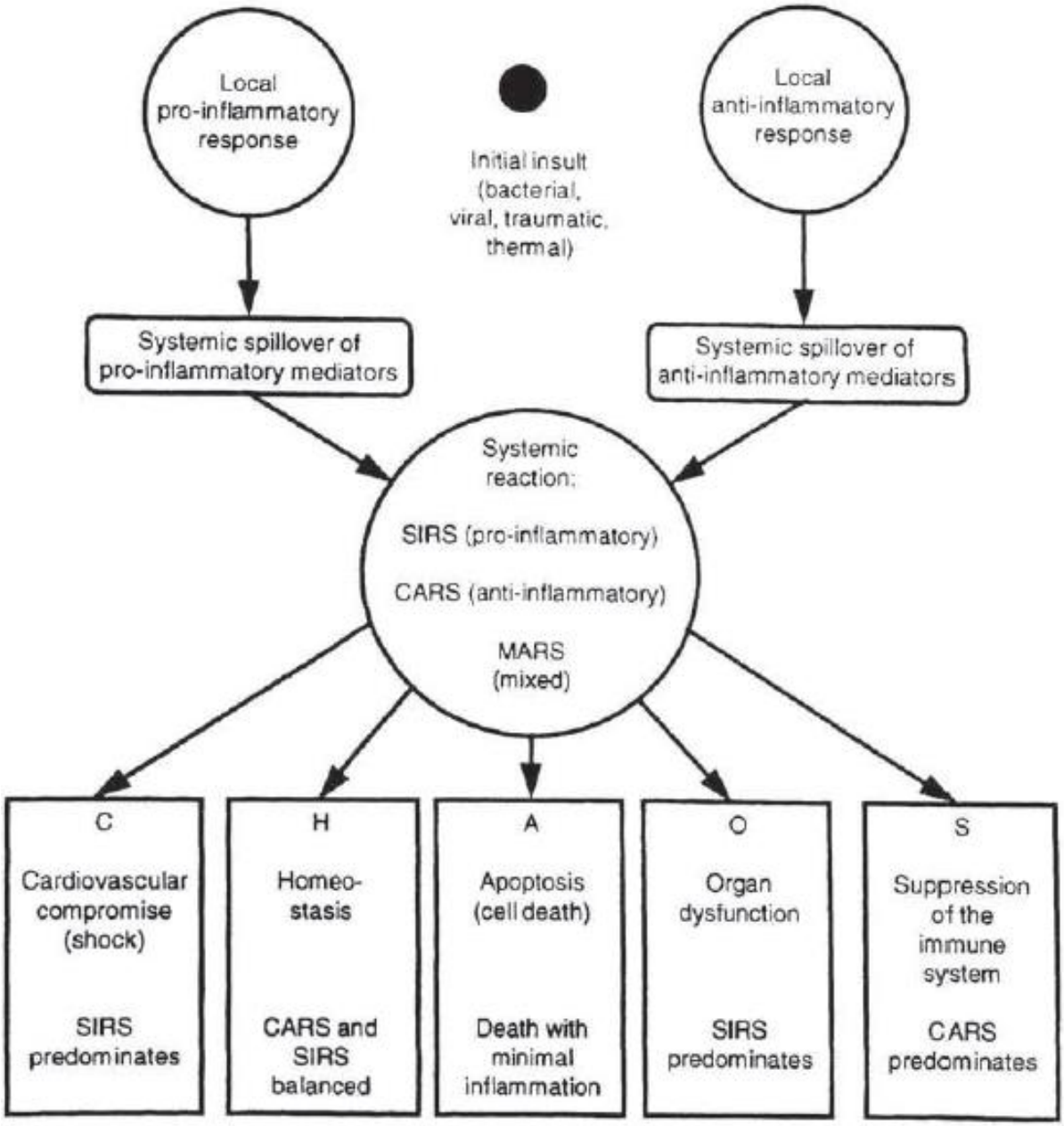

Figure 7 SIRS, CARS and CHAOS (Bone et al., 1997)

1.4 Pathophysiology:

In order to develop the concept for treating sepsis, the cause and source of SIRS will be discussed in detail in this section. The cause of sepsis is not infection itself, but the immune response of the body to an infection. It is an effect on autoimmune condition. Once the bacteria molecular pattern, which have pathogen-associated molecular pattern (PAMP), is detected, a local response is initiated which will propagate through the whole system through circulation of immune cells and mediators. The host response to an insult is not only is not confined to the local response, it is a complex process that involves participation of different cells, such as white blood and endothelial cells and a series of mediators that lead to impact on distal tissues and organs. The local production of inflammatory cytokines initiates further generation of cytokines that leads to organ dysfunction. This phenomenon called "cytokine storm", is "likely responsible for the diverse, local and remote, signs associated with infection" (Chousterman et al., 2017). As mentioned before, the cause of sepsis could be bacteria, virus, fungi and parasites. In USA, the number of gram-positive bacteria that cause sepsis has increased to reach a level equal to half of the recorded cases with gram-negative bacteria. The increased number of gram-positive bacteria cases could be due to the increase in the number of invasive interventions and associated hospital acquired bacteria (Staitieh and Martin, 2017, P.37, Martin et al., 2003).

The most common cause of sepsis is both gram-positive and gram-negative bacteria. Both will be discussed in detail, together with the way the immune system deals with them and the signaling pathways that lead to the inflammatory response.

1.4.1 Signal pathway:

Robertson and Coopersmith (2006) states that "while numerous differences exist in the pathophysiology between sepsis and non-infectious inflammation, many of the mechanisms underlying patients with SIRS are similar". SIRS is not a directly related to the insult, whether it is infection or non-infection origin, it is the immune response to that insult that can escalate in an uncontrolled manner (Robertson and Coopersmith, 2006). As previously mentioned, the main causes of sepsis are gram-positive and gram-negative bacteria. Figure 8 demonstrate the signal pathway for gram-positive and gram-negative bacteria (Bochud and Calandra, 2003).

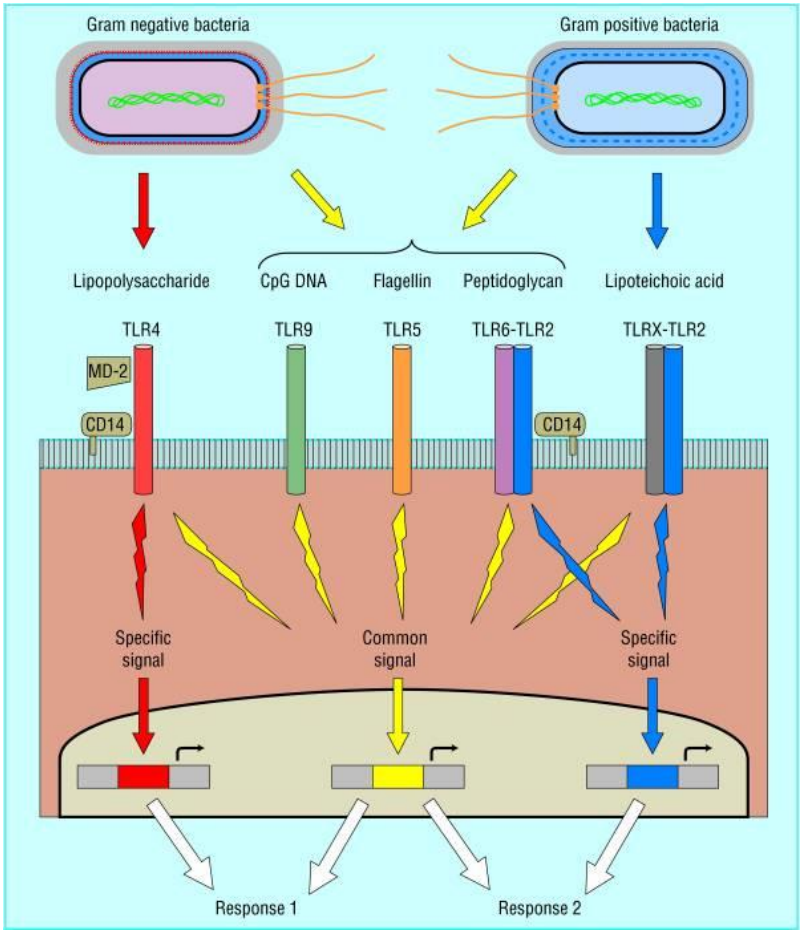

Figure 8 Gram-negative and gram-positive bacteria signal path (Bochud and Calandra, 2003)

Once the invaders, such as bacteria, enter the body, the innate immune system is the first line of response. The innate immune system is a non-specific system that is able to identify invaders such as bacteria and virus. The bacteria have PAMPs that are recognize by Pattern recognition receptors (PRRs) located on the innate immune cells surface, such as toll-like receptors (TLRs). As a result, the production of proinflammatory cytokines will be initiated through the activation of various signal pathways. (Mogensen, 2009, Chousterman et al., 2017). These key processes are detailed in the following section.

1.4.2 Immune response:

The activation of the innate immune system through PRRs will initiate the inflammatory response, which is important for the body to eliminate the insult. One key weapon in the body's armoury in the fight against infection is the ability, through several mechanisms to raise body temperature. This has the effect of reducing the ability of microorganisms to multiply and thrive. Increasing the body temperature requires more energy, which in turn requires more oxygen. Consequently, heart rate is raised to meet the higher oxygen demand. As the cells use more oxygen, they produce more carbon-dioxide as waste, thus the respiratory rate will be increased, known as tachypnea. Also, vascular changes are initiated as more blood and leukocytes are directed to the inflammation site. The inflammatory response of the innate immune system is a very complex and sophisticated network with many feedback controls. The immune system cannot be considered as a linear response system, but it is an interaction of pleiotropic and redundant systems. The inflammatory response system includes both cellular and plasma cascades. Inflammatory mediators are released during the inflammatory response that include pro-inflammatory cytokines, IL-6, IL-8, IL-1 and TNF-α, and anti-inflammatory cytokines, IL-4 and IL-

10, complement and coagulation cascades, which will activate until the insult is resolved (Censoplano et al., 2014, Castellheim et al., 2009).

Cellular and humoral components:

The activated immune cells, macrophages for example, release cytokines and chemokines. The pro-inflammatory cytokines have an effect on other immune cells to produce further inflammatory mediators. The pro-inflammatory cytokines lead to the migration of neutrophils to the infection site by expressing the adhesion molecules on the endothelial surface (Schulte et al., 2013a). The neutrophils migrate to the site of the infection in order to eliminate the threat. Neutrophil migration consists of five stages: tethering, rolling, adhesion, crawling and transmigrating (Kolaczkowska and Kubes, 2013).

Tethering and rolling stages:

Activated endothelial cells have two selectins presented on their surface, P-selectin and E-selectin. These selectins bind with the P-selectin glycosylated ligands 1 (PSGL 1) that are present on neutrophils. The binding will lead to capture of the circulating neutrophils. Also, the lymphocytes function-associated antigen 1 (LFA-1), which is present on the neutrophils, binds with intercellular adhesion molecules (ICAM), ICAM-1 and ICAM-2 that are expressed on the endothelial cells to slow the flow of neutrophils.

Adhesion stage:

Chemokines, located on the endothelial wall, and the neutrophils bind. The result of the binding activates the neutrophils. Neutrophil activation is needed for adhesion to the endothelial walls. Also, the LFA-1 and MAC-1, integrins present on the neutrophils, go through conformational changes in order to bind with ICAM-1 and ICAM-2 for firm adhesion.

Crawling stage:

Following binding, the neutrophils progress to the next stage, crawling. The crawling stage prepares the neutrophils to migrate through endothelial cell-cell junctions. The neutrophils crawl perpendicular to the blood flow and rely on the interaction between MAC-1 and ICAM-1. In order for the neutrophils to crawl along the endothelial surface, the neutrophils break bonds and make new bonds. This provokes forward movement of neutrophils on the endothelial surface.

Neutrophil transmigrating:

There are two pathways for neutrophil transmigration, categorized as paracellular and transcellular pathways. The primary pathway is paracellular in focus. In paracellular, it is required to release junctional intercellular protein bonds, especially these made by the vascular endothelial cadherin, which functions as gatekeeper for the endothelial cells. In the transcellular pathway, endothelial cells form a “transmigratory cup” similar to microvilli projections. These projections rise to cover the neutrophils and form “domes”. Figure 9 and figure 10 demonstrate neutrophil extravasation stages, both paracellular

and transcellular transmigration (Kolaczkowska and Kubes, 2013, Langer and Chavakis, 2009).

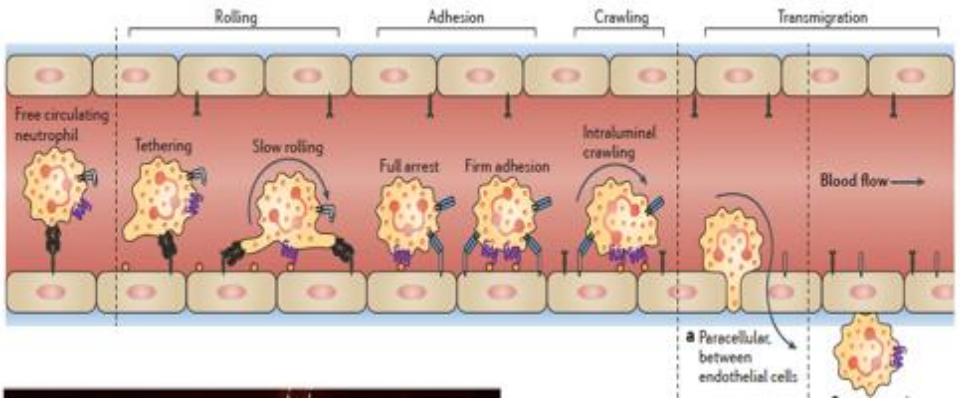

Figure 9 Neutrophils extravasation (Kolaczkowska and Kubes, 2013)

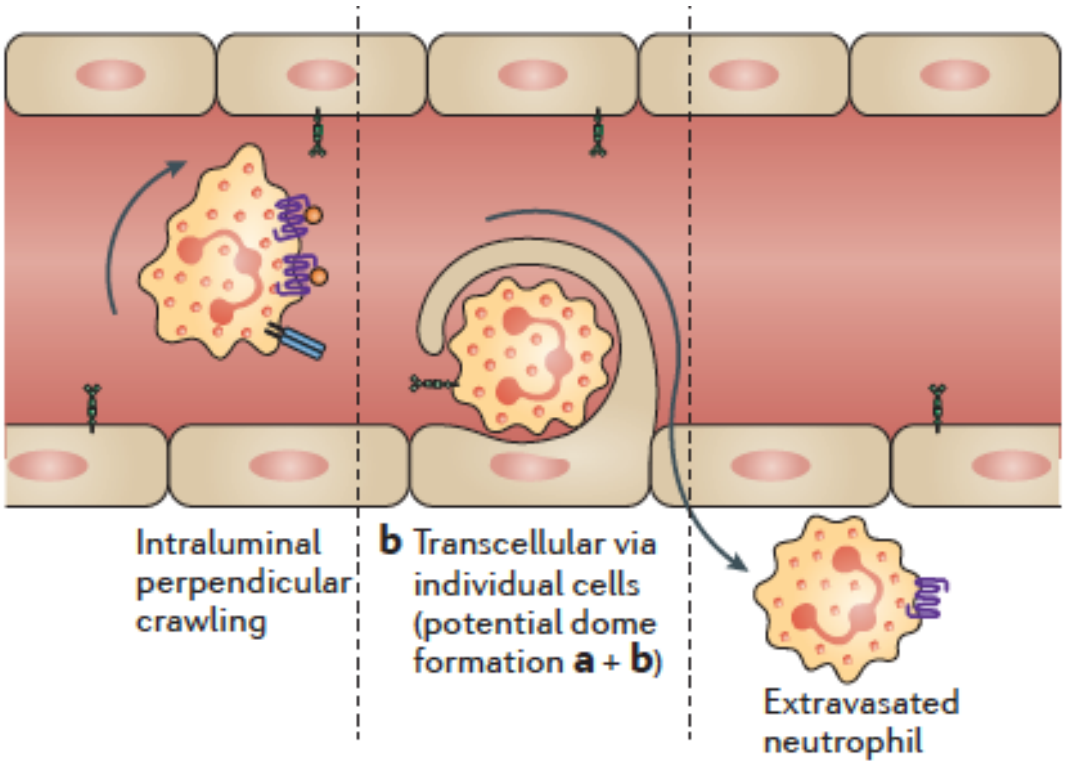

Figure 10 Transcellular neutrophils migration (Kolaczkowska and Kubes, 2013)

After neutrophil extravasation and reaching the site of infection, they will start to eliminate the pathogen through degranulation. This process, unfortunately, also results in tissue "collateral damage". There are three granules secreted by the neutrophils to destroy pathogens, azurophilic granules, specific granules and gelatinase granules. Azurophilic granules hold anti-microbial enzymes and myeloperoxidase (MPO) that is responsible for a distributive oxidative burst. Specific granules also contain anti-microbial enzymes but no MPO. Gelatinase granules have fewer anti-microbial enzymes compared to the other two, again without MPO. The neutrophils start the process of degranulation at the infection site results in the infusion of anti-microbial enzymes in the phagosome or the plasma membrane. The neutrophils then initiate an oxidative burst, which result in reactive oxygen species (ROS), through NADPH oxidase to eliminate the pathogen. The ROS lead to the production of highly reactive free radicals. The ROS is initiated when the NADPH oxidase reduce the oxygen molecule to superoxide; the superoxide forms hydrogen peroxide through rapid dismutation. MPO reacts with hydrogen peroxide, producing reactive species such as hypohalous acids. Figure 11 illustrates the chemical reactions that lead to the generation of ROS (Amulic et al., 2012, Szasz et al., 2007).

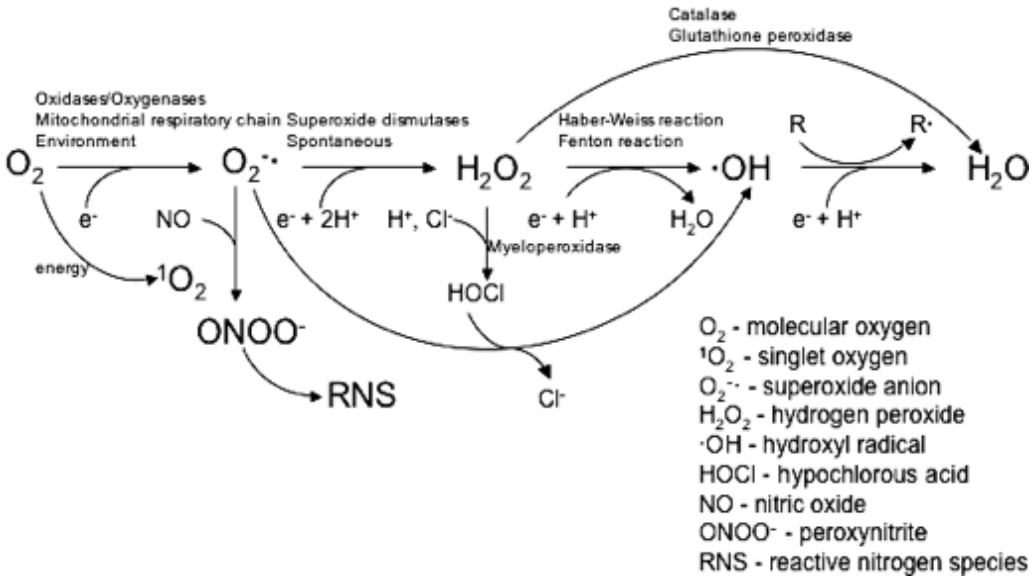

Figure 11 ROS reactions (Szasz et al., 2007)

The free radicals are removed by antioxidants in order to maintain the balance and prevent oxidative stress. The antioxidants can be categorized into two groups: enzyme antioxidants and non-enzyme antioxidants. The antioxidant enzymes include superoxide dismutase, catalase, glutathione peroxidase, thioredoxin, peroxiredoxin and glutathione transferase. The non-enzyme antioxidants are vitamin C, vitamin E, glutathione and carotenoids. Oxidative stress occur due to an imbalance between the free radicals and antioxidants (Birben et al., 2012). Neutrophils are killer cells that cannot distinguish between pathogen and host tissue. So, the immune system controls the neutrophils in order to minimize damage to host cells a process called “resolution of inflammation”, which is defined by Amulic et al. (2012) as “an active process that limits further leukocyte infiltration and removes apoptotic cells from inflamed sites”. Once the neutrophils finish their task, they die due to self-programmed death, which is known as

apoptosis. Macrophages digest the apoptosed neutrophils and release anti-inflammatory cytokines (Amulic et al., 2012).

Plasma components:

There are four plasma enzyme systems that are activated during the inflammatory response, the complement system, coagulation system, fibrinolytic system and kallikrein-kinin system. The first two systems are the main plasma based systems. These are activated by the same stimulus and are interrelated through communication (Castellheim et al., 2009).

Complement system:

The complement system is one of the components of the innate immune system that is activated when an organism invades the body. There are three pathways that activate the complement system, the classical pathway, the alternative pathway and the lectin pathway. All three pathways lead to the elimination of the pathogen. The activated complement system generates chemoattractants in order to attract the phagocytes to the invader location, to help the phagocytes to identify the pathogen in order to initiate phagocytosis and eliminate the pathogen directly by the formation of the membrane attack complex (MAC) that enters the bacteria membrane (Berends et al., 2014). The classical pathway is activated either by the interaction of immune complexes, such as IgG and IgM, with the C1 complex or by pentraxins, for example C-reactive protein, that detect the pathogens. The lectin pathway is initiated when carbohydrates located on the microorganisms binds with the collectin group that include mannose-binding lectin

(MBL) and ficolins. The alternative pathway is activated by carbohydrates, protein and lipids located on the pathogen. The result of the activation of the three pathways eventually leads to the generation of the C3a, C3b, C5a and MAC (C5b-9). The C3a and C5a are called anaphylatoxins and they guide the phagocytes to the pathogen's location. In this regard, these proteins are considered to be chemoattractant. C3a and C5a are involved in the release of cytokines. The functions of C3b is to amplify the activation of the complement system and phagocytosis. MAC causes pathogen death by disrupting the pathogen membrane leading to cell lysis (Sarma and Ward, 2011). Figure 12 illustrate the pathways of complement activation.

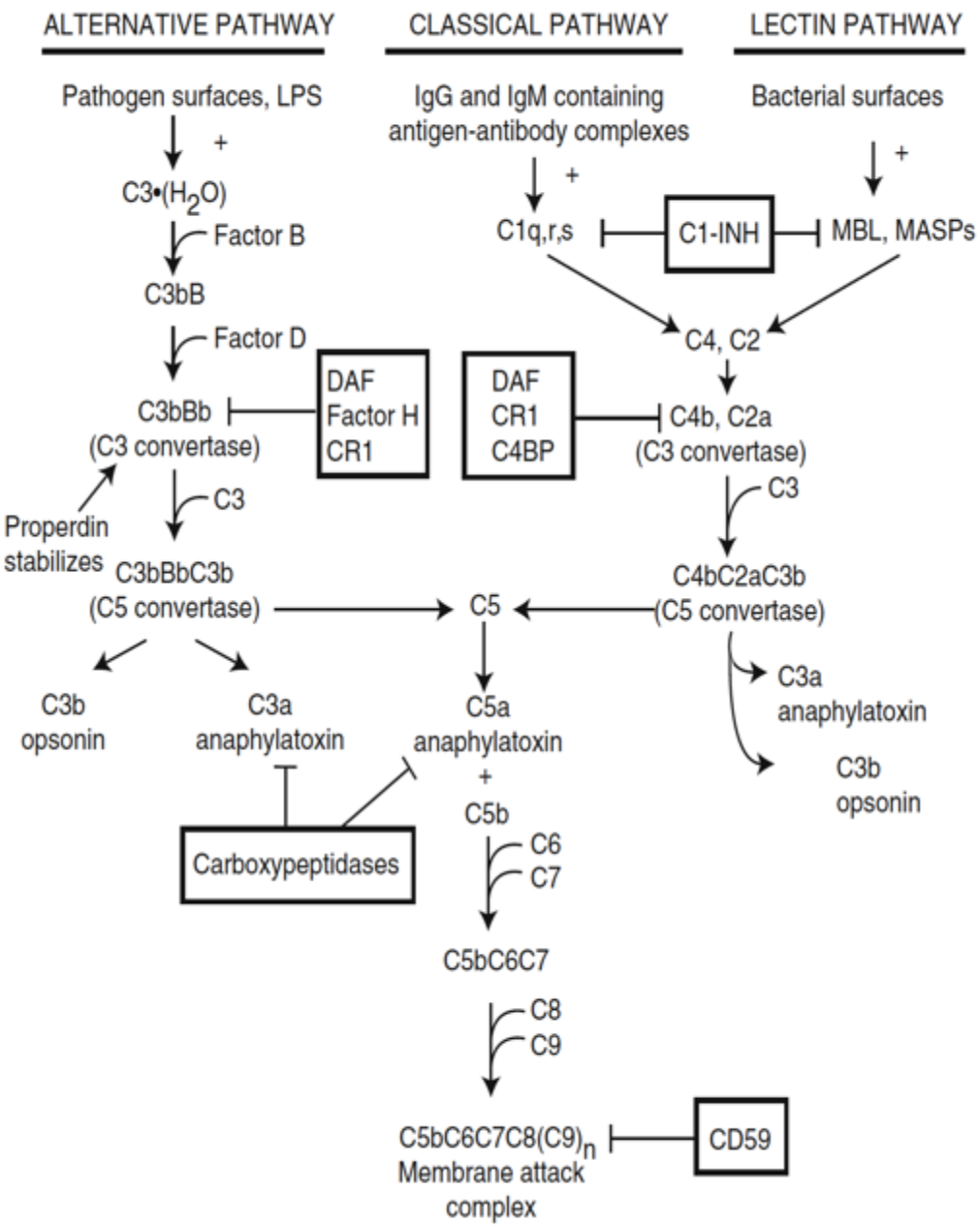

Figure 12 Complement pathways activation (Sarma and Ward, 2011)

Coagulation system:

There are two pathways for initiating coagulation cascades, intrinsic and extrinsic, both of which lead to thrombin activation. The thrombin will cleave fibrinogen to fibrin. When tissue is damaged due to direct trauma, the intrinsic pathway is initiate by Hageman factor (Factor XII) that binds with collagen, basement membrane or activated platelets. The binding will lead to the activation of cascades that eventually form thrombin. Tissue factor production activates the extrinsic pathway. During the inflammatory response, pro-inflammatory cytokines will trigger the endothelial cells and monocytes to initiate the production of tissue factor. The tissue factor activates factor VII and binds with it, the binding complex leads to thrombin activation by initiating the cascade. The activated coagulation system is regulated by anti-coagulants, which in general terms have three components. The first component is anti-thrombin that leads to deactivation of thrombin by binding to it. The second component is protein C, triggered by the thrombin-thrombomodulin complex, which is located on the endothelial cells. Protein C acts as anti-coagulant by inhibiting the activation of factor Va and factor VII. The third component is tissue factor pathway inhibitor (TFPI). TFPI deactivates the tissue factor in order to minimize the clotting cascade. TFPI binds with tissue factor and factor VIIa. TFPI deactivates the extrinsic pathway. Figure 13 demonstrates the two pathways of coagulation system activation (Sherwood and Toliver-Kinsky, 2004).

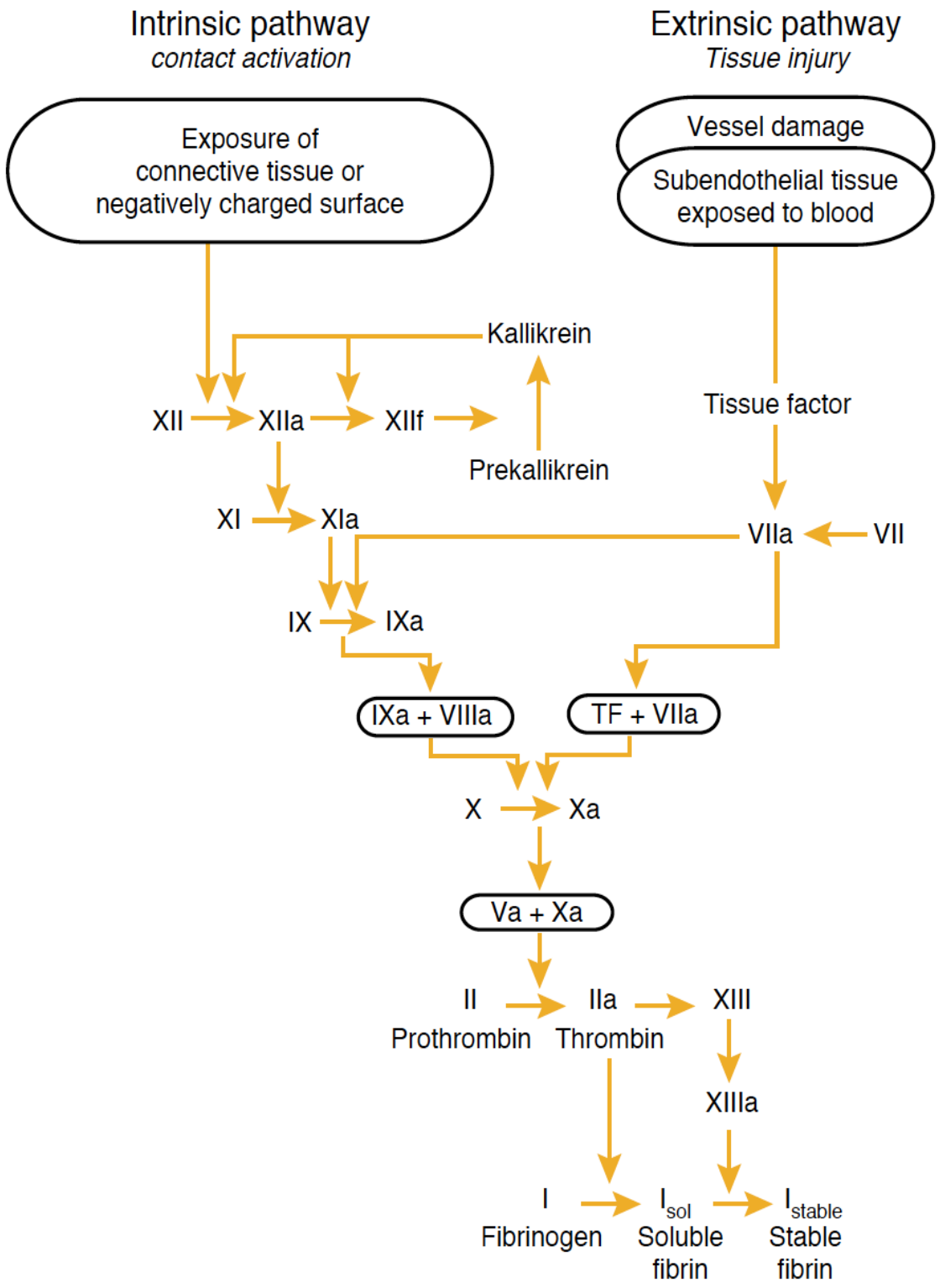

Figure 13 Coagulation system activation pathways (Sherwood and Toliver-Kinsky, 2004)

Normally, the coagulation cascades are regulated. However, should the regulation become disrupted, this will lead to disseminated intravascular coagulation (DIC). The initiation of DIC activates thrombin which results in the formation of fibrin. As a result, the consumption of coagulation factors increase which results in hypocoagulation. Moreover, the accumulation of fibrin in the microvascular system may result in organ dysfunction (Rittirsch et al., 2008).

1.4.3 Cytokines:

Dembic (2015, P. 1) has defined cytokines as "cell-to-cell messengers … structurally and genetically, cytokines are defined as polypeptides, proteins, and glycoproteins … The physiological role of cytokines, in general, is in tissue homeostasis and cellular activation, relocation and differentiation … regulating the immune system's response to trauma, inflammation, and infection". Cytokines molecular weights are less than 40 KDa. In a healthy person, the cytokines levels are very low (Netea et al., 2003, Schulte et al., 2013a). Cytokines act in three ways, by affecting the cells that produced them (autocrine), affecting neighboring cells (paracrine), and affecting cells at a distance (endocrine). Different cells are associated with the production of various cytokines. For example, macrophages produce TNF-α and IL-1. Whereas, T-cell produce IL-13 and IL-4 (Zhang and An, 2007, Opal and DePalo, 2000). Once the immune system detects an invader the host response is initiated. Cytokines are important factors in fighting pathogens through organizing the anti-microbial process. Cytokines recruit leukocytes to the site of the infection, amplifying the phagocytes anti-microbe activity, and initiating a defensive fever (Cavaillon et al., 2003). Cytokines can be classified into pro-inflammatory and anti-inflammatory variants. Pro-inflammatory cytokines such as IL-1, TNF-α and IL-8, known as chemokines, are responsible for the initiation and propagation of the inflammatory response. Pro-inflammatory cytokines especially IL-1 and TNF-α activate the inflammatory mediator cascade by binding to endothelial cells. Anti-inflammatory cytokines, such as IL-10 and IL-4, are produced for the purpose of reducing the inflammatory response. Anti-inflammatory cytokines work by suppressing

the secretion of pro-inflammatory cytokines, in addition, the anti-inflammatory cytokines have the ability to reduce the damage caused by inflammatory mediators (Dinarello, 2001, Opal and DePalo, 2000). In sepsis, if the host response cannot eliminate the pathogen, a "cytokine storm" will occur. At the first stage of sepsis, this cytokines storm is produced in order to initiate the inflammatory response, but the mass production of cytokines in sepsis in this way can lead to tissue injury and eventually failure of organs (Chaudhry et al., 2013).

Tumor Necrosis Factor α (TNF-α):

TNF-α is a pro-inflammatory cytokine with a molecular weight of 17 KDa. Immune cells, such as macrophages and non-immune cells, such as fibroblasts produce TNF-α. Macrophages produce TNF-α in 30 minutes after the detection of the pathogen and peak concentration can be reached in 60-90 minutes. TNF-α functions as the initiator of inflammatory mediators and activator of immune cells. TNF-α belongs to a group of pyrogenic cytokines and once it is produced it will promote a fever. The released TNF-α binds to progenitor cells leads to amplification of macrophage production, activating and differentiating macrophages, and increasing macrophage survival. Also, TNF-α targets endothelial cells resulting in enhancement of adhesion molecule expression. Neutrophil integrin adhesive molecules are increased by TNF-α causing extravasation of neutrophils at the site of infection. TNF-α binds to the macrophages in order to produce other pro-inflammatory cytokines such as IL-6 and IL-8, lipid mediators and reactive oxygen species, which cause organ dysfunction in sepsis. The TNF-α is known as "the master regulator" since it activates the cytokine cascade. It has been found that injection

of TNF-α in animal models results in symptoms similar to septic shock. Also, by injecting human with recombinant TNF-α cause SIRS (Schulte et al., 2013a). From this work and that of other researchers, the crucial role of TNF-α in the development of SIRS is clear.

Interleukin-1 (IL-1):

IL-1 is used to describe a family of cytokine proteins that include IL-1α and IL-1β. IL-1 is a pro-inflammatory cytokine. The main immune cell that produce IL-1 is the activated macrophages. As both TNF-α and IL-1 is secreted in 30 minutes following the initial insult and the peak is reached in 60-90 minutes. IL-1, similar to TNF-α, is one of the pyrogenic cytokines that cause fever. IL-1 has an effect on endothelial cells, macrophages and neutrophils. In addition to TNF-α, IL-1 acts on macrophages to release other pro-inflammatory cytokines such as IL-6, lipid mediators and reactive oxygen spices. Moreover, both cytokines are responsible for activating coagulation. IL-1 and TNF-α are synergetic since both of them can increase vascular permeability, pulmonary edema and hemorrhage (Schulte et al., 2013a). Administrating of IL-1 into humans in dosage of 1-10 ng/kg has resulted in fever, sleepiness, anorexia, headache, arthralgia and myalgia. However, higher dose of IL-1, 100ng/kg or more, has induced hypotension. TNF-α injection shows the same observations of IL-1, in addition to initiating the coagulation cascade (Dinarello, 1997).

Interleukin-6 (IL-6):

IL-6 is glycoprotein with molecular weight of 21 KDa. IL-6 belongs to the pro-inflammatory cytokine family and it secreted by a number of cells that include macrophages, endothelial cells, lymphocytes, smooth muscles cells and fibroblasts. IL-6 is responsible for activating T and B lymphocytes, activating the coagulation cascade and modulating hematopoiesis. In addition, IL-6 functions as a fever inducer, leukocytosis, and is involved in the production of hepatic proteins that include c-reactive protein, complement component, fibrinogen and ferritin. IL-6 elevated in the plasma is related to medical conditions that include sepsis and major surgeries. As a result, it is used as marker for evaluating sepsis, septic shock, multiple organ failure and mortality. (Schulte et al., 2013a). It has been found that after LPS injection into healthy subjects, IL-6 increases and reaches a peaks concentration in 3-4 hours (Kemna et al., 2005).

Interleukin-8 (IL-8):

IL-8 is a chemokine released by macrophages, endothelial and epithelial cells. IL-8 functions by attracting the neutrophils to the site of infection, thus it is known as a chemoattractant (Chaudhry et al., 2013). In humans, injecting IL-8 results in "time-dependent perivascular neutrophil influx". In sepsis patients, IL-8 levels in the plasma is high and this high concentration of IL-8 is correlated with mortality (Blackwell and Christman, 1996).

Interleukin-10 (IL-10):

IL-10 is a homodimeric anti-inflammatory cytokine with molecular weight of 35 KDa. It is released by many immune cells such as monocytes, macrophages, B and T lymphocytes. IL-10 inhibits the secretion of the IL-1, IL-6 and TNF-α (Schulte et al., 2013a). In mice, given IL-10 before injecting endotoxin has resulted in reduced mortality associated with endotoxin and also leads to a reduction in TNF-α. Additionally, by suppressing IL-10 production in mice, an increase in both endotoxin-induced mortality rate and the TNF-α level in the plasma have been observed. In sepsis patients, IL-10 plasma levels are high. IL-10 level in septic shock patient is higher than in sepsis patients (Blackwell and Christman, 1996). And in this way, it has been used as marker of the condition.

Interleukin-4 (IL-4):

IL-4 is an anti-inflammatory cytokine that is responsible for controlling the proliferation, differentiation and apoptosis of different immune cells such as T lymphocytes. IL-4 is released by the T_H2 lymphocytes and it functions in the production of anti-inflammatory cytokines in addition to the suppression of pro-inflammatory cytokines that are released by monocytes. IL-4 increases survival when high dosage of LPS injected in animals. IL-4 levels in plasma do not differ between survival and non-survival sepsis patients (Schulte et al., 2013a).

1.5 Chapter summary:

Cytokines are classified into either pro-inflammatory or anti-inflammatory varieties. They are produced during an inflammatory response and they are regulated by the immune system. However, a disturbance in the regulation of cytokine production results in the amplification of the inflammatory response and the activation of various, and interconnected, cellular and humoral pathways. These pathways, that include innate immune cells (WBCs) and plasma pathways (complement and coagulation systems) may lead to sepsis and its complications such as MODs and ultimately death.

Chapter 2:

Sepsis Pharmacological and Technological Treatments and Clinical Trials

2 Sepsis Pharmacological and Technological Treatments and Clinical Trials:

2.1 Introduction:

As mentioned in chapter one, sepsis is a life-threatening disease caused by a systemic response which leads to organ dysfunction and may ultimately cause death. The imbalance between the pro-inflammatory and anti-inflammatory cytokines leads the immune system to enter hyperinflammatory status. One million patients are diagnosed with sepsis each year in USA with mortality rate between 28% to 50%. However, there are currently no FDA approved pharmacological treatments for sepsis (Petersen et al., 2018). Due to the complexity of the immune system interactions that occur during the inflammatory response, treatments that target specific inflammatory mediators fail to demonstrate any real benefit. This chapter will focus on the current treatments of sepsis and associated clinical trials. Also, extracorporeal blood purification systems will be discussed and their role in targeting inflammatory mediators.

2.2 Sepsis pharmacological treatments:

Currently, the treatment for sepsis is non-specific, and it includes giving oxygen to the patient, IV fluids, antibiotics, vasopressors, inotropes and organ support devices. The aim of the current treatments for sepsis is eliminating the pathogen, preventing sepsis complications and progression, in avoiding a maladaptive septic state. Also, there are efforts introduced in the healthcare system in order to diagnose sepsis as soon as possible in order to start treatment early. These methods include diagnosis criteria, rapid response teams that are responsible for detecting sepsis and initiating treatment according to the surviving sepsis campaign (SSC). In spite of all these factors, the mortality rate among sepsis patients remains high. The international campaign for sepsis guidelines cannot provide an explanation for the high death rate in sepsis patients (Berry et al., 2017).

2.2.1 Current Treatments:

Sepsis treatment has two categories: antibiotic treatment and supporting treatment (Polat et al., 2017).

2.2.1.1 Antibiotic Treatments:

According to the SSC, once sepsis or septic shock is diagnosed, antibiotics must be given in the first hour. The antibiotics are given empirically and cover a broad-spectrum of pathogens. As the laboratory tests confirm the specific pathogen involved, antibiotics, and one or more antimicrobial are selected to target the identified microorganism. However, one of the concerns that rise with the use of antibiotics is the increase in

bacterial resistance. This issue needs to be resolve by developing new drugs that overcome the antibiotics resistance (Cohen et al., 2015, Berry et al., 2017).

In UK, the SSC bundle was used in only in 14% of the sepsis patients, so, "Sepsis Six" was developed. The "sepsis six" consists of three therapeutic and three diagnostic tasks that should be employed in the first hours of diagnosing sepsis. The three therapeutic tasks are:

1- Oxygen delivery.
2- Administration of wide spectrum of antibiotics intravenously.
3- Initiation of intravenous fluid.

The three diagnostic tasks are:

1- Take blood samples.
2- Measurement of blood count and lactate level.
3- Measurement of urine output (Daniels et al., 2011).

2.2.1.2 Supporting treatment:

Septic shock is defined as when the blood is unable to provide cells with sufficient oxygen and nutrition, and this results in organ and cellular dysfunction. Haemodynamic treatment restores normal blood circulation in tissue to deliver nutrition and oxygen to tissues. The treatment is achieved by giving fluids and vasopressors (Ruokonen et al., 2002).

Fluids:

In sepsis-3, the task force agreed that hypotension that occurs in sepsis patients is defined as MAP<65 mmHg. As a result, patients are administered with fluids with a volume of up to several litres in order to increase the MAP to the range of 80-85 mmHg and subsequently improve urine output (Singer et al., 2016, Gotts and Matthay, 2016).

Vasopressors:

In sepsis-3, septic shock is defined as sepsis with persisting hypotension and a lactate level of more than 2 mmol/L despite sufficient fluids. As a result, vasopressors such as norepinephrine and epinephrine is administered to increase MAP to more than 65 mmHg (Berry et al., 2017).

Other treatments:

One of the treatments for sepsis patients is providing efficient nutrition. Glutamine involve in the production of proteins, an energy fuel for various cells such gastrointestinal cells and immune cells. Glutamine is produced and stored in muscles. In sepsis, the demand for glutamine by organs and cells is significantly increased, often causing glutamine depletion. As a result, the lack of glutamine could lead to a decrease in the function of cells in the immune system and could reduce the integrity of the gut barrier, consequently, the bacteria translocate into the circulation. Thus, glutamine treatment can regulate the immune system in sepsis patients (Stehle and Kuhn, 2015, D'Souza and Powell-Tuck, 2004, Polat et al., 2017). Additionally, organ support devices such as mechanical ventilation and haemodialysis are used in sepsis patients with kidney and respiratory dysfunction (Polat et al., 2017).

2.3 Clinical Trials:

In 1976, first clinical trial that target treating sepsis using a high dose of corticosteroid was published, since then more than 100 clinical trials for treating sepsis have been produced. The aim of these clinical trials are either selective or non-selective treatments (Marshall, 2014). Non-selective treatments include the use of corticosteroids to suppress inflammation and selective treatments, focused on the removal of pathogen products, endotoxins for example, or inflammatory mediators such as TNF-α and IL-1. Despite successful results in animals, these techniques have not translated into human clinical trials, and failed to significantly improve survival (Marshall, 2014, Xie et al., 2014). Some of the pharmacological clinical trials will be discussed in this section.

2.3.1 Recombinant Human IL-1 Receptor Antagonist (rhIL-1ra):

IL-1 is one of the pro-inflammatory cytokines released during the inflammatory response. The IL-1 receptor antagonist (IL-1ra), which is produced in humans, is released by the immune system during the inflammatory response and binds to the IL-1 receptors. Thus, it suppresses the IL-1 cellular signal, which is discussed in section 1.4.3. In animal experiments, for a complete block of haemodynamic and physiological activity is caused by the infusion of IL-1, the concentration of rhIL-1ra concentration should be higher by 100 to 10000 fold compared to the IL-1 concentration. (Fisher et al., 1994). Fisher et al. (1994) studied the effect of rhIL-1ra on decreasing the mortality rate in sepsis patients. The aim of the study was to compare the survival rate between the study group and placebo group. The total population included in this study was 893 patients. 298 patients received 1mg/kg of intravenous rhIL-1ra while the other group,

with a population of 293 patients, received 2 mg/kg of intravenous rhIL-1ra, and the remaining patients, 302, was the placebo group. All patients were followed up during the 28 days of the study or to death. The mortality rate among the placebo group was 34%, 1 mg/kg group was 31% and 2 mg/kg group was 29%. There was no statistically significant different in the survival rate between the groups. Another clinical trial to investigate the effect of rhIL-1ra on sever sepsis and septic shock patients conducted by Opal et al. (1997) included 906 patients, in which, only 696 patients had complete data, and the placebo group was 346 patients and the study group, which received rhIL-1ra, was 350 patients. At the 28 day endpoint, the mortality rate in placebo group was 35.7% while the study group was 33.6%. There was no significant difference in survival rate between the group. Both clinical trials failed to illustrate a reduction in mortality rate among sepsis patients for rhIL-1ra.

2.3.2 Anti-TNF:

As mentioned in section 1.4.3, TNF-α is a pro-inflammatory cytokine that is produced during the inflammatory response. Administration of TNF-α intravenously into human subjects demonstrate sepsis like symptoms such as hypotension and clotting cascade activation. Abraham et al. (1995) investigated the effect of administration of TNF-α MAb, which is anti-TNF-α, in a randomized, controlled, double-blind study in different centers with a sample size of 994 patients. The patients were divided into three groups', placebo group, study group whom received 7.5 mg/kg of TNF-α Mab and the second study group whom received 15 mg/kg of TNF-α MAb. The mortality rate at 28-day point among the placebo patients was 33.1%, in 7.5 mg/kg patients was 29.5% and in the

15 mg/kg group was 31.3%. Overall, there was no statistically significant difference in mortality rate among the groups. Another clinical conducted by Abraham et al. (1998) to study the effect of TNF-α MAb in septic shock patients. The clinical trial was a randomized, double-blind, placebo-control in different centers in USA and Canada with a population of 1879 patients. The patients were assigned into two groups, the placebo group, 930 patients, and the study group, 949 patients. The study group received a single dose of 7.5 mg/kg of TNF-α MAb. The mortality rate at 28-day among the placebo patients was 42.8% and among the study group was 40.3%, which indicated there was no significant difference increase in survival rate between both groups. Also, Reinhart et al. (2001) have investigated the effect of anti-TNF-α in sepsis patients. The study was randomized, placebo-controlled, and double-blinded in 84 medical centers. The population of the patients involved was 944, where they divided into two groups. The placebo group consisted of 222 patients and 224 patients received anti-TNF-α. At the 28-day point, the mortality rate among the placebo group was 57.7% and the study group was 54%. Thus, the anti-TNF-α failed to demonstrate an increase in survival rate of the sepsis patients.

2.3.3 Activated Protein C

As discussed in section 1.4.2, during the inflammatory cascade, the cytokines lead to the activation of the coagulation cascade and suppression of fibrinolysis. Activated protein C (APC) is capable of initiating fibrinolysis and inhibiting the inflammation and coagulation cascades as illustrated in figure 14. In sepsis patients, the level of protein C is low and it has been correlated with an increase in mortality rate. The study of the effect of activated drotrecogin alfa (ADF) administration to severe sepsis patients was carried out by Bernard et al. (2001).

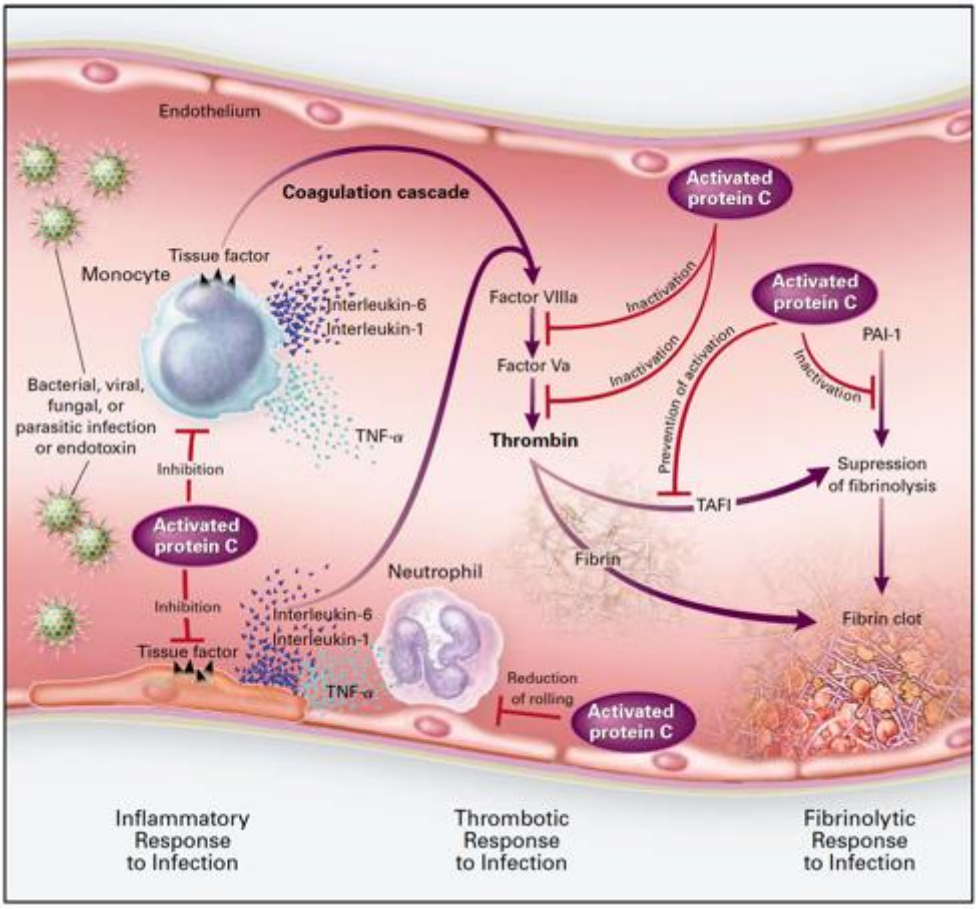

Figure 14 APC effect on the inflammatory cascade (Bernard et al., 2001)

The clinical trial included 1690 patients. There were 840 placebo patients and 850 ADF treated patients. The mortality rate at the 28-day end point was 30.8% and 24.7%, respectively. Also, the inflammatory response among ADF group was decreased since there was a significant reduction in IL-6 levels in this group. However, there was a high risk of bleeding associated with the use of ADF. Dhainaut et al. (2003) investigated the administration of ADF into severe sepsis patients in the Phase 3 Recombinant Human Activated Protein C Worldwide Evaluation in Sever Sepsis (PROWESS) trial. 1690 patients were included in this study and divided into two groups. The first group of 1271 patients with MODs (placebo 637 patients and 634 treated patients), and the second group was 419 with single organ dysfunction, placebo 203 patients and the treated 216 patients. At the 28-day end point, the mortality rate among the first group was 26.5% in the study group and in the placebo group was 33.9%. In the second group, in the study group was 19.4% and 21.1% in the placebo group. Patients with MODs benefited more in terms of reduction in mortality rate associated with ADF, but the risk of serious bleeding was high among patients whom received ADF. Abraham et al. (2005) studied the effect of administrating ADF into severe sepsis patients. The clinical trial involved 2613 patients', the placebo group included 1307 patients and the ADF group included 1333 patients. The mortality rate for placebo patients was 17% and 18.5% for ADF treated patients. Ranieri et al. (2012) investigated the effect of APC on septic shock in PROWESS-SHOCK clinical trial, with 1680 patients assigned into placebo group (834) and study group (846). The patients were assessed at 28 days and at 90 days. The mortality rate at 28-day point was 24.2% in placebo group and 26.4% in ADF group, and at 90 days was 32.7% in placebo group and 34.1% in ADF group. The risk of

bleeding increased among ADF patients compared to the placebo patients. ADF did not increase the survival rate among sepsis patients in any clinical study. Eli Lilly, the company the made Xigris (ADF), withdrew the drug from the market following the PROWESS-SHOCK trial (Agency, 2011).

2.3.4 TLR-4 antagonist:

As discussed in section 1.4.1, the TLRs detect pathogens and initiate the intracellular signal for the production of inflammatory cytokines. Theoretically, by disturbing the intracellular signal, this could lead to treating sepsis by preventing the production of cytokines. TAK-242 is a TLR-4 antagonist that suppresses TLR-4. Rice et al. (2010) studied a population of 223 severe sepsis patients dividing them into three groups, the placebo group (74 patients), the 1.2 mg/kg group (74 patients) and 2.4 mg/kg group (75 patients). The 28-day endpoint mortality rate among the three groups was 24.2%, 22% and 17.4% respectively with no statistically significant difference in mortality rate. Another TLR-4 antagonist that has been studied is Eritoran tetrasodium (E5564). This clinical trial was conducted by Tidswell et al. (2010) to investigate the effect of E5564 in reducing mortality rate among 293 severe sepsis patients. The patients were categorized into three categories, the first category is the placebo (96 patients), the second category is the 45 mg of E5564 (103 patients) and the third category is 105 mg of E5564 (94 patients), where it was administrated through central venous catheter. The mortality rate among the placebo group was 33.3%, in the 45 mg group was 32% and in the 105 mg group was 26.6%, statistically, there was no significant difference between the groups. Opal et al. (2013) studied 1961 patients, 658 patients (placebo), and Eritoran

group (1304 patients). The 28-day mortality rate in placebo patients was 26.6% and in Eritoran patients is 28.1%. The clinical trial failed to show a significant difference in reduction of mortality among the two groups.

Collectively, these studies of drugs designed to mitigate sepsis has not been successful. There have been no trials that demonstrate a benefit to patients in terms of reducing mortality rate. It is however possible that combined drug approaches may be more beneficial, but these may also introduce more complications.

2.4 Medical Technologies for treating sepsis:

Selective targeting of specific cytokines, see section 2.3, failed to improve the outcome in sepsis patients because of the complexity of the immune system interactions that occur during the inflammatory cascade (Fortenberry and Paden, 2006). The removal of the pro-inflammatory and anti-inflammatory cytokines have been suggested by Ronco in his peak concentration hypothesis, where he stated "unspecific removal of soluble mediators, be they pro or anti-inflammatory, without completely eliminating their effect, may be the most logical and adequate approach to a complex and long-running process such as sepsis" (Fortenberry and Paden, 2006).

Acute kidney failure (AKF) is diagnosed in more than half of septic shock patients as a result of the inflammatory mediators and their consequences such as hypotension and cell damage. Continuous renal replacement therapies (CRRT) are used as replacements for the kidney to remove urea and excess fluid. However, Gotloib et al. (1986) found that inflammatory mediators are removed during renal therapy. Also, since the cytokine production in sepsis is a continuous process, continuous treatment is more favorable than intermitted treatment. The extracorporeal techniques used for removing harmful molecules from the blood include haemodialysis, hemofiltration and plasma filtration, the latter will be the focus in chapter 3 (Venkataraman et al., 2003, Fortenberry and Paden, 2006, Hirasawa et al., 2012). In this section, some of the extracorporeal technologies used in treating sepsis or removing inflammatory mediators are discussed.

2.4.1 Hemodiafiltration and hemofiltration:

CRRT includes continuous hemodiafiltration (CHDF) and continuous hemofiltration (CHF). The removal of the solute and harmful molecules is a continuous and gradual process so they run continuously (Oda et al., 2002). The molecules move through a semi-permeable membrane either by diffusion or convection as illustrated in figure 15. Convection depends on the transmembrane pressure (TMP) for the molecules to pass through the membrane. The diffusion requires the presence of a solute with a different gradient, for example a dialysis solution, in order for the molecules to move from the higher gradient to lower gradient to achieve gradient balance (Shaheen et al., 2009).

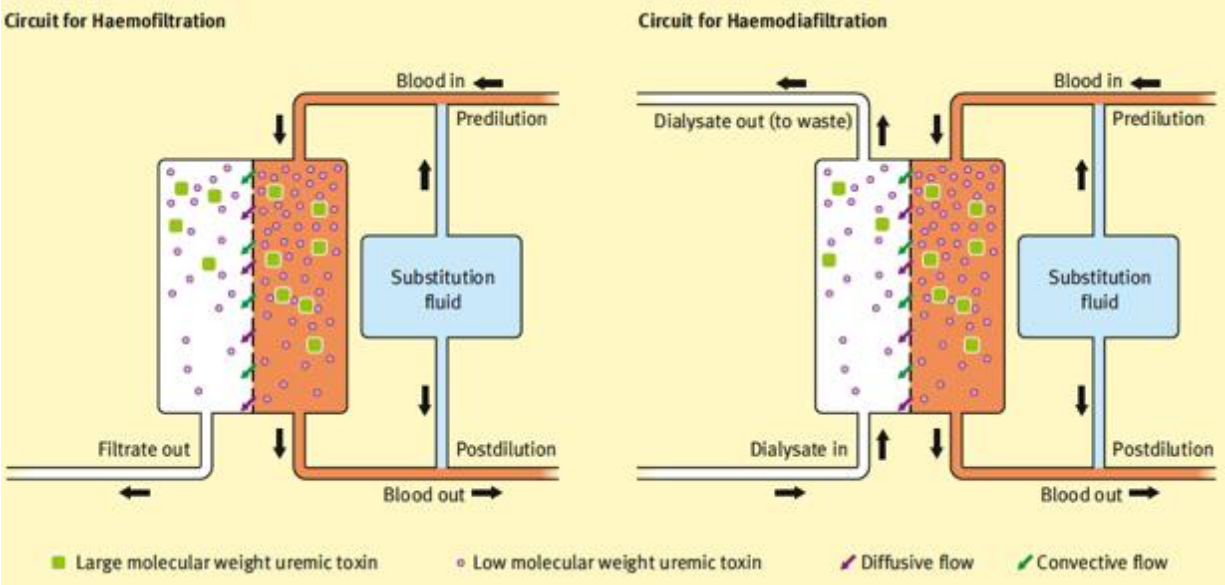

Figure 15 Convection and diffusion (Shaheen et al., 2009)

Clinical trials have investigated the effect of CHF and CHDF in the removal of inflammatory mediators. Hoffmann et al. (1995) investigated the effect of continuous veno-venous hemofiltration (CVVHF) on inflammatory mediators in plasma. The study involved 16 sepsis patients with MODS and 5 healthy subjects, where the inflammatory mediators were compared. Also, blood samples were taken before the initiation of the filtration and one hour of filtration and matching samples were taken from the ultrafiltrate. The level of inflammatory mediators before the start of the treatment in sepsis patients was high compared to the healthy subjects, in which these were undetectable. The results from both groups fail to a demonstrate a reduction in IL-6 and TNF-α cytokines after the hemofiltration treatment.

Cole et al. (2001) studied the effect of high-volume hemofiltration (HVHF) on septic shock patients. They made their hypothesis based on animal trials, where improvement in cardiac output and better blood pressure after exposed to HVHF was observed. 11 septic shock patients were categorized into two groups, where the first group were treated using CVVH and the second group with HVHF. In both groups, C3a, C5a, IL-2, IL-8, IL-10 and TNF-α were elevated pre treatment, and after treatment. In both groups, there was a reduction in the inflammatory mediators'. However, the reduction in C3a and C5a in the HVHF was greater when compared to the CVVH patients.

Cole et al. (2002b) concluded that the use of CVVH in sepsis patients did not decrease the inflammatory mediators. However, Peng et al. (2010) found that the level of cytokines was reduced significantly, such as IL-10, IL-1, IL-4. These approaches to treating sepsis remain unresolved but are often still deployed as “belt and braces” approach to treating this highly challenging patient group.

2.4.2 Hemoadsorption and activated carbon:

Hemoadsorption is a method for the removal of inflammatory mediators and it works by direct contact between the blood and a sorbent materials. There are two types of sorbent materials, materials available from nature such as charcoal, or materials that are artificially man-made such as "different resins with covalently bound groups reactive with specific ligands" (Ronco et al., 2000). The sorbent has different operating configurations depending on how is attached to an extracorporeal circuit, as illustrate in figure 16. There are many types of the hemoadsorbants such as polymyxin-B-immobilized (PMX) that are able to reduce the level of endotoxin in the plasma, and Cytosorb that is able to reduce the level of various inflammatory mediators in septic rats. Also, activated carbon (AC) has been used as a cytokine absorber. AC is a very highly adsorptive material (Ronco et al., 2000, Rimmelé and Kellum, 2011, Yushin et al., 2006) and is relatively non-selective. Some of the clinical trials and publications that used hemoadsorption and charcoals will be discussed in this section.

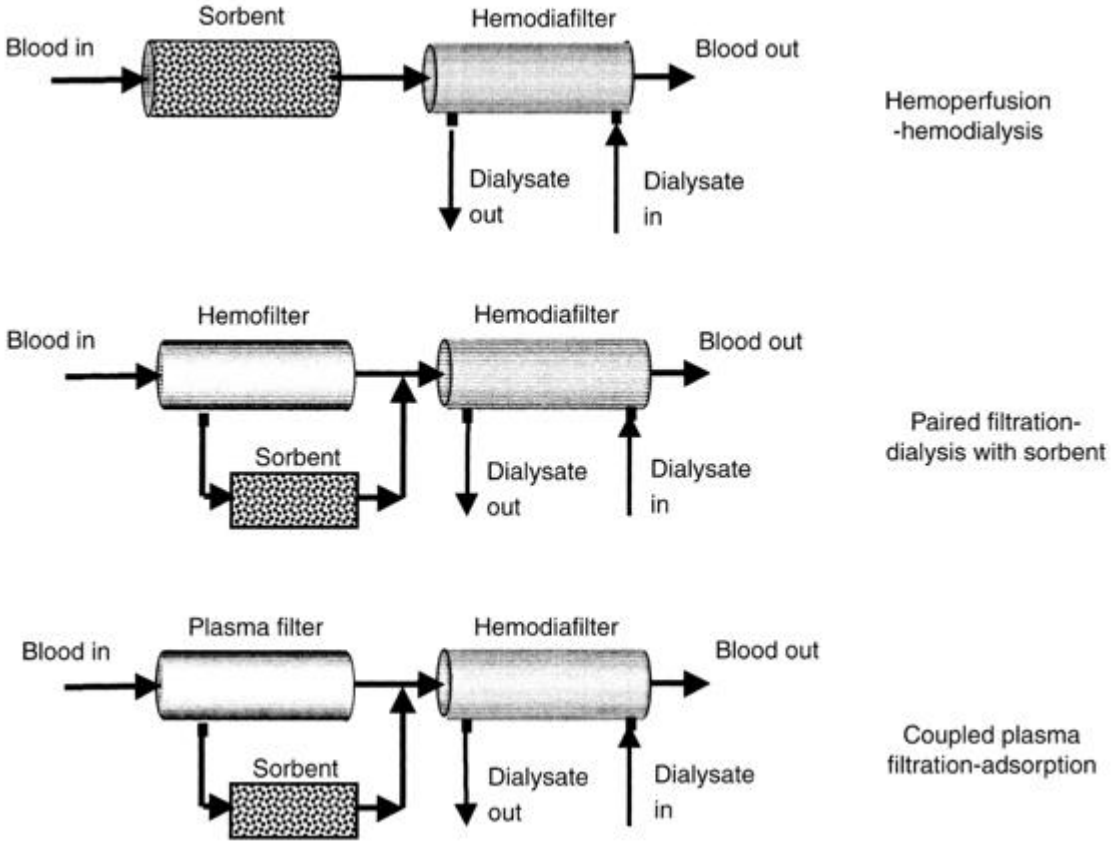

Figure 16 Adsorbent different configuration in extracorporeal circuits (Ronco et al., 2000)

2.4.2.1 PMX:

A PMX cartridge (figure 17) contains polymyxin B anti-biotics that are able to eliminate LPS endotoxin (Ronco and Klein, 2014).

Figure 17 PMX (Ronco and Klein, 2014)

Aoki et al. (1994) investigated the effect of using PMX fiber (PMX-F) on 16 sepsis patients with failure of at least two organs, where some patients received the treatment more than once. Blood tests were taken before and after the treatment for measurement of endotoxin levels in the blood. After the treatment, the level of endotoxin had declined from 76 pg/mL to 21 pg/mL. Also, Kodama et al. (1997) studied the effect of PMX-F on 37 sepsis patients with high level of endotoxin in their blood. After 14 days of the treatment, the mortality rate was 46% in patients with MOF. However, the level of endotoxin was reduced significantly and it was further declined the next day in survived patients.

Nemoto et al. (2001) assigned 98 sepsis patients into two categories, PMX-F group (54 patients) and control group (44 patients), and the endpoint of this clinical trial was 28 days. At the end of the study, the mortality rate in the PMX-F group was 59% while in the control was 89%. They found that the usage of PMX-F in patients with acute physiology and chronic health evaluation (APACHE) score, which estimates the survival rate of severe ill patients, less than 30, increased survival rate.

2.4.2.2 CytoSorb:

CytoSorb is a hemoadsorpative column able to remove inflammatory mediators from the blood. It contains highly adsorbent coated beads (figure 18). The beads are coated with polyvinylpyrrolidone in order to enhance be biocompatibility. There were two medical reports that used CytoSorb for the removal of inflammatory mediators. The first case was a septic shock patient with MOF. Due to acute kidney injury (AKI), the patient was attached to CVVHDF and a CytoSorb column was added to the extracorporeal circuit. After 60 hours, the level of IL-6 was significantly reduced from more than 5000 pg/ml to 1198 pg/ml and the CVVHDF was stopped when kidney function return to normal. In the second case, the patient was diagnosed with sepsis but it advanced into septic shock with AKI. As a result, CVVHDF was used as kidney replacement therapy. The CytoSorb column was used in conjunction with the CVVHDF. The patient improved after six hours of the initiation of the treatment and eventually recovered (Morris et al., 2015).

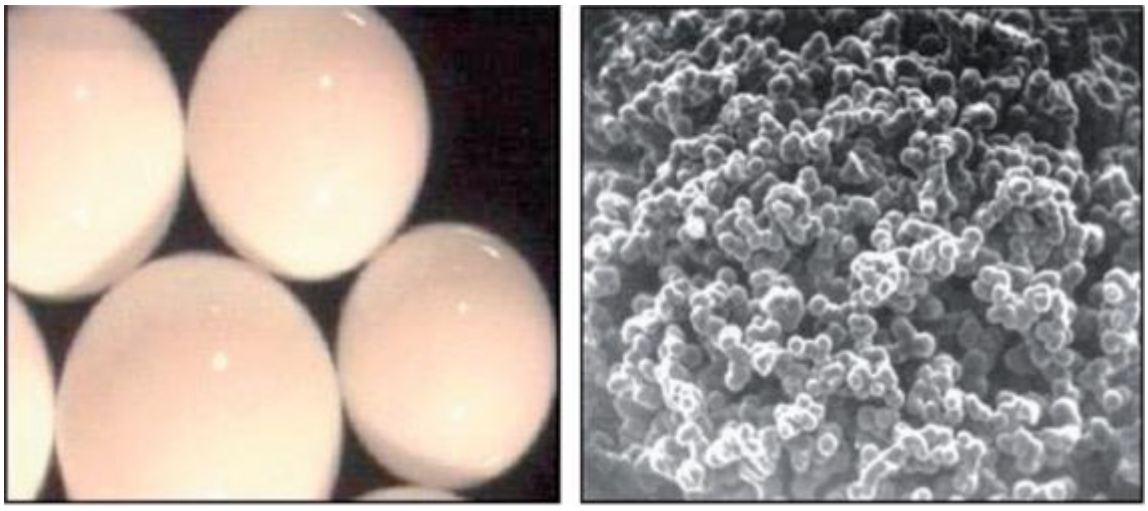

Figure 18 CytoSorb beads under microscope (Morris et al., 2015)

Träger et al. (2016) studied the effect of CytoSorb in a patient with severe respiratory failure that needed venovenous ECMO because mechanical ventilation failed to provide the patient with sufficient flow. The patients condition deteriorated and developed MOF. This corresponded to the increase in inflammatory mediators. Due to the AKI and cytokines storm, the patient required CRRT and the CytoSorb column was attach to it. After the treatment using CytoSorb, the level of cytokines, IL-6 and IL-8, were decreased and normal kidney function was restored.

2.4.2.3 Charcoal and ACs:

Cole et al. (2002a) investigated the adsorptive capabilities of uncoated charcoal (UC) in removing inflammatory mediators from the blood. 300 ml of blood was donated from six healthy subjects, an endotoxin was added to the blood and placed in a reservoir. Another 60 ml of blood was withdrawn from the subjects as a control samples. A circuit was constructed as illustrated in figure 19, consisting of of hemofiltration in addition to UC. Samples were taken every hour from three points, point A (the circulating blood), point B (outlet of the ultrafiltrate and before the inlet of the charcoal cartridge) and point C (the outlet of the charcoal cartridge), the samples are used to measure the cytokines level. After six hours, cytokines, IL-1β, IL-6, IL-8 and TNF-α were removed significantly from the blood except IL-10. Charcoal has also been used with plasmapheresis (PP) for cytokine removal and this will be discussed in chapter 3.

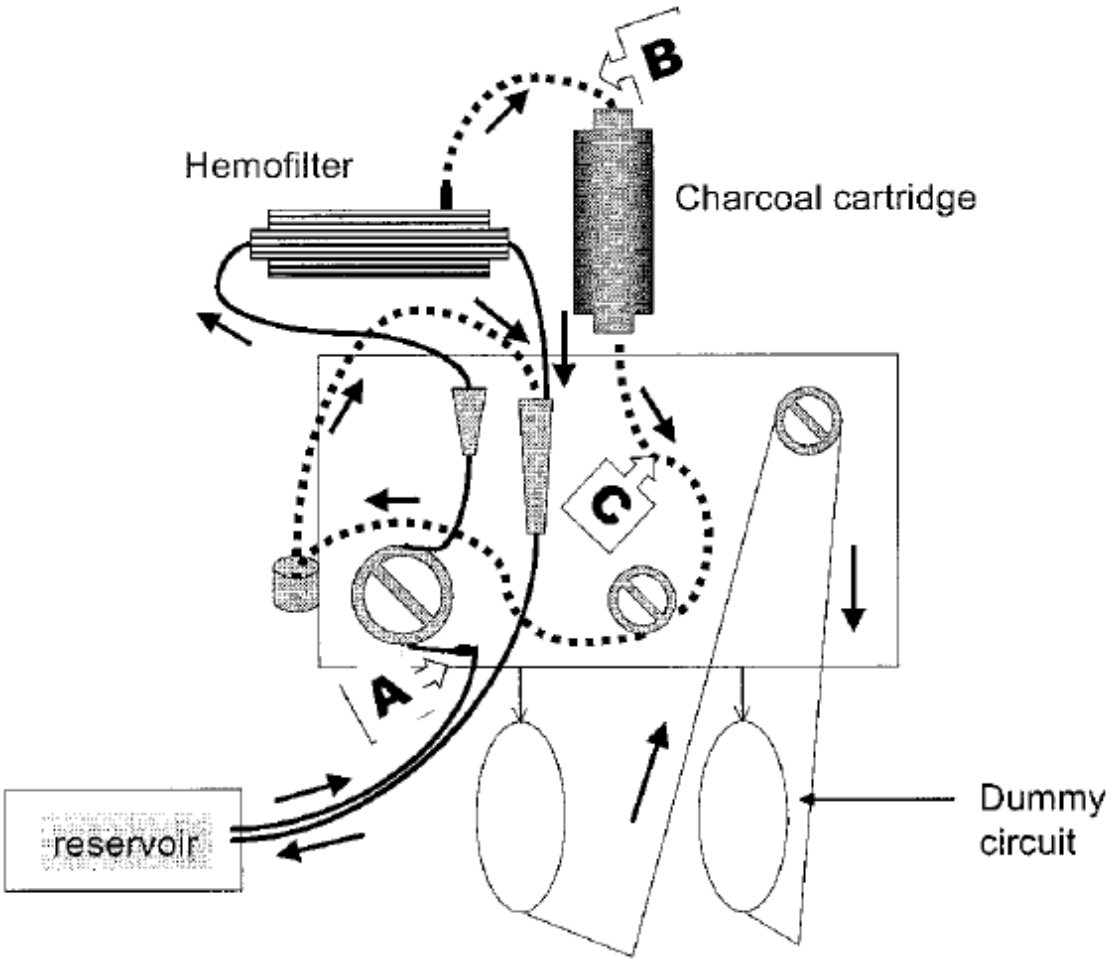

Figure 19 circuit for UC (Cole et al., 2002a)

Carbon has been studied for its ability to absorbed various inflammatory mediators. Sandeman et al. (2008) studied the effect of carbon on cytokine adsorption. They administrated cytokines (TNF, IL-6, IL-8, IL-1β) in human plasma before pumping the plasma through carbon tube for two hours. They used two types of carbon tubes, mesoporous and non-mesoporous. The mesoporous activated carbon was able to remove a significant percentage of cytokines, except TNF-α where the absorption volume is insignificant, compared to the non-porous.

Tripisciano et al. (2011) investigated the effect of activated carbon beads in adsorption of cytokines during liver failure. The carbon beads were prepared with different levels of activation (%), by heating the carbon beads at 900°C for different time periods. The activation of the carbon beads leads to an increase in the porosity of the carbon. Plasma was collected from healthy subjects and 500 pg/ml of TNF-α and IL-6 were added. The plasma samples were incubated with the carbon beads for 60 minutes in the study group, and control samples were spiked plasma without the activated carbon. The results demonstrated that as the activation of the carbon beads increased, the removal of IL-6 and TNF-α increased (figure 20).

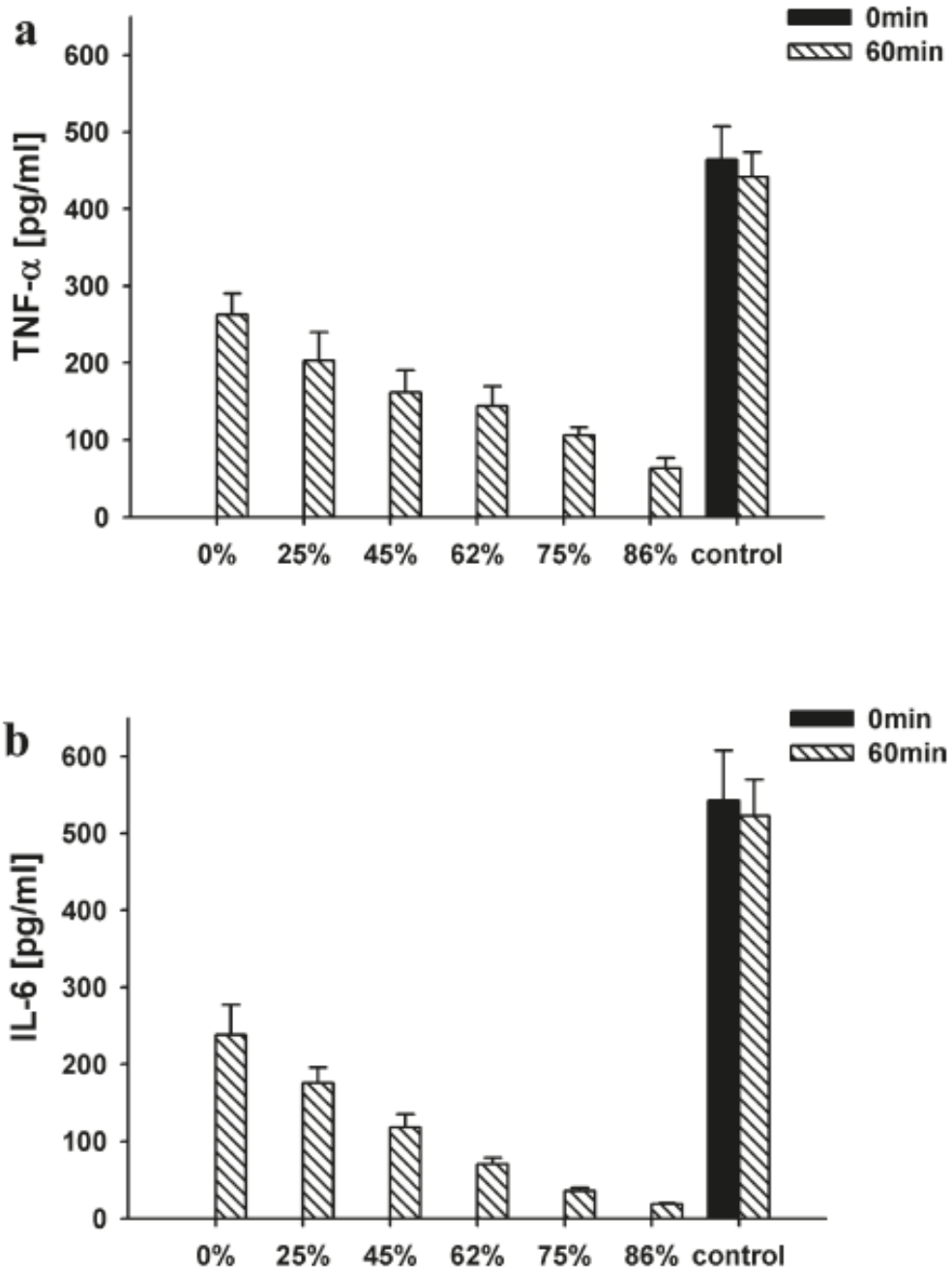

Figure 20 Activation degree on cytokines adsorption (Tripisciano et al., 2011)

Chapter 3:

Plasma filtration for the treatment of sepsis and the removal of inflammatory mediators

3 Plasma filtration for the treatment of sepsis and the removal of inflammatory mediators

3.1 Introduction:

As discussed in chapter one, the activation of inflammatory mediators occurs in plasma, thus, plasma filtration could be viewed as a beneficial process.

There are two methods for plasma separation from blood. The centrifuge method to separate the blood into its components, red blood cells (RBCs), plasma, platelets and WBCs, as illustrated in figure 21. In order to prevent hypotension when transfusing, the RBCs are mixed with the fluid as replacement for the removed plasma. The other method is filtration using membrane technology. The plasma component passes through the membrane pores, driven by the TMP. Using this method the removed plasma can be either disposed or, can be processed before being returned to patient, for example, cascade filtration plasmapheresis.

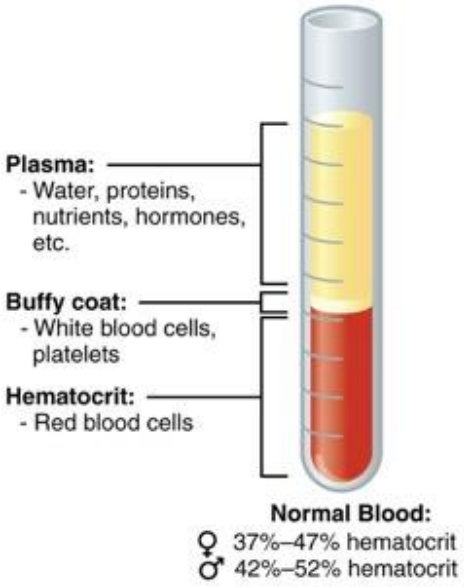

Figure 21 Blood layers after centrifuge (taken from: https://opentextbc.ca/anatomyandphysiology/chapter/an-overview-of-blood/)

This method known as plasmapheresis (PP), is used for the treatment of different conditions such as thrombotic thrombocytopenic purpura, which is a disease with unknown cause that damage red blood cells and platelets, resulting in anaemia and thrombocytopenia. PP is used for intervention in more than 60 clinical conditions according to the American Society for Apheresis (ASFA) guidelines (Reeves and Winters, 2014, Levy et al., 2001). This chapter will focus on PP and combined PP with other technologies for treating sepsis.

3.2 PP for sepsis treatment:

Iwai et al. (1998) have investigated the effect of cytokines and endotoxin reduction after one session of PP in hepatic failure patients. The number of patients in this study was 13, eight patients were diagnosed with fulminant hepatitis and the other 5 patients were diagnosed with severe form of acute hepatitis. Blood samples were taken before and after PP treatment for measurements of inflammatory mediators. The PP caused a reduction in the cytokines and endotoxin as illustrated in figure 22. The result clearly shows that a single PP is beneficial in decreasing the inflammatory mediator in the plasma.

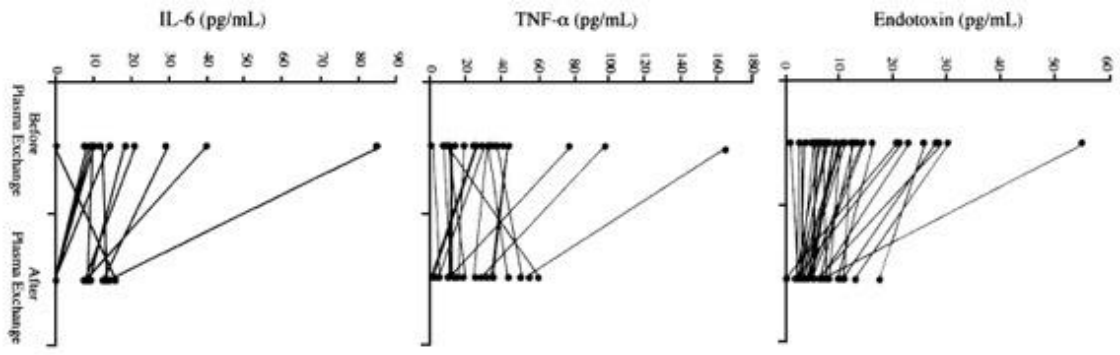

Figure 22 Cytokines and endotoxin levels before and after PE (Iwai et al., 1998)

The use of PP in fulminant hepatitis patients has been studied by Nakamura et al. (2000). More than two sessions of PP were performed, and the maximum number of sessions was 16. There were three groups in this study, the first group was fulminant hepatitis (15 patients), the second group was severe acute hepatitis (14 patients) and the third group was healthy (20 subjects). Blood samples were taken before and after each treatment. The results are demonstrated in table 4 and table 5. The PP sessions reduced the cytokine levels significantly and to a level similar to the levels in healthy subjects.

	TGF-β pg/ml	TNF-α pg/ml	IL-6 pg/ml
Fulminant hepatitis (n = 15)	62.6 ± 24.8*	64.0 ± 23.6*	19.6 ± 6.8*
Severe acute hepatitis (n = 14)	44.4 ± 16.8	22.8 ± 14.6	4.2 ± 1.1
Healthy controls (n = 20)	32.6 ± 5.6	ND	3.4 ± 0.3

Table 4 cytokines level in each group (Nakamura et al., 2000)

	TGF-β pg/ml	TNF-α pg/ml	IL-6 pg/ml
Before plasma exchange	62.6 ± 24.8	64.0 ± 23.6	19.6 ± 6.8
After first plasma exchange	42.6 ± 19.6*	20.8 ± 9.6**	6.6 ± 3.2**
After third plasma exchange	34.8 ± 6.8**	12.8 ± 2.6***	4.4 ± 1.6**

Table 5 Cytokines level before and after PE treatments (Nakamura et al., 2000)

A randomized, double-blinded study was conducted by Busund et al. (2002) to study the effect of PP on severe sepsis and septic shock patients. The patients were categorized into two groups, PP group (54 patients) and control group (52 patients). In addition to the PP, both groups were treated with conventional drug treatments, which includes antibiotics and fluid resuscitation. Two PP treatments were performed on the patients. The 28-days mortality rate in the PP group was 33.3% while in the control was 53.8%, which indicate that the PP was associated with a decrease in mortality rate. Also, in the PP group, there was a significant drop in the APACHE score after the PP sessions.

3.2.1 Hybrid technologies for sepsis and inflammatory mediators removal:

There are some studies that combine PP with different adsorptive columns or with other technologies for treating sepsis that will be discussed in this section.

3.2.1.1 PP with hemodiafiltration (HDF):

The combination of PP and HDF has been studied and published in several articles. Kumar et al. (1998) have treated a patient with fulminant meningococcal sepsis with the combined technology. The patient developed septic shock with MODS even though she received the conventional drug treatment as soon as she entered the ICU. The treatment started with HDF, however, her condition did not improve. HDF was combined with PP which resulted in better clinical conditions for the patient. Combined technologies were continued for three days, during which this the patient's condition improved. The combination of PP with HF for treating patients who develop sepsis after surgery was conducted by Schmidt et al. (2000). 19 patients received the combined technologies and their outcomes were compared with 24 patients treated using conventional means. In the combined technology patients, the mortality rate decreased in patients with one or two organ system failure, however, patients with more than two organ system failure did not benefit from the treatment. Overall, the combined approach was more effective in less complex patients.

3.2.1.2 Coupled plasma filtration with adsorption (CPFA):

There are several studies that investigated the effect of CPFA on sepsis treatment. Ronco et al. (2002) have combined CPFA technology with hemodialyzer for treating septic shock patients and compared the results with patients whom received CVVHDF technology as illustrated in figure 23. The patients were randomized to be treated with either technologies, and all patients had MODS. Blood samples were taken at different time points for the measurements of inflammatory cytokines. Despite the fact cytokine levels did not change in the combined technology group, the patients had a better clinical outcome. In these patients, the MAP was increased compared to the CVVHDF group, and they were more hemodynamic stable.

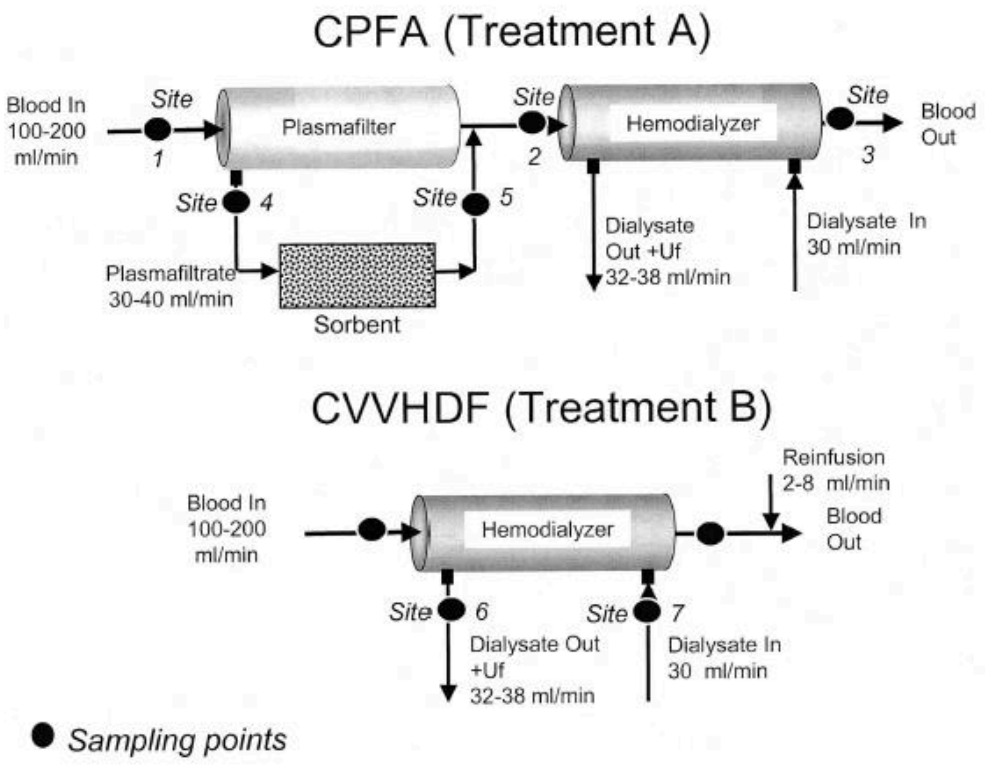

Figure 23 Combined treatment vs CVVHDF (Ronco et al., 2002)

Combination of CPFA with CVVH technologies for treating sepsis was studied by Hassan et al. (2013). The patients were divided randomly into two categories, the first is treated with combined technologies (11 patients) and the second was treated with CVVH (12 patients). The treatment started with the CPFA for four to eight hours, after that CVVH was initiated for the remaining of 24 hours. In the combined treatment, the haemostasis was established faster than in the CVVH patients. However, Livigni et al. (2014) did not agree with these findings. They studied the effect of CPFA on septic shock patients in a randomized controlled multi-centre clinical trial in Italy. The patients were divided into two groups, CPFA group, 91 patients, and control group, 93 patients. In the CPFA, out of 91 patients, 41 patients died (45.1%), while in the control group 44 patients (47.3%). As a result, there is no significant difference in mortality between both groups. Berlot et al. (2014) investigated whether the volume of the treated plasma using CPFA has an impact on outcome in sepsis patients. The patients included in this study had two or more organs failures and were treated for more than two session, each session was 10 hours. In patients who survived, the volume of the plasma treated was high compared to the patients who died. Large randomized controlled double blinded clinical trials are recommended to investigate the effect of CPFA and volume of the plasma on inflammatory mediator reduction. However, it would appear to be clear that some clinical advantages can be gained from the adoption of this approach to treat sepsis.

Chapter 4:

Thesis Objectives and Hypothesis

4 Thesis Objectives and Hypothesis

4.1 Introduction:

Sepsis is a disease that represents substantial burden on the healthcare system. Unfortunately, the mortality rate in sepsis is high despite the application of a number of treatment bundles. Also, due to the complexity of the inflammatory mediators that are involved during sepsis, targeting specific cytokines generally fail to treat the condition sepsis. As a result, nonspecific removal of the inflammatory mediators may be the best solution. The inflammatory mediators are found in the plasma; Consequently, the removal of the plasma will lead to the reduction in these cytokines.

4.2 Hypothesis

It is possible to develop an automated stand-alone plasma separation system for the treatment of sepsis

4.3 Objectives:

The objectives can be divided into phases:

1st phase: Design phase

- Design optimal blood flow pathway.
- Using computational fluid dynamics (CFD) for modelling the blood flow to calculate the shear stress, pressure drop and the behavior of the blood flow.
- 3D print prototype device for testing.

2nd phase: Optimisation and testing phase

- Determine the TMP for the critical flux.
- Compare the flux rate between two membranes with different effective pores area (EPA).
- Perform experiments for the performance of the rig by using bovine blood.
- Modify the design for better flux rate.

3rd phase: Electronic and control phase

- Design the control system for automation of the system.
- Calibration of the electronics parts for the suitable range.
- Design and print the electronics housing.

4th phase: Performance analysis phase

- Fabrication of the parts for the rig to be as an extracorporeal system.
- Perform experiments to investigate the device performance with time.

Chapter 5:

Device development

5 Device Concept:

5.1 Introduction:

In order to develop a device to generate secondary flow, the effect of shear stress on RBCs must be addressed. Thus, understanding of the blood and its composition, hemolysis and the shear stress values that could lead to RBC fracture are important. Also, the membrane characteristics of exchange device are vital when considering plasma separation from the blood. This information is essential in order to develop methods that will be used for the generation of secondary flow. These can be analysed and subsequently visualized using CFD.

5.2 Blood and its composition:

The functions performed by the blood are vital, and they include transportation of oxygen, hormones and nutrition to the cells, removal of waste such as CO2, thermoregulation, and modulation of the immune response to pathogens.

5.2.1 Compositions:

"Blood is a type of connective tissue that consists of cells surrounded by a liquid extracellular matrix" (Tortora and Derrickson, 2011, P. 729-P. 741). Approximately 45% of its volume is the formed elements and approximately 55% is the fluid plasma. most of the plasma is water, 91.5%, with the remaining proteins. The formed elements comprise RBCs, platelets and WBCs. RBCs are biconcave disks with a radius and thickness of 3.5-4 μm and 1.7-2.2 μm respectively. They contain a protein that gives the blood its red colour. Each RBC contain haemoglobin protein that binds to four oxygen molecules for gas transportation to the tissues, knows as oxyhemoglobin. In addition,

haemoglobin binds to carbon dioxide to transport it from cells to the lungs. Platelets are important for minimizing bleeding through clotting and WBCs are important for fighting pathogens that enter the body (Tortora and Derrickson, 2011, P. 729-P. 741, Diez-Silva et al., 2010, Scanlon and Sanders, 2010, P. 274).

5.2.2 Hemorheology:

Rheology is defined by Baskurt and Meiselman (2003) as "a scientific field that deals with the flow and deformation behavior of materials, with the materials under consideration being solids or fluids, including liquids and gases". Hemorheology focuses on studying the characteristics of blood flow and the deformation of blood and its components (Baskurt and Meiselman, 2003). There is a force exerted on fluids as they flow known as stress, this includes shear stress and shear rate. The shear stress is defined as the force per unit area that acts parallel to the surface, and the shear rate is the force per unit area acts perpendicular to the surface. From a rheological perspective, there are two types of fluids, Newtonian and non-Newtonian. In Newtonian fluids, the viscosity is independent of the shear stress and shear rate, while in the non-Newtonian fluids the viscosity of the fluid is dependent of the shear stress or shear rate (Baskurt and Meiselman, 2003). Blood can be Newtonian and non-Newtonian fluid. In other words, the blood plasma, which consist mostly of water is a Newtonian fluid, however, the blood components of different cells is a non-Newtonian fluid. So, the whole blood is modelled as a homogenous non-Newtonian fluid (Fasano and Sequeira, 2017, P. 40, Baskurt and Meiselman, 2003).

5.2.2.1 Blood viscosity:

Blood viscosity defined by Cho and Cho (2011) as" the resistance of blood to flow and represents the thickness and stickiness of blood". The blood viscosity depends on the shear rate, and the shear rate is related to the velocity and diameter of the blood vessels. The velocity in large arteries is high that results in low shear stress, but as the blood flows in smaller capillaries, the shear stress increases as the velocity and diameter decrease (Cho and Cho, 2011). There is another factor affecting blood viscosity, hematocrit which is represented by the percentage of the RBCs in the blood. Male adult hematocrit is around 45%. The relationship between hematocrit and shear rate is exponential as an increase by 1% in hematocrit yields an increase in the shear rate of 4%. A hematocrit increase, which occurs in polycythemia disease, leads to higher friction between the blood and vessel walls (Cho and Cho, 2011, Baskurt and Meiselman, 2003).

RBCs deformability:

Fluids with the ability to deform and restore to its original shape are known as viscoelastic fluids. RBCs are viscoelastic since they deform due to high shear rate. This occurs in smaller vessels with diameter of less than 10 μm, where the shear rate is increased due to lower velocity and smaller diameters. Once the applied force is removed, the RBCs return to normal size and shape (Fasano and Sequeira, 2017, P. 42, Baskurt and Meiselman, 2003).

RBCs aggregation:

The RBCs have the ability to aggregate and formed a linear shape similar to “stacks of coin” known as rouleaux. Shear rate influence RBCs aggregation initiated by fibrinogen and low density lipoprotein-cholesterol. In low shear rate, the RBCs start to accumulate on each other and resulted in increase in blood viscosity (Cho and Cho, 2011, Baskurt and Meiselman, 2003).

5.3 Mechanical blood trauma (Hemolysis):

Hemolysis is defined Fraser et al. (2012) by as “damage to the red blood cells, resulting in the release of hemoglobin into the blood plasma”. From the medical prospective, the acceptable free plasma haemoglobin (fpHb) is in the range of 5-10 mg/dL (50-100 mg/L) (Omar et al., 2015). As the blood flows in biomedical devices such as haemodialysis and prosthetic heart valves, it is subjected to external forces, for example, high shear stress that could lead to hemolysis or alter the RBCs rheology (Kameneva and Antaki, 2007, P.206-207). The RBCs can stand high shear stress before they rupture but only for a short exposure time, 4000 $\mathrm{N/m^2}$ for 10^{-5} (0.00001) seconds. However, for longer exposure time, 0.002 second the shear stress is 500 $\mathrm{N/m^2}$, 10^2 (100) seconds, the shear stress is 150 $\mathrm{N/m^2}$, this is demonstrated in figure 24 (Kameneva and Antaki, 2007, P.212, Maul et al., 2015b).

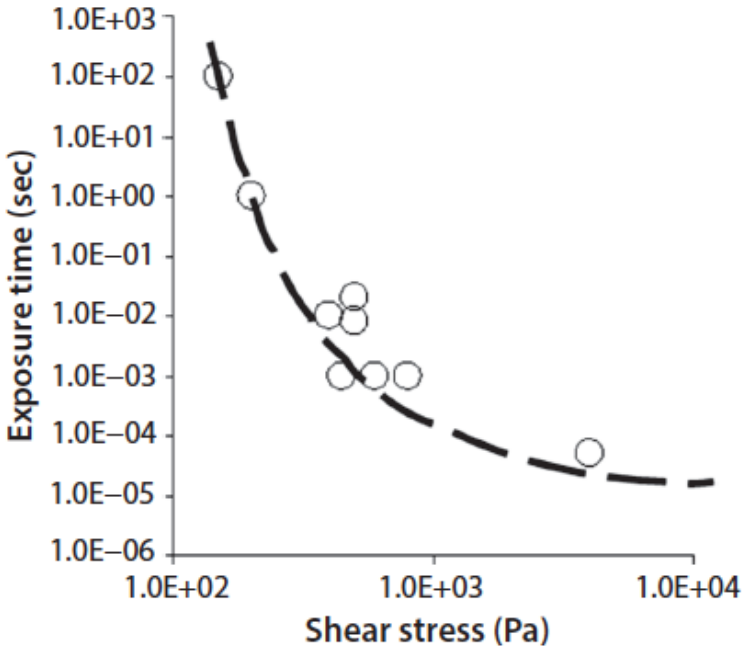

Figure 24 shear stress and exposure time relationship (Maul et al., 2015b)

Another mechanism of trauma that can occur to the RBCs when they face with shear stress lower than haemolytic shear stress is known as sub-lethal RBCs damage. In the healthy adult, the RBCs lifespan is approximately 100-120 days, however, sub-lethal damage could shorten the lifespan in addition to altering the RBCs rheology. The RBCs that face a shear stress of 120 Pa for 120 seconds have shown a reduction in their ability to deform. In addition, sublethal trauma damage increases the RBCs aggregation as seen in patients with circulatory assist device (CAD). In order to reduce the effect of sublethal damage, these patients are given erythropoietin to generate healthy and deformable RBCs. Also, giving albumin or fresh frozen plasma to CAD patients will help in reduces RBCs aggregation (Olia et al., 2016).

Another blood components that are activated due to the shear stress generated by the extracorporeal circulation are platelets and leukocytes. The shear stress that reduce the leukocytes number is in the range 10-60 Pa for a period of time, which is far less than shear stress that cause hemolysis for the same duration (150 Pa) (Radley et al., 2018, Maul et al., 2015a). Moreover, the platelets will be activated when the exposed to shear stress in the range 10-35 Pa (Alemu and Bluestein, 2007). Clearly, the shear stress that leads to the reduction in the leukocytes number and platelets activation is far less compare to the one that cause hemolysis. However, during the membrane plasmapheresis process, there was no significant reduction in platelets and leukocytes numbers (Siami and Siami, 2001).

5.4 Membranes:

Membranes are defined by Khayet and Matsuura (2011) as “a device that selectively permits the transfer of one or more compounds from a liquid and/or gas media”. Membranes for filtration are used in different fields, such as food processing and medical applications. The usage of membranes in medical applications varies from plasmapheresis (PP) to haemodialysis and hemofiltration. Generally, the membranes are divided based on the pore size and described as Ultrafiltration (UF) and Microfiltration (MF) membranes. For the application of PP, the membranes used are UF. The force used to drive the filtration separation process in UF is pressure (Cheryan, 1998, P.3).

5.4.1 Membrane characteristics for PP:

Membranes used for medical treatment differ in their properties such as the pore size and transmembrane pressure which is the acting force that required for the removal of the particles from the solution. There is a general set of requirements for the membrane for PP:

1- All protein in the plasma should pass through the membrane.
2- The membrane should have high volume porosity for higher plasma removal.
3- The membrane is hydrophilic and Wettable
4- The membrane fouling in addition to the protein adsorption should as minimum as possible.
5- Biocompatible.
6- The membrane should not be affected by the sterilization methods.

7- The performance of the filtration for treatment is constant during the operation (Wiese, 2007, P.76).

In the clinical applications, the membranes are either flat sheet or hollow fiber configurations. Figure 25 demonstrate schematic diagram for hollow fiber and flat sheet membranes that are used for plasma exchange (Wiese, 2007, P.83, P.85). In this project, flat sheet membrane will be used for the plasma separation.

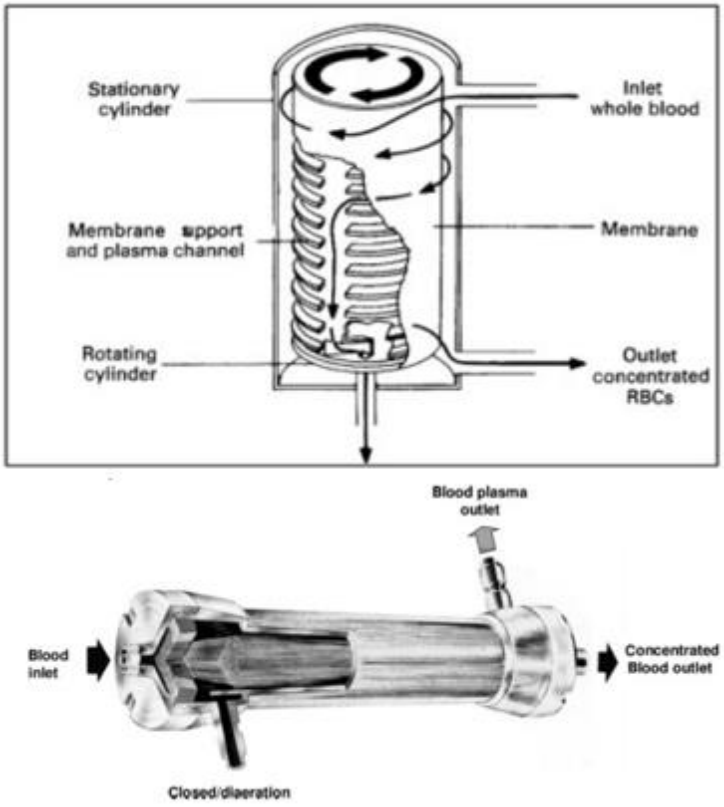

Figure 25 The top picture shows flat sheet membrane that used in rotating plasma separation device, and the bottom picture shows hollow fiber module used for plasma separation (Wiese, 2007, P.86)

5.4.1.1 Membrane porosity and pore sizes:

Currently, the membranes used for PP are hollow fiber membranes with the pore size of 0.2 μm to 0.5 μm that retain the RBCs, WBCs and platelets as illustrated in figure 26. Hollow fiber membranes for PE have a large surface area, generally they have a surface area of around 1 m^2 and are made from polymers such as cellulose acetate, polyethylene (PE) and polyethersulfone (PES) (Gashti, 2016, Wiese, 2007). Another factor that determines the usability of a membrane for PP is porosity, this can be calculated using the volume of the pores divided by the membrane total volume (Smolders and Franken, 1989). There are three methods for the determination of pores size their distribution; the bubble point, electron microscope and challenge test (Cheryan, 1998, P.72). The pore size has an effect on the filtration rate (ml/min), permeate removal rate per time, as stated by Friedman et al. (1983). They compared three different membranes used for plasma exchange with different pore sizes, 0.4 μm, 0.6 μm and 0.8 μm. They found that 0.8 μm was the highest filtration rate as illustrated in figure 27.

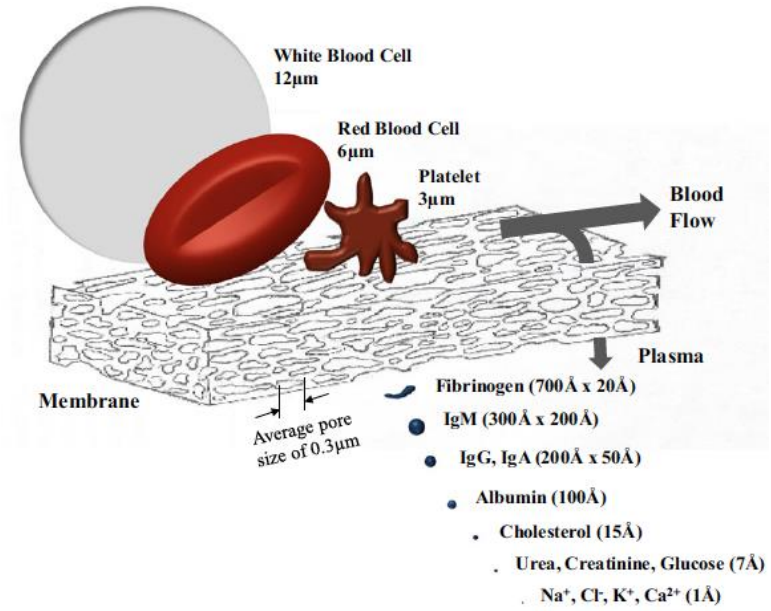

Figure 26 Comparing cells and molecules with the membrane pore size (Gashti, 2016)

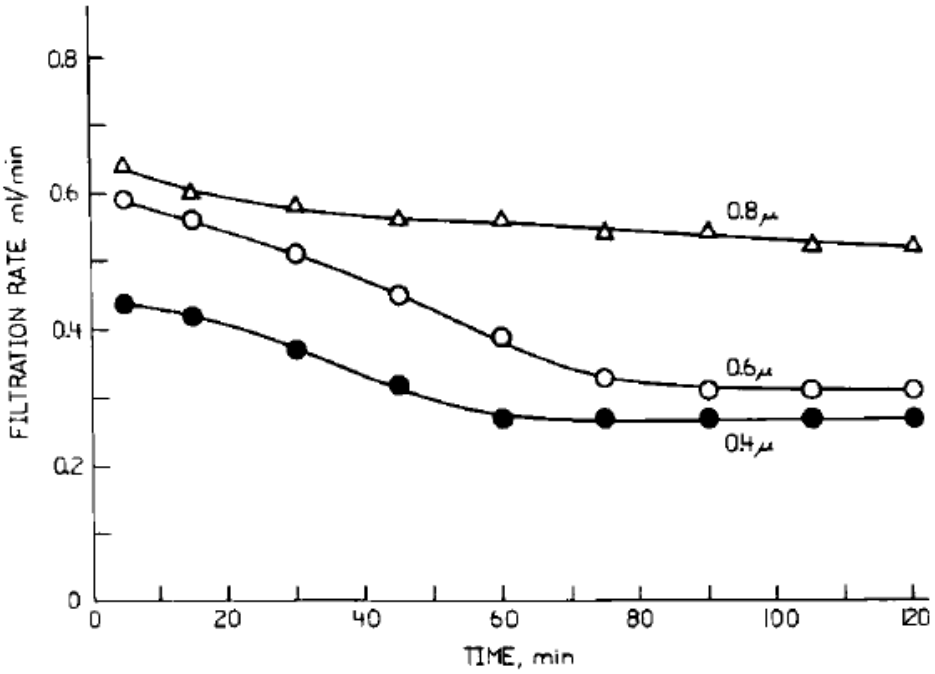

Figure 27 Comparison of three different membranes with different pore sizes used for plasma exchange technology (Friedman et al., 1983).

Bubble Point:

The bubble point test is the most common method for the measurement of membrane pore size. The pore sized is calculated based on the following equation:

$P = \frac{4\sigma cos\theta}{D}$, where σ is surface tension at the solvent/air interphase, $\theta$is liquid-liquid contact angle, P is the bubble pressure, and D is the capillary diameter. In order to calculate D, which is the pore diameter, a liquid with known surface tension and contact angle is used to wet the membrane. Once the membrane is wetted, it is positioned inside a housing and the pores are filled with a liquid, P=0. Then air is blown that force the liquid inside the pores to be pushed and as the pressure is increased, the more liquid will be removed from the pores, $P < P_B$. Once the pressure that remove all the liquid from the pores, air bubbles will be notice, $P = P_B$, and from the equation the pore size can be determined. Figure 28 shows the bubble point measurement (Cheryan, 1998, P.72-P.73).

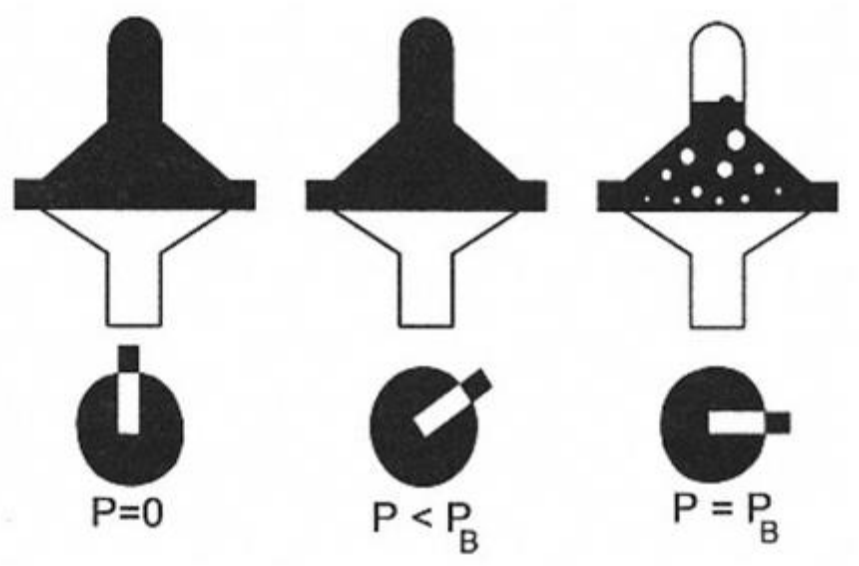

Figure 28 Bubble point method for pore size measurement (Cheryan, 1998, P.74)

Scanning electron microscope (SEM):

Direct observation is used for the measurement of membrane pore size using SEM. The SEM method can be used for membranes that have pores in the range of 0.05 µm to 2 µm, as illustrated in figure 29 (Cheryan, 1998, P.78).

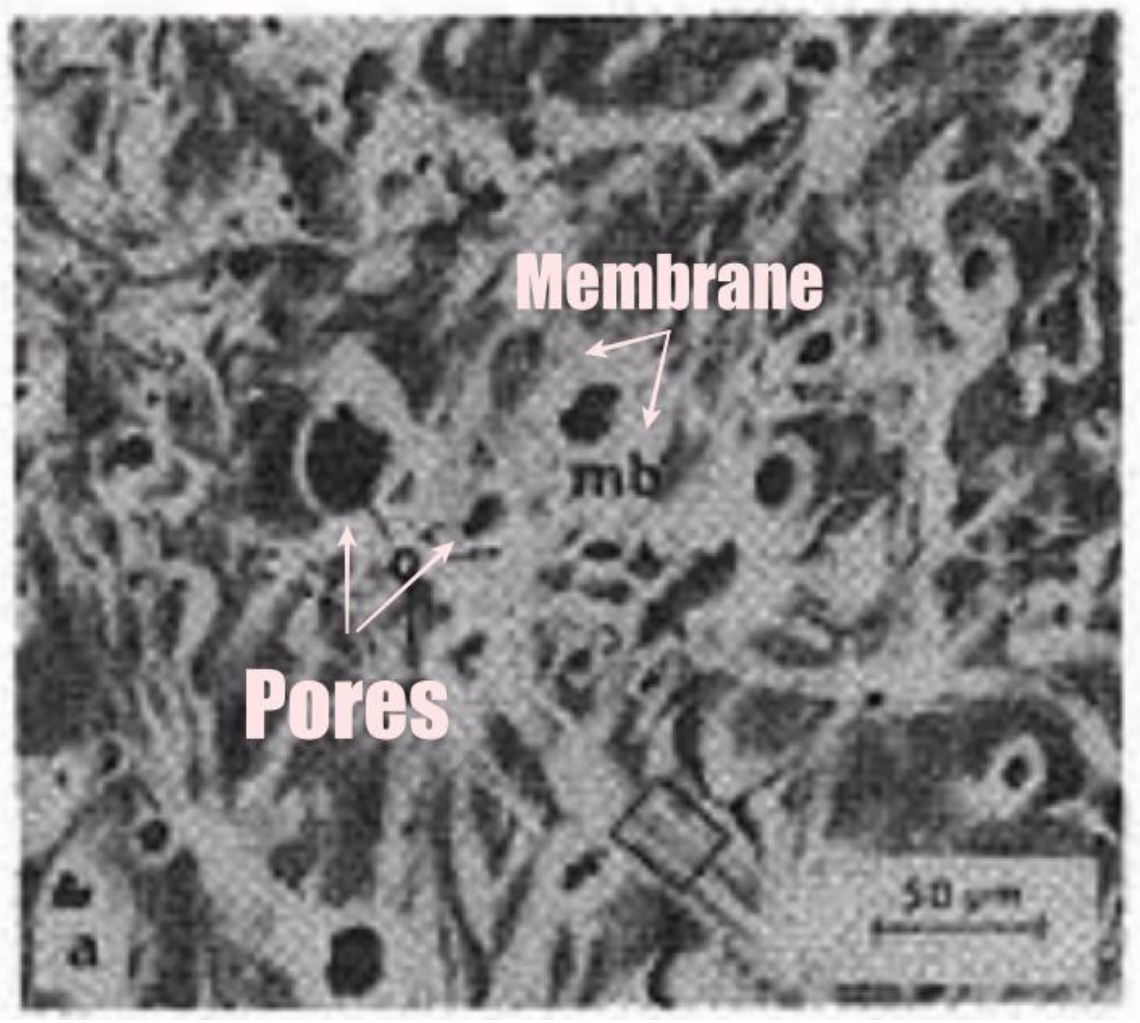

Figure 29 Membrane pore size captured using SEM (Cheryan, 1998, P.12)

Challenge test:

This test, which is also known as function measurement, is used to measure the ability of the membrane to pass the particles with different known molecular weight (MW) through the pores distribution. In UF, the challenge test is used to determine the MW cut-off (MWCO) that cannot pass through the membrane pores. Different proteins with known MWs are used in this test. Sodium chloride (MW: 58.5) and glucose (MW: 180) are used since they pass completely through membrane, while immunoglobulin (MW> 90000) is used since it is 100% rejected by the membrane. In the middle range, different proteins with different MW are used such as Inulin (MW:5000) and Myoglobin (MW:17800). Figure 30 illustrate the graph of MW distribution for different membranes (Cheryan, 1998, P.85, P.89-P.91).

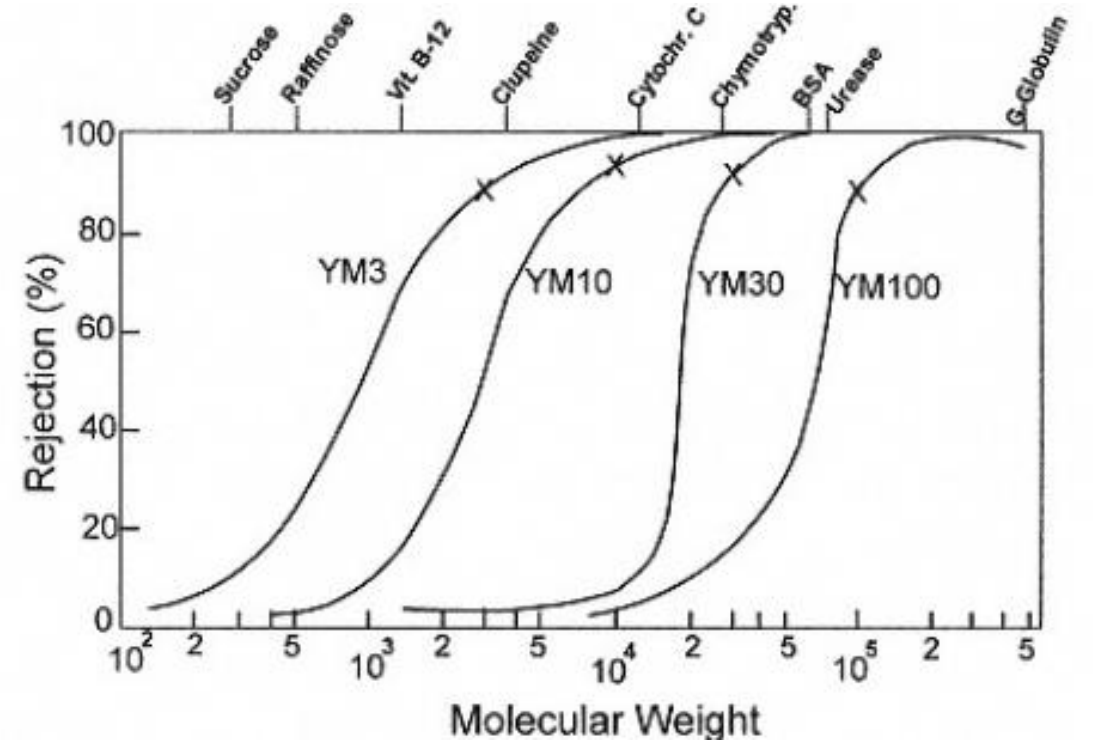

Figure 30 MW distribution for different UF membranes (Cheryan, 1998, P.93)

5.4.1.2 Wettability:

Wettability can be defined as the interaction between fluid and the membrane surface of the polymer. The contact angle is the technique that used to measure the wettability (Mulder, 1996, P.367). Different fields require different membrane wettability, for example, the membrane used for water distillation is hydrophobic. In PP, the membrane of interest should be hydrophilic. The reason for choosing hydrophilic membrane is to reduce the protein adsorption at the membrane surface. Also, these types of membranes are considered biocompatible with the blood. The contact angle is measure based on the Young's equation:

$$\gamma_L \cos\theta = \gamma_S - \gamma_{SL}$$

Where γ_L is the liquid-vapour, γ_S is the solid-vapour and γ_{SL} is the solid-liquid interfacial tension. Based on this equation, the contact angle θ can be calculated as illustrated in figure 31 (Xu et al., 2009, P.45).

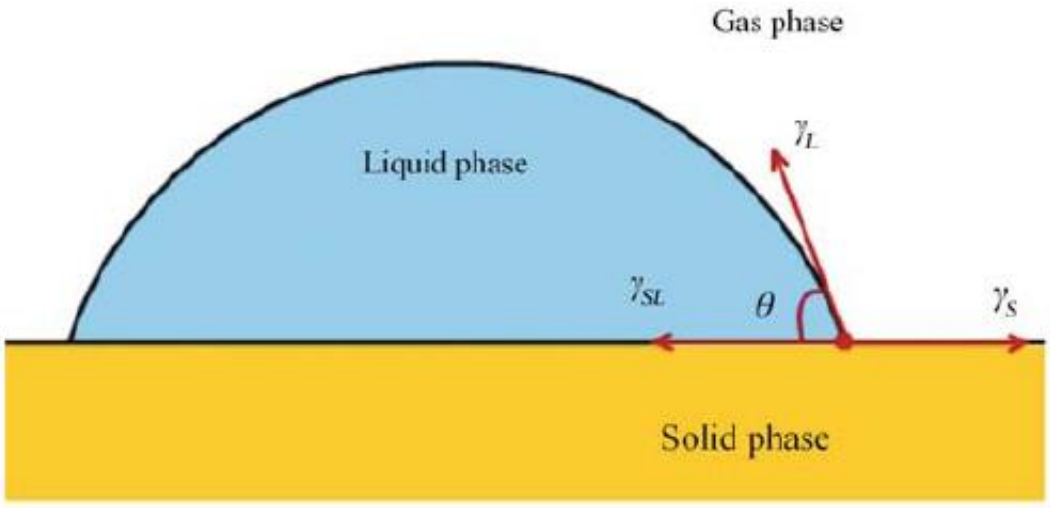

Figure 31 measurement of contact angle of a membrane (Xu et al., 2009, P.46)

The angle will indicate if the membrane is either hydrophilic or hydrophobic, as demonstrated in figure 32. If the angle is less than 90^0 , the membrane is hydrophilic, and if the contact angle is more than 90^0, the membrane is hydrophobic. The surface tension of the solid phase, the surface tension of the liquid and the interfacial tension are the three factors that affect the membrane wettability (Gugliuzza, 2016, Menzies and Jones, 2010).

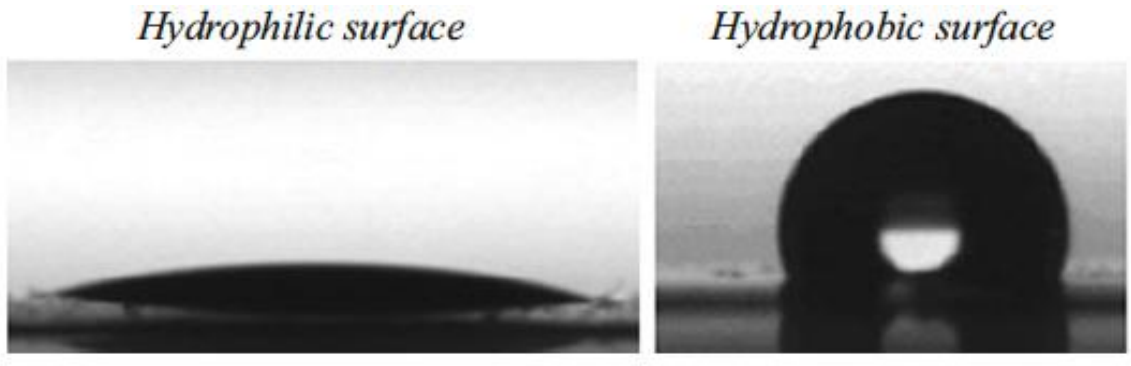

Figure 32 Liquid droplet on hydrophilic and hydrophobic membrane (Gugliuzza, 2016)

5.4.1.3 Flux and TMP:

As mention in section 2.3.1, in order to remove solute during PP, the driving force is the TMP. The TMP for PE membrane is calculated based on the following equation:

TMP $= \frac{P_{Bi}+P_{Bo}}{2} - P_F$, where P_{Bi} is the blood inlet pressure, P_{Bo} is the blood outlet pressure and P_F is the plasma filtrate pressure (Wiese, 2007, P.84). Flux can be defined as the removal of solute volume per time (ml/min). The relationship between flux and TMP is consider linear and non-linear. To clarify, as the TMP rises, the flux rate rises linearly until the flux reaches a plateau. This relationship is illustrated in figure 33. The

plateau in the TMP and filtration flux curve is caused by concentration polarization, which will be discussed in section 5.4.1.4. In region 2 (figure 33), once the plateau is reached the relationship between TMP and flux is stable, the flux will remain the same despite further increase in TMP, but the increase in pressure could cause hemolysis (Gurland et al., 1996, P.475, Wiese, 2007, P.84). The knee point, where the linear line starts to curve, is the point selected for the optimum TMP that will give reasonable filtration rate. (Allegrezza et al., 2010, P.126, Wiese, 2007). For plasmapheresis, for the first 50 mmHg, the flux increases linearly, after that it hits a plateau at 70 mmHg (Jaffrin et al., 1992).

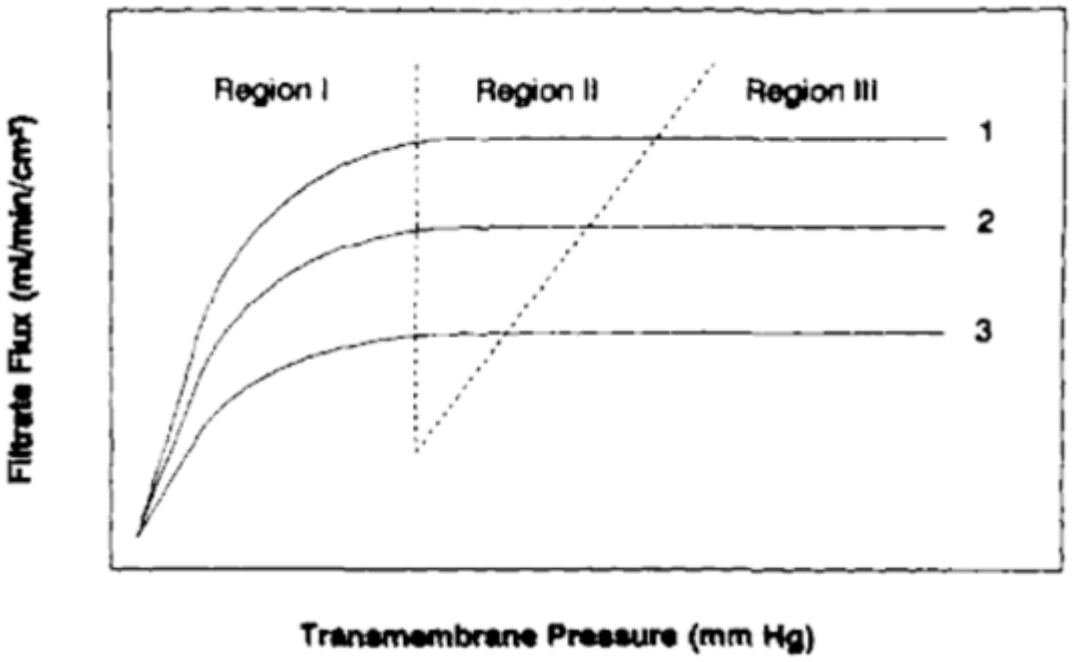

Figure 33 Relationship between TMP and flux rate (Gurland et al., 1996, P.475)

5.4.1.3.1 Critical flux:

As mentioned in section 5.4.1.3, the knee point of the flux TMP curve is selected for the optimum operation. This point is known as the critical flux. The critical flux is defined by Miller et al. (2014) as "the maximum flux that can be achieved with slight or negligible fouling". The critical flux is measured using different methods such as flux-TMP curve and stepwise method measurements (Bacchin et al., 2006). In the flux-TMP curve, the measurement of critical flux is either by applying measured the TMP and measure the flux or apply a fixed flux and measure TMP while recording the measured values. Both methods will produce the flux-TMP curve, where the critical flux can be measured (Bacchin et al., 2006). The stepwise measurement method simply is by alternating between increasing and decreasing TMP while recording the flux for measurement of critical flux (Espinasse et al., 2002).

5.4.1.4 Membrane Fouling:

Wang et al. (2017) defines membrane fouling as "initiated by the accumulation of inorganic, organic, colloidal, and biological species on the membrane surface and/or within its pores. It results in a reduced flux, a rapidly increasing transmembrane pressure, and possibly deterioration of mechanical properties". Generally speaking, there are three stages in the reduction of flux. In the first stage, the flux is reduced due to the concentration polarization layer at the beginning of the filtration process. As the proteins continue to deposit at the membrane surface and pores there is an increase in membrane resistance due to the decrease in pore size, the flux will further decreased, representing the second stage. In the final stage, the pores are completely filled with the proteins that cause complete layers to build on the membrane surface, decreasing the flux rate slowly. Figure 34 demonstrates the three stages with time (Marshall et al., 1993).

Since in PP there is an interaction between membrane surface and blood components, fouling will occur. Protein surface interaction and concentration polarization are the may cause of membrane fouling. The cause of the concentration polarization is independent of the membrane properties such as pore size and materials, but they naturally occur because the removal of the solution from the solvent leads to the concentration difference as illustrated in figure 35. As a result, the solvent will gradually start to create a layer on the membrane surface. Concentration polarization can be reduced by inducing shear stress at the membrane surface, this will be discussed in section 5.4.1.5 (Sun et al., 2003). The process of concentration polarization is reversible. Protein adsorption at the membrane surface affects the membrane material and its porosity. Fouling occurs due to the protein being absorbed in the membrane pores, which is non-reversible. As a result,

the flux decreases (Sun et al., 2003). Figure 36 demonstrates the different protein adsorption blockages at the membrane surface and pores (Saxena et al., 2009).

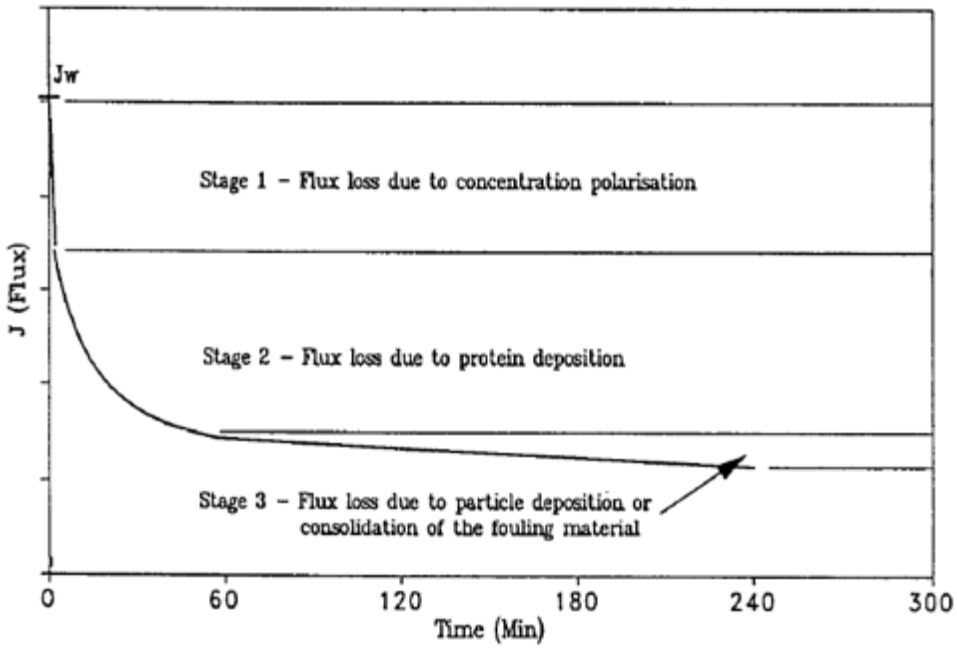

Figure 34 Stages of flux reduction with time (Marshall et al., 1993)

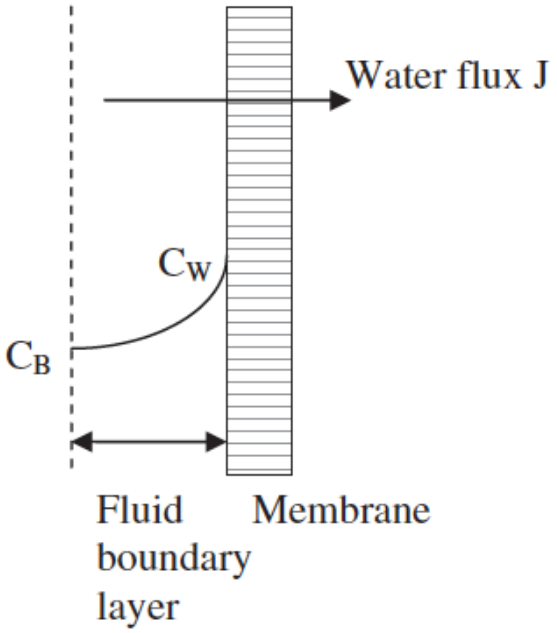

Figure 35 Concentration polarization formation (Charcosset, 2012, P.80)

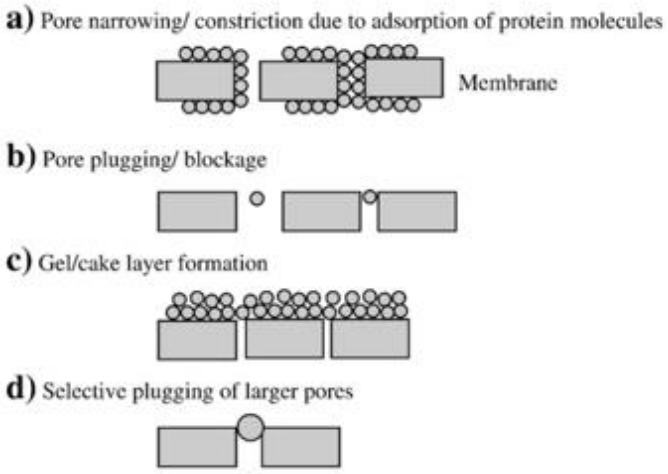

Figure 36 Different pore blockage schematic (Saxena et al., 2009)

5.4.1.5 Flux enhancement:

As mentioned in section 5.3.1.4, fouling will occur during the removal of the plasma. However, there are some methods that can minimize fouling and increase the filtration rate with time. These methods focus on inducing and increasing shear stress (Saxena et al., 2009). Before reviewing the methods of inducing shear stress, the effect of shear stress on membrane flux will be discussed.

5.4.1.5.1 Relationship between shear stress and flux:

As mentioned in the section 5.4.1.4, membrane fouling occurs due to protein deposition at the surface of the membrane that leads to pore blockage. As a result, the filtration flux reduces with time. So, by generating shear stress at the membrane surface, the process of membrane fouling can be delayed. High shear stress leads to a decrease in membrane fouling (Jaffrin, 2011). However, there are limits to the increase in the rate of the shear stress. Grandison et al. (2000) demonstrated that the increase in the shear stress leads to an increase in the flux initially. However, the flux decreases and the rate of reduction increases with a further increase in the shear stress. The cause of this was due to the rate of the difference between the deposited and removed particles. Also, Du et al. (2019) have investigated the effect of shear stress on migration of particles. They concluded that high shear stress helps to remove the large particles that leads to small particles depositing at the membrane pores. Eventually, the fouling of the membrane is enhanced.

5.4.1.5.2 Dean vortices:

Dean vortices is defined by (Jaffrin, 2011) as "helicoidal flows created by centrifugal forces in curved channels, such as coiled or helically twisted tubular membranes". The generated Dean vortices have the ability to reduce the polarization layer that resulted in increasing in filtration rate (Jaffrin, 2011). Mallubhotla and Belfort (1997) have reported that the usage of bend tube, as shown in figure 37, produce flow instability, and Dean vortices. The results showed an increase in the flux by up to 43% compared to the stable flow. Moreover, Najarian and Bellhouse (1996) have investigated the effect of combining a screw-threaded inset, illustrated in figure 38, and oscillatory flow for plasmapheresis using bovine blood. The combined method increased the flux by 7.5-fold compared with the non-oscillatory flow.

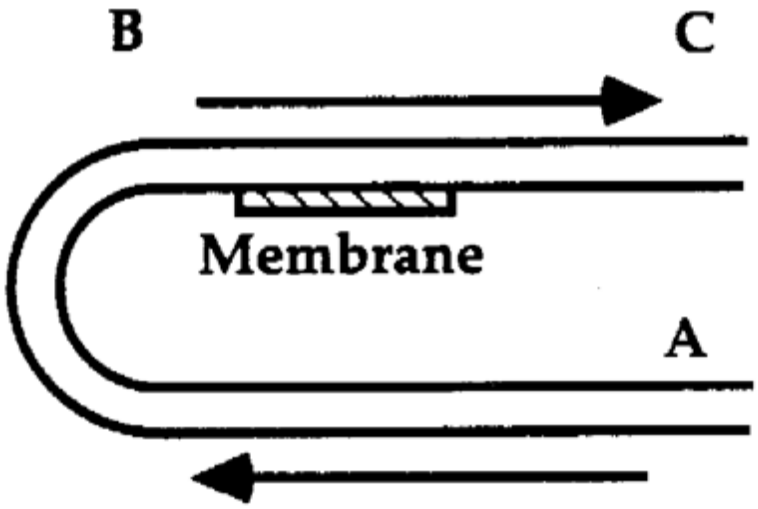

Figure 37 U-bend tube (Mallubhotla and Belfort, 1997)

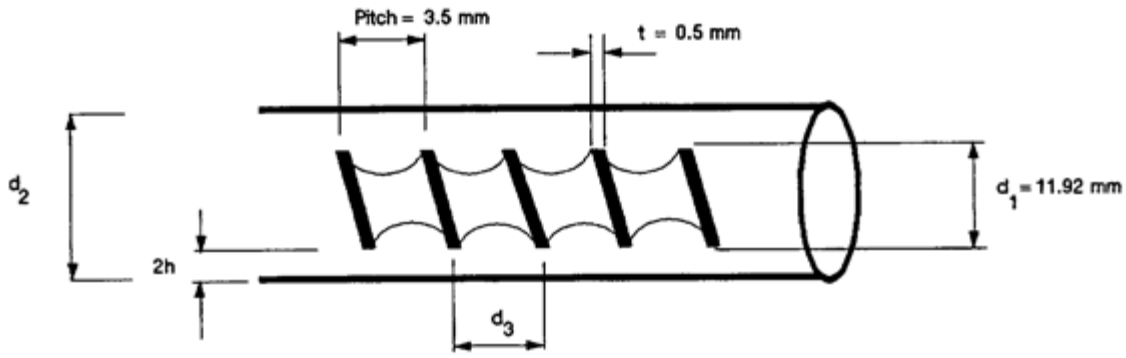

Figure 38 screw-threaded insert (Najarian and Bellhouse, 1996)

5.4.1.5.3 Pulsatile flow:

Pulsatile flow has demonstrated an improvement in flux filtration rate. Bellhouse et al. (1973) have illustrate the effect of pulsatile flow in an oxygenator system as seen in figure 39. The two pulsatile pumps were used in conjunction with other methods of generation of secondary flow. One pump was placed at the inlet while the other pump was placed at the outlet. The system known as interpulse has been used in the hospitals, however, due to the complexity, the interpulse has been withdrawn from the market (Jaffrin, 2011).

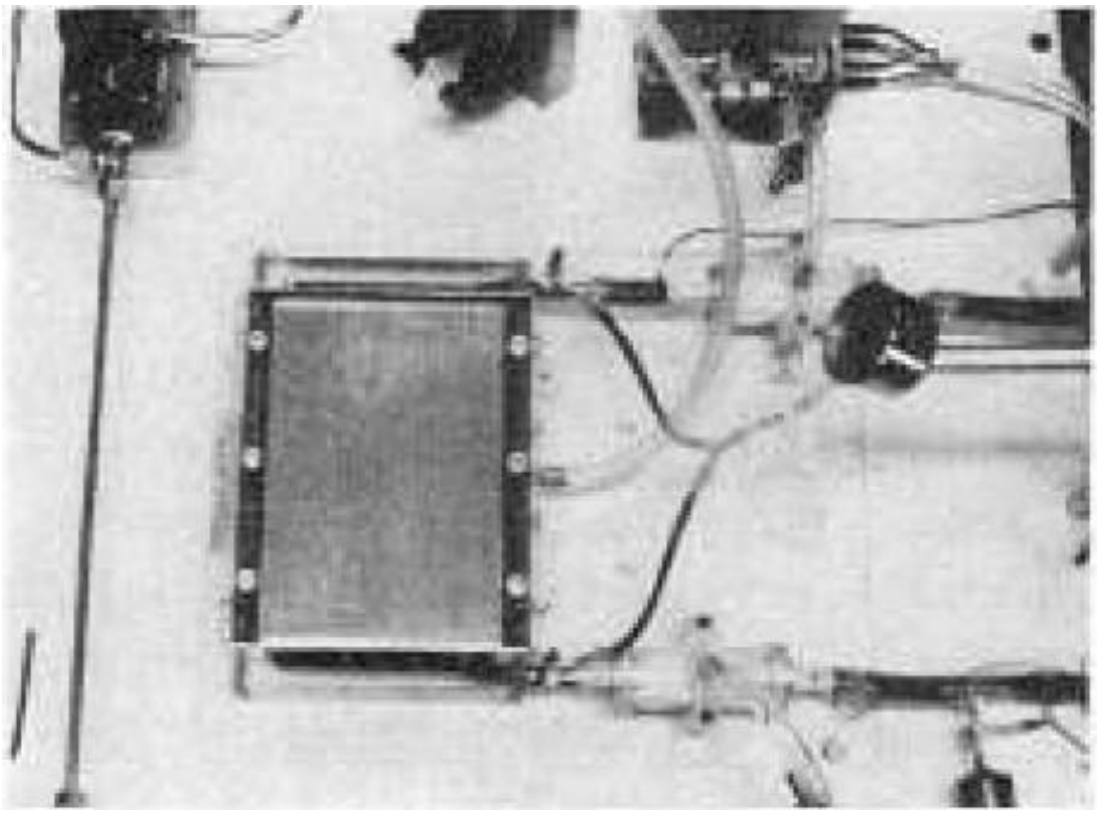

Figure 39 Dual pumps oxygenator system (Bellhouse et al., 1973)

Galletti et al. (1983) reported that the usage of oscillating blood flow has shown an enhancement in the plasma removed from the blood. They used a flat-sheet membrane with pore size of 0.4µm, and the oscillatory pulses were generated using the Scotch-yoke mechanism with different frequencies. In steady-state flow, the filtration rate was 0.5 ml/min, and once the oscillatory flow was initiate, the plasma flux was 1.5 ml/min (200% improvement), as illustrated in figure 40.

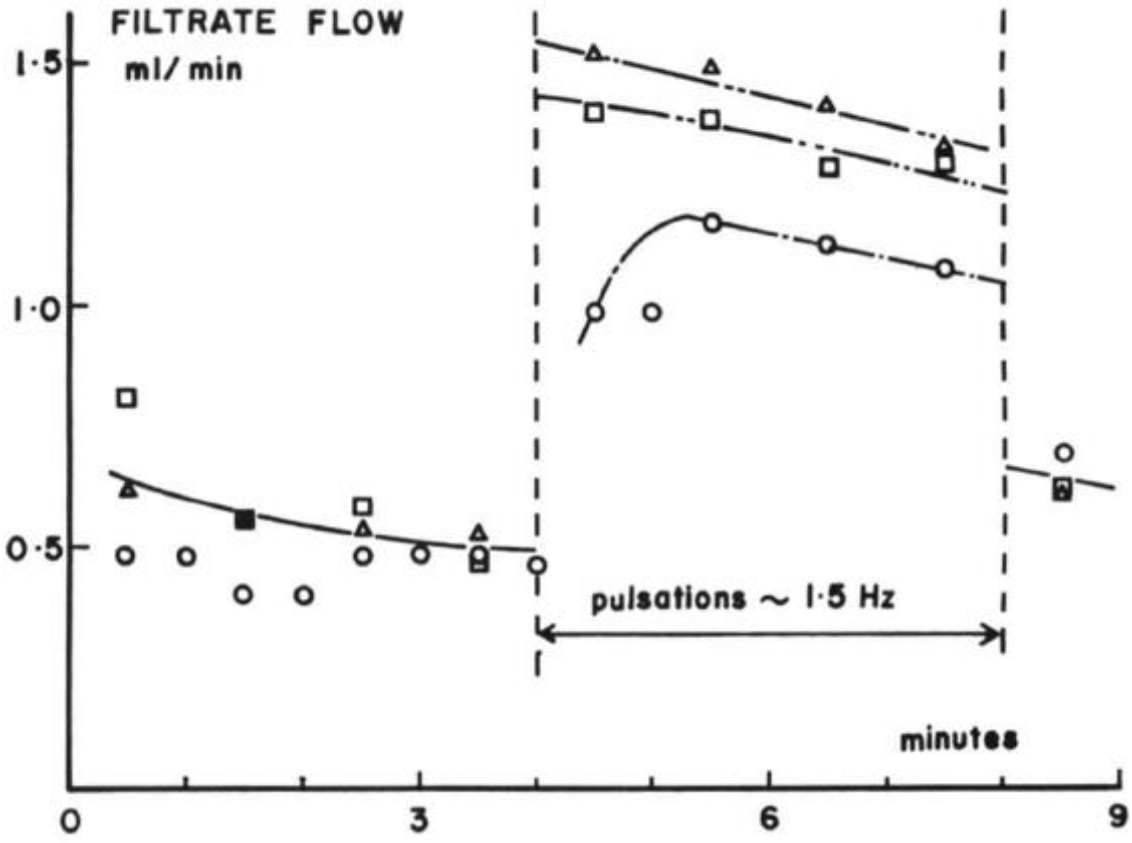

Figure 40 steady-state for 4 minutes followed by 4 minutes of pulsation flow. The last minute was continuous flow (Galletti et al., 1983)

5.4.1.5.4 Protuberances:

In order to minimize the formation of concentration polarization on the layer of the membrane, protuberances (figure 41) are used in order to generate a secondary flow. Moreover, to effectively improve the flux, the flow disturbances should occur at the interface between membrane and protuberance. Despite the usage of protuberances, the disturbances that they cause in the flow is insufficient (Belfort et al., 1994). However, there are three techniques for increasing the effectiveness of the protuberance. First, the protuberance should be placed in area with high velocity so the secondary flow is increased. Second, by placing flat sheet membrane on furrows. Lastly, the location of the protuberances should be at fixed distance from the membrane, as seen in figure 42 (Belfort et al., 1994).

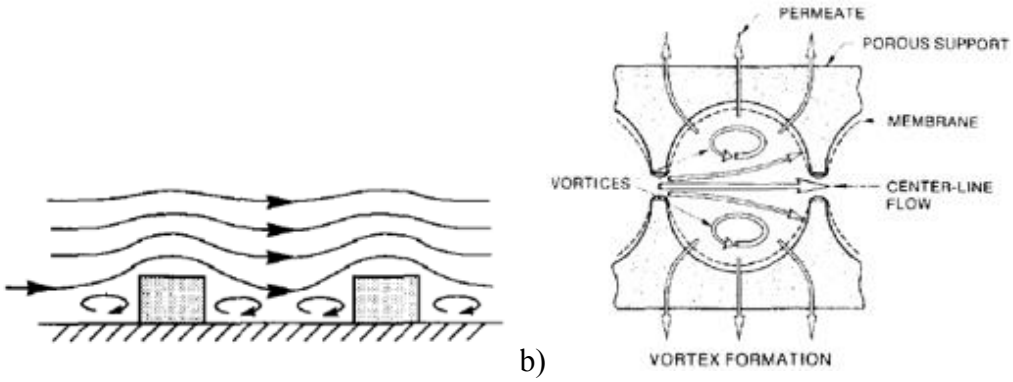

Figure 41 Protuberances. A) square shape, B) furrows (Belfort et al., 1994)

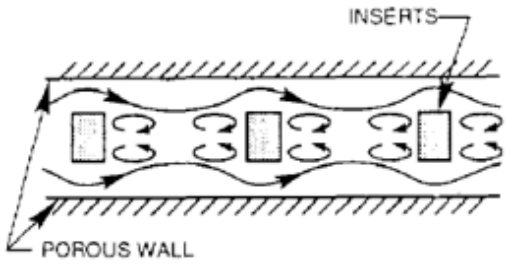

Figure 42 Protuberance distanced from membrane (Belfort et al., 1994)

The protuberance and furrows have been used in medical devices. Bellhouse et al. (1973) have used the furrows design, in addition to oscillatory flow, in an oxygenator system (figure 43). Moreover, the protuberance, in combination of oscillatory flow, has been used in a plasma separation device that has been designed by Millward et al. (1995). Figure 44 demonstrates the deflector in order to create instability in the flow for an increase in the plasma filtration. In the plasmapheresis design, the distance between deflectors was assessed at 4 mm, 16 mm and 24 mm. They found that the highest secondary flow generated when the spacing between deflectors was 4 mm compared with the 16 mm that caused the number of the deflectors to decrease by 73%, but the flux only decreased by 40% that indicate the secondary flow improve the filtration rate. For the 24 mm spacing, the flux rate is reduced.

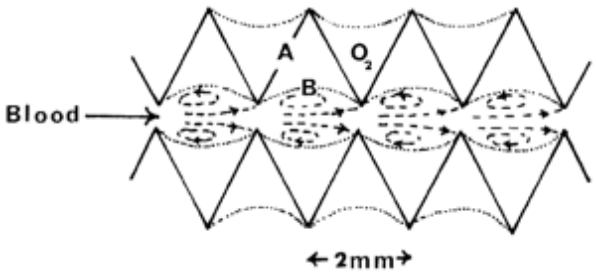

Figure 43 Furrows used in oxygenator (Bellhouse et al., 1973)

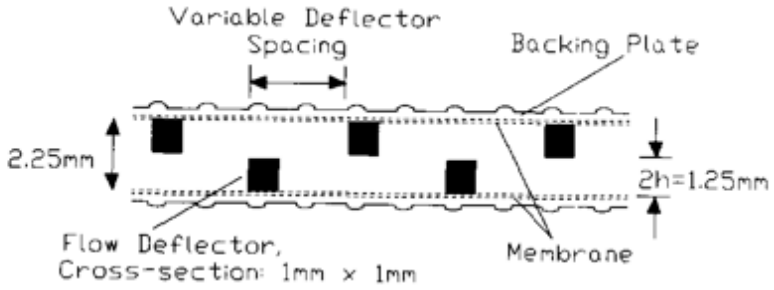

Figure 44 Protuberance used in the plasma separation device (Millward et al., 1995)

5.4.1.5.5 Bubbles:

The use of bubbles with different shapes has been investigated in order to increase the flux by creating vortices at the flat end of the bubble. Taha and Cui (2002) have studied the effect of vortices created by the Taylor bubble using CFD. As demonstrated in figure 45, the secondary flow is generated at the flat end of the bubble and improves the flux in the membrane. In addition, Wei et al. (2013) used CFD in order to explore the effect of bubble for the enhancement of the flux in membrane, the bubble formed was large spherical shaped bubble with tiny bubbles as seen in figure 46. The result of the CFD illustrate that the maximum shear stress, red region in figure 47, occur at the flat part of the spherical shape bubble.

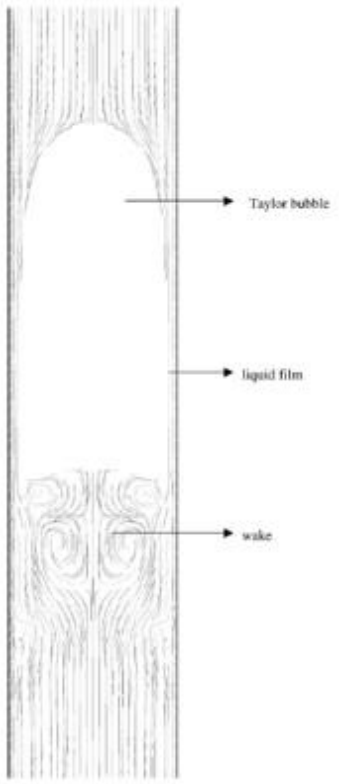

Figure 45 Secondary flow generated inside the membrane (Taha and Cui, 2002)

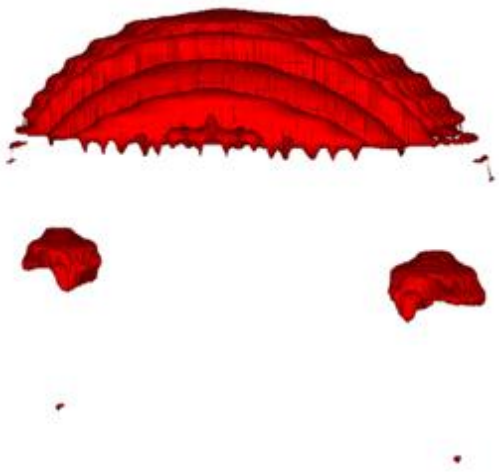

Figure 46 CFD of the bubble (Wei et al., 2013)

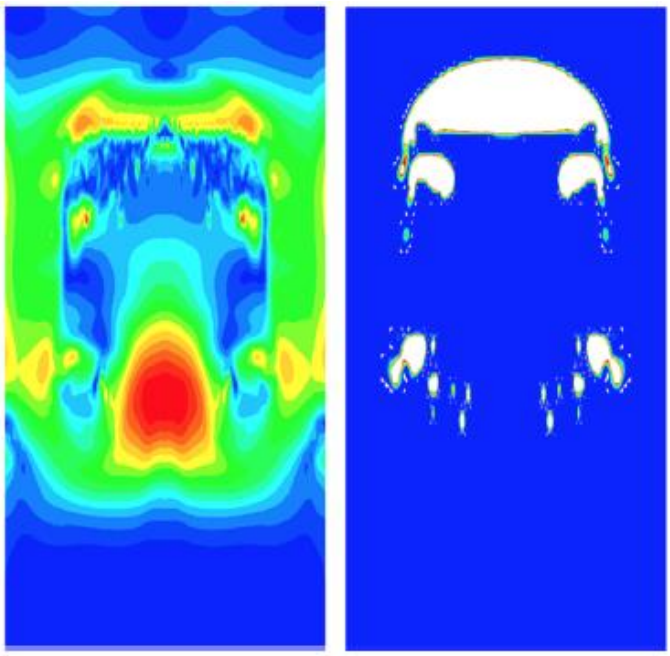

Figure 47 CFD shear stress result that occur due to the spherical shape bubble (Wei et al., 2013)

5.5 Secondary flow plasmapheresis:

In this section, plasmapheresis methods used for the induction of secondary flow will be discussed. As mentioned in the 5.3.1.5.3, Galletti et al. (1983) have used oscillatory flow that increased the plasma removal by 200%. Millward et al. (1995) flow deflectors arranged as illustrated in figure 44 in both ends that contacted the membrane in order to generate vortex waves. In addition, they used oscillatory flow that is generated using by pump bags that generate antiphase frequency in the range of 2-8 Hz. This was placed in the side of the rig, as shown in figure 48. This method has improved the filtration rate of the plasmapheresis by a factor of 3.5 compared with an un-deflected rig. Also, in addition to the deflectors, the use of the oscillatory flow, caused the flux rate to reach 0.1 cm/min (approximately 18.2 ml/min).

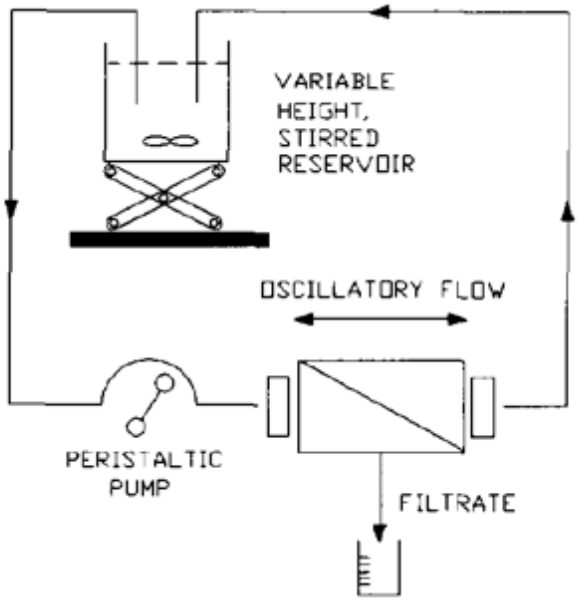

Figure 48 Schematic of the plasmapheresis setup. The pump bags are placed on the side of the rig (Millward et al., 1995)

Najarian and Bellhouse (1996) have developed a test rig that is able to improve the filtration rate of plasmapheresis. The test rig consisted of oscillatory pump bags with frequencies in the range of 0-10 Hz placed on both side of the rig (as shown in figure 49). Moreover, a helical insert, (figure 38) was used to generate vortices in the blood that flowed inside the rig. In optimum operating conditions, the flux rate was 0.06 cm/min (2.88 ml/min).

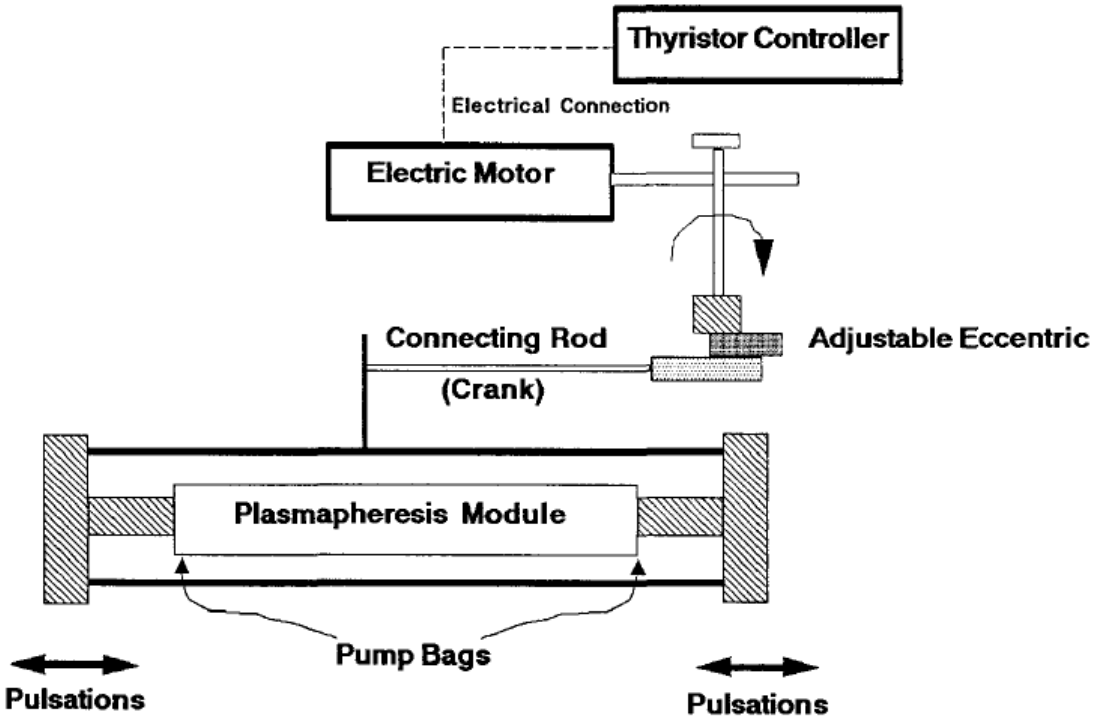

Figure 49 Schematic diagram of the test rig that illustrate the generation of the pulsation (Najarian and Bellhouse, 1996)

5.6 Device Concept:

The concept of the device is to effectively separate the plasma from the blood through the membrane. As mentioned in section 5.4.1.4, due to the concentration polarization, the proteins accumulate on the membrane surface. As a result, cake layer form that cause the reduction in filtration process with time. As a result, in order to increase the efficiency of the plasma separation and reduce the cake layer formation, the rig should employ methods to create disturbance in the blood flow. The development of the rig is divided into three phases.

1- CAD design and CFD modelling
2- 3D print of the first prototype that include testing of different membranes.
3- 3D print of the final prototype with the automation system.

Computer modelling will give an insight on the behavior of the blood flowing inside the rig that includes the secondary flow promoters. Also, the wall shear stress can be visualized and measured.

5.6.1 CAD design and CFD modelling:

The design concept was to combine three methodologies of flow disturbance described in section 5.3.1.5. The three techniques are U-bends to the create of Dean vortices, the use of flow deflectors similar to the ones that have been employed in the plasmapheresis, and the semi-circle bubble. However, the semi-circle bubble has been replaced by a semi-circle solid, to prevent risk of air embolism. The introduction of air bubbles into the blood stream can cause activation of the inflammatory response and blood clotting (Papadopoulou et al., 2014). As mentioned in 5.4.1.5.4, for effective generation of secondary flow, the distance of the protuberance should be at fixed distance. The angle

selected is 180 degree since it makes U shape. The number of U-bends is chosen to increase blood-membrane contacting area. As a result, the design is selected based on these criteria.

CAD was performed using PTC Creo Parametric 3.0 (PTC, Boston, USA) and the file was saved as STP format in order to export to the CFD modelling program. The CFD modelling was performed using Ansys Workbench Fluent 15.0 (Ansys, Canonsburg, USA). First CFD, modelling of the 2D model is shown in figure 50. In this model, the flow deflectors are not used due to the limitation of the 2-dimensional space, because in 2D model, only x-axis and y-axis plane can be drawn. The flow deflectors is drawn in the z-axis plane.

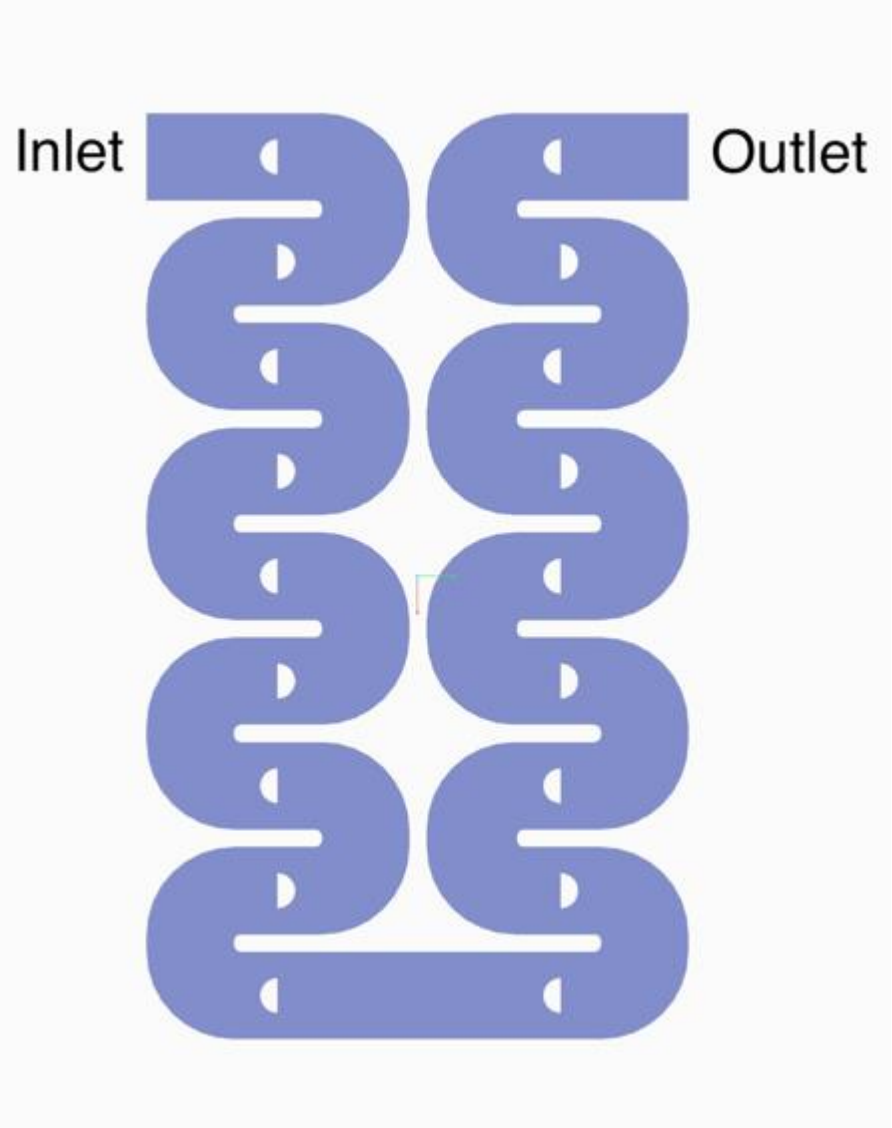

Figure 50 2D model of the part of the rig

In fluent, the model is initially meshed (figure 51). Since the blood is non-Newtonian, the model selected is Carreau model (Byun and Rhee, 2004):

$$\eta = \eta_\infty + (\eta_0 - \eta_\infty)[1 + (\lambda\gamma)^2]^{(q-1)/2}$$

where η is the coefficient of viscosity and γ is the shear rate

Where $\eta_\infty = 0.00345\ Pa\ s$, $\eta_0 = 0.056\ Pa\ s$, $\lambda = 3.313\ s$ and $q = 0.3568$.

In Ansys fluent, the density of the blood is required, and the blood density is 1050 kg/m^3 (Siebert and Fodor, 2009).

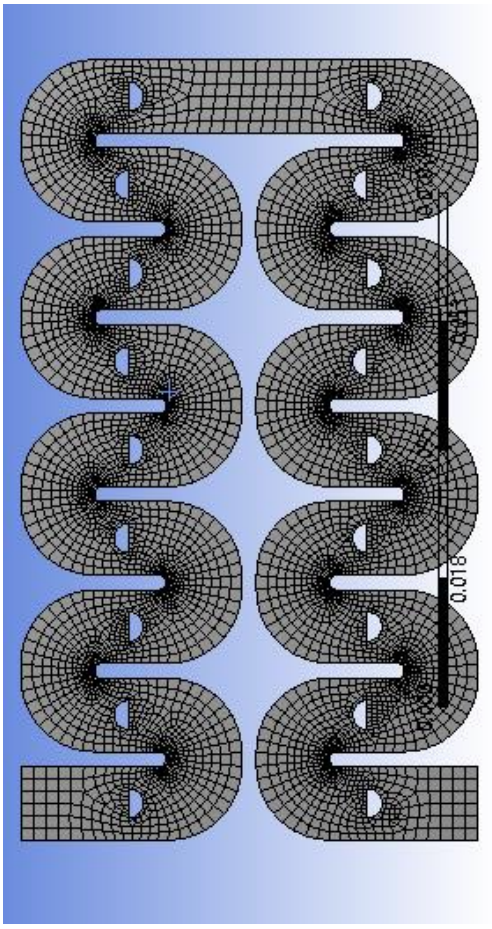

Figure 51 2D mesh of the exported 2D design

The model selected for the measurement of wall shear stress is the k-ε renormalization group (RNG) with enhanced wall treatment. The selection of the k-ε RNG model is based on the recommendation of Zhang et al. (2013). The margin of error in the k-ε RNG with enhanced wall treatment is smaller compared to other k-ε models since this model has higher accuracy. The boundary conditions for the inlet and the outlet are velocity-inlet and outflow, respectively. For the inlet velocity, a user defined function (UDF) file was created in C language to generate a square wave that resembled the flow pump. The following equation was used for the calculation of velocity from the known parameters, the flow rate (150 ml/min) and the diameter of the tube (4 mm):

$$V = \frac{Q}{A}$$

As a result, the velocity is equal to 0.2 m/s. Figure 52 shows the profile of the inlet velocity. From clinical prospective, the selected blood flow rate in plasmapheresis is 50-250 ml/min. So, the average of this range is selected (Wiese, 2007, P.73).

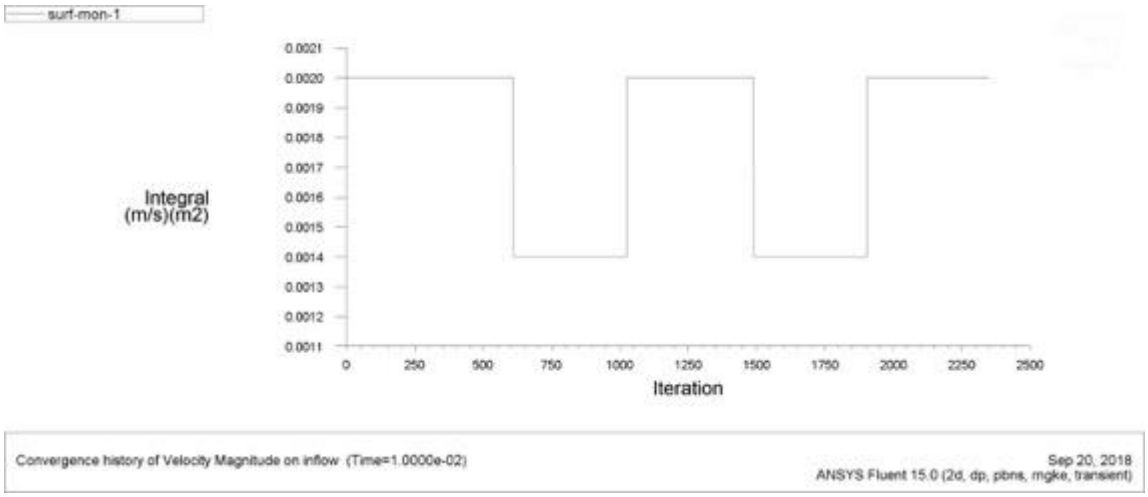

Figure 52 The square wave generated from the UDF that show the change in the velocity with time

In order to capture the changes in blood flow and wall shear stress, the time step size was selected to be 0.01 seconds and the number of time steps was 500. The time steps will run the solver for 500 time with an increment of 0.01 second for the total time of 5 seconds. Based on the boundary conditions selected for the CFD modelling, the results of the modelling are shown in figure 53, 54, 55 and 56. These show the velocity, turbulent kinetic energy, wall shear stress changes, and blood flow in the rig, respectively.

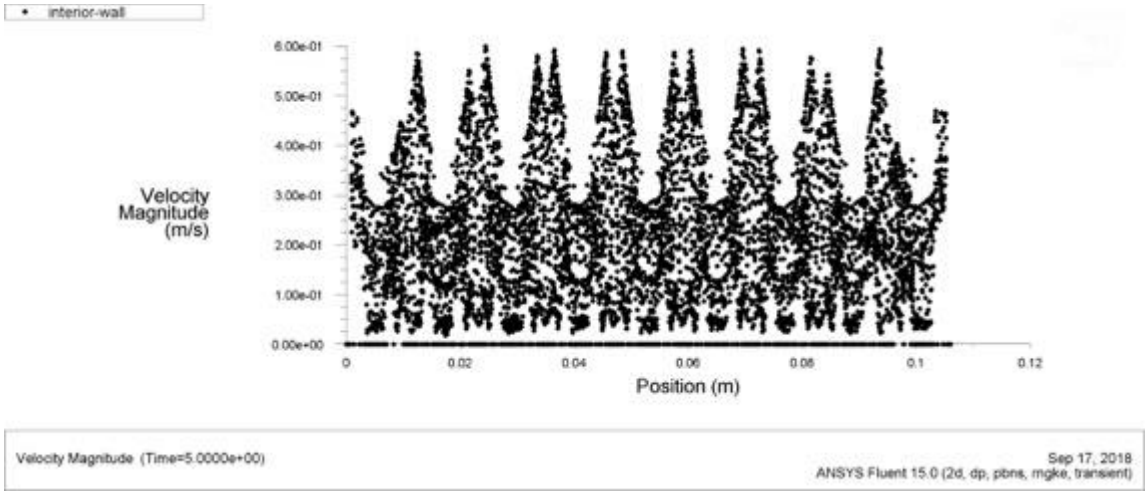

Figure 53 Blood velocity plotting through the length of the rig

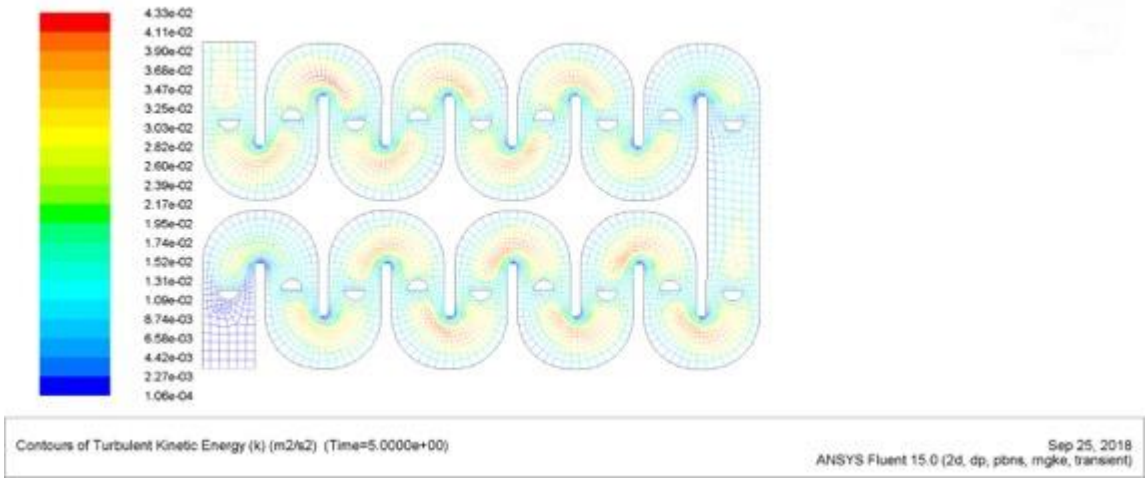

Figure 54 Turbulent kinetic energy contour

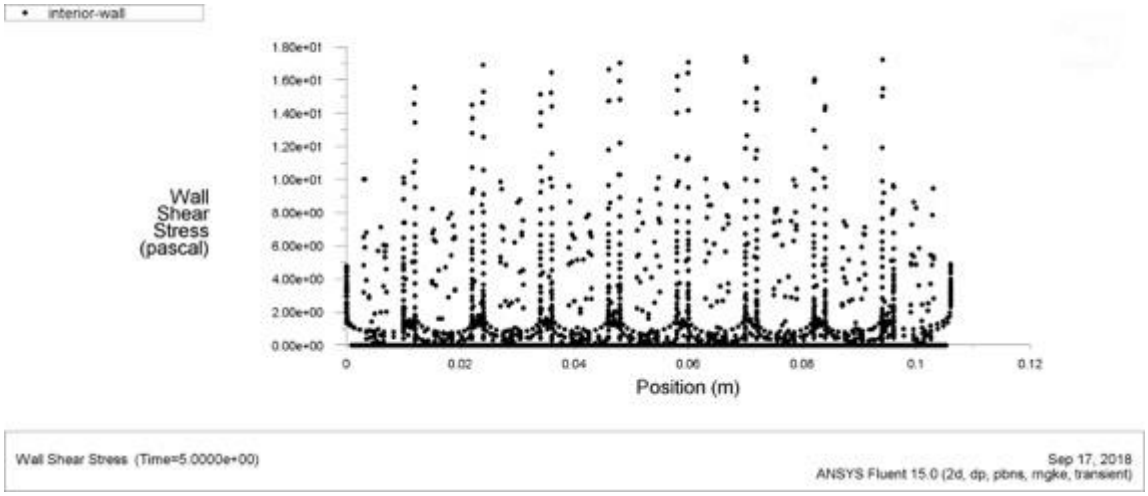

Figure 55 Wall shear stress created as the blood flow is distributed due to the flow deflectors

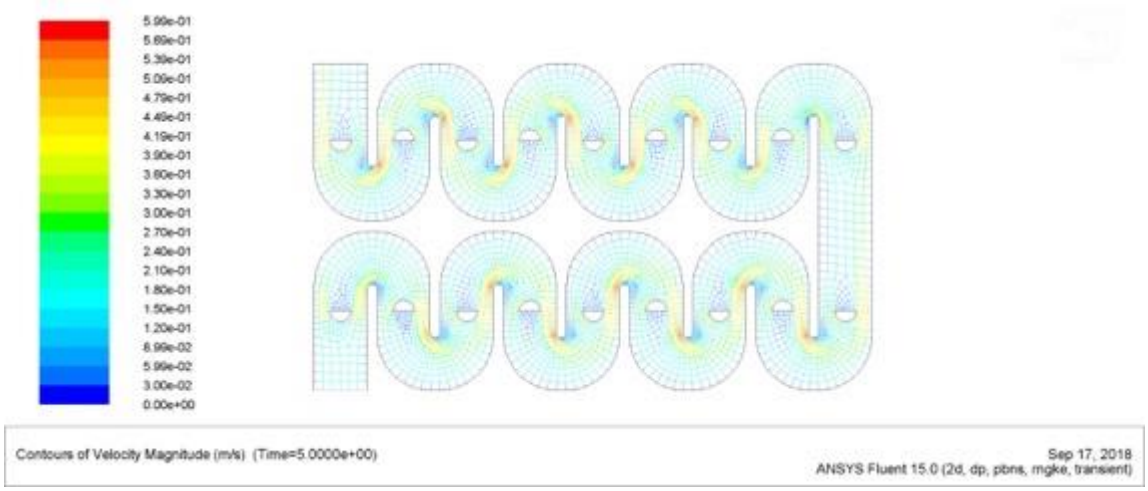

Figure 56 Blood velocity change as it flows through the rig

The wall shear stress value peaks when blood make a 180º turn. Moreover, as blood passes through the semi-circle, the wall shear stress increases. Based on the results of the 2D design, a 3D model, figure 57, was designed that contained the flow deflectors in order to investigate their behavior on blood wall shear stress. The flow deflectors height is chosen based on Millward et al. (1995), where the height in their rig is 1 mm. Different hights and distance were tested as seen in table 6 and 7. However, the distance between the deflectors is 6 mm instated of 4 mm because of the presentation of semi-circle shape. Moreover, the height selected is 1 mm, so the blood flow in a path of height of 1 mm. The reason for this selection is to minimize the jet effect caused by the reduction in the flow path due to the sudden increase in the velocity.

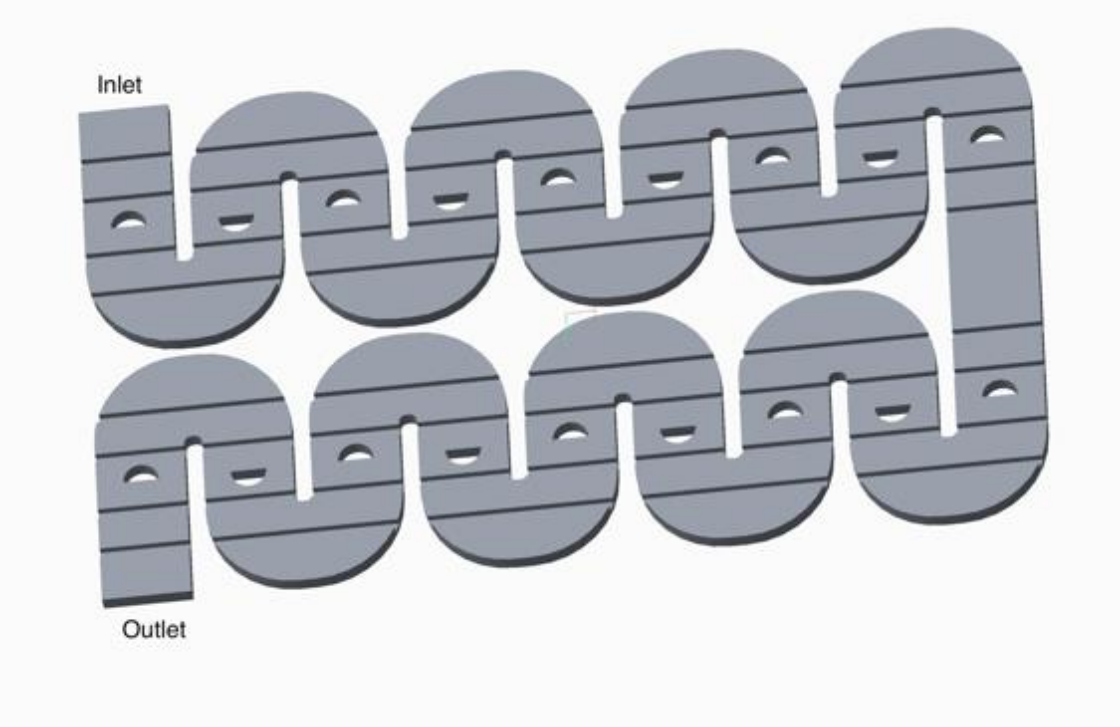

Figure 57 3D model that represent part of the device

Distance	2 mm	4 mm	6 mm	8 mm
Shear stress (Pa)	5.03	6.27	5.26	4.6

Table 6 Average shear stress for different gap distance

Height	0.6 mm	0.8 mm	1 mm	1.2 mm	1.4 mm
Shear stress (Pa)	3.13	3.93	5.25	7.59	12.17

Table 7 Average shear stress for different gap height

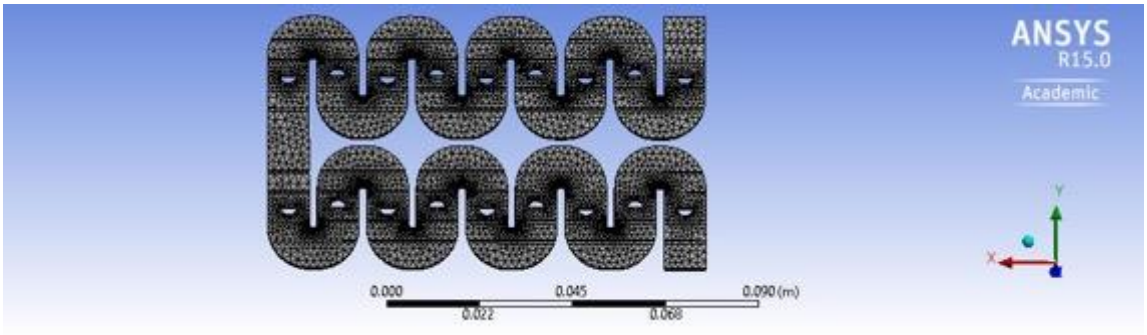

Figure 58 3D mesh of the STP file

Once the model was exported into Ansys, the same parameters applied to the 2D model were used in the 3D model. Figure 58 shown the meshed of the 3D model. The results of the modeling are represented in the figures 59, 60 and 61.

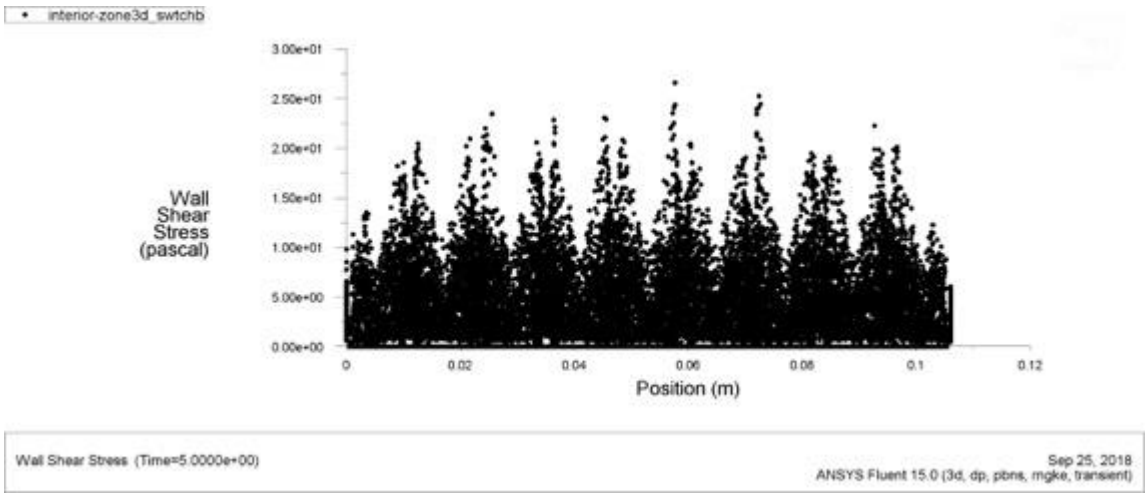

Figure 59 Wall shear stress plotting as the blood flows inside the device

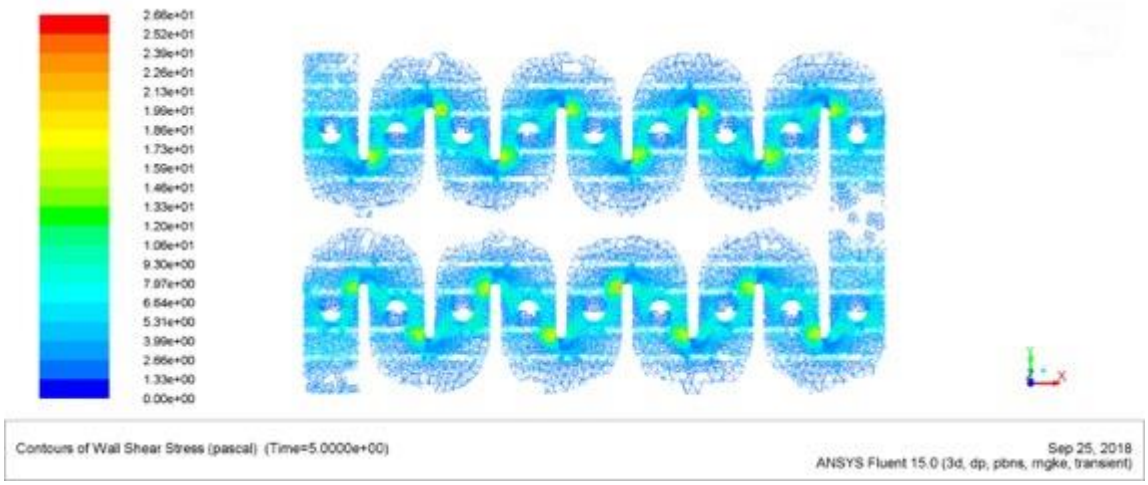

Figure 60 Wall shear stress contour inside the rig

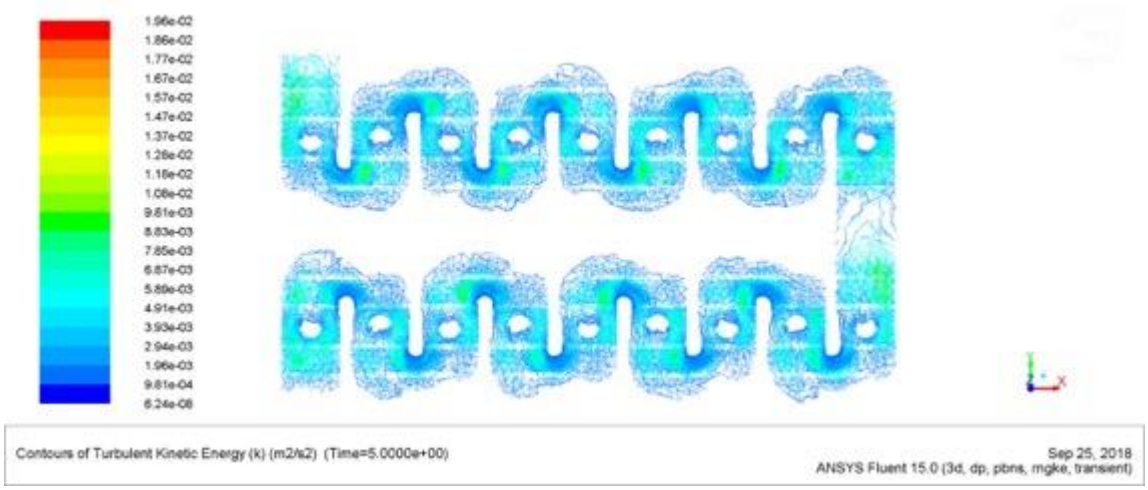

Figure 61 Turbulent kinetic energy contour

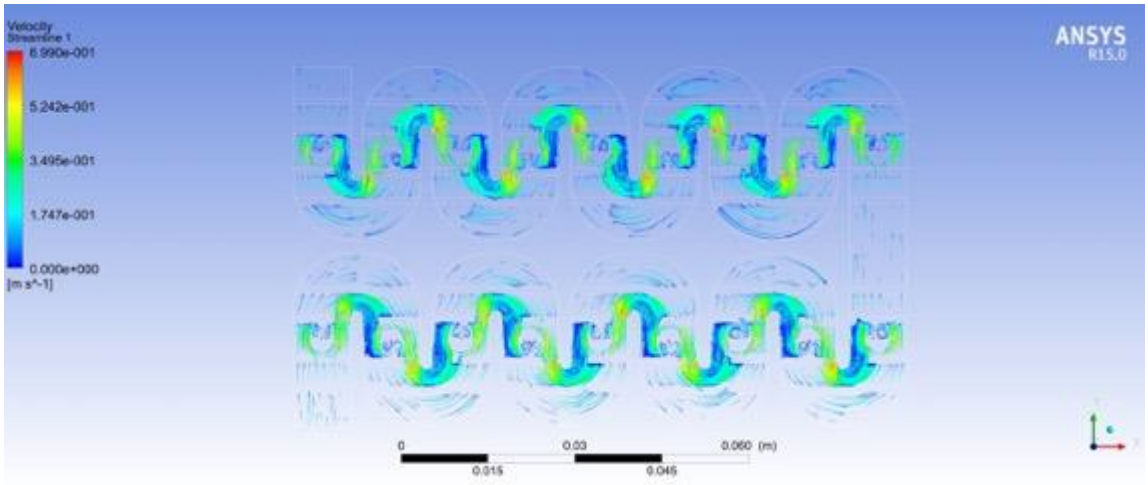

Figure 62 Velocity streamlines

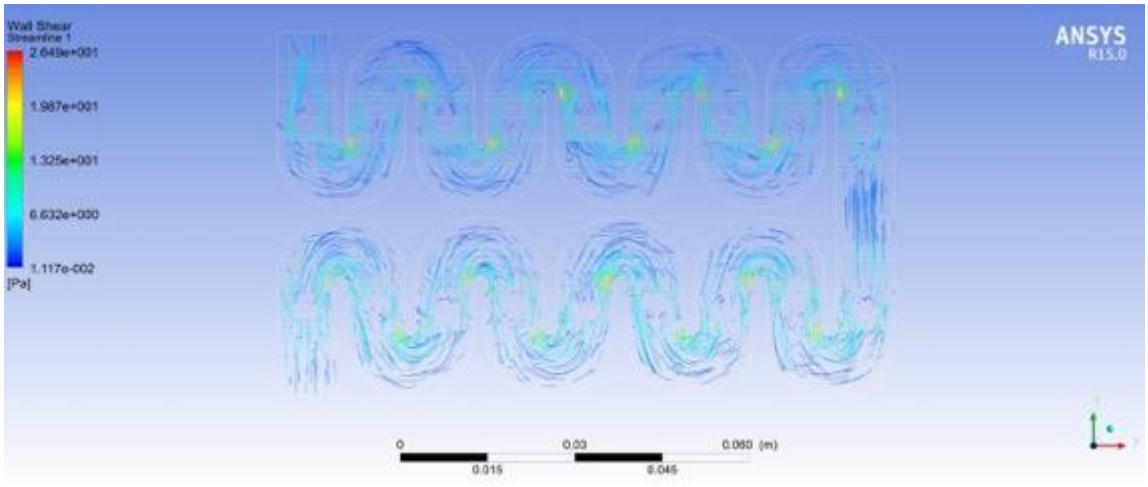

Figure 63 Wall shear stress streamlines

In figures 62 and 63, the streamlines of both the velocity and shear stress are modelled during the flow of blood through the device. The disruption of the flow occurs with the combination of the three methods of generation of secondary flow.

5.6.2 1st prototype:

From the modelling results, the methods used are able to generate wall shear stress that enhance the filtration of plasma and may resulted in reduction in cake formation layer. The first prototype was made using Creo software as shown in figure 64. The dimension of the 1st prototype was 163 X 182 mm and the thickness is 3 mm.

Figure 64 3D design of the 1st prototype device

The membrane was attached on top of the flow disruptors (including the U-bend, semi-circle, and baffles) and were glued using silicon. However, in order for the blood to follow the path, a membrane support was also designed using Creo and was laser cut using TMX65 (CTR laser, Northampton, UK), figure 65. The thickness of the membrane support is 3 mm. The membrane support is placed on the top of the membrane and glued to the membrane surface, so the membrane does not bend and force blood to follow its designed path.

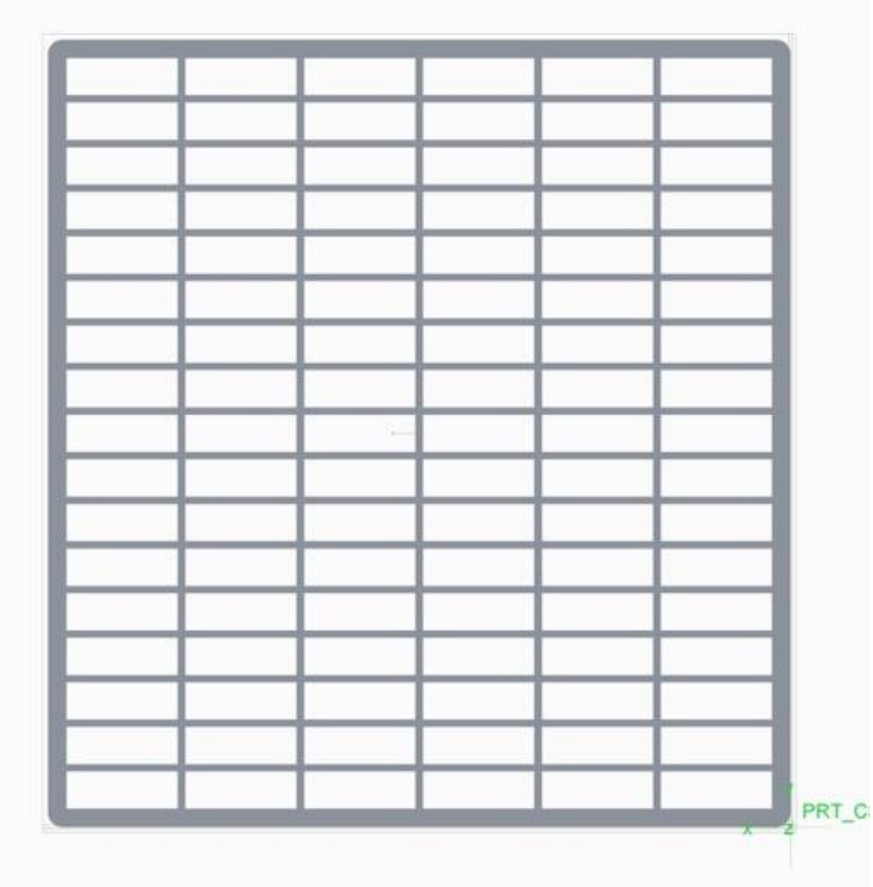

Figure 65 Membrane support design that will cause the blood to follow the path in order to reduce the cake formation

The 3D printer used is Ultimaker 2 extended (Ultimaker, Geldermalsen, Netherlands) with a layer resolution of 40 micron and the material produced by the 3D printing is polylactic acid. Figure 66 shows the printed device and figure 67 shows the device with the membrane support.

Figure 66 Printed rig with the flow deflectors

Figure 67 The rig with the membrane support

The next step was to determine the TMP to achieve the critical flux for the selected membrane. The membrane used was Whatman Track Etch polycarbonate (PC) with a pore size of 1µm. Figures 68 and 69 show SEM images of the membrane under X5 and X10 magnification that was taken using Hitachi TM-1000 electron microscope (Hitachi High-Technologies Corporation, Tokyo, Japan).

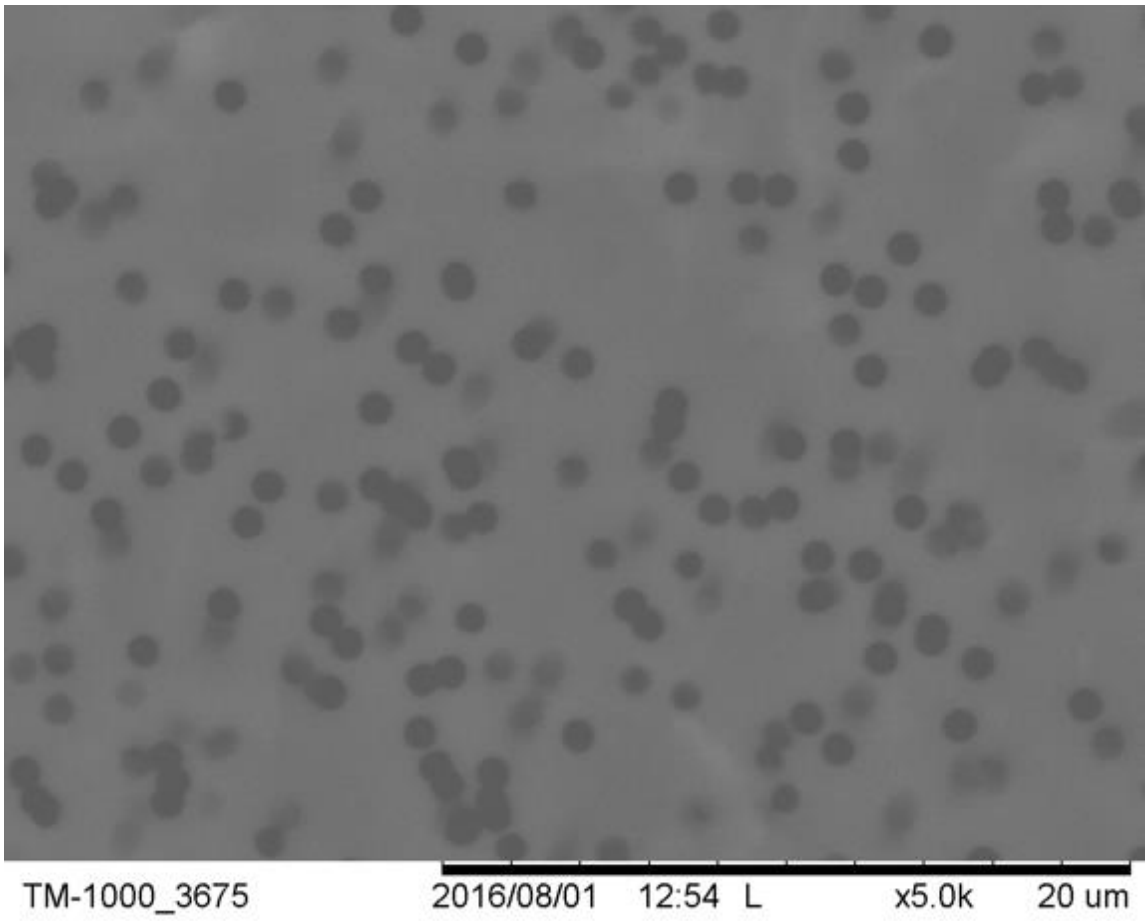

Figure 68 SEM for Whatman membrane of X5 magnification

As mentioned in section 5.4.1.1, porosity is defined as the volume of the pores divided by the membrane total volume. This factor is important for the selection of the membrane for the PP device. As seen in figure 68, the effective pore size is approximately 30%.

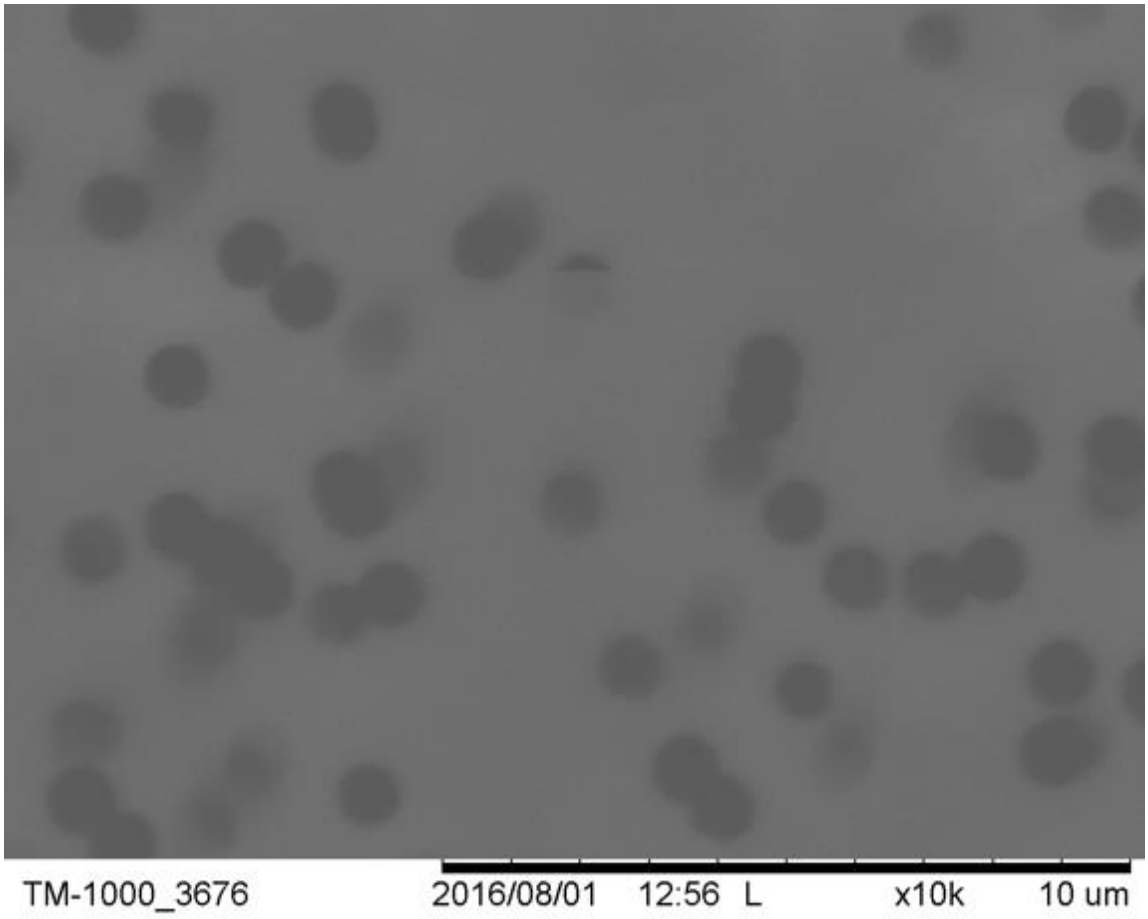

Figure 69 SEM for Whatman membrane of X10 magnification

5.6.2.1 Critical flux measurement:

As discussed in section 5.4.1.3.1, the knee point (critical flux) in the TMP-flux curve is the optimum operation of filtration rate. So, in order to determine the critical flux, an experiment is performed to generate the graph. The TMP will be increased in controlled steps and the associated flux will be measured in order to draw the TMP-flux graph. The schematic diagram for the circuit setup is shown in figure 70, where UF module is shown in the rig with the membrane and membrane support, gate clamp flow restrictor to control the TMP. Fresh bovine blood collected from an abattoir (Sandyford, Paisley, UK) in a sealed canister and treated with 10000 IU heparin sodium from porcine mucosa (Sigma Aldrich, Dorset, UK) in 50 ml of 0.9% sodium chloride solution. The membrane was cut and attached to the rig using silicon glue. The membrane support was placed on top of the membrane and glued to the rig. 500 ml of blood was used. Two factors are measured before initiating the critical flux measurement experiment; active clotting time (ACT) and hematocrit level. The ACT is used to measure the anti-coagulating effect in blood and the level kept above 400 seconds during cardiac surgery (Neema et al., 2004). ACT was measured using a Hemochron Jr Signature+ (International Technidyne Corp, Edison, USA). The hematocrit (hct%) is calculated by filling the capillary tubes with blood then placing them in a Haematospin 1400 centrifuge (Hawksley and sons ltd, Lancing, UK) in order to separate the blood into RBCs and plasma components. The capillary tubes are placed into micro-hematocrit reader (Hawksley and sons ltd, Lancing, UK) for the measurement of hct%. The membrane is then wetted with saline to create channels in pores for the removal of plasma. The blood is pumped into the rig using a stöckert roller pump (stöckert instrumente GmbH, Breisgau, Germany) and the flow rate

was at 150 ml/min. Biopac acquisition system (Biopac Systems Inc., Goleta, USA) is used to collect data from the pressure transducers attached at the inlet and the outlet of the rig. The equation for calculating the TMP is found in 5.3.1.3, but the P_F in the equation is zero since the plasma is open to the atmosphere. The circuit setup is illustrated in figure 71.

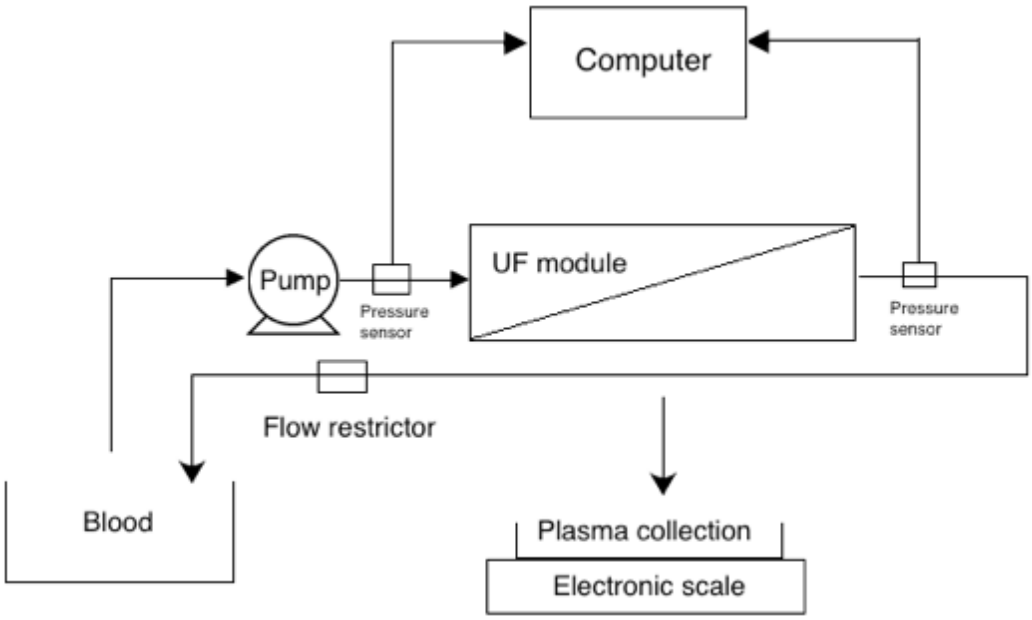

Figure 70 Schematic diagram for the critical flux measurement set-up circuit

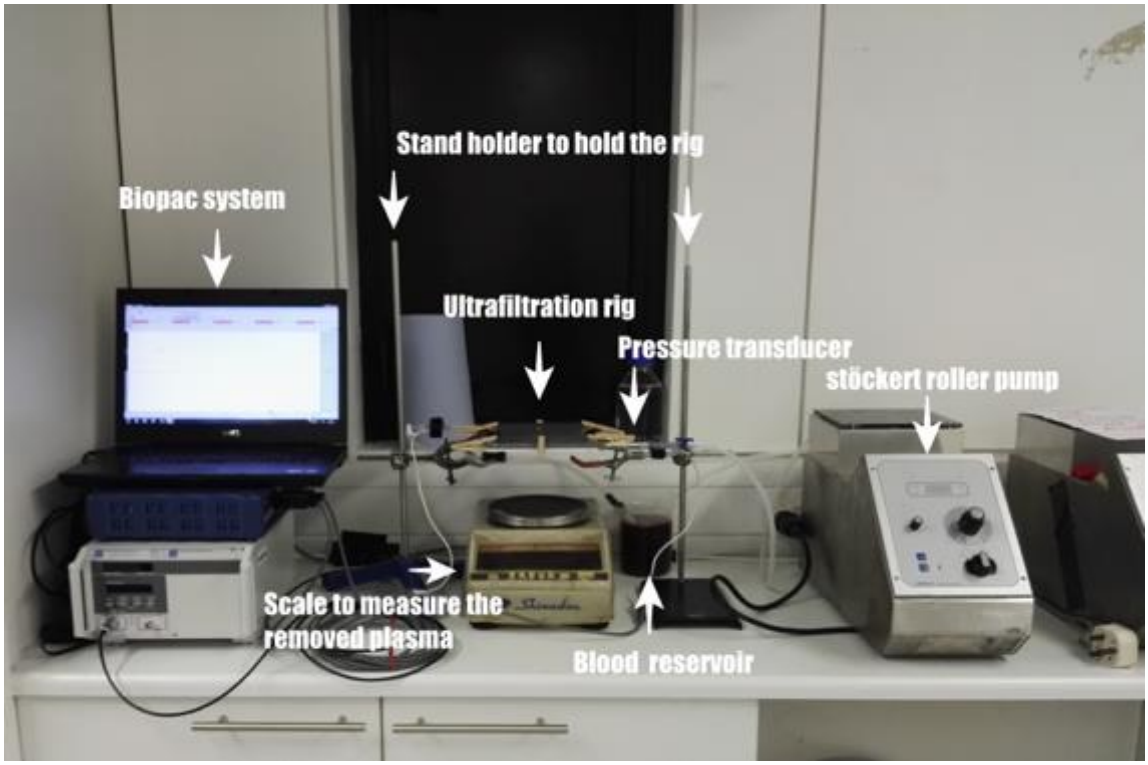

Figure 71 the circuit setup for the TMP measurement

Unfortunately, the experiment was terminated due to blood passing through the pores of the 3D printed device. So, to reduce the porosity of the 3D printed rig, a coating material was applied to the surface of the rig. The coating material used was XTC-3D (Smooth-On Inc, Easton, USA), which is a two part epoxy. The coating material reduced the volume of the blood into the rig but it did not fully prevent blood passage. In this experiment, blood in some area did not follow the designated path. The experiment shown that the flux rate is very low as seen in the table 10 and figure 72.

Time	Scale weight (g)	Flux (ml/min)	TMP (mmHg)
0	0	0	0
10	0.48	0.048	14
20	1.2	0.072	20
30	1.96	0.076	28
40	2.75	0.079	48
50	3.5	0.075	56

Table 8 Critical flux experiment for the coated rig

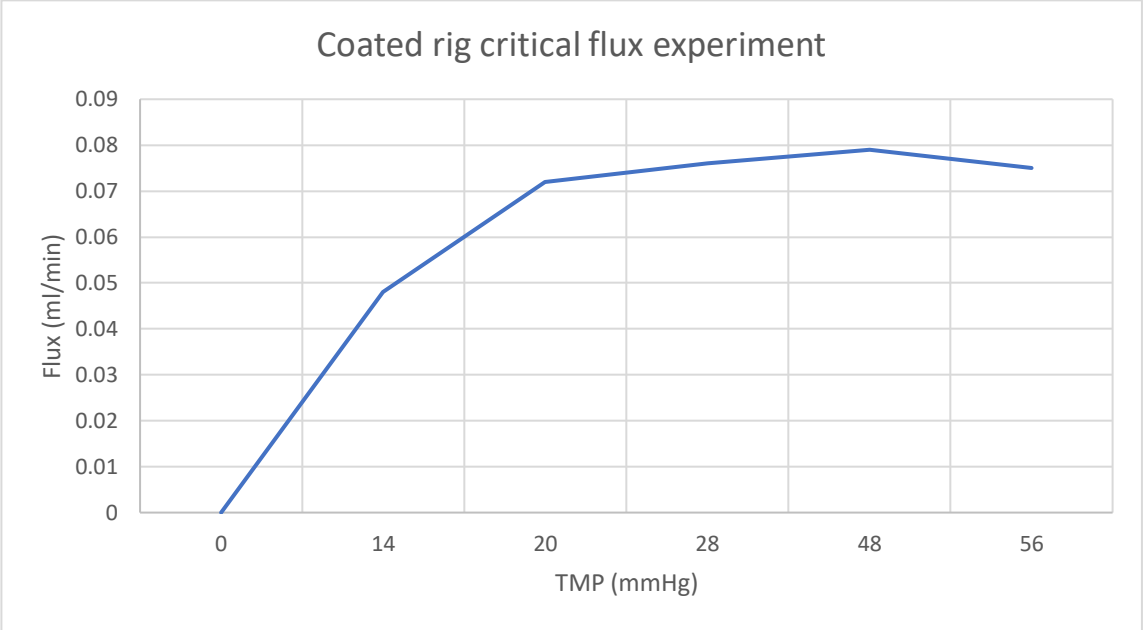

Figure 72 Plot of the flux rate vs TMP for the coated device.

5.6.3 2nd prototype:

Since the 3D printed device was porous and permitted blood leakage. The device design was further modified (figure 73).

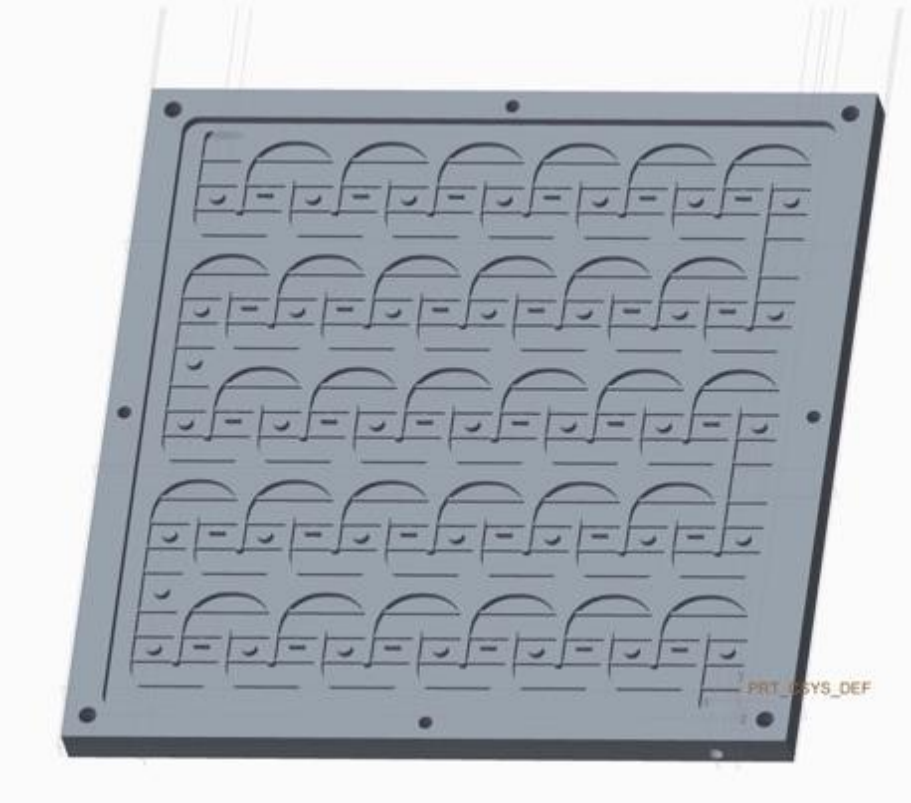

Figure 73 2nd prototype in Creo

The 2nd prototype with dimensions 184 mm X 182 mm has screw mount holes to hold the membrane support on top of the membrane, the 1st prototype dimensions were 163 mm X 182 mm. The membrane support was thicker, 5 mm, compared than the 1st prototype, 3mm, as shown in figure 74. Also, in the 1st prototype, the membrane was on the whole rig and glued to the surface of the rig, on the 2nd prototype, the membrane is placed inside the rig, where the flow disruption occurs.

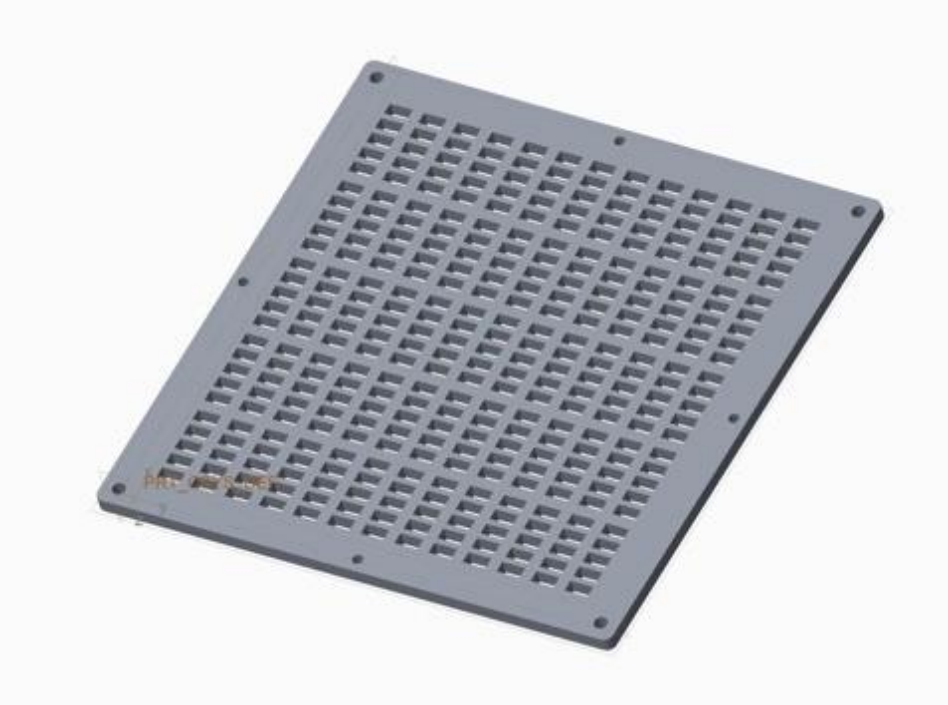

Figure 74 2nd prototype membrane support

The device was printed by the department of Design Manufacture and Engineering Management (DMEM), University of Strathclyde's high resolution 3D printer (ObJet EDEN 350, USA) that has a 16 microns resolution compared to the previous printer which has a resolution of 40 microns (figure 75). The laser cut acrylic used for the membrane support is shown in figure 76. In addition, a laser cut flow disruptor acetate sheet, figure 77, was added on the top of the rig between the membrane and the blood flow to increase the flow disturbance.

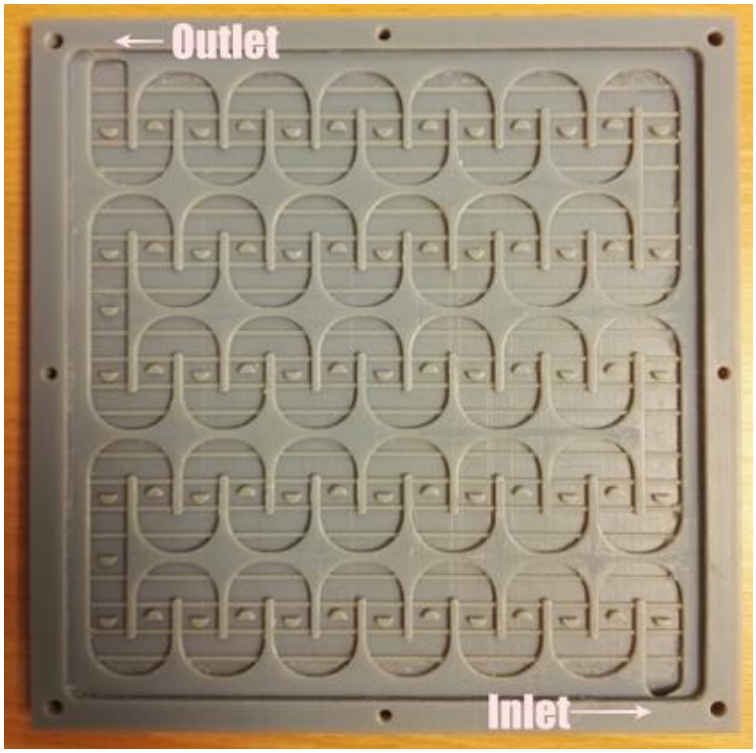

Figure 75 2nd prototype 3D printed device

Figure 76 5mm acrylic membrane support

Figure 77 Laser cut baffles acetate sheet

The measurement of critical flux was performed as mentioned before in section 5.6.2.1. The membrane was attached to the rig using silicon glue and left for four hours to dry before the start of the experiment. Also, before pumping the blood into the device, the membrane is wetted with saline. The Hct% for the blood was 30.5% and the clotting time was 468 seconds. At the start of the experiment, the gate clamp flow restrictor was fully open, and after every 10 minutes is compressed to see the appropriate increase in TMP. The total time for the experiment was 80 minutes and table 9 represent the data collected for the determination of critical flux. Figure 78 shows flux against TMP graph.

Time	Scale weight (g)	Flux (ml/min)	TMP (mmHg)
0	0	0	0
10	7.1	0.71	28
20	20.5	1.34	44
30	33.5	1.3	56
40	46	1.25	64
50	57.5	1.15	77
60	68.5	1.1	98
70	82.1	1.36	106
80	90.3	0.82	116

Table 9 Critical flux measurement results. As the TMP increase, the flux increase until it reaches a plateau and decreased

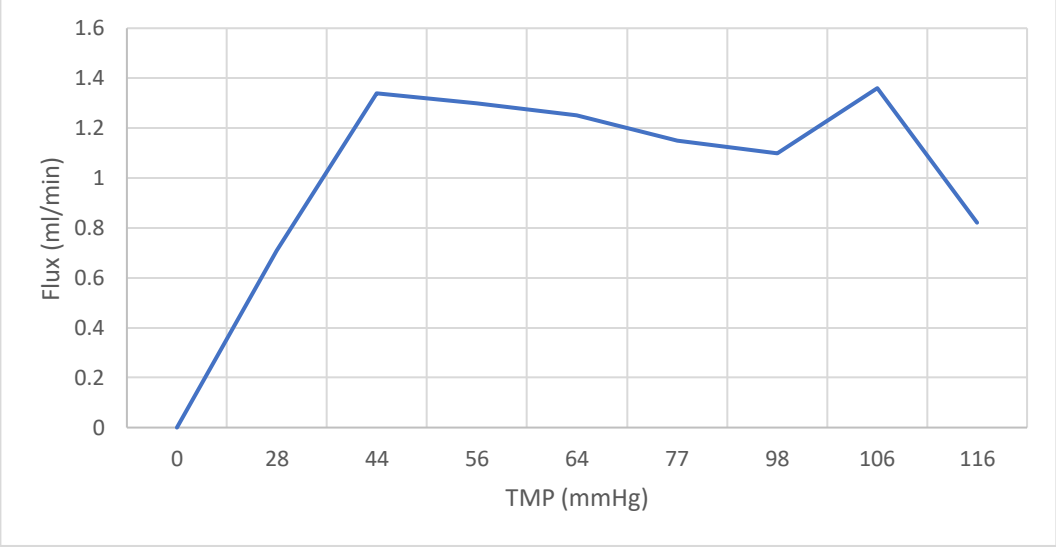

Figure 78 Flux TMP graph

When the TMP reached 106 mmHg, the membrane and the rig separated. Thus, the blood did not follow the path in some parts of the rig. Between 105-116 mmHg, RBCs appeared in the removed plasma which could indicate haemolysis occurred due to high TMP. For these reasons the experiment was terminated.

From figure 78, the flux increased with the increase in TMP, and reached a plateau at 40-50 mmHg before decreasing after 50 mmHg. As a result, the critical flux occurs in the range 40-50 mmHg. The next step was to test the device performance in the range of TMP 40-50 mmHg. At the beginning of the experiment, the TMP was 40 mmHg, however, the inlet pressure increased while the outlet pressure did not change. As a result, the clamp restrictor was unscrewed to lower TMP. Despite that, the inlet pressure did not decrease, and consequently the TMP did not reduce and the experiment was stopped. During disassembly of the rig, there was clotting inside in the rig (figure 79). In addition to the clotting, silicon glue restricted the inlet. These factors caused the TMP to increase.

Figure 79 Blood clotting inside the rig

It is thought the heparin volume is insufficient to prevent blood clotting. The heparin volume was subsequently increased to 4000 IU for 1L of bovine blood. The PC membrane, which has effective open area of 30%, was replaced with a membrane with higher pore size and porosity. The new membrane was made of PES material and is a

porous membrane that has an effective open area of 80%. A SEM of the PES membrane of X5 magnification is shown in figure 80.

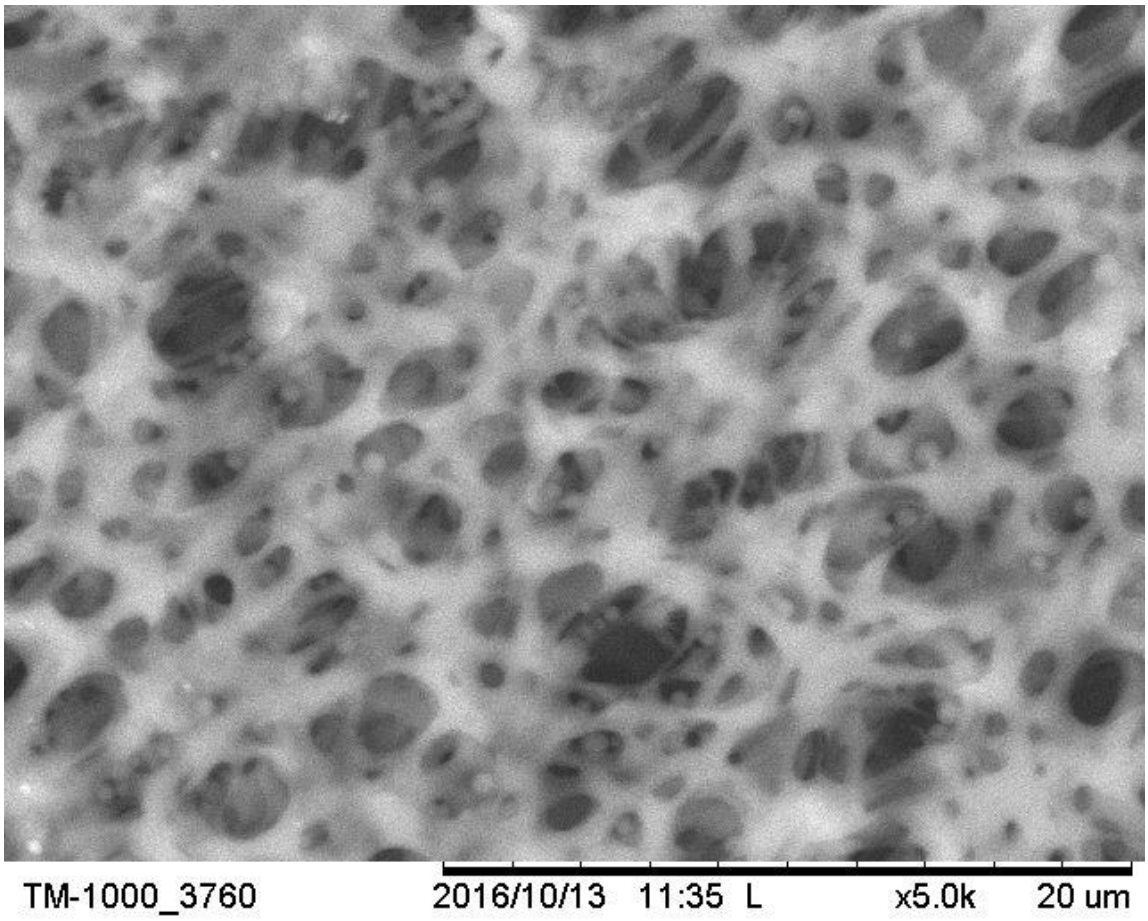

Figure 80 SEM of the PES membrane of X5 magnification

As seen from the SEM image, the PES membrane pores size is non-uniformly distributed and vary in size from 1 µm to 5 µm. The average size of the pores was 3 µm.

After the termination of the experiments and during cleaning, the silicon glue is removed using metal chisel that unfortunately leads to the removal of the 3D printed material at the inlet and the outlet side. Moreover, at TMP above 100 mmHg, the silicon glue separate that cause the blood not to follow the path. So, the silicon glue was replaced with a flow director. The material chosen was 3 mm thick expanded neoprene rubber (Delta rubber LTD, Christchurch, UK). Also, flexing in the acrylic support (figure 81), a metal cross member with dimensions of 184 mm X 182 mm was added, figure 82. This metal cross supports the material above it and maintains its shape and mechanical integrity.

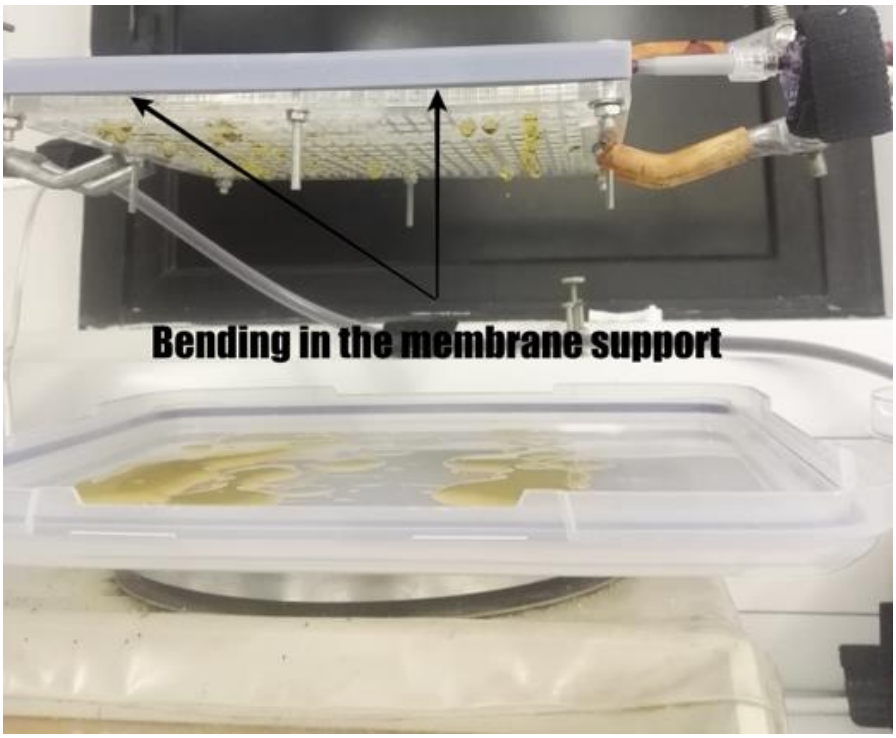

Figure 81 5 mm thick acrylic bending

Figure 82 Metal cross members shape placed on the top of acrylic support

Unfortunately, when neoprene rubber is compressed, the shape is changed and it does not return to its original shape as seen in figure 83, where there are gaps between the neoprene rubber and the rig.

Figure 83 3 mm thick neoprene rubber compressed after experiment

As a result, another material with better mechanical property was selected. we used a 3 mm thick solid neoprene rubber (Delta rubber LTD, Christchurch, UK) as illustrated in figure 84. The new material has the ability to maintain it shape.

Figure 84 3 mm thick solid neoprene rubber

The acetate flow disruptor sheet and the PES membrane show an improvement in the flux rate of 60% when compared with PC membrane. The PC membrane has an average flux of 1.02 ml/min while the PES membrane has an average flux rate of 1.63 ml/min. The PES membrane was selected for the device since it had a higher flux rate, removing plasma faster.

5.6.4 3rd prototype:

The 3rd prototype is the final phase of the 3D print rig where the size increased to 326 mm X 242 mm to investigate the effectiveness of increasing surface area of the device on the plasma filtration rate. Some changes were introduced before the 3D printing. Two cuts are made around the rig to add rubber gaskets for firm support and sealing. Also, the inlet and the outlet was made perpendicular to the rig (figure 85).

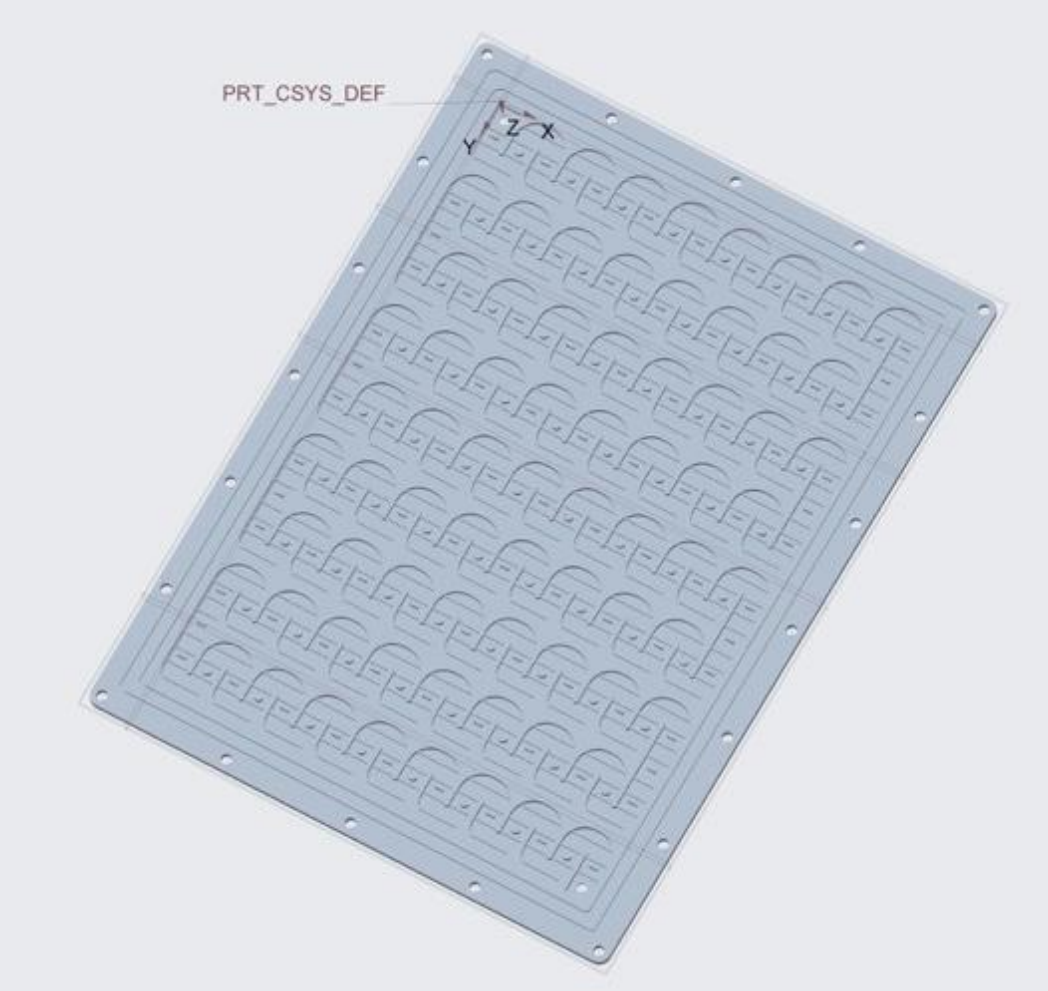

Figure 85 3rd prototype design in Creo

Also, in order to force the blood to follow the path, a 12 mm acrylic material (figure 86), was laser cut and placed and screwed in place on top of the rig. Two rubber gaskets were attached to the rig to prevent blood leakage and for structural support. Figure 87, 88 and 90 show the rig with the base and the membrane support. A metal support bar was added on top of the acrylic material for firm support, figure 90. A laser cut flow disruptor, figure 91, was added to the configuration since it improved the filtration rate as shown in the previous device configuration.

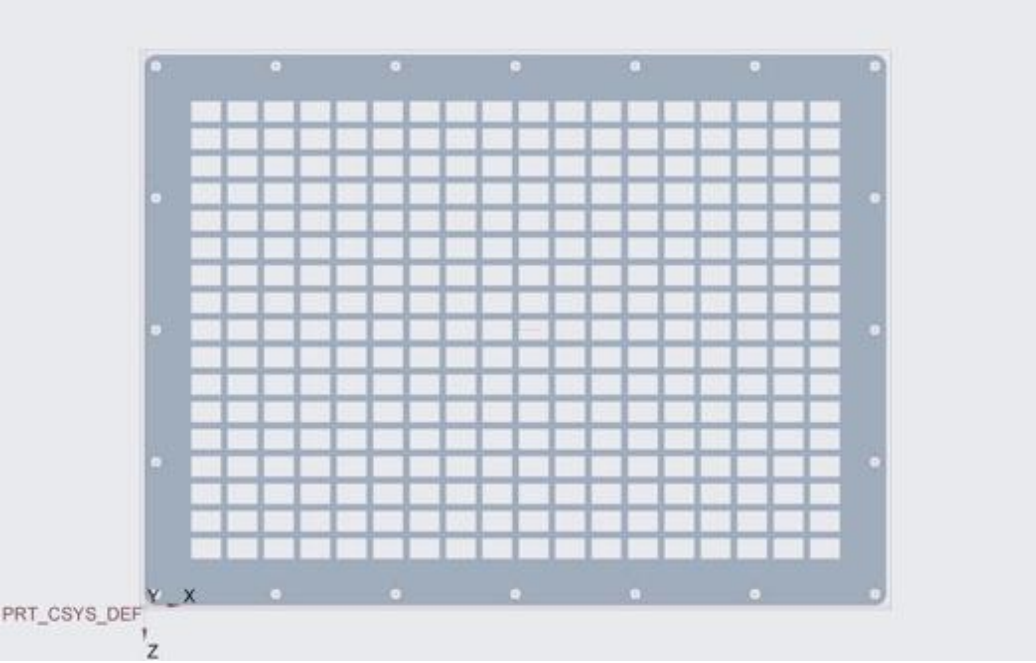

Figure 86 12 mm acrylic membrane support

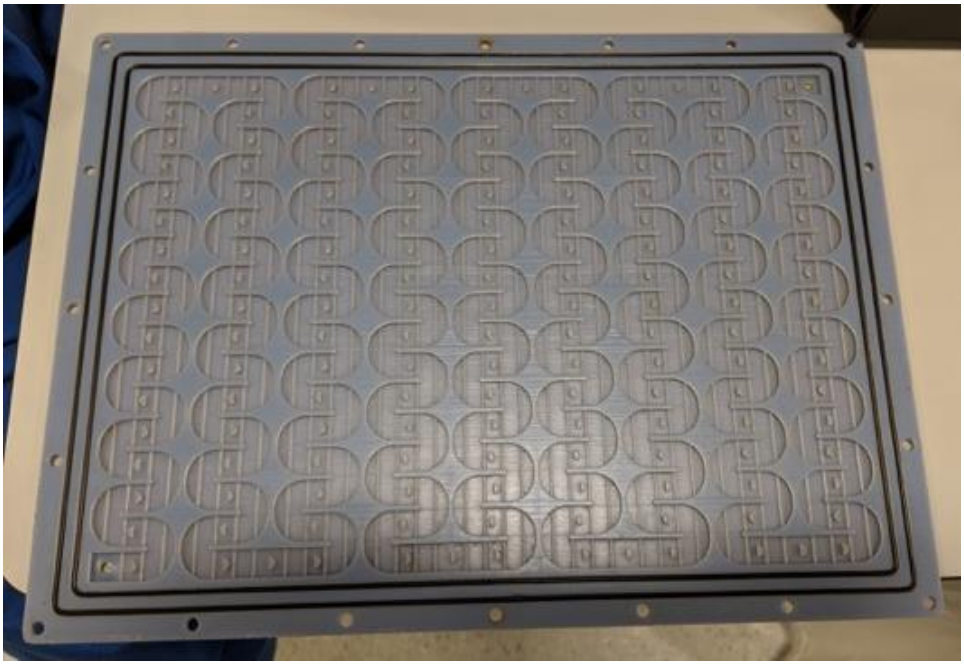

Figure 87 3D printed 3rd prototype. The gasket is placed around the rig to prevent blood leakage

Figure 88 The base of the device where the inlet and the outlet is inserted. Two gasket ring are added for prevention of leaking blood

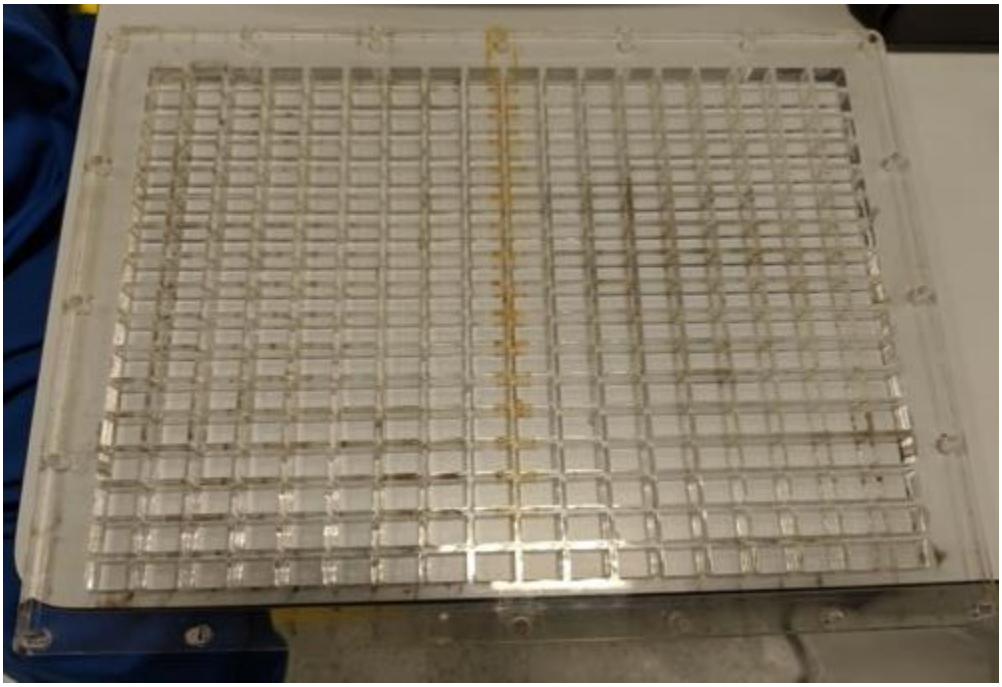

Figure 89 the 12mm acrylic membrane support

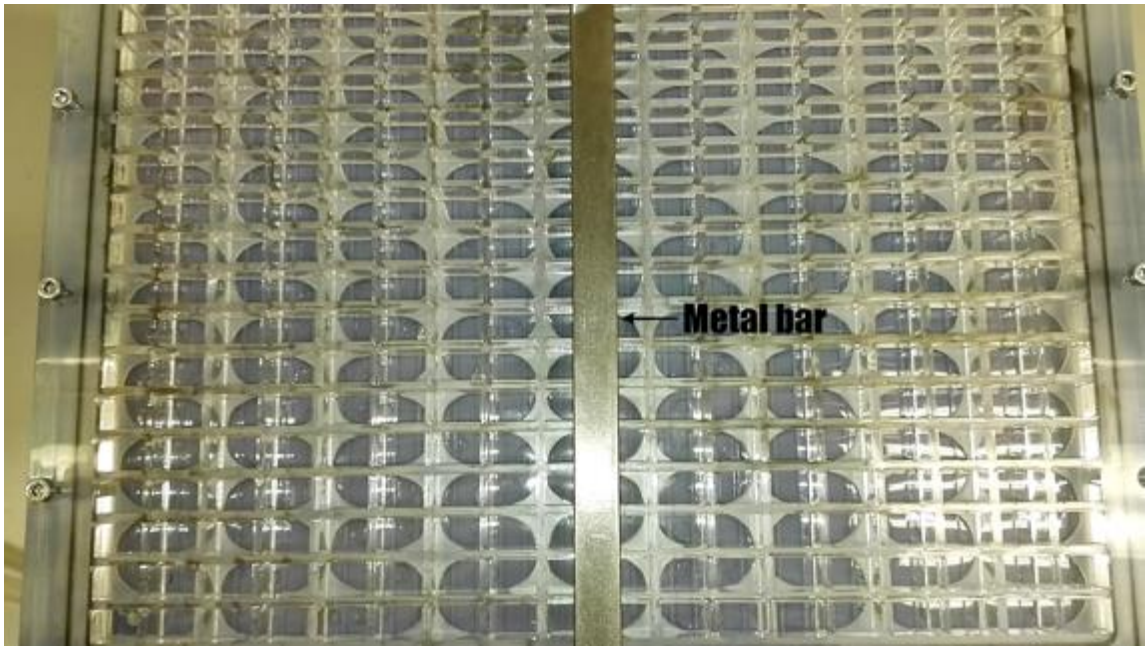

Figure 90 Metal bar for firm support to the acrylic membrane support

Figure 91 Laser cut flow disruptor acetate sheet

Experiments were performed to investigate the performance of the 3rd prototype in addition to improvement of the flux rate, figure 92. The experiment for the testing the flux rate for the rig is similar to the pervious configuration:

a) pore blood in plastic beaker
b) set up the rig and adding the membrane
c) wet the membrane using saline
d) connecting the Biopac pressure sensors
e) place the plasma collection bucket on the scale and reset the scale
f) pump the blood at 150 ml/min flow rate using the stöckert roller pump
g) maintain the TMP in the range of 40-50 mmHg
h) replace the removed plasma with saline that pumped in the blood beaker for maintain a fixed volume and reduced haemodynamic effect

The reason for using bucket to collect plasma is to have the rig and the container as one disposable part.

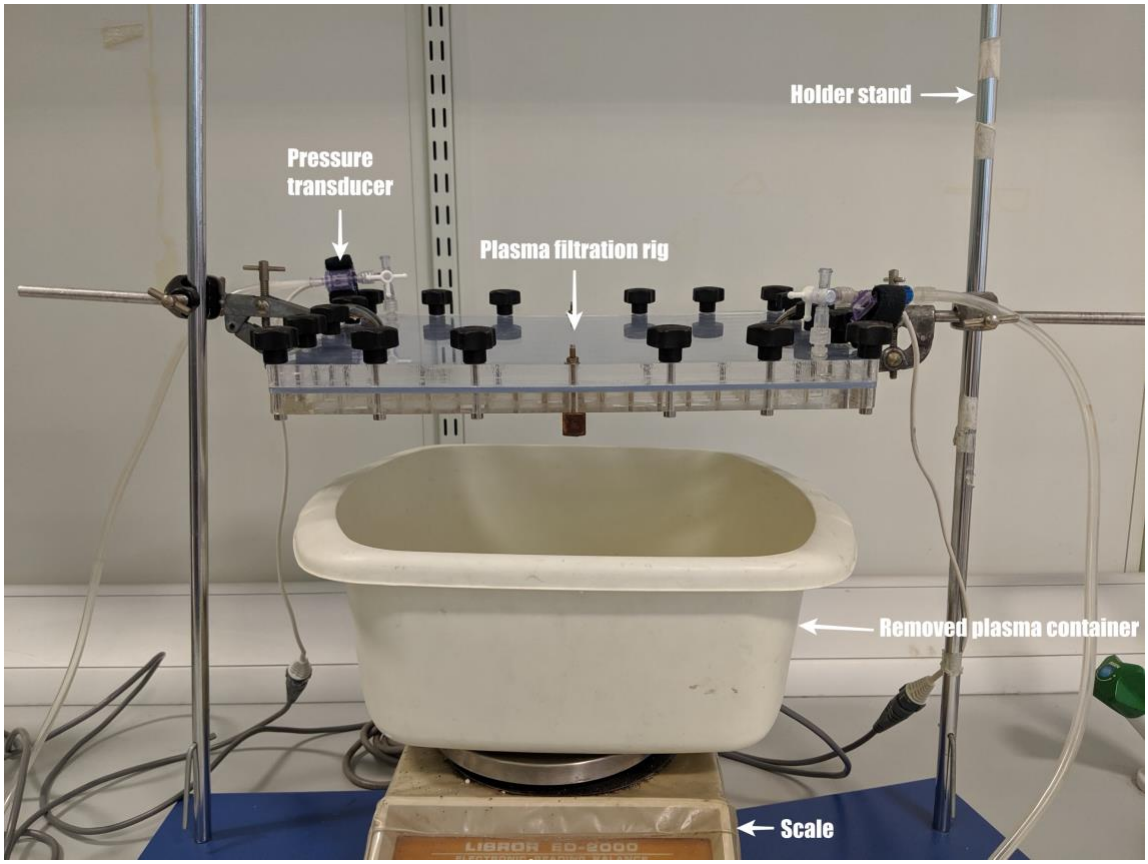

Figure 92 Experiment setup

The average flux rate for 60 minutes was 3.75 ml/min. Experiments to study the effect of setting the flow rate of the stöckert roller pump to 300 ml/min with and without the addition of membrane support permeate carrier. The material used was nylon fabric mesh (Remnant Kings, Glasgow, UK) placed on the outer side of the membrane. The idea of the nylon mesh is to absorb the plasma from the outer side of the membrane to the bucket, the idea is similar to absorptive tissues that absorb liquid from a surface, but instated of absorb and store, it acted as medium that create channels for the plasma to move from the membrane into the bucket. The flux rate without the nylon fabric was 4.10 ml/min and the addition of the fabric increase the filtration rate by 37% (5.62 ml/min). Table 10 shows the average filtration rate of the removed plasma using different flow rates and permeate carrier. The next step was to develop the automation system for the rig and assemble the rig to create a full system for testing.

Average removed plasma		
150 ml/min Flow rate	300 ml/min Flow rate	300 ml/min Flow rate with permeate carrier
3.75 ml/min	4.10 ml/min	5.62 ml/min

Table 10 Average filtration rates for the removed plasma

5.6.5 Automation control system:

The control system is a central to permitting the system to allow it to perform without human intervention, with the objective making the system “plug and play”. In order to design the control system, the key parameters need to be considered. First, to measure the TMP, two pressure sensors are needed. Second, two pumps are required; one for the replacement of the removed plasma and the second for pumping blood to the rig. Third, a linear actuator that regulates and maintains the TMP to achieve critical flux. Lastly, a load cell is necessary for the measurement of the removed plasma from the blood. An Arduino Uno (Arduino.cc, Italy) would be employed as the system microcontroller (MC).

5.6.5.1 Arduino MC:

Arduino Uno (figure 93) is a MC that can receive digital or analog signals and send digital or analog outputs as a pulse width modulation (PWM) signal. The analog to digital conversion (ADC) can range from 0-5 V. This is important with regards to pressure sensors output voltages. The A pins are analog inputs that can receive voltages from 0V to 5V and the minimum change for each step is 4.88 mV. The MC is programmed using the C++ language and these commands can upload it to the MC using a USB cable. The USB can also provide the power for the MC to operate.

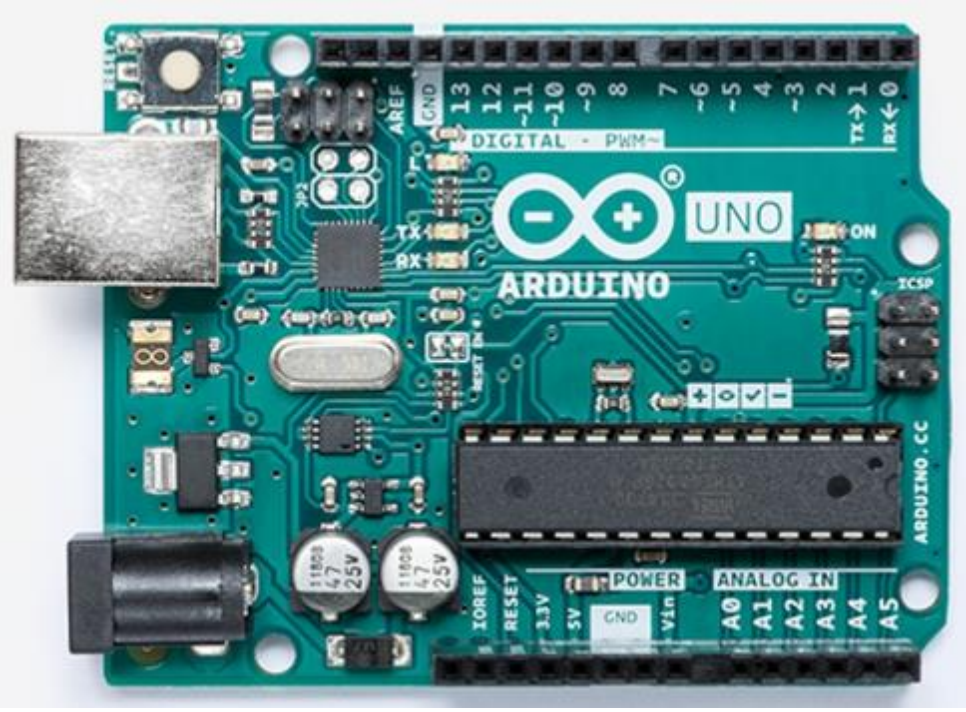

Figure 93 Arduino Uno (taken from https://store.arduino.cc/arduino-uno-rev3)

5.6.5.2 Pressure sensors:

At the early stages of the device development, a stöckert roller pump was used and its pressure profile are demonstrated in figure 94. The pressure sensors selected were 24PCBFA2G (Honeywell, Charlotte, USA) which are gauge pressure sensors. These read zero mmHg at atmospheric pressure. The voltage output of these sensors are in millivolts so a differential instrumentation amplifier is required to amplify the voltage to be in the range 0-5 V for the MC. The amplifier used was the INA125p (Texas instrument, USA. In order to amplify the input signal, a resistor value is calculated based on the gain equation, $G = 4 + \frac{60k\Omega}{R_G}, G = \frac{V_o}{V_{in}}$, provided in the datasheet. From the calculations, the resistors required to achieve the gain up to 5V are in the values of 1.2kΩ.

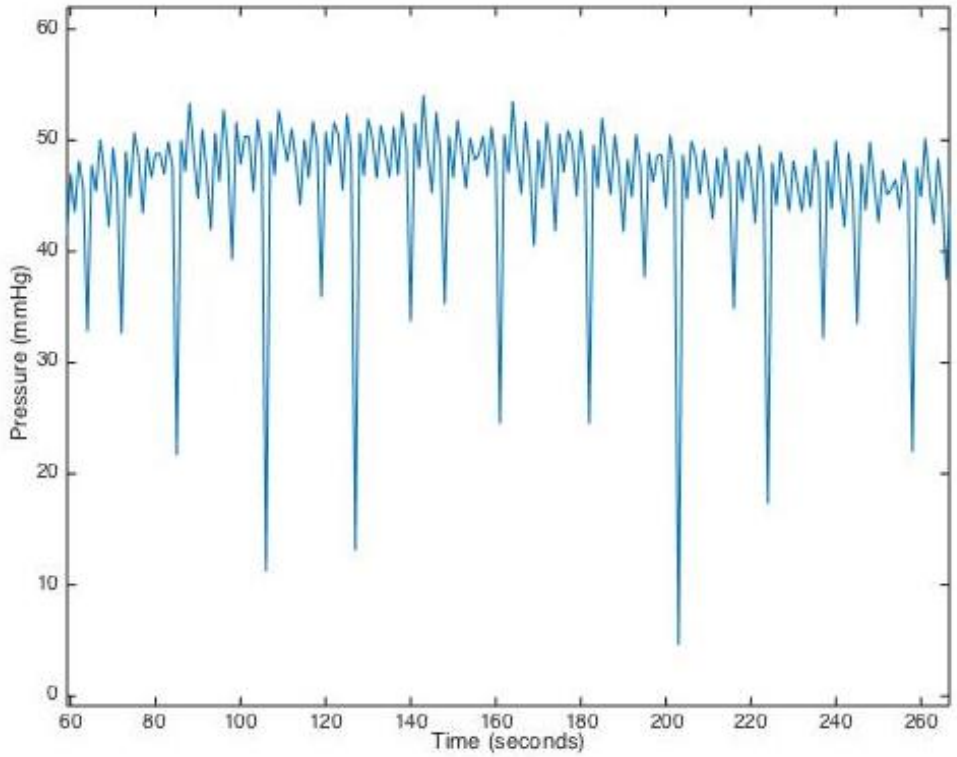

Figure 94 stöckert Roller pump profile plotted in Matlab

For calibration of the pressure sensors, a Biopac pressure sensor is connected to an encore pressure inflator (Boston Scientific Corp, Marlborough, USA) to generate pressure and measure the amplified voltage output using a digital multimeter in order to calculate the linear equation for the pressure sensors (figure 95 and 96). The maximum pressure set for each sensor is around 200 mmHg and the graphs for the inlet and outlet pressure sensors are shown in figures 97 and 98.

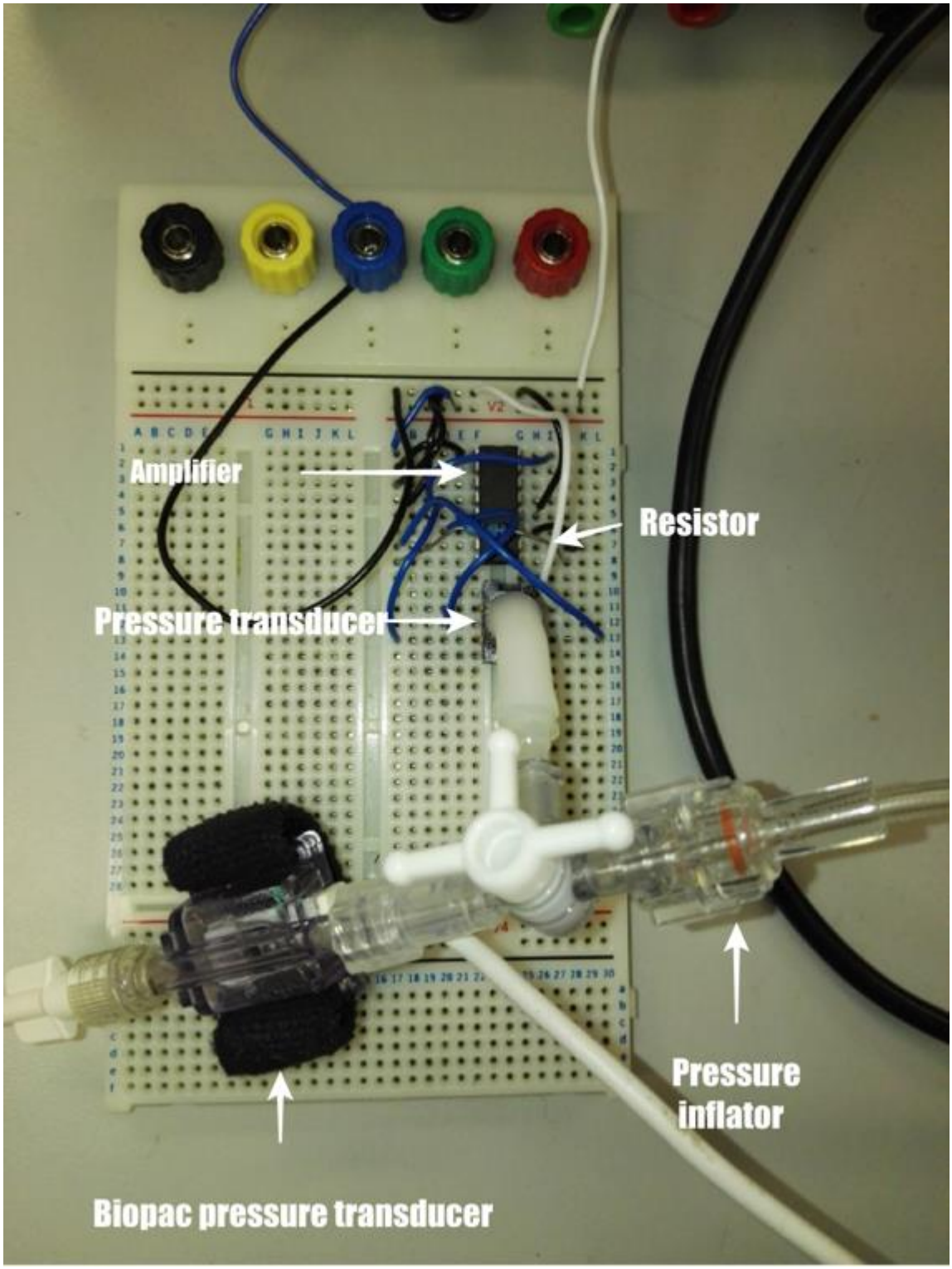

Figure 95 Pressure sensor calibration using the Biopac system

Figure 96 Encore pressure inflator generating pressure for the pressure sensor

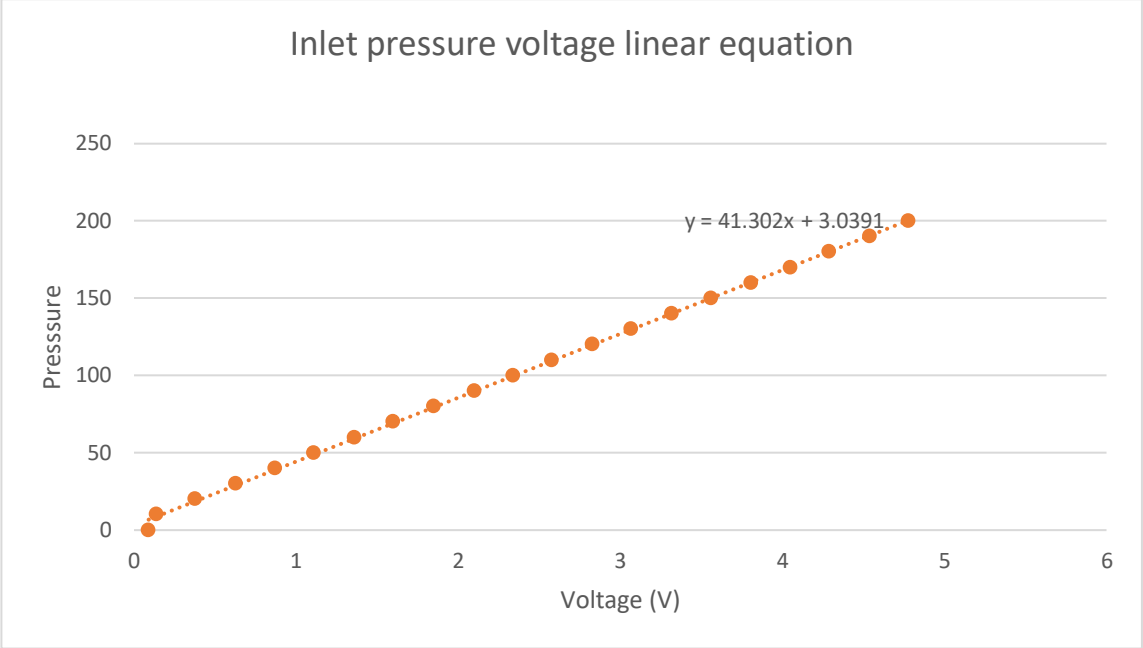

Figure 97 Inlet pressure sensor where the relationship between output voltage and the pressure is linear

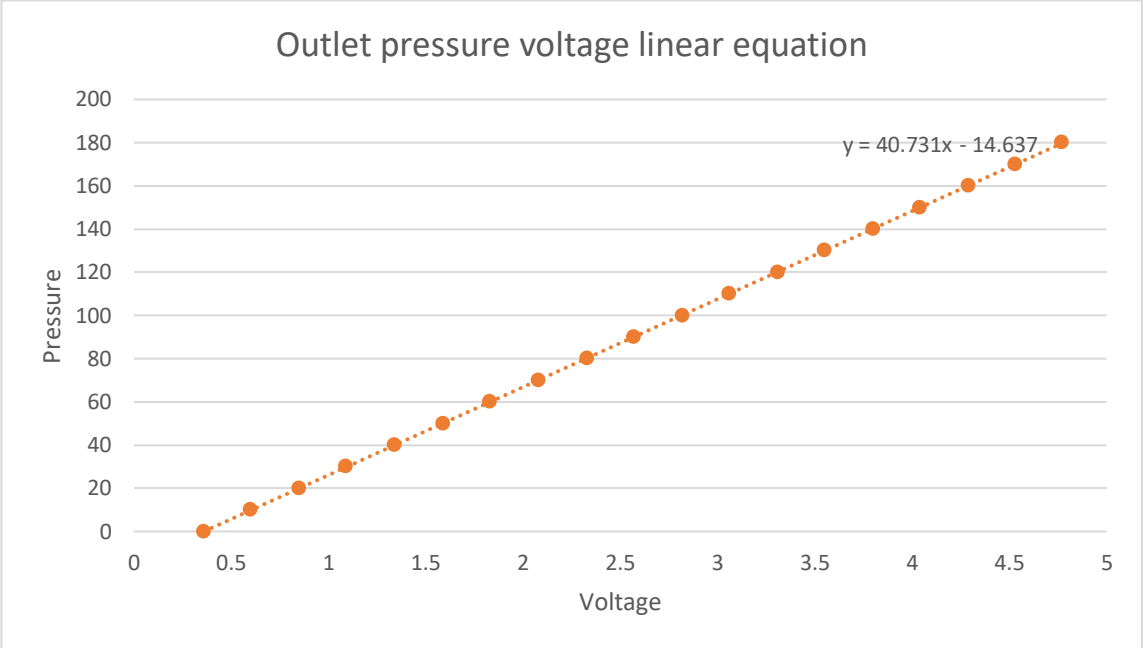

Figure 98 Outlet pressure sensor that shows the linear relationship between the output voltage and pressure

The two linear equations were used in Uno to convert the analog voltage from the INA125p into pressure. However, since the roller pump does not create uniform pressure, an average is implemented to average the change of the pressure into a single value that represents the TMP. The average pressure data readings are similar to the Biopac system readings. Latterly, the larger pump was replaced with a small roller pump (Brightwake LTD, Nottingham, UK) used in the hemosep device since it will be used for the automation system. The pressure profile for the pump is shown in figure 99. Since the roller pump pressure can go into -20 mmHg, the gauge pressure sensors cannot read negative values. Therefore, new absolute pressure sensors from 24PCDFA6A (Honeywell, Charlotte, USA) were employed. The absolute pressure sensor reads around 750 mmHg when they are open to atmosphere compared to the gauge pressure sensor that read zero mmHg when they open to atmosphere. For calibration, they were set to zero at atmospheric pressure.

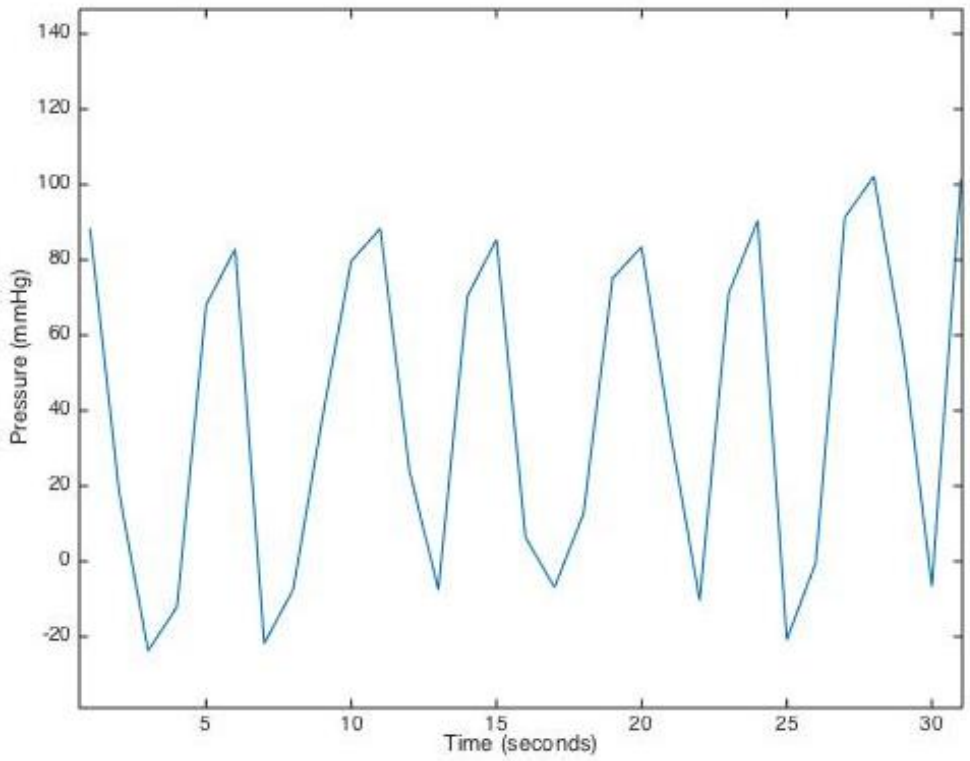

Figure 99 Roller pump pressure profile

In addition, a new single dual instrumentation amplifier, INA2126 (Texas instrument, USA), was used to replace the two INA125p. The calibration for the absolute pressure sensors were identical to the gauge pressure sensor. The linear graphs for the two pressure sensors are presented in figures 100 and 101.

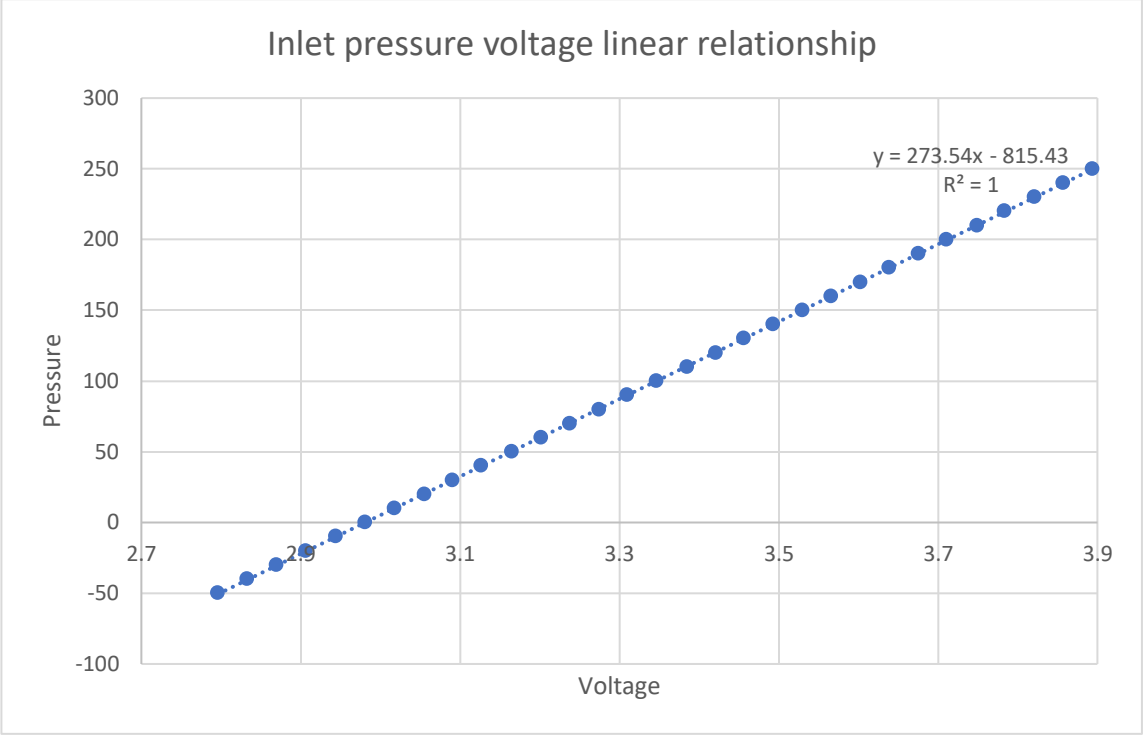

Figure 100 relationship between output voltage and inlet pressure

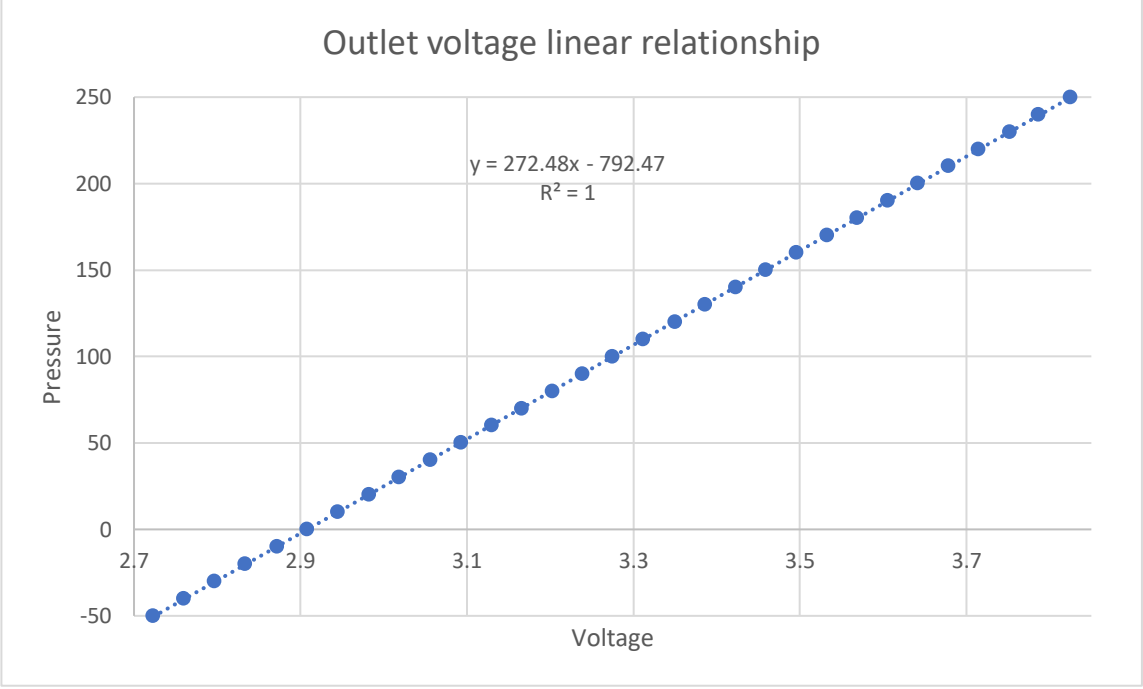

Figure 101 Relationship between output voltage and outlet pressure sensor

The pressure sensor values were similar to the Biopac pressure sensor. Since the roller pump fluctuated from negative to positive pressure, an averaging method was used that averaged 100 readings for the pressure sensors. This gave values for the TMP that fluctuated in the range of the TMP recorded by the Biopac system.

5.6.5.3 Load cell:

During plasmapheresis the removed plasma is replaced with other fluids, for example fresh frozen plasma and human serum albumin (McLeod, 2006). In order to replace the fluid that is equal to the removed plasma, a load cell was used to calculate the volume of the removed plasma. A load cell is a device that measures the weight of an item. Thus, it can measure weight of the plasma that passes out of the membrane. The load cell used in this project is Tedea-Huntleigh model 1042 5Kg (Vishay Precision Group, Malvern, USA) that can detect 1 gram of fluid weight. However, the ADC in the Arduino is 10 bits, that means that the conversion from analog will give 1024 discreet digits. Unfortunately, the minimum weight measured is approximately five grams. To solve this issue, ADC, HX711 module, with 24 bits is connected to the load cell and this will give 16777216 discreet digits, so, the minimum detected weight is 0.00029 grams. This module provided voltage for the load cell to operate and was connected to Arduino for the measurement of weight. The code for the HX711 module is written and provided by the Arduino community, since it is an open source MC, but the load cell needed to be calibrated. Before calibration, an acrylic sheet plate with dimension of 200 mm X 200 mm is made and added to the top of the load cell, (figure 102) in order to hold the container for the removed plasma. The calibration is carried out using calibrated weights, of meal construction with known weight, and the code is adjusted until the Arduino output matches the weight.

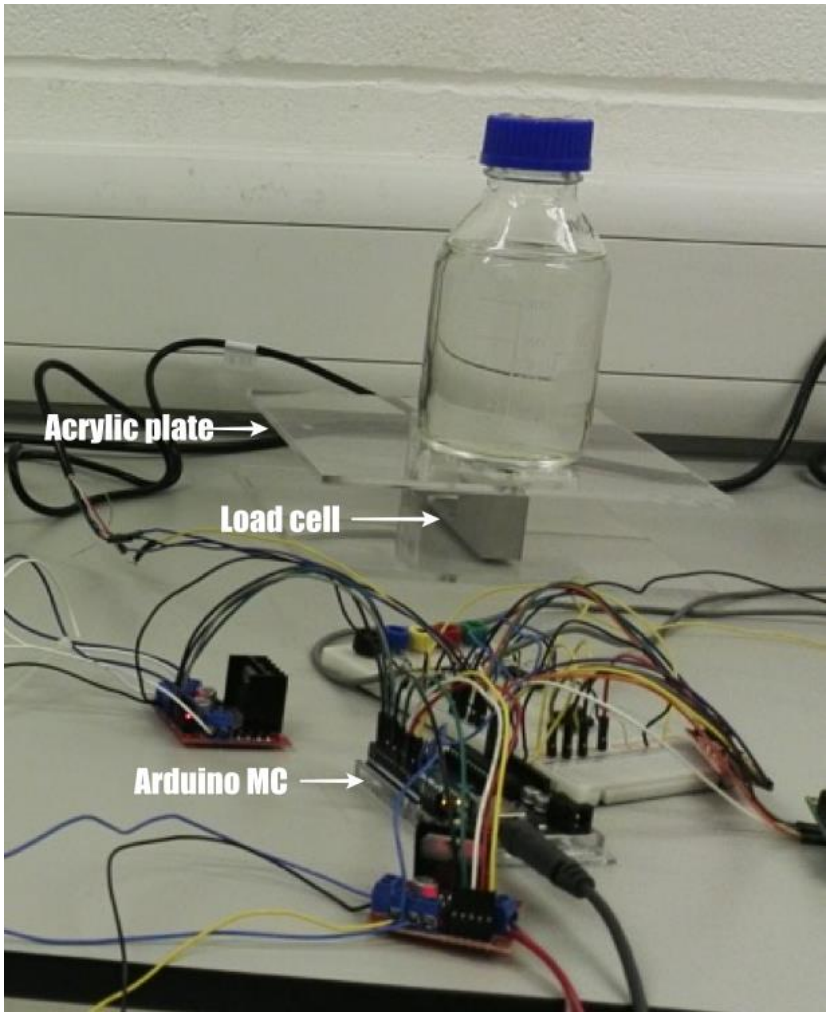

Figure 102 Loadcell with the plate on the top of it

5.6.5.4 Pumps:

There are two pumps used in the system; the membrane roller pump and the fluid replacement pump (Adafruit Industries, New York, USA). The membrane roller pump is a changeable flow rate pumps that pump the blood into the rig. The fluid replacement pump is a pump used to replace the removed plasma with saline. Both pumps are connected to the Arduino using a TB6612FNG dual motor controller (Pololu Robotics and Electronics, Las Vegas, USA). The controller receives the signal from the Arduino

as a PWM signal and controlls each pump independently by providing constant voltage for the pump to operate at the required flow rate. The roller pump was calibrated for five different flow rates, 50, 100, 150, 200, 260 ml/min, while the fluid replacement pump was calibrated to pump 10 ml of plasma replacement fluid when the system removed 10 ml of plasma from the blood. The roller pump calibration was done by increasing the PMW value and measuring the flow rate for 30 seconds (figure 103). Figure 104 shows the relationship between PWM and different flow rates. The fluid replacement pump is calibrated using time in MC. The fluid replacement fluid was set to pump only 10 ml of fluid to replace the removed plasma, and the time for the pump to operate is calculated.

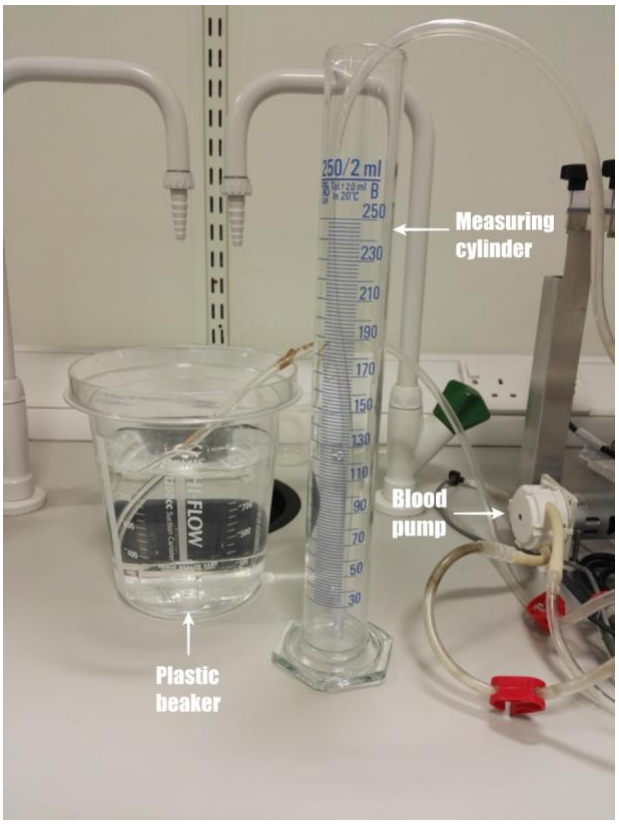

Figure 103 Calibration of the roller pump to calculate the value of the PWM for different flow rates

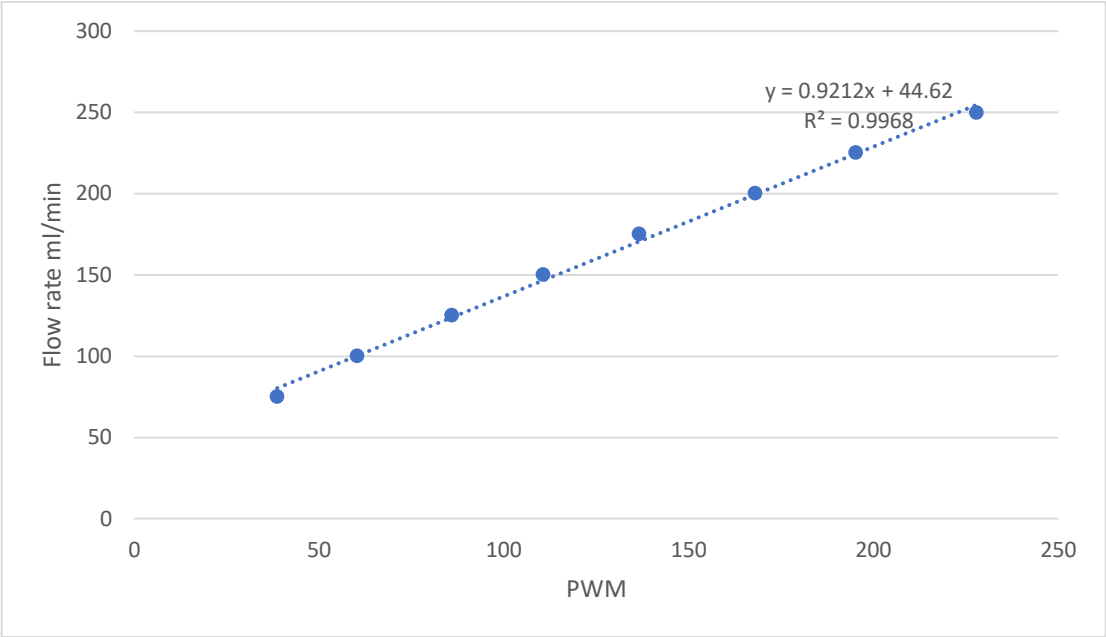

Figure 104 Relationship between Arduino PWM and flow rate

5.6.5.5 Linear actuator:

The TMP was manually adjusted using gate clamp flow restrictor. In the automation system, the rotating restrictor is replaced with 43 N electrical linear actuator (crouzet Automatismes, Valence, France), figure 105. The linear actuator is a stepper motor with a shaft, controlled by the Arduino through a DRV8824 stepper motor controller (Pololu Robotics and Electronics, Las Vegas, USA). The code for the stepper controller was provided in the Arduino forum websites, but was modified to maintain the TMP in the critical flux range. As shown in figure 106, the relationship between the low speed of the motor and the high torque is constant, then as the speed increase, the torque exponentially decreases by increasing the speed, the torque is reduced. So, by testing different speed values through modification in Arduino code and visualize if these values able to squeeze the tube. Once a speed value was generating enough torque to clamp the tube, that value was selected.

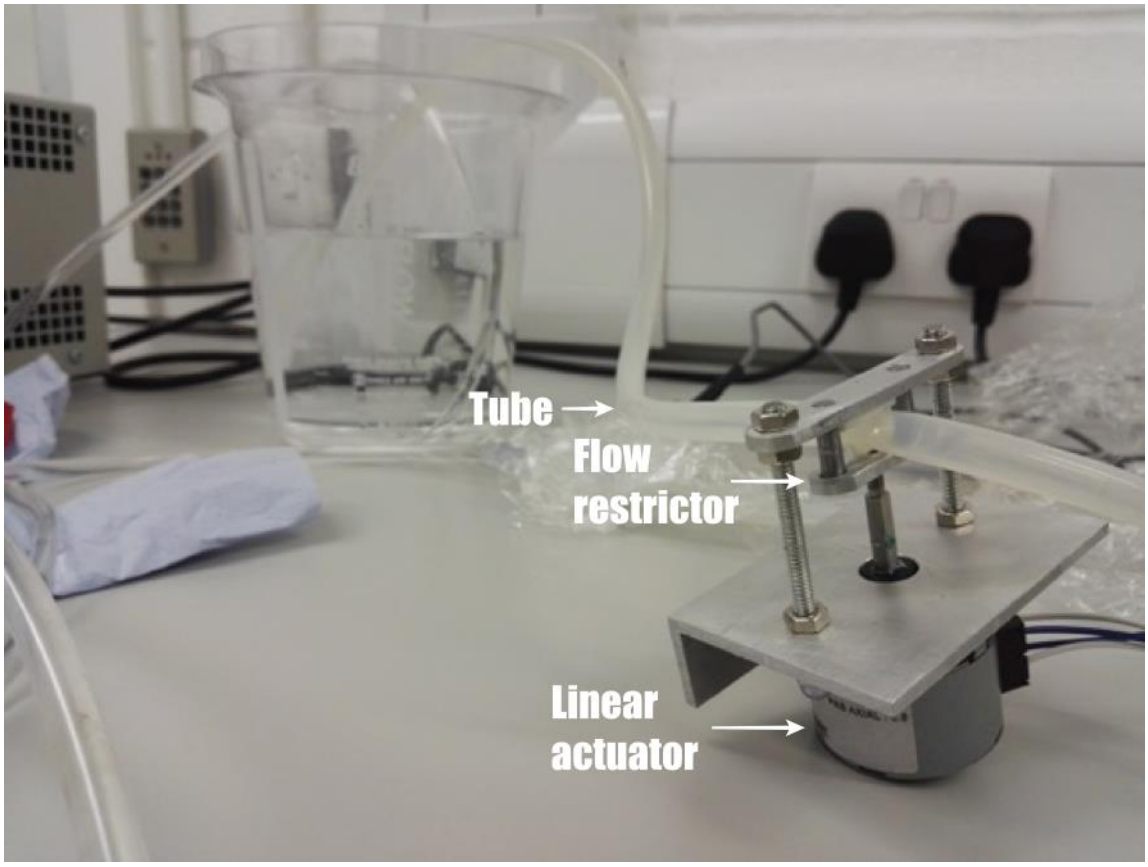

Figure 105 Linear actuator

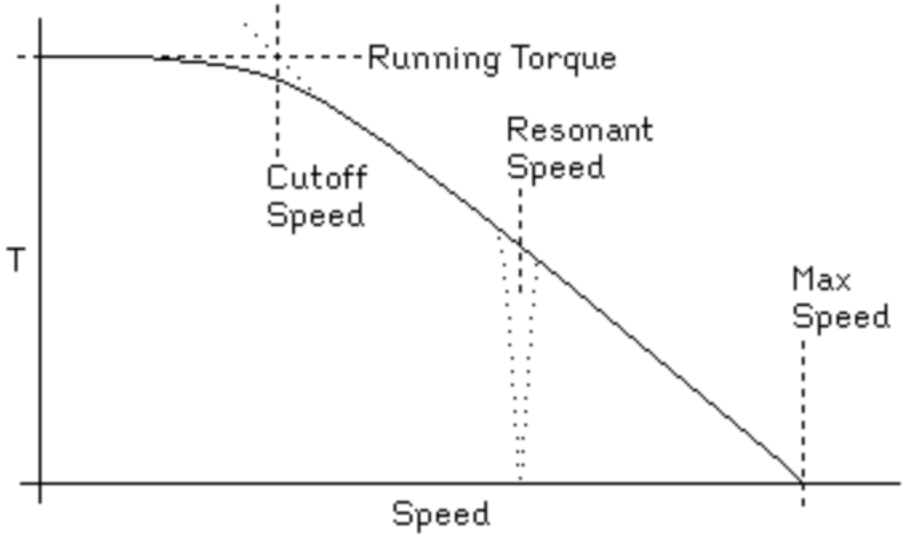

Figure 106 Relationship between torque and speed. The higher the speed the lower the torque. (Taken from http://www.hobbyprojects.com/stepping_motor_physics/torque_versus_speed.html)

5.6.5.6 Control system unit:

The next step was to combine all the components as a single control system. An SD card reader module (Tinxi, GmbH, Eggenstein-Leopoldshafen, Germany) was added to the automation system to record the data for further analysis. Power was provided from the digimess HY3003-2 DC power supply (Digimess Instruments ltd, Derby, UK) that is connected to the dual motor controller and 10 VDC voltage regulator LM7810ACT (ON semiconductor, USA) with a maximum operating current of 1 A. The voltage regulator provides power to Arduino, pressure sensors, amplifier and stepper motor controller. Four switches (Ywrobot, China) were added to the system, and each switch was assigned with a specific function (figure 109 shows the letters for the switches):

a) Switch one turned the pump on or off.
b) Switch two zeroing the scale.
c) Switch three increases the flow rate.
d) Switch four decreases the flow rate.

Also, an LCD (SunFounder, China) was added to display information needed; plasma volume removed, volume of the replacement fluid, TMP and the duration of the experiment. Moreover, LED lighting (kingbright, Taipei, Taiwan) was used as visual indicators for the TMP readings. If the TMP was lower than 40 mmHg, the LED color was yellow, red if the TMP was above 50 mmHg, and green if the TMP was in the range of 40-50 mmHg. The Arduino Uno was replaced with Arduino micro (Arduino.cc, Italy) since was smaller in size and had more analog and digital pins. Figure 107 shows the Arduino micro with all the components connected to the pins, and the system powered through a single power supply, 12 VDC that also powers the 10VDC voltage regulator.

The electrical system was able to function properly, so the next step was to implement the components into printed circuit board (PCB).

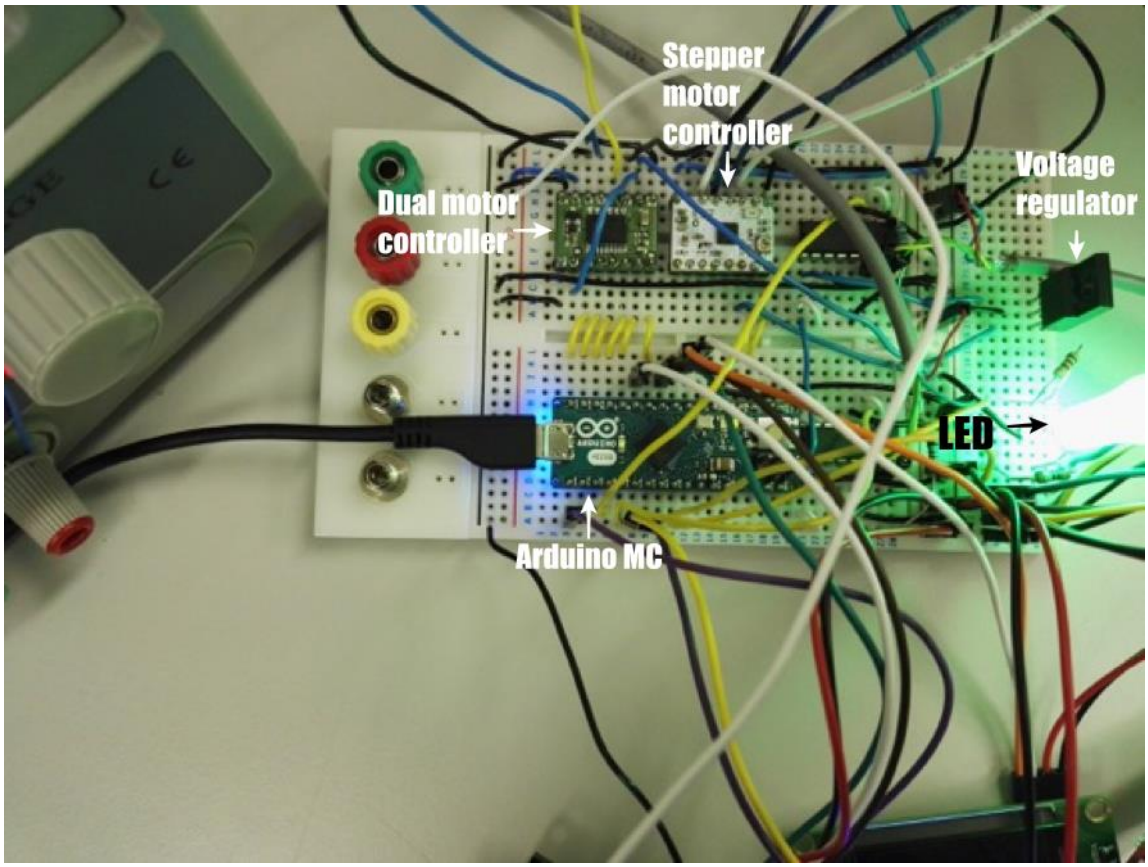

Figure 107 Testing the control system

5.6.6 Combined system:

The device concept was to develop a system to remove cytokines through plasma filtration and a cytokines filter. The device is designed to be a automation system. The rig and the plasma collection basin as seen in figure 109. The electronic components are mounted into the 3D printed housing (figure 108) and the LCD and the four switches are integrated to this.

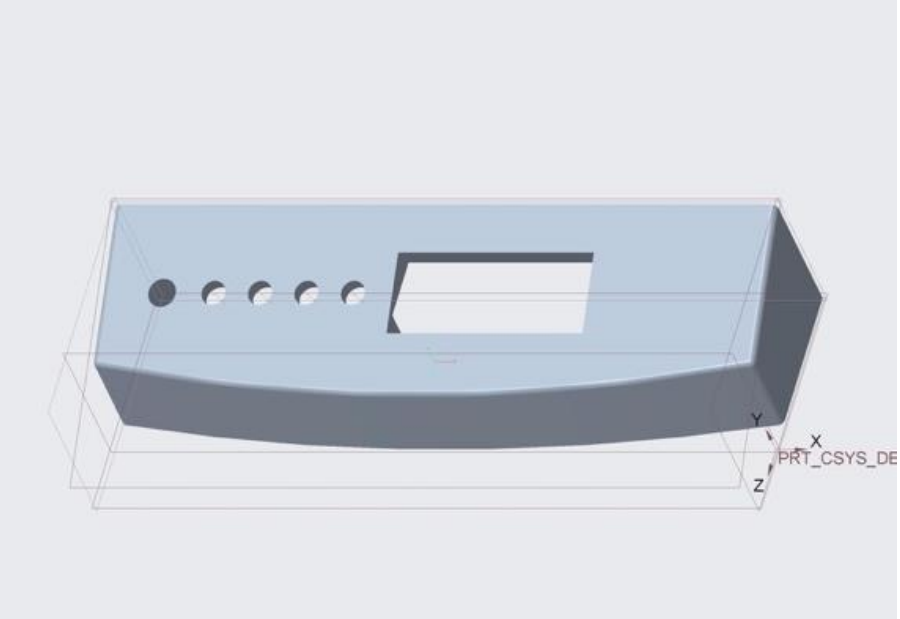

Figure 108 3D CAD of the electronic housing

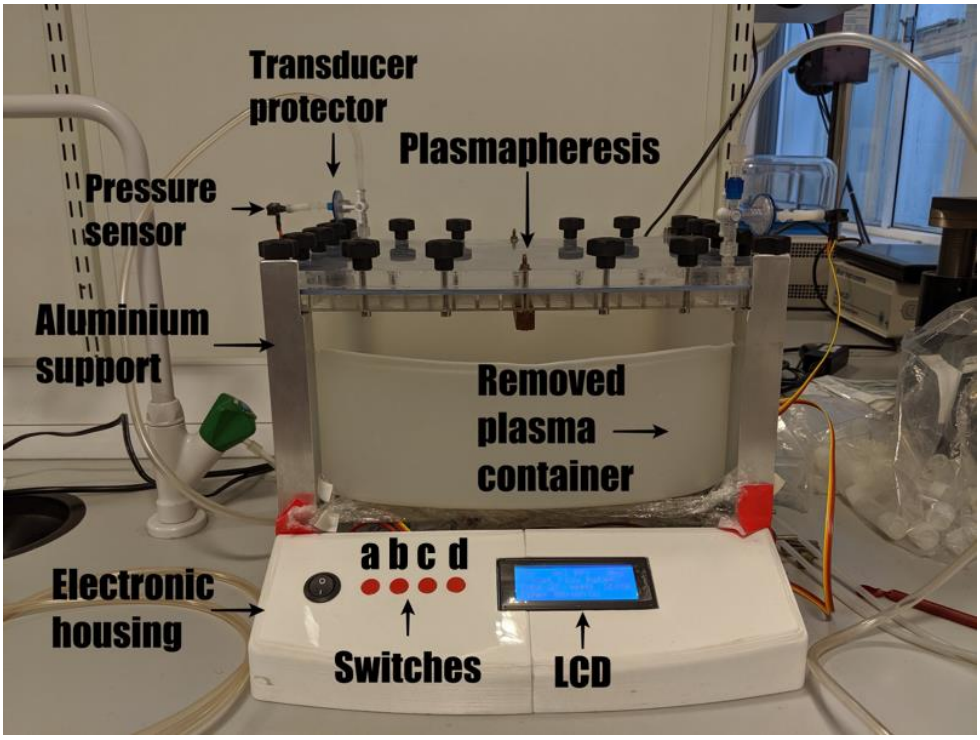

Figure 109 Combined system

To prevent the pressure sensors contacting the blood, a hydrophobic transducer protector (Millx, Burlington, USA) was placed in a three-way valve. The thermoplastic basin (D300mm X W345mm X H110mm) was made at the prosthetics and orthotics department. The aluminium square support bars (W25mm X H245 mm) were made at the workshop in the biomedical engineering department. The load cell is mounted to the base of the system.

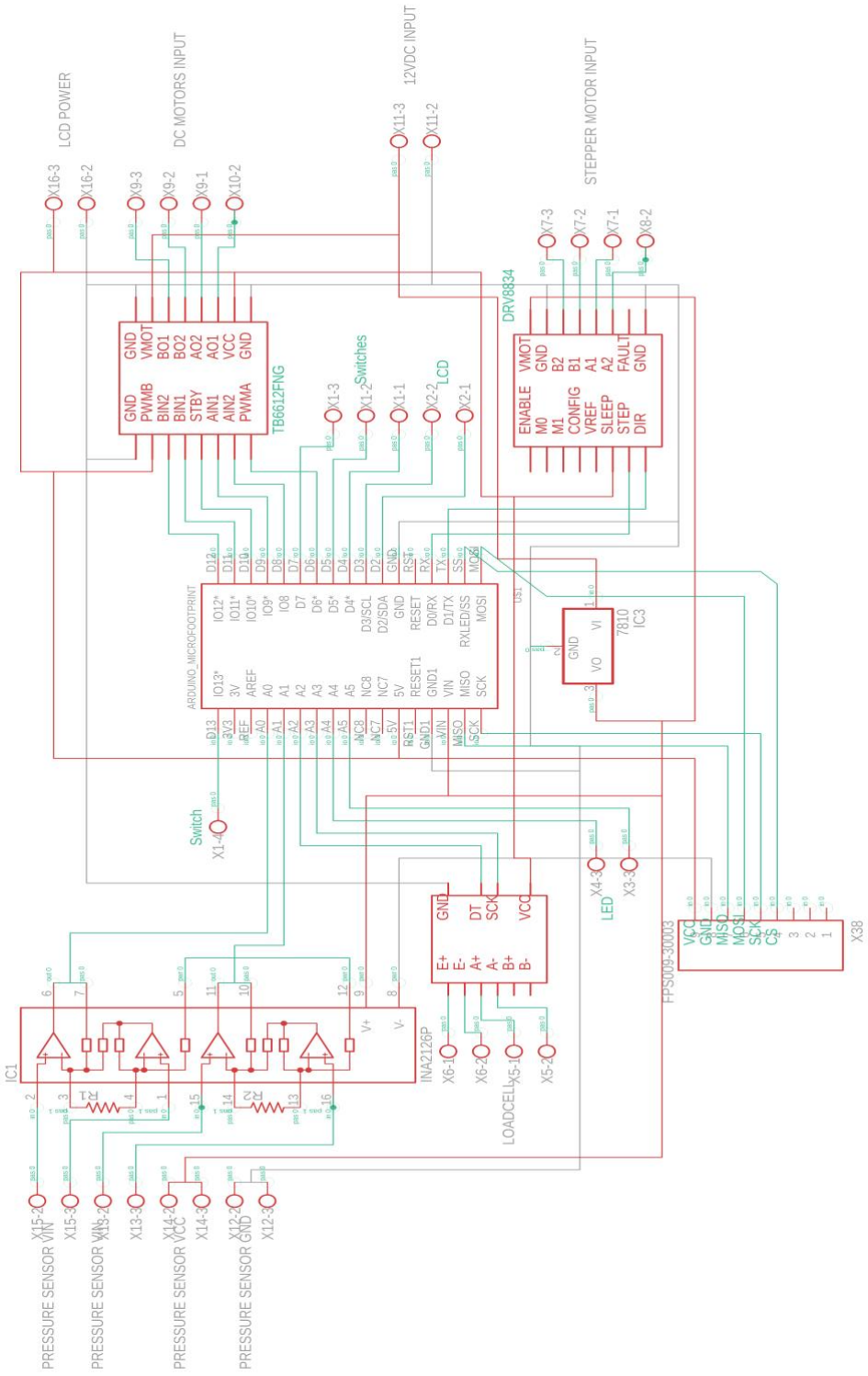

Figure 110 schematic diagram for the automation system

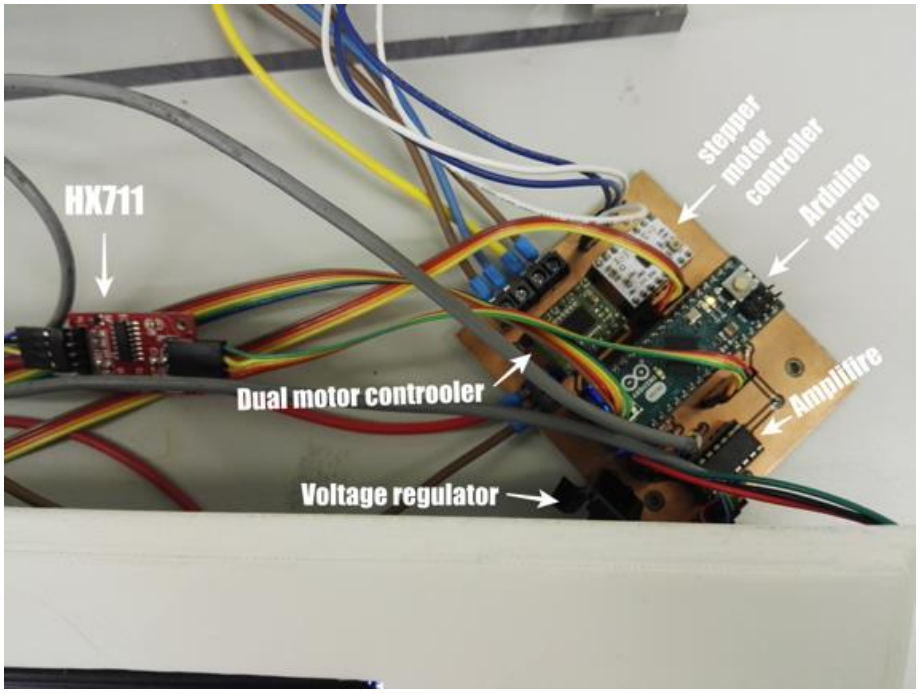

Figure 111 PCB with the components attach to the headers

Figure 110 shows the schematic diagram for the automation system that will be used for the design of the PCB circuit, which was manufactured at the electrical engineering department. The electrical components are attached to female pin headers that were soldered into the PCB (figure 111). The AC adaptor (XP power ltd, Singapore, Singapore) provided the components with electrical power to operate.

5.6.6.1 Measurement of hemolysis:

The 12 hrs experiment was conducted to mimic the clinical scenario. During this experiment, samples of the removed plasma were collected each hour for measurement of pfHb. The pfHb is used to determine the hemoglobin released into plasma due to RBCs damage. Since the RBCs is exposed to shear stress, the pfHb is calculated to measure volume of release hemoglobin. The pfHb was measured using the direct spectrophotometer based on the method presented by (Noe et al., 1984), where they calculate the hemoglobin based on the Allen correction equation:

pfHb (mg/L) = $1.68A_{415} - 0.84A_{380} - 0.84A_{450}$, where A is the absorbance

The absorbance is taken at three wavelengths to eliminate the interference caused by the presence of bilirubin in the samples.

The collected plasma samples were centrifuged and added to 96 well plates and saline was used as blank. Then, they place into the multiskan Go spectrophotometer (Thermo Scientific, Massachusetts, USA). The absorbance readings were taken at three wavelengths: 380 nm, 415 nm and 450 nm. The above equation was used to calculate the pfHb

During the 12 hrs experiment, blood smears were taken from the beaker before the initiation of the experiment, after six hours and at the termination of the experiment. These blood smears were placed under ZOE fluorescent cell imager microscope (Bio-rad, Hercules, USA) to illustrate the RBCs shape that circulate inside the plasmapheresis device.

5.6.6.2 Statistical calculation:

R^2 is defined as good to fit, in other words, how close the data to the fitted model. It range from 0 to 1, as the value of R^2 is larger, the better the data fit the model (Shtatland et al., 2002). For example, in figure 100 and figure 101, the relationship between voltage and pressure is 0.999 that indicate that it is almost a perfect fit, as the voltage increase, the current increase linearly. Moreover, the R^2 is used to determine the relationship between flux rate and TMP.

The error bars used are mean with the standard deviation (mean±SD).

Chapter 6:

Results

6 Results:

6.1 Introduction:

The aim of this project is to design and test a new device directed at plasmapheresis (PP) for the treatment of sepsis. The work including:

1- The design of the fundamental membrane exchange component

2- Maximization of the flux rate through enhanced secondary flow generation to minimize cake formation.

3- System design and configuration to facilitate control and automation function.

The early design and testing process is detailed in chapter 5.

1) Membrane configurations were studied to determine the optimum configuration for the exchange device. This work involved membrane performance testing to determine the most appropriate membrane.
2) Having modelled secondary flow structure to enhance the exchange flow of the device, physical testing of the configuration was performed.
3) Control software and sensor were designed and tested with regards to ensuring autonomous control and performance. These systems were tested under laboratory conditions.

In the present chapter, we will describe the enhancing of the performance of the first iteration of the formal device design. This will take the form of:

1- Assessing the overall performance of the exchange system with particular regard to:
    a) Overall exchange rate with and without a flow disruptor (structural acetate sheet).
2- The effect of the inclusion of a flow director on the flux rate, and to determine whether a flux rate of rigid structure is more efficient in this regard.
3- Asses the effect of controlled TMP on the flux rate.

To establish the proof of concept for each iterative step, we performed one experiment (n=1). Following this, having established the best possible configuration we performed a minimum of three experiments in each arm of the study.

6.2 2nd prototype results:

6.2.1 The effect of flow disruptor on flux:

The flux rate associated with the presence of a flow disruptor (laser cut acetate sheet shown in figure 77) was assessed under the controlled conditions stated in chapter 5, section 5.6.4. These were a flow rate of 150 ml/min at a TMP of 40-50 mmHg over a period of 60 minutes. The results of this process are shown in the following tables (table 11 and 12) and figures (figure 112 and 113).

Time (min)	Plasma removed weight (g)	Flux (ml/min)
0	0	0
10	1.6	0.16
20	3.4	0.18
30	5.5	0.21
40	7.1	0.16
50	9.1	0.2
60	11.2	0.21
Average Flux rate = 0.186 (±0.023) ml/min		

Table 11 Flux rate over 60 minutes without the flow disruptor (laser cut acetate sheet)

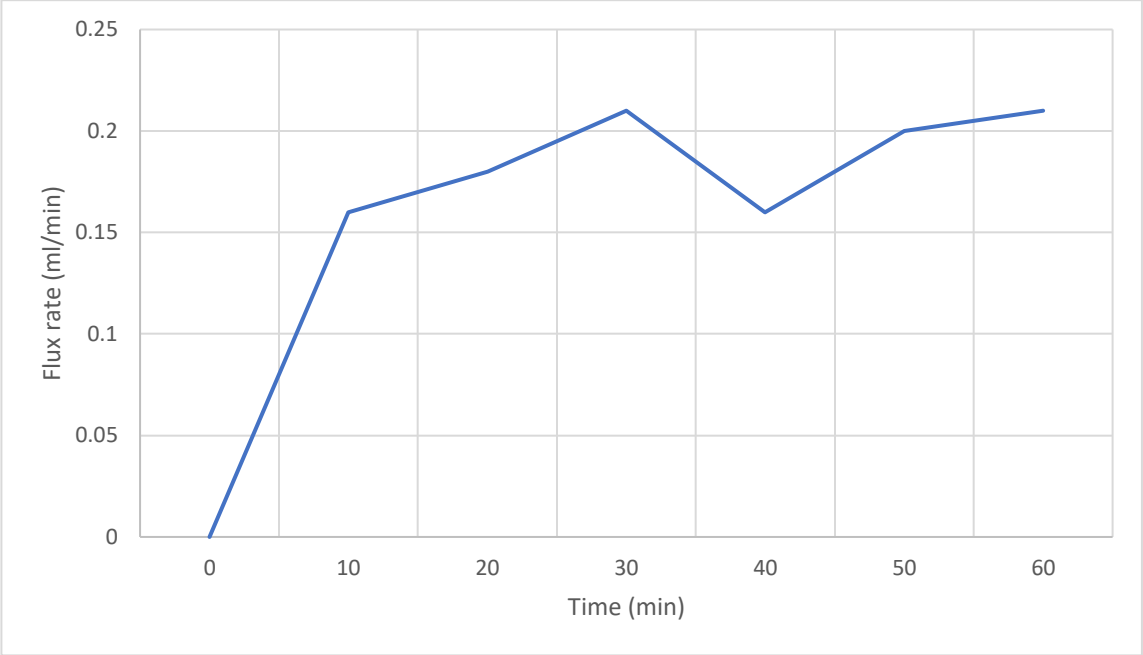

Figure 112 Flux rate over 60 minutes with the flow disruptor (laser cut acetate sheet)

Time (min)	Plasma removed weight (g)	Flux (ml/min)
0	0	0
10	5.9	0.59
20	18	1.21
30	30.8	1.28
40	41.4	1.06
50	52.5	1.11
60	62.1	0.96
Average Flux rate = 1.035 (±0.024) ml/min		

Table 12 Flux rate over 60 minutes with flow disruptor (laser cut acetate sheet)

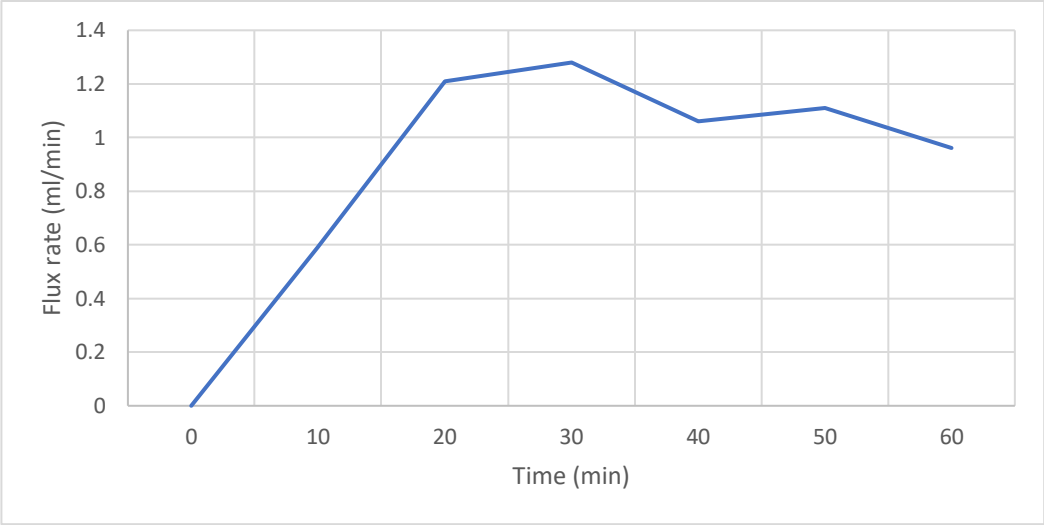

Figure 113 Flux rate over 60 minutes with flow disruptor (laser cut acetate sheet)

6.2.2 The effect of flow director on the flux:

There are two type of flow director that have been accessed, the soft neoprene and hard neoprene. The flow rate was 150 ml/min and the TMP maintained in the range of 40-50 mmHg over a period of 60 minutes. The results of this experiments are shown in the following tables (table 13 and 14) and figure (114 and 115).

Time (min)	Plasma removed weight (g)	Flux (ml/min)
0	0	0
10	6.5	0.65
20	22.9	1.64
30	37.2	1.43
40	47.1	0.99
50	61.5	1.44
60	72.4	1.09
Average Flux rate = 1.20 (±0.36) ml/min		

Table 13 The flux rate of inclusion of soft neoprene flow director

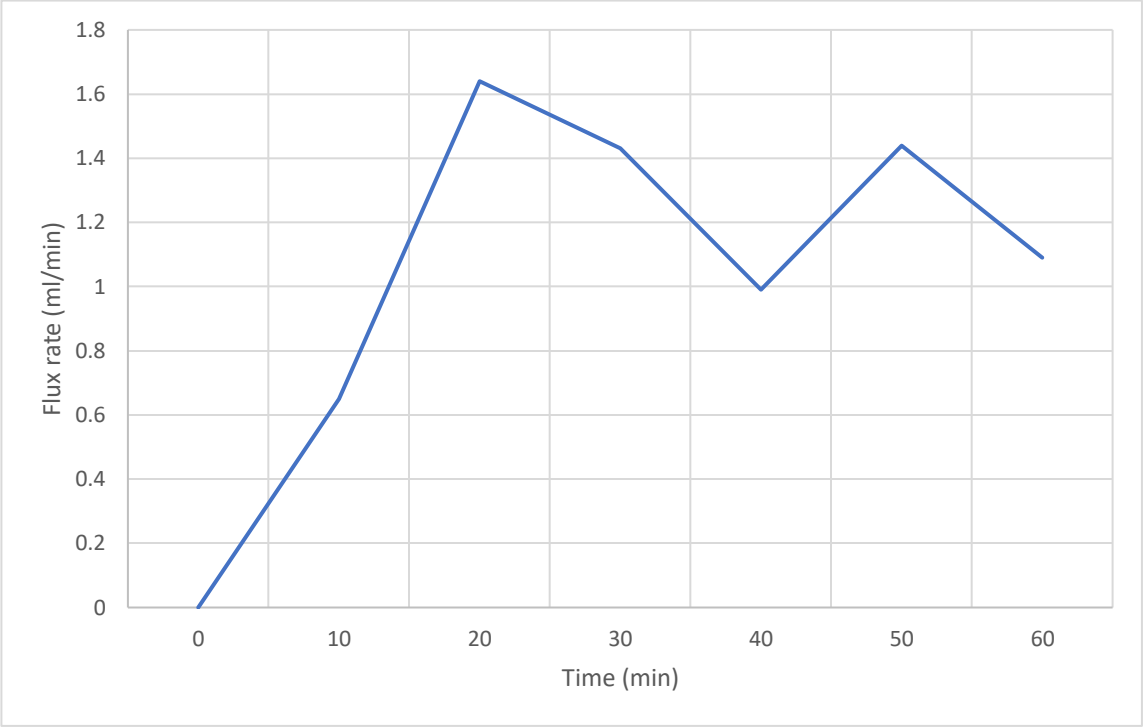

Figure 114 The flux rate of inclusion of soft neoprene flow director

Time (min)	Plasma removed weight (g)	Flux (ml/min)
0	0	0
10	15.2	1.52
20	33.2	1.8
30	52.1	1.89
40	69.2	1.71
50	86.6	1.74
60	104.5	1.79
Average Flux rate = 1.74 (±0.12) ml/min		

Table 14 The flux rate of inclusion of hard neoprene flow director

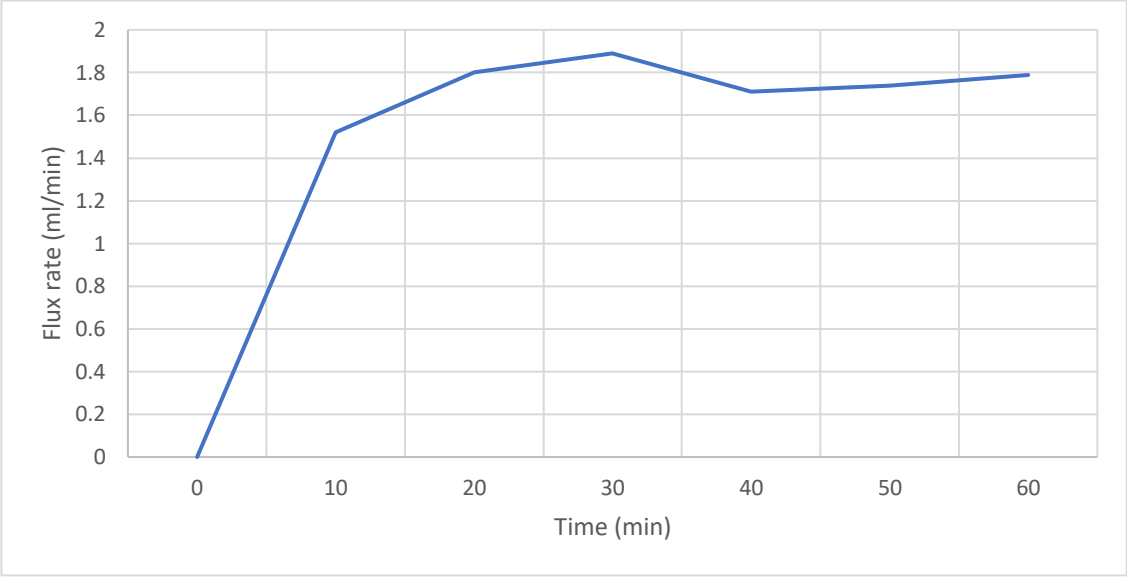

Figure 115 The flux rate of inclusion of hard neoprene flow director

6.2.3 The effect of TMP on the flux rate:

The effect of TMP on the flux rate was investigated. In these experiments (n=3), the ranges of the TMP were 40-50 mmHg, 50-60 mmHg, 60-70 mmHg and 70-80 mmHg with a fixed flow rate of 150 ml/min. The results are illustrated in the figure 116.

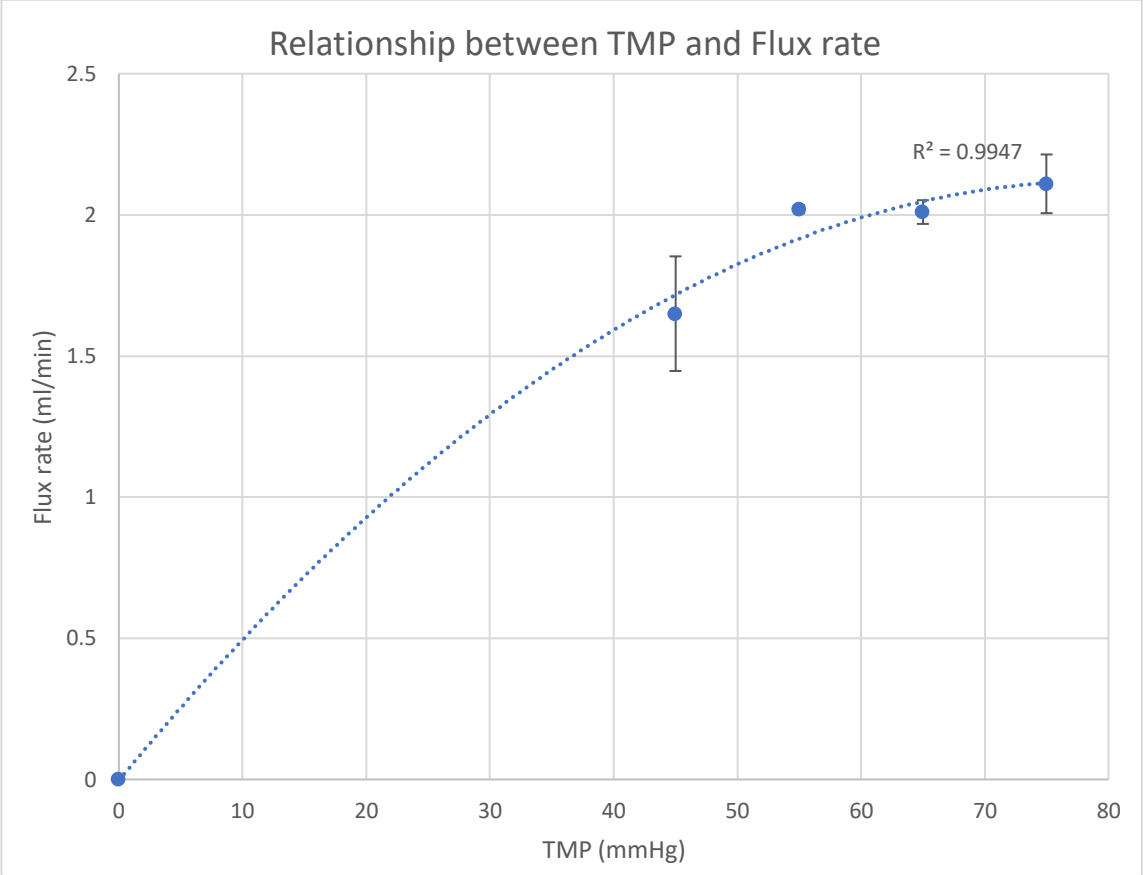

Figure 116 Relationship between TMP and flux rate

6.2.4 Summary:

These experiments confirm that the flow disruptor enhance the fluid flux (0.186 ml/min-1.035 ml/min, 456% improvement). The inclusion of a rigid flow director device in the technology leads to further exchange enhancement (1.2 ml/min-1.74 ml/min, 45% improvement). The final series of experiments, focused on determining the effect of increasing TMP illustrate that the flux increases as the TMP increases, then it reaches a plateau in the range of 50-80 mmHg. Overall, we were able to determine the impact of various design modification to optimize the exchange device. The final configuration comprises the core membrane, a flow disruptor and flow director, operating at a range of 40-80 mmHg (safe range with regards to destruction of blood components) at a flow rate of 150 ml/min. However, the flow and associated flux, was considered to be of sub-clinical proportions. A higher effective flux would be expected for efficient clinical development. Therefore, we processed a design for a larger device with a higher surface area, suited to higher flow rate, with an expected increase in flux.

6.3 3rd prototype:

The previous work and associated results suggest that to attain flux rates of clinical significance further modification and redesign of the core technology was necessary. A 3rd prototype was therefore produced that was different from previous design in that the exchange surface was expanded. This new, larger design was then tested under similar conditions to that described previously in this chapter and in chapter 5.

The first series of test runs were carried out using the larger device without the baffles arrangement, and this was compared with a 2nd prototype without baffles. The results of these tests are shown in table 15 and figure 117.

6.3.1 The effect of flow disruptor on flux:

Time	Plasma removed weight (g)	Flux (ml/min)	2nd prototype flux rate (ml/min)
0	0	0	0
10	8.9	0.89	0.16
20	29.4	2.05	0.18
30	42.5	1.31	0.21
40	54.3	1.18	0.16
50	65	1.07	0.2
60	74	0.9	0.21
Average flux rate = 1.23 (±0.43) ml/min			0.186 (±0.023) ml/min

Table 15 Data for the PES membrane without baffles acetate sheet

Simply by increasing the process surface area there was a significant difference in performance between the 2nd and 3rd prototypes devices. The difference was 561.29%.

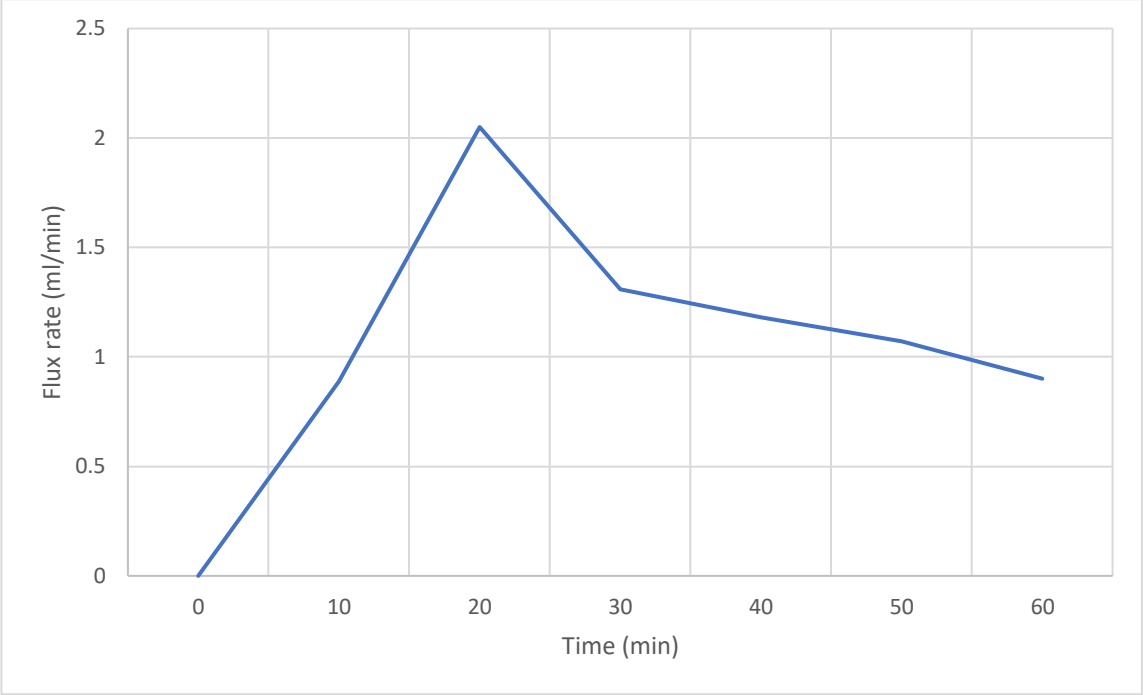

Figure 117 Flux rate for the PES membrane with acetate without baffles sheet

Further tests were carried out on this expanded prototype 3 with the additional of flow disruptor. Disruptor were shown to improve the performance of the 2nd stage prototype because it introduces a secondary flow mechanism in this experiment we investigate whether the flow disruptor would have a significant effect on the performance of the expanded prototype, or whether the increased surface area negated the need for flow disruptor.

Time (min)	Plasma removed weight (g)	Flux (ml/min)	2nd prototype flux rate (ml/min)
0	0	0	0
10	30.9	3.09	0.59
20	69.1	3.82	1.21
30	106.5	3.74	1.28
40	146.6	4.01	1.06
50	195	4.84	1.11
60	225.5	3.05	0.96
Average flux rate = 3.76 (±0.66) ml/min			1.035 (±0.024) ml/min

Table 16 Data for the 3rd prototype with the inclusion of baffles

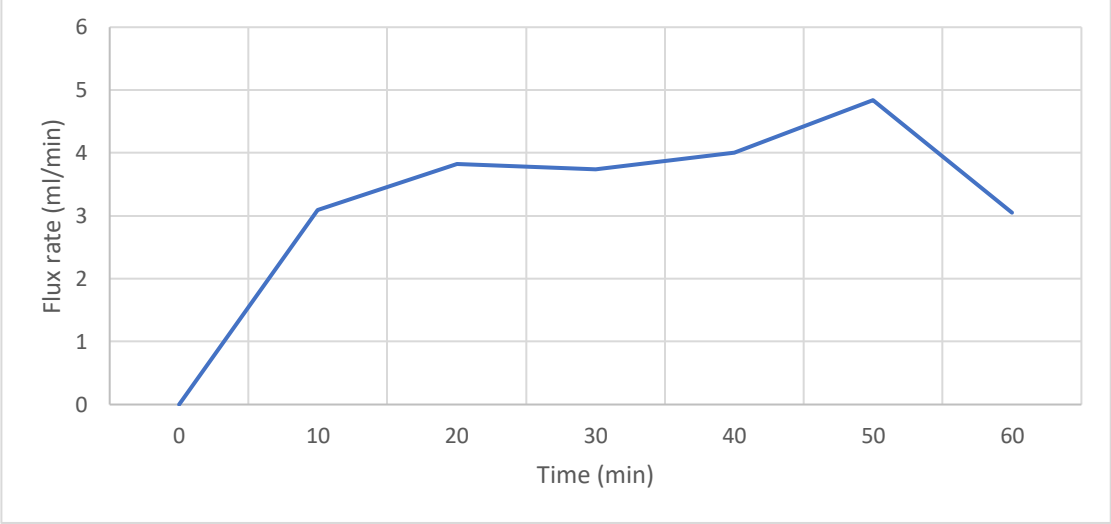

Figure 118 Plot for the 3rd prototype with the inclusion of baffles

The inclusion of the baffles increased the flux rate of the expanded device significantly (1.23 – 3.76 ml/min, 205.69%). The performance of the stage 3 prototype with baffles far exceeded that of the stage 2 prototype with baffles. This confirms the benefit of increasing the surface area for exchange, and the inclusion of flow disruptor on performance.

6.3.2 The effect of flow increase on flux:

Another factor that can influence performance and efficiency in the flow rate of blood through device. To investigate the effect of flow rate on performance we investigated incremental increasing flow rate from 150 ml/min to 300 ml/min a range that covers that anticipate in the clinical field. The result of this is shown in table 17 and figure 119.

Time (min)	Plasma removed weight (g)	Flux (ml/min)	150 ml/min flow rate Flux (ml/min)
0	0	0	0
10	26.6	2.66	3.09
20	76.1	4.95	3.82
30	121	4.49	3.74
40	172.1	5.11	4.01
50	218.5	4.64	4.84
60	246.3	2.78	3.05
Average flux rate = 4.10 (±1.09) ml/min			3.76 (±0.66) ml/min

Table 17 Data for the high flow rate of 300 ml/min

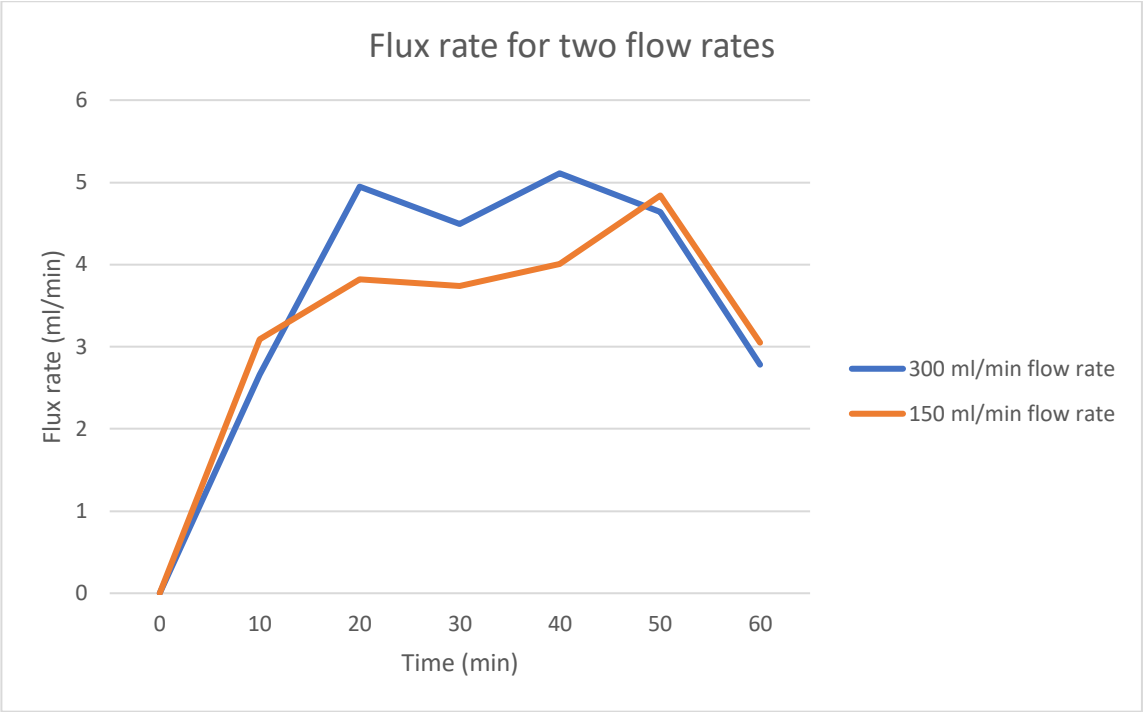

Figure 119 Flux rate plotting for high flow rate of 300 ml/min compared to 150 ml/min

The study of flow rate demonstrated that an increase in flow rate of 100% resulted in an increase in flux over the experimental period of over 9%. Given that flow rate magnitude is a primary contributor to damage to formed blood elements, this is viewed as a positive outcome, given that flow rate through the device can be kept to fairy moderate level to obtain an acceptable flux rate, and there is no significant advantage in significantly escalating blood flow.

6.3.3 The effect of permeate carrier on flux:

Having established key performance enhancing structural elements of the device, we considered whether modifications to the flux outlet conditions might offer a performance advantage. Previous investigations suggest that the inclusion of a permeate carrier, in the form of a nylon mesh structure, positioned at the permeate outlet of the device, may further enhance performance. We investigated this by comparing the performance of the device with and without the permeate carrier. The results of the process are shown in table 18 and figure 120.

Time (min)	Plasma removed weight (g)	Flux (ml/min)	Flux (ml/min) without the permeate carrier
0	0	0	0
10	36.1	3.61	2.66
20	94.1	5.8	4.95
30	154.3	6.02	4.49
40	216.4	6.21	5.11
50	278.1	6.17	4.64
60	337.2	5.91	2.78
Average flux rate = 5.62 (±0.99) ml/min			4.10 (±1.09) ml/min

Table 18 Data for the 300 ml/min flow rate in addition to the membrane support

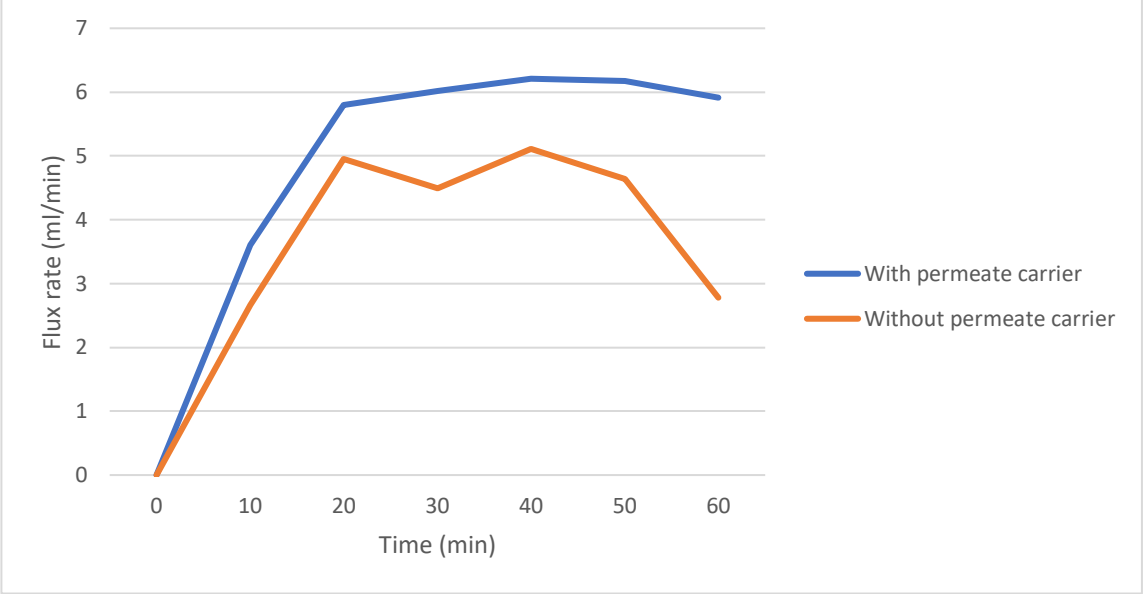

Figure 120 Data for the 300 ml/min flow rate with and without permeate carrier

The inclusion of the permeate carrier have resulted in an increase in the flux rate from 4.10 – 5.62 ml/min (37% improvement) over test period.

6.3.5 Summary:

The series of experiment was designed to examine the effect of a series of factors that may influence device performance and establish the optimal design configuration for the device. These studies established the following:

1- Increasing the surface area resulted in increased flux.

2- Increasing flow rate beyond 150ml/min resulted in only a small performance gain.

3- The inclusion of baffles in the device enhances performance irrespective of surface area.

4- The inclusion of a permeate carrier enhances performance.

These studies have taken the technology closer to an “ideal” configuration.

6.4 Testing system control:

Having established the optimum configuration of the core technology and developed the control system for automation, a series of experiments were carried out to determine the efficacy of the control system in maintaining performance under a series of control scenarios. Of critical importance is the control of blood flow rate and TMP. The following scenarios were studied in terms of the maintenance of these key factors over time for flow rate of 150, 200, 260 ml/min TMP 40-50, 50-60, 60-70 mmHg. The accuracy of the system to control these key factors over time (90 minutes) is an essential objective of this work. The results are shown in figures 121, 122, 123 and 124.

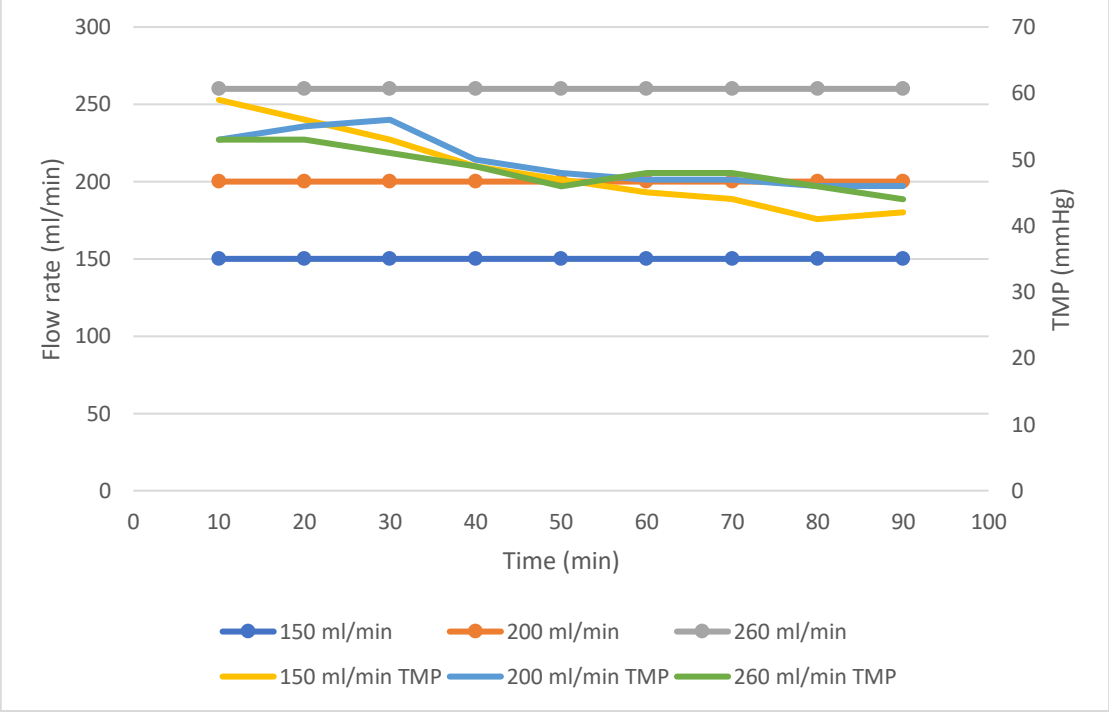

Figure 121 Controlled TMP for different flow rates. The control system was able to maintain the TMP in range of 40-50 mmHg

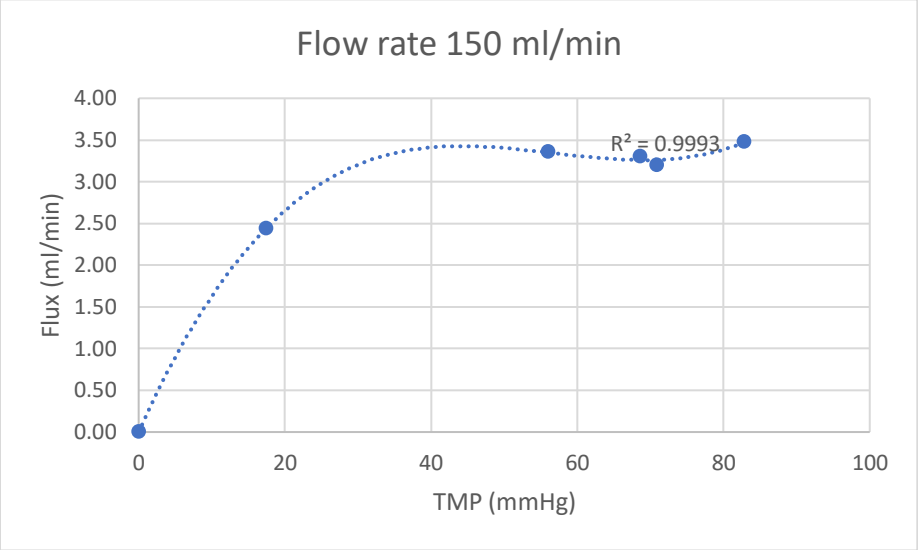

Figure 122 Filtration rate with TMP for 150 ml/min flow rate (n=3)

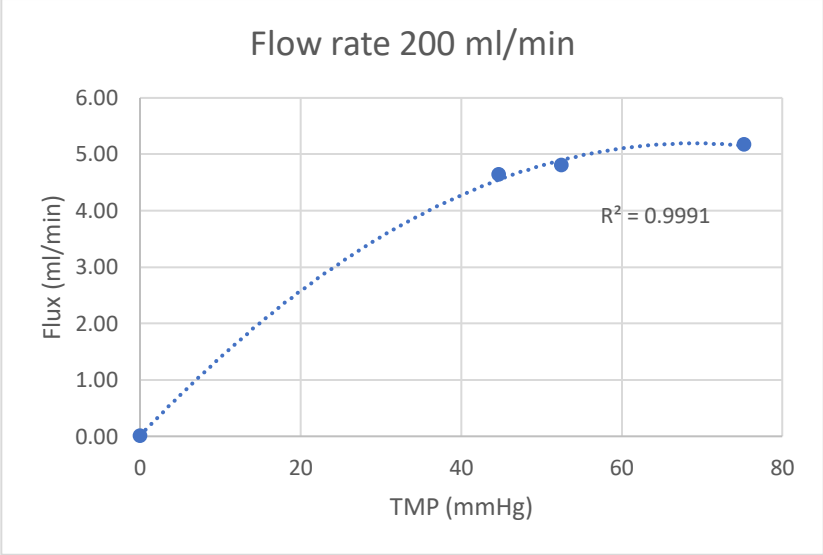

Figure 123 Flux rate with change in TMP for flow rate 200 ml/min (n=3)

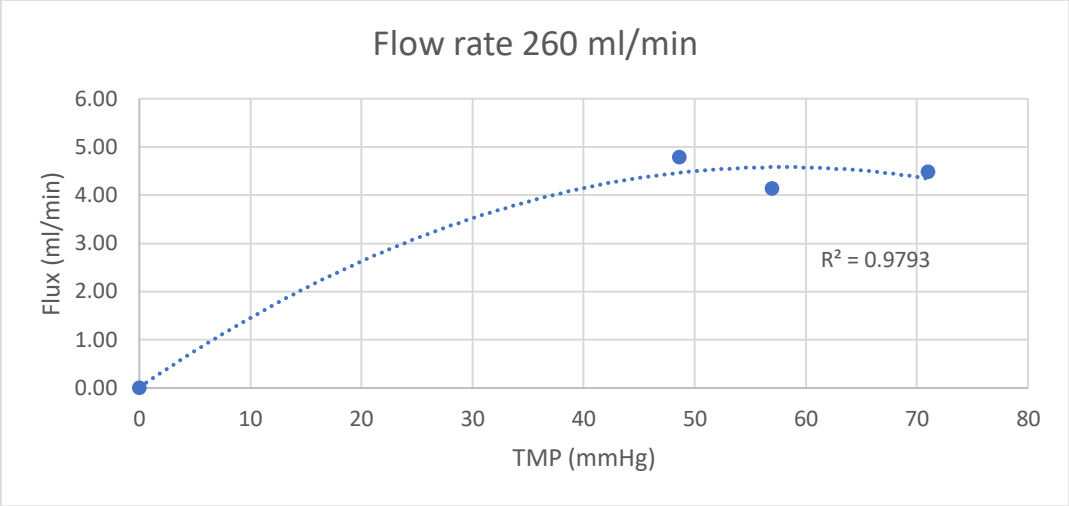

Figure 124 Filtration change with TMP for 260 ml/min flow rate (n=3)

It is clear from these studies that the system was capable of providing a high degree of control of the working environment in each scenario. The performance of the auto-controlled device during various scenarios in term of flux rate is shown in figure 125.

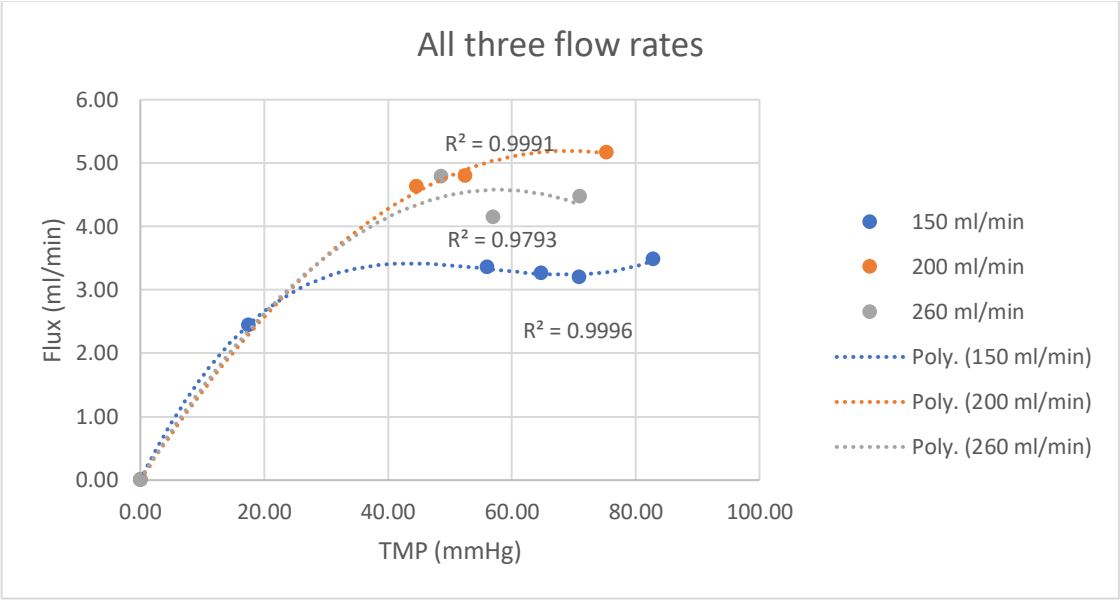

Figure 125 All the three flow flux rates with TMP combined in one graph (n=3)

6.4.1 The 12 hours experiment:

The device will be expected to function over a prolonged demonstrate where in clinical use. To somewhat simulate this scenario, we undertook to illustrate the performance of the device over a 12 hour period. Two main factors were investigated in this experiment, flux and pfHb. The result of this experiment is shown in figures 126 and 127. Figures 128 (before initiation of experiment), 129 (after 6 hrs from the start of the experiment) and 130 (at the termination of the experiment) show the RBCs taken at different time points. The circle shape in figure 130 shows RBCs that deformed after the 12 hrs experiment.

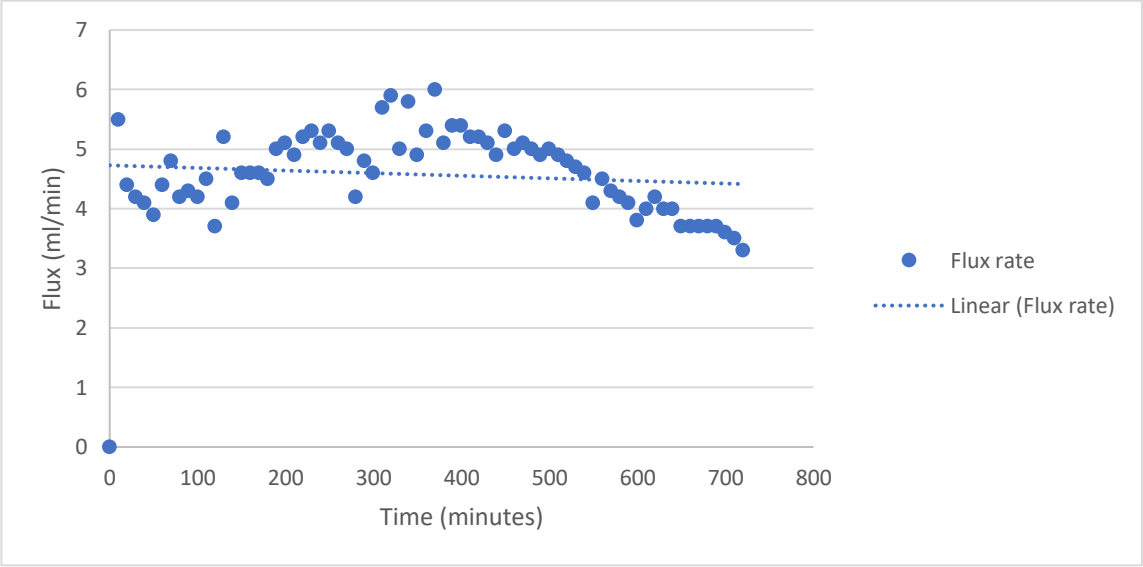

Figure 126 The filtration rate of the 12 hour experiment

The flux rate was fairly constant for the first 500 minutes, tailing off somewhere beyond that. Overall an average flux rate of 4.63 ml/min was achieved.

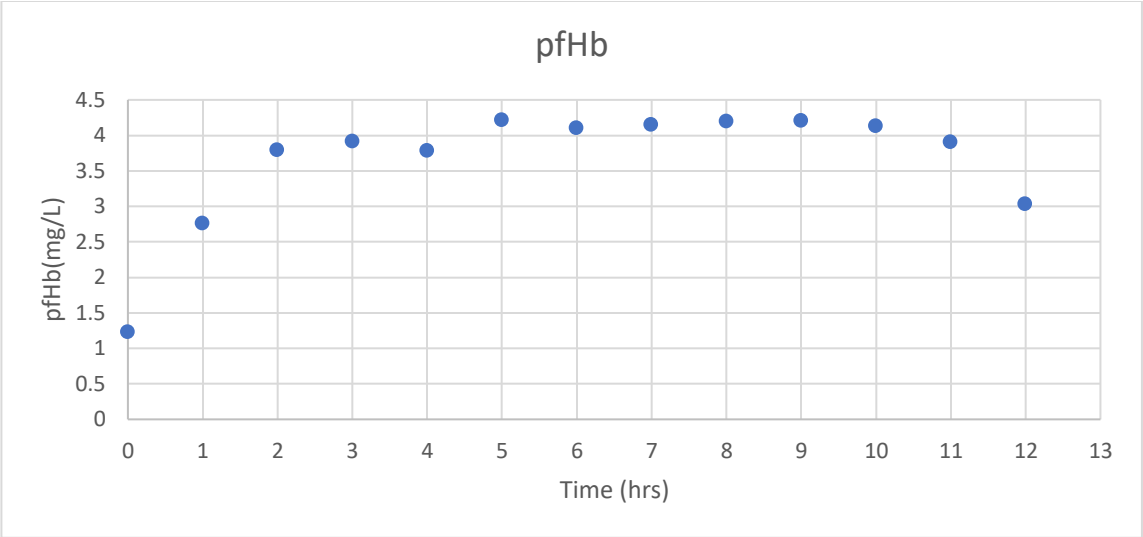

Figure 127 pfHb that measured from the samples taken from the removed plasma each hour through the experiment

There was a rise in pfHb, which measure the hemoglobin level in the removed plasma, over the first 2.5 hrs from 1.25 mg/L to around 4 mg/L. Beyond this the pfHb remained at around 4 mg/L for the duration of the experiment. There were no signs of excessive hemolysis associated with this experiment carried out over a prolonged period.

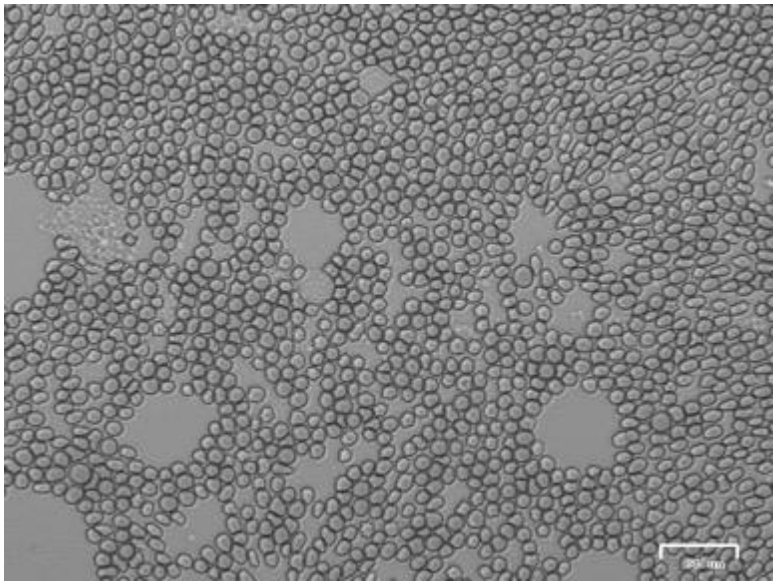

Figure 128 RBCs microscopic image taken before the start of the experiment

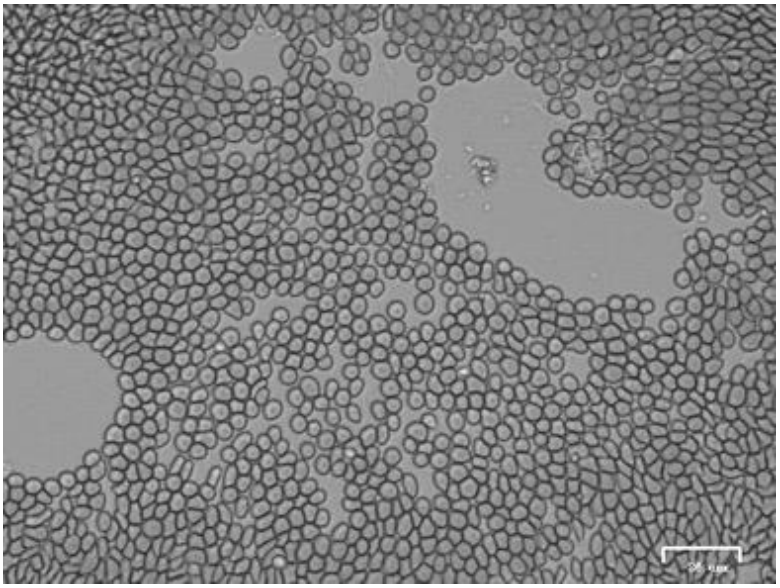

Figure 129 RBCs microscopic image taken after 6 hours of the experiment

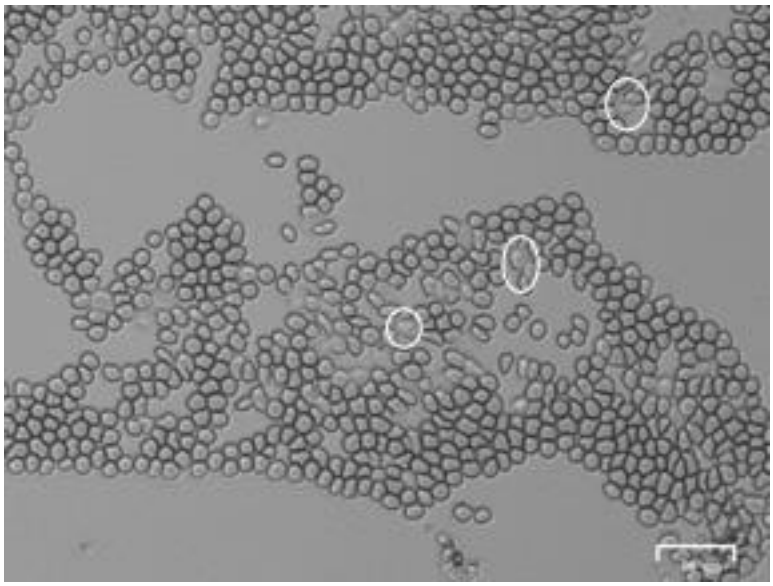

Figure 130 RBCs microscopic image taken at the termination of the experiment

There are some RBCs that was damaged as illustrated by the white circle in figure 130 due to prolong contact with shear stress.

6.4.2 Summary:

The series of experiments for each flow rate show that the flux rate increase with the increase in TMP until it reaches a plateau above 50 mmHg. At a TMP of 40-50 mmHg, a 260 ml/min flow rate has the highest flux rate. In the 12 hours experiment, the flux rate was maintained until toward the end of the experiment where it decreased slightly. The microscopic images of RBCs showed that at the end of the experiment, there was some deformation of some of the RBCs.

Chapter 7:

Discussion and Limitations

7 Discussion and limitation:

7.1 Achieved objective:

The aim of this project was to develop a simplified, stand-alone, fully automated, device to filter plasma from blood with the objective to treat sepsis. The objectives that have been met are summarized below:

1- CFD modelling of methods to generate secondary flow to reduce cake layer formation.
2- The rig has been 3D printed for investigation of the performance of the device
3- The optimum TMP for to achieve high flux for the rig was determined.
4- Different methods have been employed to increase the filtration rate.
5- Two membranes with different effective open areas (EOA) have been tested for flux optimization.
6- Larger rig has been fabricated using 3D printer and various experiments were performed to determine the impact on efficiency.
7- The automation system was developed and tested.
8- The combined system performance was tested to investigate the performance of the automated control system.

7.2 Summary of the device development:

The design of the device was based on combining different approaches for generation secondary flow to minimize the formation of the cake layer known to reduce the filtration rate. CFD modelling was performed in Ansys software to investigate the shear stress of the blood flowing through the device. The prototype was 3D printed and two membranes with different effective porous pore structures to study difference in filtration rate. Also, different measures were investigated to increase the flux rate. However, since the second prototype did not produce a clinical acceptable flux rates (>200ml/hr), a larger device was fabricated to increase the flux rate. Different configurations were employed to further improve the filtration rate. An automation system was developed to be used with the device, since the device objective is "plug, play and throw away". The role of the automation system was to control the key operational parameters of the system, to enhance and stabilize performance and to offer a high degree of operator independence. Based on the pressure readings from the inlet and the outlet pressure sensors, the MC controls the TMP by extending or retracting the linear actuator restricting or enhancing flow through the device by controlled resistance. In addition, the MC initiates the replacement of the removed plasma fluid based on load cell readings which measure the volume of the plasma removed. Auto-switches are used to start and stop the pumps, select the flow rate and to reset the scale. The automation system was added to the 3rd prototype and several experiments were performed to investigate the performance of the electronic system in controlling device performance. Moreover, using the automated system, the performance of the different flow rates on the filtration rate and TMP was studied. Ultimately, the system was run for a continuous

period of 12 hours to investigate the performance of the system over a clinically mimetic period.

7.3 CFD studies to inform design:

The combination of the methods used by Mallubhotla and Belfort (1997) (U-bend), Millward et al. (1995) (baffles) and Wei et al. (2013) (semi-circle bubble) was used to create disturbance in the flow as illustrated in the CFD results, figures 60, 61, 62, 63 and 64. The maximum shear stress was 26 pa at the confluence of these structures. In addition, the results of the TKE, which represent the intensity of turbulence, matched the shear stress. In other words, the highest values of the TKE are in the same location of the highest shear stress. So, this indicates that highest intensity of turbulent flow occurs at the highest shear stress. Due to the constrains on mesh selection, the number of elements in the mesh affects the number of the contours and the streamlines. The number of elements for the selected mesh is medium because of constrains put on computational power and time. The time to solve the CFD equation increases with the increasing mesh and element numbers.

7.4 2nd prototype results:

The use of the flow disruptor (laser cut acetate sheet) enhanced the flux rate when compared to the 1st prototype. Moreover, for the PES membrane configuration, the addition of baffles led to a significant improvement in the flux rate, in the range of 456.5%. This flow disruptor induces two benefits:

1- Generation of additional secondary flow due to creation of disruption of the flow
2- Amplifies the secondary flow that is generated by the protuberances

These two phenomena have resulted in higher shear stress, associated with an improvement in the filtration rate. Moreover, by replacing the PC membrane that has an effective open area of 30% (pore size 1μm) by a PES membrane (average pore size 3 μm) with effective open area 80% there was an improvement in flux of 60%. This improvement in the flux rate has previously been reported by (Friedman et al., 1983). The use of the flow director was investigated using 3mm thick soft neoprene and 3mm thick solid neoprene. The solid neoprene resulted in higher flux rate compared with the soft neoprene since this encourage the blood to flow the prescribed path. As the blood follows the designed path, optimal secondary flow is generate. Thus, the shear stress is higher when compared with the with soft neoprene as indicated by the difference in the flux rate (soft neoprene 1.2 ml/min) (solid neoprene 1.74 ml/min). In the series of experiments that illustrate the relationship between TMP and flux, it was clear that as the TMP increased from 40-50 mmHg to 50-60 mmHg, the flux rate increase linearly by 22% (1.65 - 2.02 ml/min). In addition, the critical flux occurs in the range of 40-50 mmHg in both membranes, possibly due to the accumulation of particles on the membrane surface associated with the separation process. This relationship between

TMP and flux in plasmapheresis has been reported by Jaffrin et al. (1992), who suggests that in the first 50 mmHg, the flux increases linearly with TMP. However, further increase in TMP does not improve the flux rate as it reached a plateau as seen in figure 116. The flux rate only improved by 4.8% as the TMP reached 70-80 mmHg. The linear increase only occurs in flux dependent region as described by Gurland et al. (1996, P.475) and Wiese (2007, P.84). The small 4.8% increase in flux due to increasing the TMP to 70-80 mmHg could be due to the high TMP forcing particles through the membrane pores, but is insignificant in term of clinical performance.

7.5 3rd prototype results:

The previous designed fail to reach a clinically acceptance plasma removal rate of around 200 ml/hr. Thus, in the 3rd prototype we increased the device size. Since the flow disruptor demonstrated that it is able to improve the flux rate, it was incorporated into the 3rd prototype. Moreover, for firm support a metal bar was added on the top of the acrylic membrane support to improve rigidity. The data presented in table 12 and figure 116 show that the larger rig was able to filtrate the plasma at a rate of 3.75 ml/min. This indicates that by increasing the surface area of the device, the plasma filtration rate is increased. However, substantially increasing the flow rate by 100% only resulted in an increase in flux rate of 9.3%. This can be explained by the shear stress limitation mechanisms mentioned by (Grandison et al., 2000). They suggest that further increase in shear stress will result in improvement in the filtration rate but once the critical shear stress is reached, further increase will lead to reduction in shear stress. So, it is possible in our model that above a flow rate of 300 ml/min, critical shear stress is reached and results in a reduction in the flux rate. By adding a nylon mesh membrane support

(permeate carrier) to the configuration, the flux rate improved by 37% (4.1 – 5.52 ml/min) for the same flow rate. The permeate carrier, which carries the solute from the outer side of the membrane to the solute collection bucket. Permeate carrier helps to collect plasma faster since it acts as a flow channel that allows the plasma to flow faster from the membrane to the acrylic support and into the collection basin.

7.6 Comparison between 2nd and 3rd prototypes:

The 2nd prototype was developed to prove the concept of generating secondary flow to minimize the cake layer formation. Also, two membranes were tested to determine which is associated with higher flux rate. Different configurations were tested to enhance the flux rate. Despite optimizing the configuration, including adding flow disruptor that amplify the shear stress and a flow director for force the blood to follow its prescribed path, the PP rate was less than 200 ml/hr in the 2nd prototype. As a result, the 3rd prototype size was increase to increase the overall plasma filtration volume. Using a thicker membrane support and adding a metal bar to enhance mechanical support, the plasma separation volume was able to exceed 200 ml/hr. Overall, enhancement in the 3rd configuration led to improvement performance, resulting in a level that is compatible with clinical requirement.

7.7 Combined system studies:

The combined system consists of the final configuration of the 3rd PP device and the control system for full automation. The basis of this PP device that it is should be simple to use. Millward et al. (1995) and Najarian and Bellhouse (1996) developed devices for PP, however, there devices are complex and employed a mechanical pillow to induce secondary flow through fluid oscillation. In the combined system, the oscillatory flow is generated using the contact and release mechanisms of the roller pump.

Several experiments were performed to investigate the effect of TMP on the flux rate using three flow rates, 150 ml/min, 200 ml/min and 260 ml/min. The results show that, as the TMP increase, the flux rate also increases, until 50 mmHg where it reaches a plateau. This supports the findings from clinical Plasmapheresis, where the flux is linear until the TMP is 50 mmHg (Jaffrin et al., 1992). In our 12 hour experiment, the automation device was able to separate plasma from the blood effectively with consistency. This suggests that the generation of secondary flow is sufficient to minimizes the cake layer formation which would cause a decay in exchange rate. After 600 minutes, the flux rate dropped slightly, most likely due to the membrane pores being blocked by cells deposited as an effect of filtration. The pfHb data confirm that minimal haemolysis occurred during the plasma separation, a level well below acceptable level suggested by (Omar et al., 2015). The microscopic images of the RBCs taken before initiation of the experiment, after six hours and at the end of the experiment show the condition of RBCs that circulate inside the device. (Olia et al., 2016) stated that longer exposure to shear stress could deform RBCs. The microscopic image taken at the end of the experiment show that some RBCs have deformed, but not significant numbers.

7.8 Limitation:

There are some limitations that could have an impact on the scope of the data and quality of research:

1- The plasmapheresis optimum operation is at a TMP in the range of 40-50 mmHg. This can be achieved by modifying the flow rate to decrease and increase, if thrombosis occur, in order to maintain the effective TMP range. However, the C++ code written for the automation system takes up than 70% of the MC memory. Even though the automation system is working effectively, adding further codes for controlling the flow rate could cause the system to not function as required.

2- Due to time constraints, the cytokines removed through the removed plasma was not measured. However, we have confidence from previous experiments that this will function adequately (Coutts, 2016).

3- The cake layer that form due to the protein deposition on membrane surface was not measured and analyzed using SEM directly. However, the data shown, indirectly, that the cake layer effect was reduced as the device was able to maintain almost constant flux rate for 9 hours.

Chapter 8:

Conclusion and Future Work

8 Conclusion and future work:

8.1 Conclusion:

A full scale design was produced using a combination of 3D printer and fabrication and the total plasma flux, together with methods designed to enhance flux were introduced. A series of approaches were taken to evaluate performance, including various pumping solution, and membrane support configurations. A final ideal configuration was derived, which resulted in a clinically acceptable filtration rate, in the region of excess of 200 ml/hr at a TMP in the region of 50 mmHg. A key aspect of the proposed technology is that it should be largely autonomous, in effect "plug and play" and a considerable efforts was applied to the design the control algorithms, electronics and sensor technologies required to achieve these. After a period of defining and refining the various components a fully compensatory fluid balance mechanism was derived that permitted long term automated maintenance of fluid balance in the flowing blood perfusate and a similar arraignment for volumetric control of the transferred replacement solution. After a number of issues associated with minimizing haemolysis and maximizing the fluid (plasma) flux through enhanced secondary flow generation, a final configuration was derived that was tested over a prolonged period, in this case, 12 hours. The experiment was highly successful, resulting in the maintenance of good flux (200+ ml/hr) and fluid balance, with only minimal levels of hemolysis (<4 mg/L). Overall the primary objectives of the project were met, through the development of a fully functional and consistent plasma removal and replacement system that was fully automated. We did not achieve the full integration of the cytokine adsorption technology for technical reasons. However, this aspect of the work will form a key part of our future work.

8.2 Future work:

This project was successful in terms of its primary focus, the development of fully automated plasma separation for the treatment of sepsis. There remain however a number of areas that require future development these include:

a) The integration of cytokine filter technology to reduce the cytokine storm present during sepsis. We have identified a new approach to this, activated carbon cloth, which offer better manufacture potential for this. An integrated filter technology will be developed using this material, for this application.

b) Further work is required on the alarm element of the system to inform users of imbalance in flow, TMP, fluid together with the development of a software algorithm which integrates these key features.

c) The system needs to be tested on a large animal model of sepsis to prove its efficacy and efficiency.

References:

ABRAHAM, E., ANZUETO, A., GUTIERREZ, G., TESSLER, S., SAN PEDRO, G., WUNDERINK, R., DAL NOGARE, A., NASRAWAY, S., BERMAN, S., COONEY, R., LEVY, H., BAUGHMAN, R., RUMBAK, M., LIGHT, R. B., POOLE, L., ALLRED, R., CONSTANT, J., PENNINGTON, J. & PORTER, S. 1998. Double-blind randomised controlled trial of monoclonal antibody to human tumour necrosis factor in treatment of septic shock. NORASEPT II Study Group. *Lancet,* 351**,** 929-33.

ABRAHAM, E., LATERRE, P.-F., GARG, R., LEVY, H., TALWAR, D., TRZASKOMA, B. L., FRANÇOIS, B., GUY, J. S., BRÜCKMANN, M., REA-NETO, Á., ROSSAINT, R., PERROTIN, D., SABLOTZKI, A., ARKINS, N., UTTERBACK, B. G. & MACIAS, W. L. 2005. Drotrecogin Alfa (Activated) for Adults with Severe Sepsis and a Low Risk of Death. *New England Journal of Medicine,* 353**,** 1332-1341.

ABRAHAM, E., WUNDERINK, R., SILVERMAN, H. & ET AL. 1995. Efficacy and safety of monoclonal antibody to human tumor necrosis factor α in patients with sepsis syndrome: A randomized, controlled, double-blind, multicenter clinical trial. *JAMA,* 273**,** 934-941.

AGENCY, E. M. 2011. *Xigris (drotrecogin alfa (activated)) to be withdrawn due to lack of efficacy* [Online]. Available: http://www.ema.europa.eu/ema/index.jsp?curl=pages/news_and_events/news/2011/10/news_detail_001373.jsp&mid=WC0b01ac058004d5c1 [Accessed 3/6/2018 2018].

ALEMU, Y. & BLUESTEIN, D. 2007. Flow-induced Platelet Activation and Damage Accumulation in a Mechanical Heart Valve: Numerical Studies. *Artificial Organs,* 31**,** 677-688.

ALLEGREZZA, A., IRELAND, T., KOOLS, W., PHILLIPS, M., RAGHUNATH, B., WILKINS, R. & XENOPOULOS, A. 2010. Membranes in the Biopharmaceutical Industry. *In:* KLAUS-VIKTOR PEINEMANN, S. P. N. (ed.) *Membranes for the Life Sciences.* Wiley-VCH Verlag GmbH & Co. KGaA.

AMULIC, B., CAZALET, C., HAYES, G. L., METZLER, K. D. & ZYCHLINSKY, A. 2012. Neutrophil function: from mechanisms to disease. *Annual review of immunology,* 30**,** 459-489.

AOKI, H., KODAMA, M., TANI, T. & HANASAWA, K. 1994. Treatment of sepsis by extracorporeal elimination of endotoxin using polymyxin B-inimobilized fiber. *The American journal of surgery,* 167**,** 412-417.

BACCHIN, P., AIMAR, P. & FIELD, R. W. 2006. Critical and sustainable fluxes: Theory, experiments and applications. *Journal of Membrane Science,* 281**,** 42-69.

BASKURT, O. K. & MEISELMAN, H. J. Blood rheology and hemodynamics. Seminars in thrombosis and hemostasis, 2003. Copyright© 2003 by Thieme Medical Publishers, Inc., 333 Seventh Avenue, New York, NY 10001, USA. Tel.:+ 1 (212) 584-4662, 435-450.

BELFORT, G., DAVIS, R. H. & ZYDNEY, A. L. 1994. The behavior of suspensions and macromolecular solutions in crossflow microfiltration. *Journal of Membrane Science,* 96**,** 1-58.

BELLHOUSE, B. J., BELLHOUSE, F. H., CURL, C. M., MACMILLAN, T. I., GUNNING, A. J., SPRATT, E. H., MACMURRAY, S. B. & NELEMS, J. M. 1973. A HIGH EFFICIENCY MEMBRANE OXYGENATOR AND PULSATILE PUMPING SYSTEM, AND ITS APPLICATION TO ANIMAL TRIALS. *ASAIO Journal,* 19**,** 72-79.

BERENDS, E. T., KUIPERS, A., RAVESLOOT, M. M., URBANUS, R. T. & ROOIJAKKERS, S. H. 2014. Bacteria under stress by complement and coagulation. *FEMS microbiology reviews,* 38**,** 1146-1171.

BERLOT, G., AGBEDJRO, A., TOMASINI, A., BIANCO, F., GERINI, U., VIVIANI, M. & GIUDICI, F. 2014. Effects of the volume of processed plasma on the outcome, arterial pressure and blood procalcitonin levels in patients with severe sepsis and septic shock treated with coupled plasma filtration and adsorption. *Blood purification,* 37**,** 146-151.

BERNARD, G. R., VINCENT, J. L., LATERRE, P. F., LAROSA, S. P., DHAINAUT, J. F., LOPEZ-RODRIGUEZ, A., STEINGRUB, J. S., GARBER, G. E., HELTERBRAND, J. D., ELY, E. W., FISHER, C. J., JR. & RECOMBINANT HUMAN PROTEIN, C. W. E. I. S. S. S. G. 2001. Efficacy and safety of recombinant human activated protein C for severe sepsis. *N Engl J Med,* 344**,** 699-709.

BERRY, M., PATEL, B. V. & BRETT, S. J. 2017. New Consensus Definitions for Sepsis and Septic Shock: Implications for Treatment Strategies and Drug Development? *Drugs,* 77**,** 353-361.

BIRBEN, E., SAHINER, U. M., SACKESEN, C., ERZURUM, S. & KALAYCI, O. 2012. Oxidative stress and antioxidant defense. *World Allergy Organization Journal,* 5**,** 9.

BLACKWELL, T. S. & CHRISTMAN, J. W. 1996. Sepsis and cytokines: current status. *Br J Anaesth,* 77**,** 110-7.

BOCHUD, P.-Y. & CALANDRA, T. 2003. Pathogenesis of sepsis: new concepts and implications for future treatment. *BMJ : British Medical Journal,* 326**,** 262-266.

BONE, R. C., BALK, R. A., CERRA, F. B., DELLINGER, R. P., FEIN, A. M., KNAUS, W. A., SCHEIN, R. & SIBBALD, W. J. 1992. Definitions for sepsis and organ failure and guidelines for the use of innovative therapies in sepsis. The ACCP/SCCM Consensus Conference Committee. American College of Chest Physicians/Society of Critical Care Medicine. *Chest Journal,* 101**,** 1644-1655.

BONE, R. C., GRODZIN, C. J. & BALK, R. A. 1997. Sepsis: A New Hypothesis for Pathogenesis of the Disease Process. *Chest,* 112**,** 235-243.

BOTERO, J. S. H. & PÉREZ, M. C. F. 2012. The history of sepsis from ancient Egypt to the XIX century. *Sepsis-an ongoing and significant challenge.* InTech.

BROUGHTON, G. I., JANIS, J. E. & ATTINGER, C. E. 2006. A Brief History of Wound Care. *Plastic and Reconstructive Surgery,* 117**,** 6S-11S.

BUSUND, R., KOUKLINE, V., UTROBIN, U. & NEDASHKOVSKY, E. 2002. Plasmapheresis in severe sepsis and septic shock: a prospective, randomised, controlled trial. *Intensive Care Med,* 28**,** 1434-9.

BYUN, H. S. & RHEE, K. 2004. CFD modeling of blood flow following coil embolization of aneurysms. *Medical Engineering & Physics,* 26**,** 755-761.

CASTELLHEIM, A., BREKKE, O. L., ESPEVIK, T., HARBOE, M. & MOLLNES, T. E. 2009. Innate Immune Responses to Danger Signals in Systemic Inflammatory Response Syndrome and Sepsis. *Scandinavian Journal of Immunology,* 69**,** 479-491.

CAVAILLON, J.-M., ADIB-CONQUY, M., FITTING, C., ADRIE, C. & PAYEN, D. 2003. Cytokine Cascade in Sepsis. *Scandinavian Journal of Infectious Diseases,* 35**,** 535-544.

CENSOPLANO, N., EPTING, C. L. & COATES, B. M. 2014. The Role of the Innate Immune System in Sepsis. *Clinical Pediatric Emergency Medicine,* 15**,** 169-176.

CHARCOSSET, C. 2012. Ultrafiltration. *In:* CHARCOSSET, C. (ed.) *Membrane Processes in Biotechnology and Pharmaceutics.* Amsterdam: Elsevier.

CHAUDHRY, H., ZHOU, J., ZHONG, Y., ALI, M. M., MCGUIRE, F., NAGARKATTI, P. S. & NAGARKATTI, M. 2013. Role of cytokines as a double-edged sword in sepsis. *In vivo (Athens, Greece),* 27**,** 669-684.

CHERYAN, M. 1998. *Ultrafiltration and Microfiltration Handbook,* Lancaster, CRC Press.

CHO, Y.-I. & CHO, D. J. 2011. Hemorheology and microvascular disorders. *Korean circulation journal,* 41**,** 287-295.

CHOUSTERMAN, B. G., SWIRSKI, F. K. & WEBER, G. F. 2017. Cytokine storm and sepsis disease pathogenesis. *Seminars in Immunopathology,* 39**,** 517-528.

CHUN, T. T., POTZ, B. A., YOUNG, W. A. & AYALA, A. 2017. Overview of the Molecular Pathways and Mediators of Sepsis. *In:* WARD, N. S. & LEVY, M. M. (eds.) *Sepsis: Definitions, Pathophysiology and the Challenge of Bedside Management.* Cham: Springer International Publishing.

COHEN, J., VINCENT, J. L., ADHIKARI, N. K., MACHADO, F. R., ANGUS, D. C., CALANDRA, T., JATON, K., GIULIERI, S., DELALOYE, J., OPAL, S., TRACEY, K., VAN DER POLL, T. & PELFRENE, E. 2015. Sepsis: a roadmap for future research. *Lancet Infect Dis,* 15**,** 581-614.

COLE, L., BELLOMO, R., DAVENPORT, P., TIPPING, P., UCHINO, S., TETTA, C. & RONCO, C. 2002a. The effect of coupled haemofiltration and adsorption on inflammatory cytokines in an ex vivo model. *Nephrology Dialysis Transplantation,* 17**,** 1950-1956.

COLE, L., BELLOMO, R., HART, G., JOURNOIS, D., DAVENPORT, P., TIPPING, P. & RONCO, C. 2002b. A phase II randomized, controlled trial of continuous hemofiltration in sepsis. *Critical Care Medicine,* 30**,** 100-106.

COLE, L., BELLOMO, R., JOURNOIS, D., DAVENPORT, P., BALDWIN, I. & TIPPING, P. 2001. High-volume haemofiltration in human septic shock. *Intensive care medicine,* 27**,** 978-986.

COUTTS, E. R. 2016. *Evaluation of adsorbent haemoperfusion in interventional therapy of sepsis.* Thesis [Eng. D] -- University of Strathclyde, 2016.

D'SOUZA, R. & POWELL-TUCK, J. 2004. Glutamine supplements in the critically ill. *Journal of the Royal Society of Medicine,* 97**,** 425-427.

DANIELS, R. 2011. Surviving the first hours in sepsis: getting the basics right (an intensivist's perspective). *J Antimicrob Chemother,* 66 Suppl 2**,** ii11-23.

DANIELS, R., NUTBEAM, T., MCNAMARA, G. & GALVIN, C. 2011. The sepsis six and the severe sepsis resuscitation bundle: a prospective observational cohort study. *Emergency Medicine Journal,* 28**,** 507.

DAVIES, M. G. & HAGEN, P. O. 1997. Systemic inflammatory response syndrome. *Br J Surg,* 84**,** 920-35.

DELANO, M. J. & WARD, P. A. 2016. The Immune System's Role in Sepsis Progression, Resolution and Long-Term Outcome. *Immunological reviews,* 274**,** 330-353.

DEMBIC, Z. 2015. Chapter 1 - Introduction—Common Features About Cytokines. *The Cytokines of the Immune System.* Amsterdam: Academic Press.

DHAINAUT, J. F., LATERRE, P. F., JANES, J. M., BERNARD, G. R., ARTIGAS, A., BAKKER, J., RIESS, H., BASSON, B. R., CHARPENTIER, J., UTTERBACK, B. G., VINCENT, J. L. & RECOMBINANT HUMAN ACTIVATED PROTEIN, C. W. E. I. S. S. G. 2003. Drotrecogin alfa (activated) in the treatment of severe sepsis patients with multiple-organ dysfunction: data from the PROWESS trial. *Intensive Care Med,* 29**,** 894-903.

DIEZ-SILVA, M., DAO, M., HAN, J., LIM, C.-T. & SURESH, S. 2010. Shape and biomechanical characteristics of human red blood cells in health and disease. *MRS bulletin,* 35**,** 382-388.

DINARELLO, C. A. 1997. Proinflammatory and anti-inflammatory cytokines as mediators in the pathogenesis of septic shock. *Chest,* 112**,** 321s-329s.

DINARELLO, C. A. 2001. Anti-Cytokine Therapies in Response to Systemic Infection. *Journal of Investigative Dermatology Symposium Proceedings,* 6**,** 244-250.

DU, X., ZHANG, K., YANG, H., LI, K., LIU, X., WANG, Z., ZHOU, Q., LI, G. & LIANG, H. 2019. The relationship between size-segregated particles migration phenomenon and combined membrane fouling in ultrafiltration processes: The significance of shear stress. *Journal of the Taiwan Institute of Chemical Engineers,* 96**,** 45-52.

ESPINASSE, B., BACCHIN, P. & AIMAR, P. 2002. On an experimental method to measure critical flux in ultrafiltration. *Desalination,* 146**,** 91-96.

FASANO, A. & SEQUEIRA, A. 2017. Hemorheology and Hemodynamics. *In:* FASANO, A. & SEQUEIRA, A. (eds.) *Hemomath: The Mathematics of Blood.* Cham: Springer International Publishing.

FISHER, C. J., JR, DHAINAUT, J. A., OPAL, S. M. & ET AL. 1994. Recombinant human interleukin 1 receptor antagonist in the treatment of patients with sepsis syndrome: Results from a randomized, double-blind, placebo-controlled trial. *JAMA,* 271**,** 1836-1843.

FLEISCHMANN, C., SCHERAG, A., ADHIKARI, N. K., HARTOG, C. S., TSAGANOS, T., SCHLATTMANN, P., ANGUS, D. C. & REINHART, K. 2016. Assessment of global incidence and mortality of hospital-treated sepsis. Current estimates and limitations. *American journal of respiratory and critical care medicine,* 193**,** 259-272.

FORTENBERRY, J. D. & PADEN, M. L. Extracorporeal therapies in the treatment of sepsis: experience and promise. Seminars in pediatric infectious diseases, 2006. Elsevier, 72-79.

FRASER, K. H., ZHANG, T., TASKIN, M. E., GRIFFITH, B. P. & WU, Z. J. 2012. A Quantitative Comparison of Mechanical Blood Damage Parameters in Rotary Ventricular Assist Devices: Shear Stress, Exposure Time and Hemolysis Index. *Journal of Biomechanical Engineering,* 134**,** 081002-081002-11.

FRIEDMAN, L. I., HARDWICK, R., DANIELS, J. R., STROMBERG, R. R. & CIARKOWSKI, A. A. 1983. Evaluation of membranes for plasmapheresis. *Artificial organs,* 7**,** 435-442.

FUNK, D. J., PARRILLO, J. E. & KUMAR, A. 2009. Sepsis and Septic Shock: A History. *Critical Care Clinics,* 25**,** 83-101.

GALLETTI, P. M., RICHARDSON, P. D. & TRUDELL, L. A. 1983. OSCILLATING BLOOD FLOW ENHANCES MEMBRANE PLASMAPHERESIS. *ASAIO Journal,* 29**,** 279-282.

GASHTI, C. N. 2016. Membrane-based Therapeutic Plasma Exchange: A New Frontier for Nephrologists. *Seminars in Dialysis,* 29**,** 382-390.

GOTLOIB, L., BARZILAY, E., SHUSTAK, A., WAIS, Z., JAICHENKO, J. & LEV, A. 1986. Hemofiltration in septic ards. the artificial kidney as, an artificial endocrine lung. *Resuscitation,* 13**,** 123-132.

GOTTS, J. E. & MATTHAY, M. A. 2016. Sepsis: pathophysiology and clinical management. *BMJ,* 353.

GRANDISON, A. S., YOURAVONG, W. & LEWIS, M. J. 2000. Hydrodynamic factors affecting flux and fouling during ultrafiltration of skimmed milk. *Lait,* 80**,** 165-174.

GUGLIUZZA, A. 2016. Membrane Wettability. *In:* DRIOLI, E. & GIORNO, L. (eds.) *Encyclopedia of Membranes.* Berlin, Heidelberg: Springer Berlin Heidelberg.

GURLAND, H., SAMTLEBEN, W., LYSAGHT, M. J. & WINCHESTER, J. F. 1996. Extracorporeal Blood Purification Techniques: Plasmapheresis and Hemoperfusion. *In:* JACOBS, C., KJELLSTRAND, C. M., KOCH, K. M. & WINCHESTER, J. F. (eds.) *Replacement of Renal Function by Dialysis.* Dordrecht: Springer Netherlands.

HAN, C., SIM, S.-J., KIM, S.-H., SINGH, R., HWANG, S., KIM, Y. I., PARK, S. H., KIM, K. H., LEE, D. G., OH, H. S., LEE, S., KIM, Y. H., CHOI, B. K. & KWON, B. S. 2018. Desensitized chimeric antigen receptor T cells selectively recognize target cells with enhanced antigen expression. *Nature Communications,* 9**,** 468.

HASSAN, J., CADER, R. A., KONG, N. C., MOHD, M., RAHMAN, A. R. & HOD, R. 2013. Coupled plasma filtration adsorption (CPFA) plus continuous veno-venous

haemofiltration (CVVH) versus CVVH alone as an adjunctive therapy in the treatment of sepsis. *EXCLI journal,* 12**,** 681.

HERNANDEZ BOTERO, J. S. & FLORIAN PEREZ, M. C. 2012. The History of Sepsis from Ancient Egypt to the XIX Century.

HIRASAWA, H., ODA, S., NAKAMURA, M., WATANABE, E., SHIGA, H. & MATSUDA, K. 2012. Continuous Hemodiafiltration with a Cytokine-Adsorbing Hemofilter for Sepsis. *Blood Purification,* 34**,** 164-170.

HOFFMANN, J. N., HARTL, W. H., DEPPISCH, R., FAIST, E., JOCHUM, M. & INTHORN, D. 1995. Hemofiltration in human sepsis: Evidence for elimination of immunomodulatory substances. *Kidney international,* 48**,** 1563-1570.

IWAI, H., NAGAKI, M., NAITO, T., ISHIKI, Y., MURAKAMI, N., SUGIHARA, J. I., MUTO, Y. & MORIWAKI, H. 1998. Removal of endotoxin and cytokines by plasma exchange in patients with acute hepatic failure. *Critical care medicine,* 26**,** 873-876.

JAFFRIN, M. Y. 2011. Hydrodynamic Techniques to Enhance Membrane Filtration. *Annual Review of Fluid Mechanics,* 44**,** 77-96.

JAFFRIN, M. Y., DING, L. H. & LAURENT, M. J. 1992. Kinetics of concentration-polarization formation in crossflow filtration of plasma from blood: experimental results. *Journal of Membrane Science,* 72**,** 267-275.

KAMENEVA, M. V. & ANTAKI, J. F. 2007. Mechanical Trauma to Blood. *In:* BASKURT, O. K., HARDEMAN, M. R. & RAMPLING, M. W. (eds.) *Handbook of Hemorheology and Hemodynamics.* Netherlands: IOS Press.

KEMNA, E., PICKKERS, P., NEMETH, E., VAN DER HOEVEN, H. & SWINKELS, D. 2005. Time-course analysis of hepcidin, serum iron, and plasma cytokine levels in humans injected with LPS. *Blood,* 106**,** 1864-1866.

KHAYET, M. & MATSUURA, T. 2011. Formation of Flat Sheet Phase Inversion MD Membranes. *In:* KHAYET, M. & MATSUURA, T. (eds.) *Membrane Distillation.* Amsterdam: Elsevier.

KODAMA, M., TANI, T., HANASAWA, K., HIRATA, K., HIRASAWA, H., ODA, S., OTSUKA, T., YAMAMOTO, Y., KANESAKA, S. & TAKAHASHI, Y. 1997. Treatment of sepsis by plasma endotoxin removal: hemoperfusion using a polymyxin-B immobilized column. *Journal of endotoxin research,* 4**,** 293-300.

KOLACZKOWSKA, E. & KUBES, P. 2013. Neutrophil recruitment and function in health and inflammation. *Nature reviews. Immunology,* 13**,** 159.

KUMAR, A., KANAGASUNDARAM, N. S., COLLYNS, T. A. & DAVISON, A. M. 1998. Plasma exchange and haemodiafiltration in fulminant meningococcal sepsis. *Nephrology, dialysis, transplantation: official publication of the European Dialysis and Transplant Association-European Renal Association,* 13**,** 484-487.

LANGER, H. F. & CHAVAKIS, T. 2009. Leukocyte-endothelial interactions in inflammation. *J Cell Mol Med,* 13**,** 1211-20.

LEVY, G. G., NICHOLS, W. C., LIAN, E. C., FOROUD, T., MCCLINTICK, J. N., MCGEE, B. M., YANG, A. Y., SIEMIENIAK, D. R., STARK, K. R., GRUPPO, R., SARODE, R., SHURIN, S. B., CHANDRASEKARAN, V., STABLER, S. P., SABIO, H., BOUHASSIRA, E. E.,

UPSHAW, J. D., GINSBURG, D. & TSAI, H.-M. 2001. Mutations in a member of the ADAMTS gene family cause thrombotic thrombocytopenic purpura. *Nature,* 413**,** 488-494.

LEVY, M. M., FINK, M. P., MARSHALL, J. C., ABRAHAM, E., ANGUS, D., COOK, D., COHEN, J., OPAL, S. M., VINCENT, J.-L. & RAMSAY, G. 2003. 2001 SCCM/ESICM/ACCP/ATS/SIS International Sepsis Definitions Conference. *Intensive Care Medicine,* 29**,** 530-538.

LEWIS, D. H., CHAN, D. L., PINHEIRO, D., ARMITAGE-CHAN, E. & GARDEN, O. A. 2012. The immunopathology of sepsis: pathogen recognition, systemic inflammation, the compensatory anti-inflammatory response, and regulatory T cells. *J Vet Intern Med,* 26**,** 457-82.

LIVIGNI, S., BERTOLINI, G., ROSSI, C., FERRARI, F., GIARDINO, M., POZZATO, M. & REMUZZI, G. 2014. Efficacy of coupled plasma filtration adsorption (CPFA) in patients with septic shock: a multicenter randomised controlled clinical trial. *BMJ open,* 4**,** e003536.

MAJNO, G. 1991. The Ancient Riddle of σηψις (Sepsis). *The Journal of Infectious Diseases,* 163**,** 937-945.

MALLUBHOTLA, H. & BELFORT, G. 1997. Flux enhancement during Dean vortex microfiltration. 8. Further diagnostics1This paper is part 8. Previous papers of the series can be found in 6, 7, 8, 9, 10, 11. Papers 3 and 7 are submitted and in preparation, respectively.1. *Journal of Membrane Science,* 125**,** 75-91.

MARSHALL, A. D., MUNRO, P. A. & TRÄGÅRDH, G. 1993. The effect of protein fouling in microfiltration and ultrafiltration on permeate flux, protein retention and selectivity: A literature review. *Desalination,* 91**,** 65-108.

MARSHALL, J. C. 2014. Why have clinical trials in sepsis failed? *Trends in Molecular Medicine,* 20**,** 195-203.

MARTIN , G. S., MANNINO , D. M., EATON , S. & MOSS , M. 2003. The Epidemiology of Sepsis in the United States from 1979 through 2000. *New England Journal of Medicine,* 348**,** 1546-1554.

MAUL, T., KAMENEVA, M. V. & WEARDEN, P. D. 2015a. Damage to leukocytes. *Mechanical Blood Trauma in Circulatory-Assist Devices.* ASME Press.

MAUL, T., KAMENEVA, M. V. & WEARDEN, P. D. 2015b. *Testing blood trauma in circulatory assist devices,* New York, NY, ASME.

MCCORMACK, D., RUDERMAN, A., MENGES, W., KULKARNI, M., MURANO, T. & KELLER, S. E. 2016. Usefulness of the Mortality in Severe Sepsis in the Emergency Department score in an urban tertiary care hospital. *The American Journal of Emergency Medicine,* 34**,** 1117-1120.

MCLEOD, B. C. 2006. Therapeutic apheresis: use of human serum albumin, fresh frozen plasma and cryosupernatant plasma in therapeutic plasma exchange. *Best Practice & Research Clinical Haematology,* 19**,** 157-167.

MENZIES, K. L. & JONES, L. 2010. The Impact of Contact Angle on the Biocompatibility of Biomaterials. *Optometry and Vision Science,* 87**,** 387-399.

MILLER, D. J., KASEMSET, S., PAUL, D. R. & FREEMAN, B. D. 2014. Comparison of membrane fouling at constant flux and constant transmembrane pressure conditions. *Journal of Membrane Science,* 454**,** 505-515.

MILLWARD, H., BELLHOUSE, B., SOBEY, I. & LEWIS, R. 1995. Enhancement of plasma filtration using the concept of the vortex wave. *Journal of membrane science,* 100**,** 121-129.

MOGENSEN, T. H. 2009. Pathogen Recognition and Inflammatory Signaling in Innate Immune Defenses. *Clinical Microbiology Reviews,* 22**,** 240-273.

MORRIS, C., GRAY, L. & GIOVANNELLI, M. 2015. Early report: The use of Cytosorb™ haemabsorption column as an adjunct in managing severe sepsis: initial experiences, review and recommendations. *Journal of the Intensive Care Society*.

MULDER, M. 1996. *Basic Principles of Membrane Technology*, Springer.

NAJARIAN, S. & BELLHOUSE, B. J. 1996. Enhanced microfiltration of bovine blood using a tubular membrane with a screw-threaded insert and oscillatory flow. *Journal of Membrane Science,* 112**,** 249-261.

NAKAMURA, T., USHIYAMA, C., SUZUKI, S., SHIMADA, N., EBIHARA, I., SUZAKI, M., TAKAHASHI, T. & KOIDE, H. 2000. Effect of plasma exchange on serum tissue inhibitor of metalloproteinase 1 and cytokine concentrations in patients with fulminant hepatitis. *Blood purification,* 18**,** 50-54.

NEEMA, P. K., SINHA, P. K. & RATHOD, R. C. 2004. Activated Clotting Time during Cardiopulmonary Bypass: Is Repetition Necessary during Open Heart Surgery? *Asian Cardiovascular and Thoracic Annals,* 12**,** 47-52.

NEMOTO, H., NAKAMOTO, H., OKADA, H., SUGAHARA, S., MORIWAKI, K., ARAI, M., KANNO, Y. & SUZUKI, H. 2001. Newly Developed Immobilized Polymyxin B Fibers Improve the Survival of Patients with Sepsis. *Blood Purification,* 19**,** 361-369.

NETEA, M. G., VAN DER MEER, J. W. M., VAN DEUREN, M. & JAN KULLBERG, B. 2003. Proinflammatory cytokines and sepsis syndrome: not enough, or too much of a good thing? *Trends in Immunology,* 24**,** 254-258.

NOE, D. A., WEEDN, V. & BELL, W. R. 1984. Direct spectrophotometry of serum hemoglobin: an Allen correction compared with a three-wavelength polychromatic analysis. *Clinical Chemistry,* 30**,** 627-630.

ODA, S., HIRASAWA, H., SHIGA, H., NAKANISHI, K., MATSUDA, K. I. & NAKAMURA, M. 2002. Continuous hemofiltration/hemodiafiltration in critical care. *Therapeutic Apheresis and Dialysis,* 6**,** 193-198.

OLIA, S. E., MAUL, T. M., ANTAKI, J. F. & KAMENEVA, M. V. 2016. Mechanical Blood Trauma in Assisted Circulation: Sublethal RBC Damage Preceding Hemolysis. *The International Journal of Artificial Organs,* 39**,** 150-159.

OMAR, H. R., MIRSAEIDI, M., SOCIAS, S., SPRENKER, C., CALDEIRA, C., CAMPORESI, E. M. & MANGAR, D. 2015. Plasma Free Hemoglobin Is an Independent Predictor of

Mortality among Patients on Extracorporeal Membrane Oxygenation Support. *PloS one,* 10**,** e0124034-e0124034.

OPAL, S. M. & DEPALO, V. A. 2000. Anti-inflammatory cytokines. *Chest,* 117**,** 1162-72.

OPAL, S. M., FISHER, C. J., DHAINAUT, J.-F. A., VINCENT, J.-L., BRASE, R., LOWRY, S. F., SADOFF, J. C., SLOTMAN, G. J., LEVY, H., BALK, R. A., SHELLY, M. P., PRIBBLE, J. P., LABRECQUE, J. F., LOOKABAUGH, J., DONOVAN, H., DUBIN, H., BAUGHMAN, R., NORMAN, J., DEMARIA, E., MATZEL, K., ABRAHAM, E. & SENEFF, M. 1997. Confirmatory interleukin-1 receptor antagonist trial in severe sepsis: A phase III, randomized, doubleblind, placebo-controlled, multicenter trial. *Critical Care Medicine,* 25**,** 1115-1124.

OPAL, S. M., LATERRE, P., FRANCOIS, B. & ET AL. 2013. Effect of eritoran, an antagonist of md2-tlr4, on mortality in patients with severe sepsis: The access randomized trial. *JAMA,* 309**,** 1154-1162.

PAPADOPOULOU, V., TANG, M.-X., BALESTRA, C., ECKERSLEY, R. J. & KARAPANTSIOS, T. D. 2014. Circulatory bubble dynamics: From physical to biological aspects. *Advances in Colloid and Interface Science,* 206**,** 239-249.

PENG, Z., PAI, P., HONG-BAO, L., RONG, L., HAN-MIN, W. & CHEN, H. 2010. The impacts of continuous veno-venous hemofiltration on plasma cytokines and monocyte human leukocyte antigen-DR expression in septic patients. *Cytokine,* 50**,** 186-191.

PETERSEN, B. K., YANG, J., GRATHWOHL, W. S., COCKRELL, C., SANTIAGO, C., AN, G. & FAISSOL, D. M. 2018. Precision medicine as a control problem: Using simulation and deep reinforcement learning to discover adaptive, personalized multi-cytokine therapy for sepsis. *arXiv preprint arXiv:1802.10440*.

POLAT, G., UGAN, R. A., CADIRCI, E. & HALICI, Z. 2017. Sepsis and Septic Shock: Current Treatment Strategies and New Approaches. *The Eurasian Journal of Medicine,* 49**,** 53-58.

RADLEY, G., ALI, S., PIEPER, I. L. & THORNTON, C. A. 2018. Mechanical shear stress and leukocyte phenotype and function: Implications for ventricular assist device development and use. *The International Journal of Artificial Organs,* 42**,** 133-142.

RANIERI, V. M., THOMPSON, B. T., BARIE, P. S., DHAINAUT, J.-F., DOUGLAS, I. S., FINFER, S., GÅRDLUND, B., MARSHALL, J. C., RHODES, A., ARTIGAS, A., PAYEN, D., TENHUNEN, J., AL-KHALIDI, H. R., THOMPSON, V., JANES, J., MACIAS, W. L., VANGEROW, B. & WILLIAMS, M. D. 2012. Drotrecogin Alfa (Activated) in Adults with Septic Shock. *New England Journal of Medicine,* 366**,** 2055-2064.

REEVES, H. M. & WINTERS, J. L. 2014. The mechanisms of action of plasma exchange. *British journal of haematology,* 164**,** 342-351.

REINHART, K., MENGES, T., GARDLUND, B., HARM ZWAVELING, J., SMITHES, M., VINCENT, J.-L., MARIA TELLADO, J., SALGADO-REMIGIO, A., ZIMLICHMAN, R., WITHINGTON, S., TSCHAIKOWSKY, K., BRASE, R., DAMAS, P., KUPPER, H., KEMPENI, J., EISELSTEIN, J. & KAUL, M. 2001. Randomized, placebo-controlled

trial of the anti-tumor necrosis factor antibody fragment afelimomab in hyperinflammatory response during severe sepsis: The RAMSES Study. *Critical Care Medicine,* 29**,** 765-769.

RICE, T. W., WHEELER, A. P., BERNARD, G. R., VINCENT, J.-L., ANGUS, D. C., AIKAWA, N., DEMEYER, I., SAINATI, S., AMLOT, N. & CAO, C. 2010. A randomized, double-blind, placebo-controlled trial of TAK-242 for the treatment of severe sepsis. *Critical care medicine,* 38**,** 1685-1694.

RIMMELÉ, T. & KELLUM, J. A. 2011. Clinical review: blood purification for sepsis. *Critical Care,* 15**,** 205.

RITTIRSCH, D., FLIERL, M. A. & WARD, P. A. 2008. Harmful molecular mechanisms in sepsis. *Nature Reviews Immunology,* 8**,** 776.

ROBERTSON, C. M. & COOPERSMITH, C. M. 2006. The systemic inflammatory response syndrome. *Microbes and Infection,* 8**,** 1382-1389.

RONCO, C., BRENDOLAN, A., DAN, M., PICCINNI, P., BELLOMO, R., DE NITTI, C., INGUAGGIATO, P. & TETTA, C. 2000. Adsorption in sepsis. *Kidney International,* 58**,** S148-S155.

RONCO, C., BRENDOLAN, A., LONNEMANN, G., BELLOMO, R., PICCINNI, P., DIGITO, A., DAN, M., IRONE, M., LA GRECA, G. & INGUAGGIATO, P. 2002. A pilot study of coupled plasma filtration with adsorption in septic shock. *Critical care medicine,* 30**,** 1250-1255.

RONCO, C. & KLEIN, D. J. 2014. Polymyxin B hemoperfusion: a mechanistic perspective. *Critical Care,* 18**,** 309.

RUOKONEN, E., PARVIAINEN, I. & UUSARO, A. 2002. Treatment of impaired perfusion in septic shock. *Annals of Medicine,* 34**,** 590-597.

SANDEMAN, S. R., HOWELL, C. A., MIKHALOVSKY, S. V., PHILLIPS, G. J., LLOYD, A. W., DAVIES, J. G., TENNISON, S. R., RAWLINSON, A. P. & KOZYNCHENKO, O. P. 2008. Inflammatory cytokine removal by an activated carbon device in a flowing system. *Biomaterials,* 29**,** 1638-1644.

SARMA, J. V. & WARD, P. A. 2011. The complement system. *Cell and Tissue Research,* 343**,** 227-235.

SAXENA, A., TRIPATHI, B. P., KUMAR, M. & SHAHI, V. K. 2009. Membrane-based techniques for the separation and purification of proteins: An overview. *Advances in Colloid and Interface Science,* 145**,** 1-22.

SCANLON, V. C. & SANDERS, T. 2010. *Essentials of Anatomy and Physiology,* Philadelphia, UNITED STATES, F. A. Davis Company.

SCHMIDT, J., MANN, S., MOHR, V. D., LAMPERT, R., FIRLA, U. & ZIRNGIBL, H. 2000. Plasmapheresis combined with continuous venovenous hemofiltration in surgical patients with sepsis. *Intensive Care Medicine,* 26**,** 532-537.

SCHULTE, W., BERNHAGEN, J. & BUCALA, R. 2013a. Cytokines in sepsis: potent immunoregulators and potential therapeutic targets--an updated view. *Mediators Inflamm,* 2013**,** 165974.

SCHULTE, W., BERNHAGEN, J. & BUCALA, R. 2013b. Cytokines in sepsis: potent immunoregulators and potential therapeutic targets—an updated view. *Mediators of inflammation,* 2013.

SCOTT, A., KHAN, K., COOK, J. & DURONIO, V. 2004. What is "inflammation"? Are we ready to move beyond Celsus? *British journal of sports medicine,* 38**,** 248-249.

SHAHEEN, I., HARVEY, B. & WATSON, A. R. 2009. Haemofiltration therapy. *Paediatrics and Child Health,* 19**,** 121-126.

SHERWOOD, E. R. & TOLIVER-KINSKY, T. 2004. Mechanisms of the inflammatory response. *Best Practice & Research Clinical Anaesthesiology,* 18**,** 385-405.

SHTATLAND, E. S., KLEINMAN, K. & CAIN, E. M. 2002. One more time about R2 measures of fit in logistic regression. *NESUG 15 Proceedings,* 15**,** 222-226.

SIAMI, G. A. & SIAMI, F. S. 2001. Membrane Plasmapheresis in the United States: A Review Over the Last 20 Years. *Therapeutic Apheresis,* 5**,** 315-320.

SIEBERT, M. W. & FODOR, P. S. Newtonian and non-newtonian blood flow over a backward-facing step–a case study. Proceedings of the COMSOL Conference, Boston, 2009.

SINGER, M., DEUTSCHMAN, C. S., SEYMOUR, C. & ET AL. 2016. The third international consensus definitions for sepsis and septic shock (sepsis-3). *JAMA,* 315**,** 801-810.

SMOLDERS, K. & FRANKEN, A. 1989. Terminology for membrane distillation. *Desalination,* 72**,** 249-262.

STAITIEH, B. & MARTIN, G. S. 2017. Epidemiology of Sepsis: Current Data and Predictions for the Future. *In:* WARD, N. S. & LEVY, M. M. (eds.) *Sepsis: Definitions, Pathophysiology and the Challenge of Bedside Management.* Cham: Springer International Publishing.

STEHLE, P. & KUHN, K. S. 2015. Glutamine: An Obligatory Parenteral Nutrition Substrate in Critical Care Therapy. *BioMed Research International,* 2015**,** 7.

SUN, S., YUE, Y., HUANG, X. & MENG, D. 2003. Protein adsorption on blood-contact membranes. *Journal of Membrane Science,* 222**,** 3-18.

SZASZ, T., THAKALI, K., FINK, G. D. & WATTS, S. W. 2007. A comparison of arteries and veins in oxidative stress: producers, destroyers, function, and disease. *Experimental Biology and Medicine,* 232**,** 27-37.

TAHA, T. & CUI, Z. F. 2002. CFD modelling of gas-sparged ultrafiltration in tubular membranes. *Journal of Membrane Science,* 210**,** 13-27.

THURSTON, A. J. 2000. Of Blood, Inflammation and Gunshot Wounds: The History of the Control of Sepsis. *Australian and New Zealand Journal of Surgery,* 70**,** 855-861.

TIDSWELL, M., TILLIS, W., LAROSA, S. P., LYNN, M., WITTEK, A. E., KAO, R., WHEELER, J., GOGATE, J., OPAL, S. M. & ERITORAN SEPSIS STUDY, G. 2010. Phase 2 trial of eritoran tetrasodium (E5564), a toll-like receptor 4 antagonist, in patients with severe sepsis. *Crit Care Med,* 38**,** 72-83.

TORTORA, G. J. & DERRICKSON, B. 2011. *Principles of anatomy and physiology,* Hoboken, N.J., Wiley.

TRÄGER, K., SCHÜTZ, C., FISCHER, G., SCHRÖDER, J., SKRABAL, C., LIEBOLD, A. & REINELT, H. 2016. Cytokine reduction in the setting of an ARDS-Associated inflammatory response with multiple organ failure. *Case reports in critical care,* 2016.

TRIPISCIANO, C., KOZYNCHENKO, O. P., LINSBERGER, I., PHILLIPS, G. J., HOWELL, C. A., SANDEMAN, S. R., TENNISON, S. R., MIKHALOVSKY, S. V., WEBER, V. & FALKENHAGEN, D. 2011. Activation-dependent adsorption of cytokines and toxins related to liver failure to carbon beads. *Biomacromolecules,* 12**,** 3733-3740.

VENKATARAMAN, R., SUBRAMANIAN, S. & KELLUM, J. A. 2003. Clinical review: extracorporeal blood purification in severe sepsis. *Critical Care,* 7**,** 139.

WANG, K., ABDALA, A. A., HILAL, N. & KHRAISHEH, M. K. 2017. Chapter 13 - Mechanical Characterization of Membranes. *In:* HILAL, N., ISMAIL, A. F., MATSUURA, T. & OATLEY-RADCLIFFE, D. (eds.) *Membrane Characterization.* Elsevier.

WEI, P., ZHANG, K., GAO, W., KONG, L. & FIELD, R. 2013. CFD modeling of hydrodynamic characteristics of slug bubble flow in a flat sheet membrane bioreactor. *Journal of Membrane Science,* 445**,** 15-24.

WIESE, F. 2007. Membranes for Blood Fractionation/Apheresis. *Membranes for the Life Sciences.* Wiley-VCH Verlag GmbH & Co. KGaA.

XIE, K., LIU, L., YU, Y. & WANG, G. 2014. Hydrogen gas presents a promising therapeutic strategy for sepsis. *Biomed Res Int,* 2014**,** 807635.

XU, Z., WAN, L. & HUANG, X. 2009. Techniques for Membrane Surface Characterization. *In:* XU, Z., WAN, L. & HUANG, X. (eds.) *Surface Engineering of Polymer Membranes.* Berlin, Heidelberg: Springer Berlin Heidelberg.

YUSHIN, G., HOFFMAN, E. N., BARSOUM, M. W., GOGOTSI, Y., HOWELL, C. A., SANDEMAN, S. R., PHILLIPS, G. J., LLOYD, A. W. & MIKHALOVSKY, S. V. 2006. Mesoporous carbide-derived carbon with porosity tuned for efficient adsorption of cytokines. *Biomaterials,* 27**,** 5755-5762.

ZHANG, J., ZHANG, P., FRASER, K. H., GRIFFITH, B. P. & WU, Z. J. 2013. Comparison and Experimental Validation of Fluid Dynamic Numerical Models for a Clinical Ventricular Assist Device. *Artificial Organs,* 37**,** 380-389.

ZHANG, J. M. & AN, J. 2007. Cytokines, inflammation, and pain. *Int Anesthesiol Clin,* 45**,** 27-37.

Appendices:

Arduino code for the automation system:

```
/*
 * This code (in combination with the assembled device) will:
 *  1 - Monitor inlet and outlet pressure and control a linear actuator accordingly to maintain TMP between 40-50 mmHg.
 *  2 - Measure the volume of plasma removed as measured by a load cell, and replace an equal amount of fluid (in 10ml incements) using a peristaltic pump.
 *  3 - Set the flow rate of the blood to either 100ml/min, 150ml/min or 200ml/min using a peristaltic pump.
 *  4 - Define and set up the functionality of a 4 button module to: 1) reset scale 2) increase blood flow rate 3) decrease flow rate 4) start/stop pumps
 *  5 - Display on the LCD the volume removed, volume replaced, TMP, SD card initialisation check, and time
 *  6 - Record the values of volume removed, volume replaced, TMP, and time as a .csv file on a microSD card
 *
 * COMPONENTS LIST:
 *  Arduino Micro
 *  HX711 load cell amplifier
 *  Pololu DRV8834 stepper motor driver
 *  Pololu TB6612FNG dual motor driver
 *  Crouzet 80910501 linear actuator
 *  Adafruit peristaltic liquid pump
```

```
*   Hemosep peristaltic liquid pump
*   Tedea Huntleigh 1042 single point load cell
*   2 x Texas Instruments INA125P instrumentation amplifier
*   2 x Honeywell 24PC pressure sensor
*   YwRobot 4 button module
*   Catalex v1.0 microSD card adapter
*   SainSmart IIC/I2C/TWI Serial 2004 20x4 LCD module
*   RGB LED
*
*  ARDUINO PIN CONNECTIONS:
*   D0 = DRV8834 STEP
*   D1 = DRV8834 DIR
*   D2 = LCD SDA
*   D3 = LCD SCL
*   D4 = SW1
*   D5 = SW2
*   D6 = TB6612FNG PWMA
*   D7 = SW3
*   D8 = TB6612FNG AIN2
*   D9 = TB6612FNG AIN1
*   D10 = TB6612FNG STBY
*   D11 = TB6612FNG BIN1
*   D12 = TB6612FNG BIN2
*   D13 = SW4
```

```
*   A0 = Inlet pressure sensor (INA125P pin 11)
*   A1 = Outlet pressure sensor (INA125P pin 11)
*   A2 = HX711 DT
*   A3 = HX711 SCK
*   A4(D22) = Red LED and DRV8834 SLEEP
*   A5(D23) = Green LED
*   SCK = microSD SCK
*   SS = microSD CS
*   MISO = microSD MISO
*   MOSI = microSD MOSI
*/

//INCLUDING THE LIBRARIES - this section of the code includes the additional libraries required by different elements of the device electronic control system

#include <HX711.h> // include the library for the HX711

#include <LiquidCrystal_I2C.h> // include the library for the LCD display

#include <AccelStepper.h> // include the library for controlling the linear stepper motor

#include <SD.h> // include the library for using the microSD card

#include <SPI.h> // include the library for Serial Peripheral Interface (SPI) communication with the microSD card
```

// DEFINING ARDUINO PINS - This section defines the arduino pins according to their function

#define SW1 4 // button to reset the scale to zero defined as pin 4

#define SW2 5 // button to increase the blood flow rate defined as pin 5

#define SW3 7 // button to decrease the blood flow rate defined as pin 7

#define SW4 13 // button to start the blood and fluid replacement pumps defined as pin 13

#define AIN1 9 // AIN1 pin of TB6612FNG dual motor driver which drives positive terminal of the blood pump (motor A) defined as pin 9

#define AIN2 8 // AIN2 pin of TB6612FNG dual motor driver which drives negative terminal of the blood pump (motor A) defined as pin 8

#define PWMA 6 // PWMA pin of TB6612FNG dual motor driver which controls pulse-width modulation (and therefore speed) of the blood pump (motor A) defined as pin 6

#define BIN1 11 // BIN1 pin of TB6612FNG dual motor driver which drives positive terminal of the fluid replacement pump (motor B) defined as pin 11

#define BIN2 12 // BIN1 pin of TB6612FNG dual motor driver which drives negative terminal of the fluid replacement pump (motor B) defined as pin 12

#define STBY 10 // STBY pin for TB6612FNG dual motor driver - must be driven HIGH to take driver out of standby mode and allow the blood and fluid replacement pumps to be started defined as pin 10

#define redSLEEP 18 // red pin of the RGB LED and the SLEEP pin for the DRV8834 stepper motor driver - when driven HIGH will put the driver into sleep mode and stop power consumption by the linear stepper motor defined as pin 22

#define green 19 // green pin of the RGB LED defined as pin 23

HX711 scale(A5, A4); // the DT and SCK pins of the HX711 Load Cell Module defined as pin A2 and A3 respectively

AccelStepper stepper(1, 0, 1); // the step and direction pins of the DRV8834 stepper motor driver defined as pins 0 and 1 respectively

// DEFINING VARIABLES FOR KEEPING TIME - this section of the code defines the time variables

unsigned long elapsed, over; // the variables 'elapsed' and 'over' (used to express the number of milliseconds elapsed since the device started in hours, minutes and seconds) are defined as integers which can have a very large but only positive value

float h,m,s; // the variables 'h', 'm', and 's' (used to display and record the hours minutes and seconds elapsed since the device starts) are defined as numbers which have a decimal value

unsigned long previousseconds = 0 / 1000; // the variable 'previousseconds' (used to monitor the number of seconds the fluid replacement pump has operated for) is defined as an integer which can have a very large but only positive value

unsigned long seconds = 0; // the variable 'seconds' (used to monitor the number of seconds the fluid replacement pump has operated for) is defined as an integer which can have a very large but only positive value

// DEFINING VARIABLES FOR MONITORING PRESSURE - This section defines the variables used for measuring pressure

const int numReadings = 99; // the variable 'numReadings' (used to determine the the number of TMP readings which are collected into an array for averaging) is defined as a constant integer which is equal to 299. the value 299 is chosen as the he first value in the array is referred to as value 0, thus value 299 will the the 300th TMP reading

int TMPIndex = 0; // the variable 'TMPIndex' (used to determine which value in the array 'TMPArray' is being inspected by its position in the array) is defined as an integer which is initially = 0

int TMPArray[numReadings]; // the array 'TMPArray' which contains a number of values equal to the variable 'numReadings' (used to store TMP values for averaging) is created

int TMPtotal = 0; // the variable 'TMPtotal' (used to determine the sum of all the values in the array 'TMPArray') is defined as an integer which is initially = 0

int currentTMP = 0; // the variable 'currentTMP' (used to store the current TMP which is calculated by [(InletPressure + OutletPressure) / 2] is defined as an integer which is initially = 0

int TMP = 0; // the variable 'TMP' (used to store the average of the 300 values in the TMP array 'TMPArray') is defined as an integer which is initially = 0

// DEFINING VARIABLES FOR REPLACING FILTERED FLUID - this section of the code defines variables for automatically controlling the replacement of filtered fluid

int volumeremoved; // the variable 'volumeremoved' (used to store values read from the load cell) is defined as an integer

int replacementpumpcounter = 0; // the variable 'replacementpumpcounter' (used to counts how many times the fluid replacement pump has operated) is defined as an integer which is initially = 0

boolean motorson = false; // the variable 'motorson' (used to determine if the blood and fluid replacement pumps are on (motorson = true) or off (motorson is false)) is defined as boolean term which is initially false

int volumereplaced = 0; // the variable 'volumereplaced' (used to determine the volume of replaced fluid) is defined as an integer which is intially = 0

int Interval = 10; // the variable 'interval' (used to determine how long the fluid replacement pump should operate for) is defined as an integer which is initially = 10. The value 10 represents 10 seconds which equates to 10 ml replaced

// OTHER DEFINITIONS - this section defines the other remaining variables

int Speed = 45; // the variable 'speed' (used to control the speed of the blood pump motor and thus the blood flow rate) is defined as an integer which is initially = 91. The value 91 chosen as it is 46 less than 137 (46 being the speed increment used later which equates to a 50ml/min increment in flow rate). Starting from 91 allows for the "Set Flow Rate" promt on the LCD display when the device is turned on.

LiquidCrystal_I2C lcd(0x27,20,4); // define the LCD display area (20x4)

File myfile; //

int sdstate = 0; // the variable 'sdstate' (used to display on the LCD if the microSD card has initialised or not) is defined as an integer which is intially = 0

unsigned long debouncetimer = 0; // the variable 'debouncetimer' (used to determine the time for which a button must be pressed for the action to be registered) is defined as an integer which can have a very large but only positive value

// SETUP - the 'setup' section of the code which will run once only

void setup()

{

// DEFINING ARDUINO INPUTS AND OUTPUTS - this section of the code defines the digital pins status on the arduino as either input or output

pinMode(SW1, INPUT); // the pin on the arduino associated with SW1 (button to reset the scale to zero) is defined as an input pin

pinMode(SW2, INPUT); // the pin on the arduino associated with SW2 (button to increase the blood flow rate) is defined as an input pin

pinMode(SW3, INPUT); // the pin on the arduino associated with SW3 (button to decrease the blood flow rate) is defined as an input pin

pinMode(SW4, INPUT); // the pin on the arduino associated with SW4 (button to start the blood and fluid replacement pumps) is defined as an input pin

pinMode(AIN1, OUTPUT); // the pin on the arduino associated with AIN1 (the positive terminal of the blood pump) is defined as an output pin

pinMode(AIN2, OUTPUT); // the pin on the arduino associated with AIN2 (the negative terminal of the blood pump) is defined as an output pin

pinMode(BIN1, OUTPUT); // the pin on the arduino associated with BIN1 (the positive terminal of the fluid replacement pump) is defined as an output pin

pinMode(BIN2, OUTPUT); // the pin on the arduino associated with BIN2 (the negative terminal of the fluid replacement pump) is defined as an output pin

pinMode(PWMA, OUTPUT); // the pin on the arduino associated with PWMA (the pulse-width modulation speed control of the blood pump) is defined as an output pin

pinMode(STBY, OUTPUT); // the pin on the arduino associated with STBY (the standby pin for TB6612FNG dual motor driver - must be driven HIGH to take driver out of standby mode and allow the blood and fluid replacement pumps to be started) is defined as an output pin

pinMode(redSLEEP, OUTPUT); // the pin on the arduino associated with redSLEEP (the red element of the RGB LED and the SLEEP pin for the DRV8834 stepper motor driver - when driven LOW will put the driver into sleep mode and stop power consumption by the linear stepper motor) is defined as an output pin

pinMode(green, OUTPUT); // the pin on the arduino associated with green (the green element of the RGB LED) is defined as an output pin

// INITIALISATION OF COMPONENTS - this section of the code initialises the various parameters and components nevessary for the operation of the device

Serial.begin(9600); // start the communication with the computer

lcd.init(); // initialise the LCD

lcd.backlight(); // illuminate the LCD

stepper.setMaxSpeed(24); // set the maximum speed of the stepper motor. The value of 24 is calculated by [360 (degrees per revolution)/ 15 degrees] (taken from the datasheet)

stepper.setSpeed(10); // set the operating speed of the linear stepper motor. A speed of 10 is sufficiently low to provide the force required to restrict outlet tube

scale.set_scale(870); // set load cell calibration. The value of 870 is obtained by calibrating the scale with known weights; see the README for details

scale.tare(); // reset the scale to zero

for (int i = 0; i < numReadings; i++) {

TMPArray[i] = 0;

} // all values in the array 'TMPArray' (ranging from value '0' to value 'numReadings') to are set to be initially equal to zero:

// CREATING A DATA LOG FILE ON THE MICRO SD CARD - this section of the code creates the data log file on the microSD card

if(SD.begin(SS)) // if the microSD card and library are initialized. (Use of Serial Peripheral Interface (SPI) bus begins with chip/slave select pin set as the SS pin on arduino micro)

{

```
  sdstate = 1; //the variable 'sdstate' (used to display on the LCD if the microSD card has initialised or not) is set equal to 1

  }

  String header = "Time, TMP, Volume Removed, Volume Replaced"; // a string of text called 'header' is created containing the text "Time, TMP, Volume Removed, Volume Replaced" which will form the four column headers of the comma-separated values (.csv) file

  myfile = SD.open("testing.csv", FILE_WRITE); // a comma-separated value (.csv) file called "testing.csv" is opened or created on the microSD card, ready to be written to

  myfile.println(header); // the string of text called 'header' is printed to a new line of testing.csv

  myfile.close(); // the comma-separated value (.csv) file called "testing.csv" is closed

}

// LOOP - the 'loop' section of the code will run repeatedly during the operation of the device

void loop()

{

  // TIMER - this section of the code expresses the number of milliseconds elapsed since the device started in hours, minutes and seconds

  elapsed = millis(); // the variable 'elapsed' is set to be determined by the number of milliseconds elapsed since the device started

  int h = (elapsed/3600000); // the variable 'h' is set to be equal to the number (as an integer) of milliseconds elapsed divided by 3600000 (i.e. the number of hours) since the device started

  over=elapsed%3600000; // the variable 'over' is initially set to be equal to the remaining number of milliseconds when the variable 'elapsed' is divided by 3600000

  int m = (over/60000); // the variable 'm' is set to be equal to the number (as an integer) of milliseconds in the variable 'over' divided by 60000 (i.e. the number of minutes) since the device started, excluding those accounted for by the variable 'h'
```

over=over%60000; // the variable 'over' is updated to be equal to the remaining milliseconds when the variable 'elapsed' is divided first by 3600000 and then 60000

int s = (over/1000); // the variable 's' is set to be equal to the number (as an integer) of milliseconds in the updated variable 'over' divided by 1000 (i.e. the number of seconds) since the device started, excluding those accounted for by variables 'h' and 'm'

// INITIALISE THE BLOOD PUMP - this section of the code initializes the blood pump so that it will begin is soon as the STBY pin of the TB6612FNG dual motor driver is set HIGH

digitalWrite(AIN1, HIGH); // the positive terminal of the blood pump is set HIGH and the negative terminal of the blood pump is set LOW so the motor will turn when the STBY pin of the TB6612FNG dual motor driver is set HIGH

digitalWrite(AIN2, LOW); // the positive terminal of the blood pump is set HIGH and the negative terminal of the blood pump is set LOW so the motor will turn when the STBY pin of the TB6612FNG dual motor driver is set HIGH

// CONTROL BUTTONS - this section of the code determines the operation of the four control buttons

if (digitalRead(SW1) == LOW) // if the scalereset button is pressed (SW1 is LOW)

{

scale.tare(); // reset the scale

}

if ((digitalRead(SW2) == LOW) && (Speed >= 45 && Speed < 229) && ((elapsed - debouncetimer) >= 300)) // if the flowrateup button is pressed (SW2 is LOW) and the blood flow rate is between 100-150ml/min (91<=speed<=183) and the button press duration is longer than 500ms

{

Speed = Speed + 46; // increase speed by 46, thus increasing the blood flow rate by 50ml/min

analogWrite(PWMA, Speed); // start running the blood pump at the new higher speed (equal to the new value of speed)

debouncetimer = elapsed;

```
  }

  else if ((digitalRead(SW2) == LOW) && (Speed == 229) && ((elapsed - debouncetimer) >= 300)) // if the flowrateup button is pressed (SW2 variable is LOW) and the blood flow rate is already at the maximum of 200ml/min (speed>=229) and the button press duration is longer than 500ms

  {

    Speed = 255;

    analogWrite(PWMA, Speed); // continue running the blood pump at the maximum flow rate of 200ml/min

    debouncetimer = elapsed;

  }

  if ((digitalRead(SW3) == LOW) && (Speed == 255 ) && ((elapsed - debouncetimer) >= 300)) // if the flowratedown button is pressed (SW3 variable is LOW)  and the blood flow rate is between 150-200ml/min (183<=speed<=229) and the button press duration is longer than 500ms

  {

    Speed = 229; // decrease speed by 46, thus decreasing the blood flow rate by 50ml/min

    analogWrite(PWMA, Speed); // start running the blood pump at the new lower speed (equal to the new value of speed)

    debouncetimer = elapsed;

    }

    if ((digitalRead(SW3) == LOW) && (Speed <= 229 && Speed >=137) && ((elapsed - debouncetimer) >= 300))

    {

    Speed = Speed - 46; // decrease speed by 46, thus decreasing the blood flow rate by 50ml/min

    analogWrite(PWMA, Speed); // start running the blood pump at the new lower speed (equal to the new value of speed)
```

```
  debouncetimer = elapsed;

  }

  else if ((digitalRead(SW3) == LOW) && (Speed == 91) && ((elapsed - debouncetimer) >= 300)) // if the flowratedown button is pressed (SW3 variable is LOW)  and the blood flow rate is already at the minimum of 100ml/min (speed=137) and the button press duration is longer than 500ms

  {

   analogWrite(PWMA, 91); // continue running the blood pump at the minimum flow rate of 100ml/min

   debouncetimer = elapsed;

  }

 if ((digitalRead(SW4) == LOW) && (motorson == false) && ((elapsed - debouncetimer) >= 300) && (Speed != 45)) // if the motorstart button is pressed (SW4 variable is LOW) and the motorson variable is false and the button press duration is longer than 500ms

 {

  digitalWrite(STBY, HIGH); // the standby pin of the TB6612FNG dual motor driver is set HIGH, taking the driver out of standby mode and starting the blood and fluid replacement pumps

  motorson = !motorson ; // the motorson variable is changed from false to true (i.e. telling the arduino that the motor state has changed from off to on)

  debouncetimer = elapsed;

 }

 else if ((digitalRead(SW4) == LOW) && (motorson == true) && ((elapsed - debouncetimer) >= 300) && (Speed != 45)) // if the motorstart button is pressed (SW4 variable is LOW) and the motorson variable is true and the button press duration is longer than 500ms

 {
```

digitalWrite(STBY, LOW); // the standby pin of the TB6612FNG dual motor driver is set LOW, putting the driver into standby mode and stopping the blood and fluid replacement pumps

motorson = !motorson ; // the motorson variable is changed from true to false (i.e. telling the arduino that the motor state has changed from on to off)

debouncetimer = elapsed;

}

// MONITORING PRESSURE - this section of the code is used for the pressure sensors output, converting the voltage into pressure and the dealy is used to linearize the pressure output.

currentTMP = (0.681 * analogRead(A3) + 0.6825 * analogRead(A2)) - 802; //the variable 'currentTMP' is set equal to the average of the calibrated inlet and outlet pressure sensor readings, according to a simplfied equation incorpating [TMP = (Pin + Pout) / 2] and values from sensor calibration data

TMPtotal = TMPtotal - TMPArray[TMPIndex]; // the value in the array 'TMPArray' whose position is referred to by the current value of the variable 'TMPIndex' (e.g. TMPArray[0] refers to the first value in the array) is subtracted from the sum of all the values in that array ('TMPtotal') to give a new total

TMPArray[TMPIndex] = currentTMP; // the value in the array 'TMPArray' whose position is referred to by the current value of the variable (e.g. TMPArray[0] refers to the first value in the array)'TMPIndex' is set equal to the current TMP

TMPtotal = TMPtotal + TMPArray[TMPIndex]; // the value in the array 'TMPArray' whose position is referred to by the current value of the variable 'TMPIndex' (e.g. TMPArray[0] refers to the first value in the array) is replaced by this new TMP value and added to the sum of all the values in that array ('TMPtotal') to give a new total

TMPIndex = TMPIndex + 1; // the value of the variable 'TMPIndex' is incremented by 1

if (TMPIndex >= numReadings) // if the value of the variable 'TMPIndex' is greater than or equal to the variable 'numReadings' (i.e. if the end of the array 'TMPArray' has been reached)

```
  {
   TMPIndex = 0; // the value of the variable 'TMPIndex' is set to be equal to 0 (i.e. return to the first value in the array)
  }
 if (TMPIndex % 10 == 0) // if the remainder of value of the variable 'TMPIndex' is equal to 0 (i.e. every 10 'currentTMP' readings)
  {
   TMP = TMPtotal / numReadings; // the variable 'TMP' is set to be equal to the average of all values in the array 'TMPArray'
  }
  delay(1);
 // MAINTAINING THE TRANSMEMBRANE PRESSURE (TMP) - this section controls the stepper motor in order to maintain the TMP between 40-50 mmHg.

 if ((TMP<40) && (motorson == true)) // if TMP is below 40mmHg
 {
   stepper.setSpeed(+5); // the stepper motor speed is set to 5 and direction is set to positive (closing the outlet)
   stepper.runSpeed(); // the stepper motor is started
   digitalWrite(redSLEEP, HIGH); // the red and green elements of the RGB LED are lit giving an amber colour to signal TMP<40
   digitalWrite(green, HIGH); // the red and green elements of the RGB LED are lit giving an amber colour to signal TMP<40
 }
 else if ((TMP>50) && (motorson == true)) // if TMP over 50mmHg
 {
```

stepper.setSpeed(-5); // the stepper motor speed is set to 5 and direction is set to negative (closing the outlet)

stepper.runSpeed(); // the stepper motor is started

digitalWrite(redSLEEP, HIGH); // only the red element of the RGB LED is lit giving a red colour to signal TMP>50

digitalWrite(green, LOW); // only the red element of the RGB LED is lit giving a red colour to signal TMP>50

}

else if ((TMP>=40) && (TMP<=50) && (motorson == true)) // otherwise if TMP is between 40mmHg and 50mmHg

{

stepper.setSpeed(0); // the stepper motor speed is set to 0 (not moving)

stepper.runSpeed(); // the stepper motor is started

digitalWrite(redSLEEP, LOW); // only the green element of the RGB LED is lit giving a green colour to signal 40<TMP<50, additionally the SLEEP pin of the DRV8834 stepper motor driver is set LOW, putting the driver into sleep mode and stopping power consumption by the linear stepper motor

digitalWrite(green, HIGH); // only the green element of the RGB LED is lit giving a green colour to signal 40<TMP<50

}

if (motorson == false)

{

digitalWrite(redSLEEP, LOW);

digitalWrite(green, LOW);

}

// REPLACING THE FILTERED FLUID - this section of the code determines the operation of the fluid replacement pump

volumeremoved = scale.get_units(1); // open the comunication with the HX711 load cell module and read the value from the load cell

unsigned long currentMillis = millis(); // the variable 'currentMillis' (used to monitor the number of milliseconds the fluid replacement pump has operated for) is defined as an integer which may have a very large but only positive value

unsigned int seconds = currentMillis / 1000; // the variable 'seconds' (used to monitor the number of seconds the fluid replacement pump has operated for) is defined as an integer which which can only be positive

if ((seconds - previousseconds) > Interval) //

{

if (((volumeremoved - volumereplaced) >= 10) && (volumeremoved != 0)) // and if the difference between the volume of filtered fluid and the volume of replace fluid is greater than or equal to 10ml

{

digitalWrite(BIN1, LOW); // the positive terminal of the fluid replacement pump is set LOW and the negative terminal of the fluid replacement pump is set HIGH so the motor will turn and the pump will operate

digitalWrite(BIN2, HIGH); // the positive terminal of the fluid replacement pump is set LOW and the negative terminal of the fluid replacement pump is set HIGH so the motor will turn and the pump will operate

replacementpumpcounter++; // the counter which monitors the number of times the fluid replacement pump has operated increments by 1

previousseconds = seconds; //

}

else // otherwise

{

digitalWrite(BIN1, LOW); // positive and negative terminals of the fluid replacement pump are both set HIGH so the motor will not turn and the pump will not operate

digitalWrite(BIN2, LOW); // positive and negative terminals of the fluid replacement pump are both set HIGH so the motor will not turn and the pump will not operate

}

}

volumereplaced = replacementpumpcounter * 10; // calculate the volume of fluid replaced from the number of times the fluid replacement pump operated. One 10-second operation is equal to 10ml of fluid replaced.

// PRINTING TO THE LCD SCREEN - this section of the code determines what is printed to the LCD

char fluidbuffer [20]; // create a twenty character text buffer called 'fluidbuffer'

sprintf(fluidbuffer, "RM:%4dml RP:%4dml", volumeremoved, volumereplaced); // set the format of the the twenty characters in 'fluidbuffer': first three characters "RM:" followed by the variable 'volumeremoved' (the weight and thus volume of filtered fluid) expressed as four digits followed by two characters "ml", then a space, then three characters "RP:" followed by the variable 'volumereplaced' (the volume of replaced fluid) expressed as four digits followed by two characters "ml"

lcd.setCursor (0,0); // starting from the first position in the first row of the LCD

lcd.print(fluidbuffer); // print on the LCD the buffer 'fluidbuffer' as formatted

if (Speed == 91) // if the flow rate is 50ml/min (Speed = 91)

{

lcd.setCursor(0,1); // starting from the first position in the second row of the LCD

lcd.print("Flow Rate: 50ml/min"); // print on the LCD "Flow Rate: 200 ml/min" exactly as it appears between the quotation marks

}

if (Speed == 137) // if the flow rate is 100ml/min (Speed = 137)

```
{
  lcd.setCursor(0,1); // starting from the first position in the second row of the LCD
  lcd.print("Flow Rate: 100ml/min"); // print on the LCD "Flow Rate: 100 ml/min" exactly as it appears between the quotation marks
 }
 if (Speed == 183) // if the flow rate is 150ml/min (Speed = 183)
 {
  lcd.setCursor(0,1); // starting from the first position in the second row of the LCD
  lcd.print("Flow Rate: 150ml/min"); // print on the LCD "Flow Rate: 150 ml/min" exactly as it appears between the quotation marks
 }
 if (Speed == 229) // if the flow rate is 200ml/min (Speed = 229)
 {
  lcd.setCursor(0,1); // starting from the first position in the second row of the LCD
  lcd.print("Flow Rate: 200ml/min"); // print on the LCD "Flow Rate: 200 ml/min" exactly as it appears between the quotation marks
 }
 if (Speed == 255)
 {
  lcd.setCursor(0,1); // starting from the first position in the second row of the LCD
  lcd.print("Flow Rate: Maximum"); // print on the LCD "Flow Rate: 200 ml/min" exactly as it appears between the quotation marks
 }
 if (Speed == 45)
 {
  lcd.setCursor(0,1); // starting from the first position in the second row of the LCD
```

```
  lcd.print("  *Set Flow Rate*"); // print on the LCD "  *Set Flow Rate*" exactly as it appears between the quotation marks

 }

  lcd.setCursor(0,2); // starting from the first position in the third row of the LCD

  lcd.print("TMP: "); // print on the LCD "TMP" exactly as it appears between the quotation marks

  lcd.setCursor(5,2); // starting from the sixth position in the third row of the LCD

  lcd.print(TMP); // print on the LCD the value of variable 'TMP'

  lcd.print("    "); // print on the LCD three blank spaces where the value of variable 'TMP' will be printed to hold this space

  lcd.setCursor(9,2); // starting from the tenth position of the third row of the LCD

  lcd.print("mmHg"); // print on the LCD "mmHg" exactly as it appears between the quotation marks

 lcd.setCursor(15,2); // starting from the fifteenth position in the fourth row of the LCD

 lcd.print("SD:"); // print on the LCD "SD:" exactly as it appears between the quotation marks

 if (sdstate == 1)

 {

  lcd.setCursor(18,2); // starting from the eighteenth position in the fourth row of the LCD

  lcd.print("OK");   // print on the LCD " OK" exactly as it appears between the quotation marks

 }

 else

 {

  lcd.setCursor(18,2); // starting from the eighteenth position in the fourth row of the LCD
```

lcd.print("ER"); // print on the LCD " ER" exactly as it appears between the quotation marks

}

char timebuffer[14]; // create a nine character text buffer called 'timebuffer'

sprintf(timebuffer, "Time: %02d:%02d:%02d", h, m, s); // set the format of the nine characters in 'timebuffer': first a space, followed by the hours (variable 'h'), minutes (variable 'm') and seconds (variable 's') each be expressed as two digits seperated by a colon (hh:mm:ss)

lcd.setCursor(0,3); // starting from the first position in the fourth row of the LCD

lcd.print(timebuffer); // print on the LCD the buffer 'timebuffer' as formatted

// LOGGING DATA TO THE MICRO SD CARD - this section of the code determines what data is logged to the microSD card

myfile = SD.open("testing.csv", FILE_WRITE); // the comma-separated value (.csv) file "testing.csv" on the microSD card created in the setup is opened, ready to be written to

String sddata = String(timebuffer) + "," + String(TMP) + "," + String(volumeremoved) + "," + String(volumereplaced); // a string of text called 'sddata' is created comprised of four smaller text strings containing the values of 'timebuffer' 'TMP' 'volumeremoved' and 'volumereplaced', each separated by a comma

myfile.println(sddata); // the string of text called 'sddata' is written to a new line of the file "testing.csv"

myfile.close(); // the comma-separated value (.csv) file called "testing.csv" is closed

}

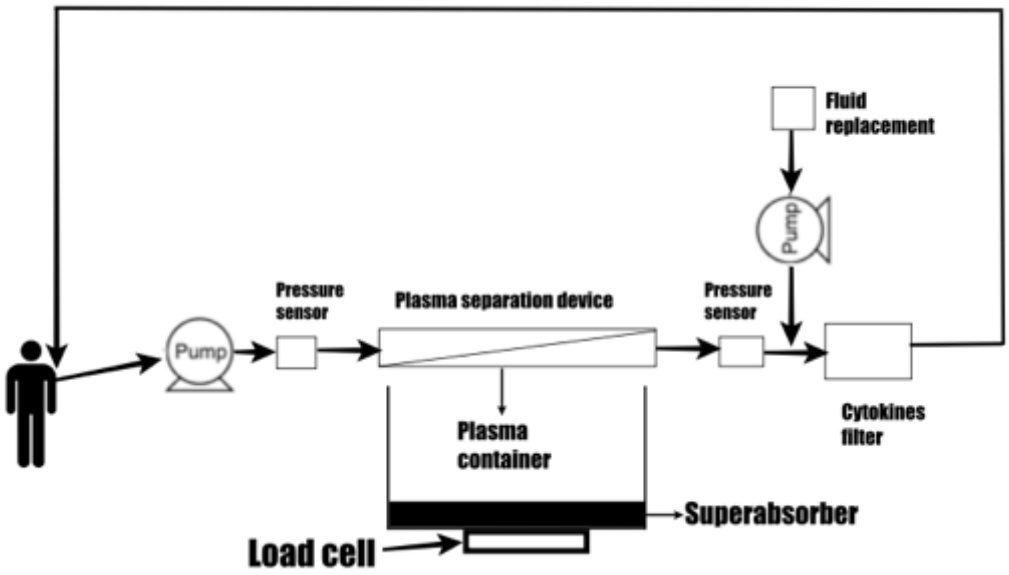

Appendix 1 Schematic diagram of the device